Synthetic Digital Circuits Using Neuronal Molecular Communications

Geoflly de Lima Adonias

School of Science and Computing

South East Technological University

This dissertation is submitted for the degree of

Doctor of Philosophy

Supervisors: Dr Sasitharan BALASUBRAMANIAM
Dr Michael Taynnan BARROS

August 2022

DECLARATION

I hereby certify that this material, which I now submit for assessment on the programme of study leading to the award of Doctor of Philosophy, is entirely my own work and has not been taken from the work of others save to the extent that such work has been cited and acknowledged within the text of my work.

Signed: _____   ID: 20078154

To my wife Bianca Leonessa.

ACKNOWLEDGMENT

"When education is not liberating, the dream of the oppressed is to become the oppressor."

Paulo Freire

Synthetic Digital Circuits Using Neuronal Molecular Communications

G. L. Adonias

Abstract

Neuron-based synthetic biology systems have been proposed in the past couple of decades as potential candidates for more precise treatment of neurodegeneration and, as building blocks of a platform for the design and development of novel therapeutics. Advances in the synthetic engineering of cells in parallel with the solid paradigm of communication engineering gave birth to a new interdisciplinary field known as Molecular Communications. Since its birth, researchers have been focusing on characterising the existing biological communication channels and developing theoretical models to pave the way for experimentalists to study, test and refine models of biological cells without the need for specialised equipment. Molecular Communications aims to facilitate the implementation of complex synthetic circuits capable of operating autonomously during short- and long-term periods with higher levels of compatibility with the biological environment and increased accuracy for minimising side effects.

The focus of this PhD thesis is to develop artificial synthetically engineered neuron-based circuits able to perform bio-computational tasks and, promptly act on specific malfunctioning processes inside the human nervous system. A model and analysis of neuron-based logic gates and circuits are proposed. This mathematical framework, from the perspective of information and communication theory, provides a way of analysing the highly stochastic processes of neuronal communications and, integrates well-known communication metrics and techniques (e.g. queue theory and information capacity). This thesis also presents a modelling approach for the analysis of demyelination, either induced by a viral infection or locally with specific drugs, that shines a light on the effects of demyelination and remyelination processes concerning the signal propagation in a single neuron and, also, within synaptic connections. Creating artificial bio-compatible circuits able to interface with natural cells can potentially lead to new forms of tackling neurological disorders and cognitive enhancements limitations that play a major role on the Internet of Bio-NanoThings.

Circuitos Digitais Sintéticos Usando Comunicações Moleculares Neuronais

G. L. Adonias

Resumo

Os sistemas de biologia sintética baseados em neurônios foram propostos nas últimas décadas como possíveis candidatos para um tratamento mais preciso da neurodegeneração e, como base para uma plataforma para o projeto e desenvolvimento de novas terapias. Avanços na engenharia sintética de células em paralelo com o sólido paradigma da engenharia das comunicações deram origem a um novo campo interdisciplinar conhecido como Comunicações Moleculares. Desde o seu nascimento, pesquisadores têm se concentrado na caracterização dos canais de comunicação biológica existentes e no desenvolvimento de modelos teóricos para abrir caminho para que experimentalistas estudem, testem e refinem modelos de células biológicas sem a necessidade de equipamentos especializados. A comunicação molecular visa facilitar a implementação de circuitos sintéticos complexos, capazes de operar de forma autônoma durante períodos de curto e longo prazo, com melhor compatibilidade com o ambiente biológico e maior precisão para minimizar possíveis efeitos colaterais.

O foco desta tese de doutorado é desenvolver circuitos baseados em neurônios sintéticos artificiais, capazes de realizar tarefas bio-computacionais e, prontamente, agir em processos específicos de mau funcionamento dentro do sistema nervoso humano. Um modelo e uma análise de portas e circuitos lógicos baseados em neurônios são propostos. Esta estrutura matemática, da perspectiva da teoria da informação e comunicação, fornece uma maneira de analisar os processos altamente estocásticos das comunicações neuronais e integra métricas e técnicas de comunicação tradicionais (por exemplo, teoria da fila e capacidade de informação). Esta tese também apresenta uma abordagem de modelagem para a análise da desmielinização, induzida por uma infecção viral ou localmente com drogas específicas, que destaca os efeitos dos processos de desmielinização e remielinização no que diz respeito à propagação do sinal em um único neurônio e, também, dentre conexões sinápticas. A criação de circuitos artificiais biocompatíveis capazes de interagir com células naturais pode potencialmente levar a novas formas de lidar com distúrbios neurológicos e limitações de aprimoramento cognitivo que desempenham um papel importante na Internet das Bio-NanoCoisas.

LIST OF FIGURES

LIST OF TABLES

CONTENTS

CHAPTER 1

INTRODUCTION

The human brain is one of the most mysterious organs of the body. It was only in the early 20th century that humanity started to grasp a more profound understanding of the brain's essential role in vital bodily functions. With the seminal work of Santiago Ramón y Cajal, it was described how the nervous system is made up of independent nerve cells that communicate with each other [1]. With the growing understanding of electricity and the technological advances that fuelled a so-called "neuroscientific revolution" and allowed the construction of powerful tools such as microscopes, humanity could fathom a much better understanding of the dynamics of the brain and its very complex anatomy. Even though today is possible to comprehend, model and simulate specific behaviours concerning neurons and their connections with other neurons (i.e. synapses), brain research is very much a work in progress and, it is hard to estimate its outcomes.

The brain acts as a machine, it processes streams of information and decides whether that information is relevant for storage, as in short- and long-term memories, or to trigger a reaction as in, activating a mechanical movement such as picking up an item or walking. The brain contains roughly more than 80 billion cells arranged into different morphological and electrical types. Those types divide the brain into densely interconnected "modules" known as the cortex. These connections can be "strengthened" as a kind of memory muscle that is

1

crucial for learning and memory recall. This means that the stronger a specific connection pattern gets, the more skillfully a specific task will be performed by the person or the more vivid a memory will be in a person's mind. Even nowadays, the mechanisms of how neuronal activity is transformed into experiences are unclear. The cortex is responsible for most of the information processing inside the brain and many researchers have been trying to understand how the brain modulates and encodes information, which brings information and communication theory (ICT) to neuroscience for an interdisciplinary approach to neuronal information processing. Neuroscientists are still working on correctly mapping the billions of neurons and their respective connections aiming to understand how the neuronal microcircuitry works and their potential continuous dynamic rearrangements. This fundamental limitation is one of the factors holding advances in the treatment of neurodegeneration, as an alternative to currently available treatments. Synthetic biology can potentially provide a useful set of novel techniques to give scientists the ability to non-invasively record neuronal activity and act upon malfunctioning cells inside the brain while the knowledge of neuronal dynamics keep expanding [2–4].

1.1 SYNTHETIC BIOLOGY

Synthetic biology (SB) is a multidisciplinary field that puts engineering and biology together aiming to not only design but also assemble and deploy artificial components. Such components are capable of reprogramming cells for manipulation and augmentation of cellular and neuronal functions to accomplish specific tasks [5, 6]. The possibility of assembling synthetic cells (SC) from scratch has been used as the foundation for more sophisticated and biocompatible approaches for the control and mimicry of some cellular functions and structures. This technology is at the centre of regenerative methods for the nervous system and allows the development of novel precise treatment, diagnostics and biocomputing systems that could act at a cellular level [7–9]. Synthetic biologists aim to construct living synthetic

cells that are not only highly energy-efficient but also of minimal complexity. Also, aligned with current research in nano-scale networks [10], the field could hugely impact the design of modern biologically synthetic cells.

Building synthetic cells from scratch is also known as a "bottom-up" approach and it originated from studies on biomimicry where the goal is the construction of models that emulate elements found in nature [11]. Electronic systems such as the ones found in today's computers and mobile phones are examples of highly complex systems that were built using the bottom-up approach. It consists of many small fully-functional components that were put to work together as a single "electronic organism". Researchers around the world have been working on such components and their findings range from logic gates [12–14] to integrated circuits such as oscillators [15]. Undoubtedly, this does not undermine "top-down" efforts which are generally performed by injecting artificial code into a host cell that can be executed either in parallel or instead of the cell's own program [11]. For example, the work of Gibson et al. [16] take advantage of the top-down approach where his team inserted a man-design DNA genome into a cell that did not contain its genome to create a cell that is controlled only by synthetic chromosome.

The idea of using mammalian cells, such as neurons, as computing elements inside the body is not new. For instance, in the 1940s, McCulloch and Pitts envisioned that cells inside the brain would possess logic gate capabilities [17]. Their work had a profound contribution to advancements in machine learning (ML) and artificial neural networks (ANN) theories. However, only recently this concept has been progressed and is gaining more and more momentum as researchers are, for example, finding ways of making neuronal networks act as logic gates by strengthening or weakening specific synaptic connections [14, 18]. Moreover, the literature also shows that neuronal arrangements can also work as dynamic logic gates by taking into account the neurons' previous activities and frequency of stimulation at their input

terminals [13]. On the other hand, it is also possible to control the logic gate performance of neurons by manipulating non-neuronal cells (e.g. astrocytes) in a tripartite synapse [19].

As scientists apply proven and well-documented engineering concepts to the design of synthetic biology systems, we look forward to a degree of controllability and reliability on these systems that would improve biocompatibility, prevent unwanted immune response and increase the level of certainty on predicting their outputs to allow us to fine-tune our models for specific applications such as filtering high-frequency spike firing. The similarities between the design of electronic and synthetic biology systems are encouraging but still present challenges that are unknown to the common engineering design. High stochasticity on the movement of synthetically engineered cells, mutation of biological systems and noise from processes originating from inside and outside the human body can affect the precision of artificial systems and compromise their reliability. Another important aspect to be taken into account is the ability that these systems should have to exchange information with each other. In the biological environment, this is usually performed with the use of molecules, which enables communication capabilities that can be exploited with the help of concepts borrowed from information and communication theory (ICT). This is done in order to quantify the performance of the cellular network with regard to information processing. It is important to emphasise that performance quantification is one of the aspects covered by the field of Molecular Communications.

1.2 MOLECULAR COMMUNICATIONS

Molecular Communications (MC) has been proposed over a decade ago, it was first introduced as a new paradigm for the transmission and reception of information modulated and encoded into molecules at the macroscopic, microscopic, and nanometric scales. Molecules released by the transmitter (T_x) are diffusely propagated in the medium (communication channel) and detected by the receiver (R_x) as an end-to-end communication system inspired by natural

biological processes [20–23]. As different types of cells in the human body communicate through the exchange of molecules, scientists have already proposed several models that use them as information carriers which include but are not limited to bacteria [24], calcium signalling [25], pheromones [26], molecular motors [27] and neurotransmitters [28].

Neurotransmitters are the main molecules responsible for carrying information between neurons in a synapse and these molecules have been drawing the attention of ICT researchers to MC research with neurons. The focus of this work is the information carried by action potentials (neuro-spike communication) that comprises periods of strong depolarisation of the neuronal membrane. Action potentials (AP) are heavily influenced by the structure of the neuron, morphological and electrophysiological characteristics can impact both the shape of the spike and its firing pattern. However, neurodegeneration can also induce changes in the neuronal structure causing a sort of "noise" added to the neuronal communication channel and presenting itself as yet another challenge for the study and characterisation of neuron-based MC systems. Different spike-firing patterns give researchers the possibility of not only modulating [29, 30], but also encoding [31–38] neuronal information through the synthetic engineering of neurons, opening a world of possibilities for the implementation of biocomputational units that should be stable and biocompatible enough for novel applications [10, 39]. We hope that future implementations provide better compatibility with natural and existent synthetic neurons in order to extend and improve current applications.

MC shows incredible potential as an alternative to conventional wireless communications, especially in environments such as an aqueous medium, where electromagnetic (EM) waves are strongly attenuated [40] or where the thermal effects induced by EM waves can damage human tissues [41]. Such promising benefits have been helping redirect part of the communication theory research to the nano-scale, i.e. nano-communications [42] and, although several works are describing neuronal communication and the detection and analysis of sequences of action potentials, there is still quite a gap to bridge, especially between theory

and implementation. MC has the potential to boost the research and development of novel targeted therapeutics based on synthetically engineered cells. From a therapeutic perspective, this is an important step towards more efficient targeted therapies because traditional drug delivery systems suffer from insufficient pharmacokinetics and unreliable distribution of the drugs themselves. Hence, MC could be the system to provide not only satisfactory therapeutic results but also the possibility of *in vivo* progress monitoring and the ability to, if needed, make changes in the process on the go [43]. For this reason, SB and MC must complement each other aiming to narrow the gap between theoretical approaches and practical implementations.

1.3 ENGINEERING COMMUNICATIONS SYSTEMS WITH NEURONS

Neurons communicate with each other through an electrochemical process known as *synapse*. It starts with electrical impulses, known as *action potentials* or *spikes*, travelling down the structure of the neuron and triggering the release of neurotransmitters into the synaptic cleft, as illustrated in Fig. 1.1 [44, 45]. This process enables the brain to process information ranging from the control and maintenance of basic vital functions to the encoding and storage of short- and long-term memories.

Neurons not only have inspired the development of artificial neural networks but also provide a multitude of concepts for potential communication systems that could take advantage of mimicking neuronal electrochemical signalling. Neurons are thought to encode information not only as a single unit but also as a network through the strengthening of specific synapses that allow a distinct group of neurons to fire action potentials nearly at the same time and each of those connection patterns represent something different. Malfunctioning neurons affected by neurodegenerative diseases such as epilepsy [46], Parkinson's disease
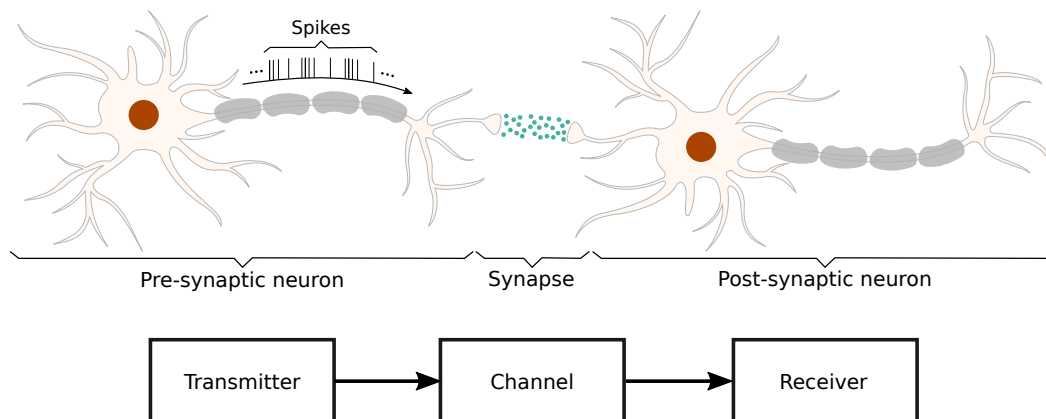
Fig. 1.1 Neuronal communication (synapse) and its analogous block diagram of a conventional communications system.

(PD) [47] and Alzheimer's disease (AD) [48] can compromise the integrity of the information within a neuronal network. Acute neurodegeneration can also be indirectly induced by viral infections that present neurotropic characteristics. These infections trigger cytokine storms as pro- and anti-inflammatory responses of the immune system to fight the infection, however, these processes can affect healthy tissue and, indirectly, cause more serious neurological manifestations [49, 50]. This degeneration can induce changes in the rate with which action potentials are fired and propagated within such a network. This results in either an increase in the frequency of firing, e.g. seizures, or a decrease due to an abnormal neuronal cell death rate [51].

Current solutions for neurodegeneration are often uncomfortable for a patient to live with, they are usually large enough to be felt inside the head and noticed from the outside and, also, they compromise the patients' lifestyles as some have reported being extra careful to not damage or dislocate the device when performing routine daily tasks [52]. Therefore, aiming to address those concerns and to exploit the rich dynamics of a neuronal network, researchers have been working on synthetically engineered neurons that react to a specific stimulus, such as light [53–57] to control neuronal firing either for the correction of malfunctioning connections or for the enhancement of sensory, motor and/or cognitive abilities.

The rate and timing of firing in response to stimuli can be applied to the design of neuron-based logic gates (detailed discussion later in Section 4.1). These synthetic logic gates can be interconnected via synaptic connections to build specific logic circuits and more complex components. This document focuses on the computational experiments performed on neuronal networks for neurons modelled not only as themselves but also as electronic components and control systems created to push the field towards more accurate and precise platforms for the simulation, design and development of targeted therapeutics, diagnostics and ability enhancements.

1.4 RESEARCH SCOPE AND OBJECTIVES OF THE THESIS

The engineering of synthetic circuits using neurons still poses several challenges such as compatibility with the biological medium and energy efficiency. Aiming to address those challenges, mathematical models are created to facilitate and speed up the study of such complex systems. The employed techniques help quantify the dynamics of the system, often analysed *in vitro* or *in vivo*, provide a way to formalise the biological knowledge currently available, and obtain a replicable methodology [58]. This PhD research work involves the analysis of biological behaviours and the modelling and simulation of molecular communications systems using neurons. It is also focused on techniques based on both computational synthetic biology and molecular communications to address the following challenges:

1. Establish a novel method for analysing the synthetic systems ability to communicate at the nano-scale for neurons.

2. Model biological processes using conventional communications systems techniques.

3. Shine light on neuronal characteristics that are fundamental to the development of novel neuron-based molecular communication systems.

The study is based on integrating various computational and mathematical models of neurons, and this includes models that govern the neural signalling when they are engineered as well as models when neurons are affected by diseases. The thesis also incorporates the use of data obtained from the literature that describes wet-lab experiments and, also, provided by collaborators, which will support the investigation on the design of a neuron-based molecular communications system capable of addressing the challenges mentioned above.

1.4.1 OBJECTIVES

This PhD research work aims to investigate and model the molecular communications processes that support the operation of neuron-based communication systems. This research is dedicated to applying information and communication theory for the analysis and reliability of neuron-based molecular communications modelled under circuit systems theory to study and propose solutions that can provide new insights for neuroscience and support the treatment of neurodegenerative diseases in the future. Its ultimate goal is to pave the way for future frameworks of novel precise treatment of neurodegeneration. As a result, the following objectives are defined to address the current limitations and challenges of this form of communication.

1. **Designing and developing computing functionalities from the interconnection of neurons:** Synthetic engineering of cells usually requires wet-lab experiments and *in vitro* testing. However, validating this through computational modelling and simulations can provide more accurate design and lower the costs for wet-lab experimental work. This in turn will provide a new tool for future synthetic biology engineering of neurons to sense and treat diseases.

2. **Developing computational models for neuronal signalling using circuit theory for the treatment of neurodegeneration:** The development of novel treatments takes

9

years to get to a stage where it is safe for the general public. With the development of accurate computational models reflecting the neurons' ability to exchange information, we can apply well-documented circuit theory concepts to analyse and quantify the neuronal signalling to efficiently and accurately propose new insights about neurodegeneration.

3. **Studying the effects of diseases based on molecular communications interactions among neurons to understand their communication behaviour:** By bridging biology and engineering, molecular communications are helping advance the knowledge on the communication between neurons paving the way for more reliable approaches that minimise the overall uncertainty of the neuronal communication channel.

4. **Using real wet-lab experimental data to understand changes in neural molecular communications:** Computational models can provide a better understanding of biological processes, however, the use of data collected from wet-lab experiments can drastically improve the performance of our models. This data can help understand details intrinsically present in biological systems and validate the findings obtained via simulation.

1.5 RESEARCH QUESTIONS

In the previous sections, several challenges posed towards the development of neuron-based communications systems were introduced (e.g., mutation of biological systems, noise from neighbouring biological processes, biocompatibility and biostability). This research work aims to contribute to the development of solutions to tackle the aforementioned issues. This is formally described through the following hypothesis:

Computational neuron-based molecular communications models can advance our understanding of the impact of neurodegeneration on neuronal communications and support the development of novel precise treatment of neurodegenerative diseases.

These potentially novel approaches to neurodegeneration will take advantage of neuron-based molecular communications for processing neuronal information, which in this thesis, is also studied in terms of circuit and systems theory where neurons can perform complex computational tasks. Firstly, the thesis will propose the use of neurons as logic gates and, consequently, logic circuits. This is then expanded to more complex circuits such as filters modelled by known control systems tools and, finally, myelination processes (which describe the production of myelin that act as layers of electrical insulation wrapped around the axon) at a single neuron level is investigated to understand how it interacts with other bodily functions and viral infections. These analyses will be able to offer relevant data on the reliability of those synthetically engineered neurons and their communication among a natural neuronal network. This hypothesis led to several research questions which were designed to fulfil all the required aspects for proposing synthetic neuronal communication systems.

First Research Question (RQ1) - *How can different logic gate operations and logic circuits be developed from neuron-based molecular communications?*

Currently, synthetic neurobiologists can engineer neurons to perform tasks like logic operations. However, several challenges exist such as neuronal control in real-time slowing down the development and application of more complex genetic circuits. The modelling of internal and external communication processes is an important step towards the solution of those aforementioned challenges. Therefore, in this research, we will model and analyse the molecular communications that exist behind engineered neuronal logic gates which should allow them to work in a more stable and controllable way. The development of neuronal logic gates represents quite a big step towards building more complex circuits. By modelling complex neuronal processes,

we can use the same approaches to connect these logic gates to form bigger and more complex logic circuits. By keeping default parameters related to the relevant synaptic connections in a process similar to the one performed for connections inside the gates themselves, we can connect inputs and outputs of different gates with each other and form circuits that can perform more complex operations such as arithmetic operations with spikes as bits or filtering specific spike firing frequency bands.

Second Research Question (RQ2) - *How can logic circuits be developed to create filters or amplifiers, using neuronal networks by theoretically analysing the non-linear dynamics of neural molecular communications?*

Neuron models are known for their highly non-linear behaviour and many factors such as spike firing rate may compromise the performance of neuronal logic gates and circuits and pose themselves as yet another challenge. With the aid of linearization techniques, we can analyse such systems by assessing their local stability of an equilibrium point and use concepts of systems and control theory to propose models and frameworks for more robust electronic components built with biophysical models of neurons.

Third Research Question (RQ3) - *How to model functionalities of logic gates and circuits for the analysis of their reliability and efficiency?*

Networks of neurons are quite hard to model. This is not limited to our understanding of the brain functions, but also there are too many processes to account for. We intend to simplify complex functionalities to a point that we can have a good approximation of the way they actually work. One approach is to use queueing-theoretical concepts over logic gates operation allowing a satisfactory prediction of the behaviour of neurons acting as gates. On the other hand, such a non-linear system can be linearised and derived as a control system, where systems theory concepts can be applied for analytical

analysis and possibly the proposal of mathematical frameworks that could increase the efficiency on a specific task such as filtering to improve accuracy when performing logical operations.

Fourth Research Question (RQ4) - *How can we model and simulate changes in neuron structure and analyse their impact on their communication behaviour?*

Like any other cell in the body, neurons are subjective to processes that could either strengthen or weaken their structure. These processes could be characterised, for example, by neurodegeneration, myelination, or the immune system's response to infections. To understand the rate with which these effects affect the neuronal structure we first need to understand how those processes work and their most relevant dynamics so it is possible to reproduce them in our simulation. There are several models of neurons and one of the most biologically plausible is the Hodgkin-Huxley which provides the dynamics and kinetics of ions and ionic channels and allow us to link the natural behaviour of the membrane to the effects of external agents that could either compromise or improve the structure of the neuron.

Fifth Research Question (RQ5) - *How viral infections can affect the performance of neuronal molecular communications systems and what communication analysis can be performed?* Some viruses present neurotropic properties, in order words, they can invade and replicate themselves within the nervous systems. This may not always be the root cause for degeneration but it most likely will lead to pro-inflammatory processes carried out by the host's immune system. These processes are triggered to fight the infection but, as a side effect, they can also damage healthy tissue which compromises not only the propagation of the neuronal signal but also neuronal connections. To understand whether this can lead to more serious neurodegenerative diseases and quantify their effects, we intend to mathematically model and account for these external factors and evaluate the neuronal performance by applying well-known

concepts from communication engineering and information theory that should provide us with a solid understanding of how the neuron is being affected aiming to adapt and propose solutions that would minimise the damage and improve the system's performance.

1.6 DOCUMENT ORGANISATION

The remainder of the thesis is organised as follows. Chapter 2 presents background information on computational neuroscience and the biological processes for neuronal communication. Chapter 3 discusses approaches for the analysis of the communication between neurons from the perspective of molecular communications and, in Chapter 4, we present methods for the design and development of biological computing units based on synthetically engineered neurons. Chapter 5 presents a summary of the research contribution which can be reviewed in further detail throughout Chapters 6-11. A discussion about the insights and findings proposed by the research work in this thesis is presented in Chapter 12 and, finally, the conclusion and future works are presented in Chapter 13.

CHAPTER 2

COMPUTATIONAL NEUROSCIENCE AND NEURONAL COMMUNICATIONS

Computational Neuroscience is a field of study that covers subjects from molecular and cellular studies to human psychology and psychophysical methods which are described by different types of behaviour by the nervous system. By putting together theoretical analysis and computational modelling, it is possible to understand and characterise how and why the nervous system operates the way it does. The construction of models helps to bridge different levels of description of the nervous system even though it can be difficult to identify the appropriate level of modelling and achieve the best balance possible between complexity and performance. It is important to put enough details to mimic as many dynamics as possible while keeping it simple enough to generate meaningful results. Furthermore, when multiple concepts from different fields of study are put together such as biology, communications engineering, control and systems theory can help the design and implementation of complex synthetically engineered biological systems, as well as expand the understanding of biological systems. In this chapter, the mechanisms and dynamics of the electrical and chemical aspects of the communication among neurons are described. This chapter also provides an overview

of the modelling of these communication processes and how it accounts for the diverse characteristics of neurons.

2.1 NEURONAL COMMUNICATION

Neurons are generally divided into three main parts: *dendrites*, *soma* and *axon*. The *dendrites*, i.e. post-synaptic terminals, receive stimuli from other cells and can help distinguish different neuron morphological types by the way the dendritic trees are projected onto neighbouring neurons. The main section of the cell is the *soma*. This is the place where most of the expression of proteins and genes and it is where all stimuli are received by the pre-synaptic cells are summed up. The membrane potential, when at rest, is negatively polarised due to the distribution of ions with regards to the extracellular medium. In the case of depolarisation of the membrane, the neuron should fire a spike down the *axon*. The *axon* is where the spike is propagated toward the pre-synaptic terminals of the neuron at its far end, passing neuronal information forward to post-synaptic neurons connected to it [28, 59].

The generation and propagation of action potentials is the electrical part of neuronal communication. After the spike reaches the pre-synaptic terminals, it triggers the release of synaptic vesicles that contain molecules (neurotransmitters) that are diffused in a small gap between pre- and post-synaptic terminals, known as the *synaptic cleft*, characterising this second stage as the chemical part. For this reason, the communication between neurons is an electrochemical process. Those neurotransmitters should probabilistically bind to neuroreceptors located on the post-synaptic terminals and drive a change in the membrane conductance which leads to the gating of ionic channels. These channels control the flow of ions which may excite the neuron, triggering the firing of an action potential or inhibit it, depending on the type of neurotransmitters received [28]. As aforementioned in Section 1.2, this electrochemical signalling process is within the context of molecular communications which employs manipulations to the spike firing pattern and neurotransmitter release for

the control of information transfer between two neurons. This whole process is known as *synapse* and is illustrated in Fig. 2.1.
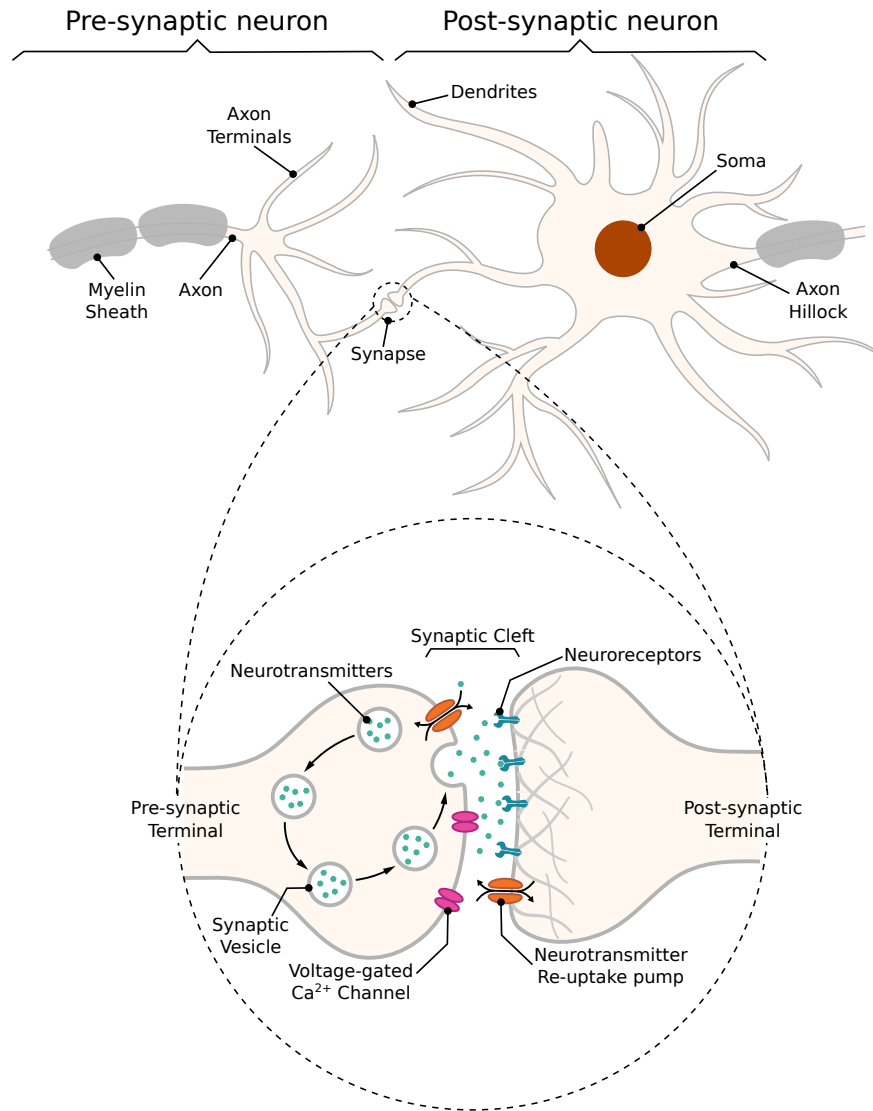
Fig. 2.1 Detailed illustration of a synapse.

In an **excitatory** synapse, the membrane potential of the postsynaptic neuron, which rests at approximately -65 mV, starts to depolarise until it reaches a threshold, θ, for action potential initiation. On the other hand, if it is an **inhibitory** synapse, the membrane should get hyper-polarised making it nearly impossible for the neuron to fire a spike. After reaching θ, the membrane potential should increase towards a maximum peak of depolarization, and

then the repolarisation process starts to drive the potential towards its resting state. For a brief moment, the neuronal membrane will repolarise itself past the reference value of potential when at rest making the membrane hyper-polarised and this short moment is known as the *refractory period*. This period can be further subdivided as *absolute refractory period* (ARP) which lasts around 1-2 ms during which the neuron is unable to fire again regardless of the strength of the stimuli, and as *relative refractory period* (RRP) which follows the ARP and, a response in the potential of the neuron may be evoked depending on the strength of the stimuli [60].

2.2 MATHEMATICAL MODELLING OF NEURONAL PROCESSES

2.2.1 THE HODGKIN-HUXLEY (HH) CONDUCTANCE-BASED MODEL

The response of the neuron is highly non-linear and the model must not be too simple as to lose relevant characteristics of the neuron and not too complex as to compromise the performance of the model. For that reason, we chose to use Hodgkin and Huxley non-linear model [61, 62] as it perfectly describes the influence of ionic and synaptic conductances in the propagation of the action potentials and, it is one of the most biologically plausible models for computational neuroscience showing consistency with existing biological knowledge [63].

In Fig. 2.2, we see how Hodgkin and Huxley used circuit theory and, consequently, mathematical equations to build an equivalent circuit that reproduces the behaviour of a neuron in which C is the membrane capacitance. Each voltage-gated ionic channel is represented by its respective conductances g_{Na} and g_K and the leak channel by the linear conductance g_l. It is important to note that the membrane capacitance is proportional to the surface area of the soma of the neuron and both the capacitance and its resistance helps estimate at which speed its potential reacts to the flow of ions through the membrane. The logarithmic ratio between intra- and extra-cellular ions define the reversal potentials E_{Na}
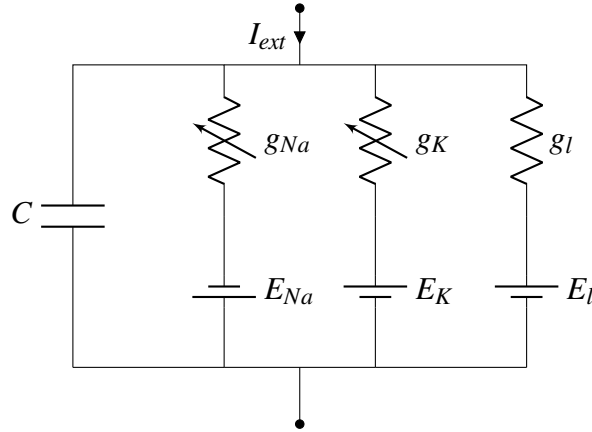
Fig. 2.2 Hodgkin-Huxley circuit representation of a neuronal compartment showing the membrane capacitance (C), the external current (I_{ext}), the variable conductances for the Sodium (g_{Na}) and Potassium (g_K), the reversal potentials for Sodium (E_{Na}) and Potassium (E_K), the linear conductance (g_l) and the leak reversal potential (E_l).

and E_K establishing a gradient that will drive the ionic flow [64], where Na and K represent Sodium and Potassium, respectively.

When an external stimulus, I_{ext}, is applied, it triggers either the activation or inactivation of the ionic channels that control the exchange of ions that result in depolarisation (or hyperpolarisation when inhibitory) of the membrane of the cell. These dynamics are modelled as

$$C\frac{dV}{dt} = -I_l - I_{Na} - I_K - I_{syn} + I_{ext},\qquad(2.1)$$

where V is the membrane potential and I_x are the ionic currents where x can be either a specific ion (Na, K) or the leak channel (l). Those currents are described as

$$I_l = g_l(V - E_l),\qquad(2.2)$$

$$I_{Na} = g_{Na}m^3h(V - E_{Na}),\qquad(2.3)$$

$$I_K = g_K n^4 (V - E_K), \tag{2.4}$$

where *m* and *h* are the activation and inactivation variables of the sodium channel, respectively, and *n* is the activation variable of the potassium channel, following the conventional approach described by Hodgkin and Huxley [62] and stated as

$$\frac{dm}{dt} = \alpha_m(V)(1 - m) - \beta_m(V)m, \tag{2.5}$$

$$\frac{dh}{dt} = \alpha_h(V)(1 - h) - \beta_h(V)h, \tag{2.6}$$

$$\frac{dn}{dt} = \alpha_n(V)(1 - n) - \beta_n(V)n, \tag{2.7}$$

in which the values of the rate constants α_x^i and β_x^i for the *i*-th ionic channel and, *x* represents *m*, *n* or *h*, can be defined as

$$\alpha_m = \frac{0.1(V + 40)}{1 + e^{-(V+40)/10}}, \tag{2.8}$$

$$\beta_m = 4e^{-(V+65)/20}, \tag{2.9}$$

$$\alpha_h = 0.07e^{-(V+65)/20}, \tag{2.10}$$

$$\beta_h = \frac{1}{1 + e^{-(V+35)/10}}, \tag{2.11}$$

$$\alpha_n = \frac{0.01(V + 55)}{1 - e^{-(V+55)/10}}, \tag{2.12}$$

$$\beta_n = 0.125e^{-(V+65)/80}. \tag{2.13}$$

Also, we present a simplified approach for the synaptic inputs from pre-synaptic cells, I_{syn}, in which the ionic channels that are activated by neurotransmitters arriving at the neuroreceptors is represented as

$$I_{syn} = g_{syn}(V - E_{syn}), \tag{2.14}$$

where the synaptic conductance, g_{syn}, and the synaptic reversal potential, E_{syn}, are used to describe many different types of synapses, and the latter may assume different values according to the types of neuroreceptors. The g_{syn} can be described as a superposition of exponentials, thus

$$g_{\text{syn}} = \sum_f \bar{g}_{\text{syn}} e^{-(t-t^{(f)})/\tau} H(t - t^{(f)}), \tag{2.15}$$

where τ is a time constant, $\bar{g}_{\text{syn}}$ is the peak synaptic conductance, $t^{(f)}$ is the arrival time of a pre-synaptic action potential and $H(\cdot)$ is the Heaviside step function [65].

The larger the cell diameter, the lower the spontaneous firing rate [66]. Furthermore, each ionic channel can be studied as containing one or more physical gates which can assume either a permissive or a non-permissive state when controlling the flow of ions. The channel is open when all gates are in the permissive state and it is closed when all of them are in the non-permissive state [67].

2.3 CONCLUDING REMARKS

As presented in this chapter, the dynamics of a neuronal communication channel can be expressed in terms of mathematical models such as the one presented in Section 2.2.1, it

makes use of a set of ordinary differential equations to capture the highly non-linear characteristics of neuronal membrane potentials and reproduce its behaviour. Researchers have been considering interdisciplinary approaches aiming to take advantage of those dynamics as is the case of Molecular Communications. However, some challenges still remain and need to be addressed. For instance, it is still unclear how neurons encode and modulate information to transform it into experience or to trigger motor functions even though many techniques have already been proposed [34, 35, 37, 68, 69]. Furthermore, a solid understanding of the way neurons communicate is essential on the quest to propose more efficient ways for measuring the reliability of the neuronal communication channel, since densely packed "random" connectomes of neurons can compromise the processing of information especially if there is a second source of stimulation such as optogenetics stimulators [53, 70] which can impact the performance of the system and integrity of the information.

There has been a tremendous effort from scientists around the world to model and simulate the brain in as much detail as possible to account for the plurality of a morphologically- and behaviourally-rich network of neurons. These models are certainly useful, however, there is not much relevant information on the control of neuronal information itself. In the works that will be later presented in Chapter 5, models based on the Hodgkin-Huxley formalism (see Section 2.2.1) were used for the analysis and development of models of synthetically engineered neurons as well as more complex neuronal circuits. The primary goal is to apply models that provide a good balance between efficiency and biological plausibility aiming to construct synthetic biological circuits with a high degree of fidelity when compared to real biological systems. Thus, this thesis presents results that push the boundaries of neuronal molecular communications supported by simulations of widely-used and -praised models of neurons.

CHAPTER 3

Neuron-based Molecular Communications

Molecular communications is a relatively new communication paradigm that takes advantage of molecular dynamics between cells within the human body to control the exchange of biological information. It borrows concepts from conventional information and communication theory aiming to create robust and scalable techniques for interfacing natural cells with synthetically engineered ones and potentially allowing more efficient targeted therapeutics, biochemical sensing, biocompatible sensor and actuator networks and the enhancement of cognitive abilities.

One of the different approaches for this kind of communication system is the use of neurons (either natural or synthetically engineered) as both ends of a communication channel, i.e. transmitter and receiver. This revolutionary thinking on the use of biological components as part of a communication system has been supporting scientific advances in the analysis of neurodegeneration and its direct or indirect causes. In this chapter, a discussion on the analysis of neurons and their connections from the perspective of molecular communications is presented. It also provides insights into how demyelination-induced degeneration can be

studied and, how foreign agents such as viruses, can indirectly trigger damaging neurological manifestations that can negatively affect the nervous system and its role in the human body.

3.1 MOLECULAR COMMUNICATION ANALYSIS OF NEURONS

As synthetic biology has been trying to bridge the gap between biology and engineering, scientists have also been working on ways to benchmark these biological communication channels using conventional information and communication theory. Computational and synthetic neurobiologists need to find proven concepts for the quantification of communication systems and by re-using well-known metrics. This will not only contribute towards a solid understanding of the capabilities of communication at a cellular level but also help narrow that knowledge gap even faster.

An early example is the work of Balevi and Akan [28], where the authors proposed a simple model of hippocampal neurons that accounts for a unidimensional diffusion of neurotransmitters in a bipartite synapse based on an assumption that there is a probabilistic factor to the process of binding neurotransmitters to neuroreceptors in the post-synaptic terminal. Ramezani et al [71] derived analytical expressions of a synapse with models from hippocampal neurons for a single input single output (SISO) communication channel. In this work, they proposed a three-dimension diffusion of molecules in a bipartite synapse following a Brownian motion.

As aforementioned, many models are applying concepts of information theory to benchmark the whole neuronal communication system. One example is the work of Veletić et al [72], who propose that communication between neurons resemble a conventional *peer-to-peer* (P2P) communication channel and their analysis could lead to implications for future P2P applications as they investigated the electrochemical and molecular paradigms of neuronal communication from a purely engineering perspective. Veletić and Balasingham [73] also use information theory to evaluate the performance of biological neuronal networks

showing a relationship of dependence between rate-coded neuronal information and synaptic connections, and morphological variety of connected neurons even though they are considering only SISO systems while in reality one neuron usually sends information to several others resembling a SIMO (single input multiple outputs) system. Barros [74] evaluates the performance of a cortical micro-column under the influence of noise and neuronal stimulation which lowers the capacity of the micro-circuitry channel, especially over time, resembling a common fast fading channel.

Furthermore, some studies emphasise a (MISO) multiple input single output system such as Cacciapuoti et al. [75] who proposed the analysis of the pre-synaptic terminals as multi-array transmitters since it is possible to find different dynamics between many connections to the same post-synaptic neuron, such as the probability of vesicle release. The modelling and characterization of the stochastic behaviour of the pre-synaptic terminals validated through numerical simulations reflected complex biophysical mechanisms of a synapse. Khan et al. [76] proposed an analysis of the synapse as a tri-dimensional space where the neurotransmitters are diffused and can, potentially, be re-absorbed by the transmitting neuron. Their results were validated by using Monte Carlo Simulation which also showed itself to be much faster in runtime when compared to the Monte Carlo approach. Khan and Akan [77] have analyzed the MISO neuro-spike communication system and how its mutual information and maximum achievable sum rate are affected by dynamic spiking thresholds helping to select neurons for particular applications in bionanonetworks studies. Lotter et al. [78] proposed a model for the synaptic diffusive molecular communication channel where they assess the impact of molecule re-uptake that propagates through the synaptic cleft following a Brownian motion.

All of the aforementioned studies in this section have served as progressive steps in the analysis of neuronal networks from the perspective of molecular communications as well as to contribute to the research and development of artificial neural communications and

facilitate the connection between real and artificial cells to further advance the treatment of neurodegenerative diseases. However, these works do not explore the real impact of neuronal information when artificially modulated and dispatched in between the natural signalling as well as the plurality of synthetic logic circuits inside a morphologically- and behaviourally-rich network of neurons (Fig. 4.1). One of the most detailed examples of models of neurons are the ones proposed by Markram et al. [59], the authors provide a digital reconstruction of the neocortical microcircuitry of rat's somatosensory cortex with fully-functioning models of neurons possessing different morphological and electrical behaviours which can support the development of analytical frameworks to be used as platforms for precise simulation of the effects of computing agents inside the brain.

3.2 BIOLOGICAL PROCESSES OF DEMYELINATION

Demyelination occurs when the myelin sheath sustains damage. Myelin sheath is the protective coating that wraps itself around the axon providing insulation and supporting action potential propagation. Diseases such as multiple sclerosis (MS) can be characterised as a functional impairment induced not only by the loss of myelin sheath but also by the failure of remyelination. Myelination in the CNS (central nervous system) is performed by oligodendrocytes while Schwann cells are responsible for the same process in the PNS (peripheral nervous system) [79]. Myelin sheath is important for the insulation and conduction enhancement in the axonal pathway [80], therefore, demyelination can impair the conduction of action potentials through the axon, attenuate the signal and compromise the communication between neurons leading to a deficiency in specific brain functions depending on which neurons are suffering demyelination. It can occur due to viral infections [81], vitamin deficiency [82], toxic, chemical or autoimmune substances [83] or a complete failure on the myelination process [84].

It is not an easy task to establish the sequence of events that leads to human demyelinating disease, but there is some evidence that myelin proteins are damaged first followed by a breakdown of the lipid bilayer [80]. In general, the permeabilization of the blood-brain barrier (BBB) precedes the process of demyelination. The BBB is a partially permeable structure of endothelial cells that regulates the transport of serum factors and neurotoxins between the circulating blood and extracellular fluid in the CNS [85]. One cause can be the activation of microglial cells, which are the resident macrophage cells in the brain and act as the main form of immune defence in the CNS and, potentially, damage the BBB facilitating the entry of toxic and autoimmune substances and accelerating the degradation of myelin sheaths [80, 86].

3.3 IMPACT OF VIRAL INFECTIONS ON THE NERVOUS SYSTEM

Nerve cells are not immune to viral infections and they can be affected by the so-called *neuroinvasive* viruses [87]. When a virus exhibits the ability to infect the nervous system, they are known to possess neurotropic properties and this type of virus can replicate itself within the nervous system [49]. These viruses can negatively impact basic functions performed by both central (CNS) and peripheral nervous systems (PNS) and even lead to severe nerve damage by triggering pro-inflammatory immune response [88]. Scientists have found that several viruses exhibit this kind of behaviour. For instance, the Zika virus (ZKV) [89] can infect the peripheral nervous system (PNS) and, sometimes, spread to the central nervous system (CNS). The human immunodeficiency virus (HIV) [90] can infect the CNS and cause *neuroinflammation* induced by an immune response of the body and, consequently, lead to neurodegeneration [91].

Studies have also shown that the novel coronavirus, SARS-CoV-2, may be able to invade the nervous system [92–95]. By hijacking and exhausting the cell's machinery for replication purposes, viruses can cause strong structural and biochemical damages to the host cell until the cell is killed. The body's defence mechanisms are triggered to avoid further damage to healthy cells and tissues by performing numerous toxic-metabolic processes, such as cytokine storms. These processes can potentially lead to inflammation and neurodegeneration as a side effect of the fight against the infection [81]. A recent survey [96] gathered information on the use of molecular communications for the modelling and analysis of infectious diseases, however, it did not account for effects caused by those infections. The need for novel molecular communications models able to reproduce the dynamics of biophysical processes performed by this kind of disease can instigate in-depth analysis not only of healthy cellular behaviour but also of dynamics needed for treatments based on synthetic biology. Further advancements can potentially lead to more efficient ways to stop neuroinflammation and restore "collateral damage" done to neurons [97].

3.4 CONCLUDING REMARKS

The construction of systems at the nano-scale with the capability of exchanging information using molecules has been made possible by advancements in synthetic biology research. There is quite a significant plurality of molecular communication systems aiming to understand not only how cells interact with each other but, also, their behaviour with regards to neuroinvasive viruses. Furthermore, literature is still a bit scarce when it comes to the study of the effect caused by viruses that do not attack primarily the nervous system have on neurological functions, especially when it could potentially lead to neurodegeneration such as demyelination.

In an effort to understand how these processes are linked together, this thesis also aims to connect all related processes and model an end-to-end cause-and-effect phenomenological

description of how viral infections can affect neuronal molecular communications. This project intends to further extend the analysis of neuronal systems and evaluate their communication performance to lay the groundwork accounting for the biological processes of neurodegeneration.

CHAPTER 4

ENGINEERING NEURON-BASED SYNTHETIC COMPUTING UNITS

Advances in the field of bioengineering and nanotechnology are giving scientists and researchers the right tools to engineer devices at the micro- and nano-scales inspired by biological dynamics and materials [98]. These devices, known as *bio-nanomachines*, are a biologically-inspired ramification of *nanomachines*. They are thought to be fully functioning synthetically engineered components capable of interacting with natural cells and molecules in the biological environment. It is envisioned that these nanomachines should address many of the challenges that still remain for synthetic biologists, especially in terms of biocompatibility, biostability and energy efficiency [99].

With the interdisciplinarity of molecular communications and nanonetworks, many researchers have been able to model and propose synthetically engineered biocomputing units able to precisely control a cell's behaviour and, by controlling neuronal dynamics, it increases the chances of creating a logic operating neuronal system that could help to push the boundaries of alternatives for precise treatment of diseases at a cellular and molecular level. In this chapter, a discussion on the advances of the use of neurons or network of

neurons as logic gates are presented as well as how non-neuronal cells may play an important role in the control of neuronal behaviour.

4.1 NEURONAL LOGIC GATES
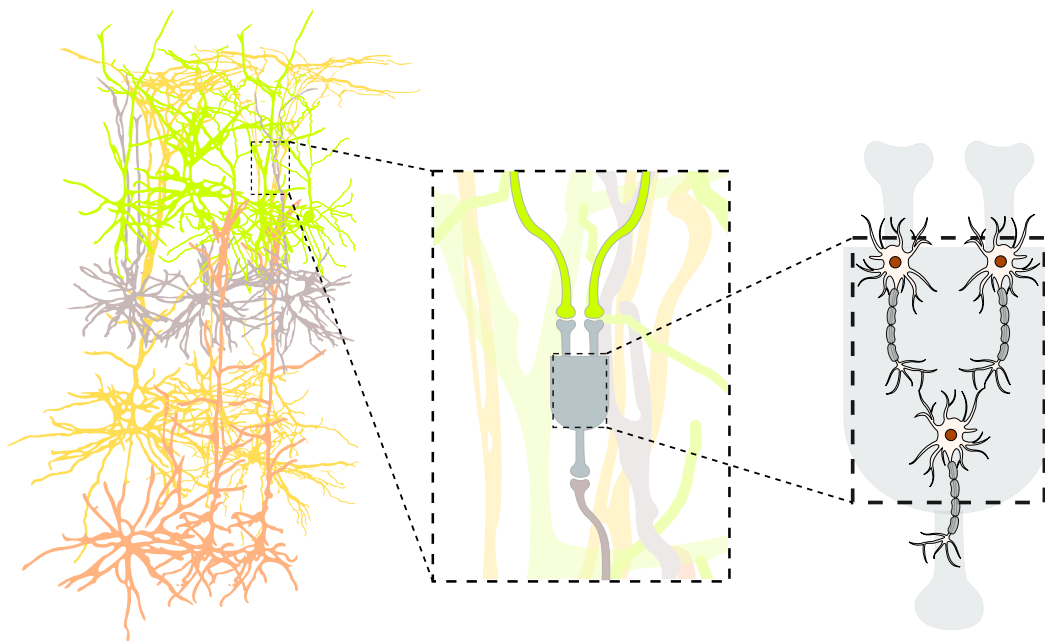
Fig. 4.1 Representation of a neuronal logic gate inside a cortical column. Three neurons compose a logic gate, two of them acting as inputs and one as the output of the gate. A gate establishes synaptic connections with natural neurons inside the cortical column.

To this day, biocomputing still remains a challenge for synthetic biologists but it has the potential of paving the way for the development of more biocompatible alternatives for the treatment of diseases [100]. These alternatives should be possible by building logic operating biocomponents that are capable of establishing a communication channel with natural cells within the human body. Drug design and discovery is the conventional way for the treatment of neurodegenerative disorders. The issue with this approach is that, despite its challenging process, new drugs usually have less than a 10% success rate for approval by the competent authorities [101]. Several factors contribute to this relatively low success rate but it is important to highlight the limited availability of biophysically plausible models and a

limited understanding of the biological processes involved in the diseases as well as many clinical trials for the study of potential side effects. For that reason, researchers are hopeful that biocomputing will be the mechanism that will allow them to perform precise control of a cell's behaviour and any other neurodegenerative effect [101]. Such designs could be improved and speeded up by the development of realistic frameworks capable of assessing the side effects of newly-discovered drugs without the ethical implications of clinical trials of current approaches.

In the 1940s, the idea that the brain comprises small units with logic gating capabilities was proposed by McCulloch and Pitts [17] and, although there was not much interest in their work during that time mainly due to the lack of technology to control the highly dynamic behaviour of the neurons, it did contribute to advancements in the fields of artificial neural networks and machine learning [13]. However, in the past few years, the scientific community has been witnessing an increase in the interest in biological logic gates constructed from brain cells driven by the emergence of cellular reprogramming techniques aiming to augment cellular capabilities through synthetic biology [6]. By allowing the control of neuronal dynamics, the possibility of creating logic operating engineered systems to interact with natural and engineered cells may lead to the development of better alternatives for the treatment of diseases at the cellular level [100].
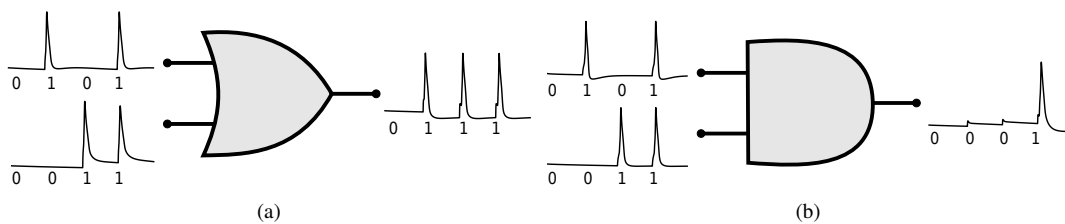
Fig. 4.2 Sampling spiking trains as bits; responses of both a (a) neuronal OR gate, and a (b) neuronal AND gate.

This idea of using neurons and non-neuronal cells as computing agents or as part of a computing "arrangement" that may comprise one or more neuronal and non-neuronal cells (Fig. 4.2), has been progressed by several works. As a first example, the work of

Vogels and Abbott [14] investigated how the manipulation of specific synaptic connections, either by strengthening or weakening some of them, may evoke different logic gates within a homogeneous network of *integrate-and-fire* models of neurons. Goldental et al [13] proposed that, unlike conventional electronic logic gates that consistently follow its truth-table, neuronal logic gates are dynamic and their functionalities depend on the frequency at the input, the activity of their interconnections and the history of their respective activities. Their experiments followed a procedure that enforced stimulations on neuronal circuits within a network of cortical cells *in vitro*.

Furthermore, Song et al [19] proposed that, in a *tripartite synapse*, the influence of astrocytes may help to control logic gating operations of neurons, but only a single type of neuron with a unique spiking pattern is used. Feinerman et al. [102] created three different neuronal logic devices using hippocampal neuronal cultures *in vitro*. The first one was a simple threshold component that would fire when it reaches a sufficiently high amplitude on the input, then they put two threshold components in parallel allowing the propagation of the signal only if the inputs are coincidental, in other words, their second device was an AND gate. The last component they built was a diode that used an asymmetric variation of the threshold component. According to the authors, the devices are very reliable with an average of 7% error across all three components.

We can also find in the literature evidence that neurons may act like filters, such as the work of Fortune and Rose [103] where they studied the effects of passive and active membrane conductances as mechanisms responsible for temporal filtering of spike trains. On the other hand, experiments conducted by Plesser and Geisel [104] on integrate-and-fire models of neurons showed that noise improved signal-to-noise ratio, if the neuron is fed with a periodic input, within a specific frequency range showing a bandpass filtering behaviour. Even with the tremendous effort of the scientific community so far, it has yet to investigate how synthetically engineered neuronal logic gates can be applied in neuroscience and the

impact synthetic neuronal computing units could have on a type-rich biological neuronal network and do not yield analytical models that could be used to describe the filtering capabilities of a neuron induced by specific drugs. Potential applications such as digital filters or amplifiers can help control abnormal spike firing patterns and provide the possibility to construct more complex circuits to perform more complex tasks.

4.2 DISCUSSION

Biological computation is still in its early stages of development even though there are several concepts already available in the literature. The models proposed by this PhD research provides the possibility of pushing the improvement of current devices used for the treatment of neurodegeneration. Surely there is a long way to translate the models shown here to fully validated solutions, especially in terms of the scale of the proposed systems but the capability of being reconfigurable and of having its accuracy more precisely estimated build the basis for more complex and robust systems.

With the construction of synthetically engineered neurons that resemble common, well-known electronic circuits, it is possible to adapt well-documented telecommunication systems and circuits metrics to properly analyse the performance of these biocomputing units and their role in molecular communication systems whilst accounting for the biological properties of neurons. A properly performed characterisation of those systems allied with the investigation in this chapter is an important step towards the design of a biocompatible synthetically engineered neuronal circuit. The proposed applications are based on the wireless nature of the synapse and focus on the single- and multi-unit interaction among neurons.

THESIS RESEARCH SUMMARY

This PhD research has produced six research articles which include four journal articles, one conference short paper and one workshop paper. Each of these articles significantly contributed towards answering the five research questions (RQ) posed in the first chapter of this document (Section 1.5).

5.1 ADDRESSING RESEARCH QUESTIONS WITH PUBLICATIONS

The study of the research questions has been continuous, meaning that the produced papers address partially more than one of the proposed RQs. This chapter presents a mapping of each publication to the specific RQ it addresses as depicted in Table 5.1.

Table 5.1 Association between the research questions and publications.

Questions	Publications
RQ1	TNB, NANOCOM, MOLCOM
RQ2	FCN
RQ3	TNB, FCN, MOLCOM
RQ4	PHYSBIO
RQ5	TNSRE

Furthermore, the summary and contributions of each publication are briefly discussed below.

1. **TNB** (*Chapter 6*) - G. L. Adonias, A. Yastrebova, M. T. Barros, Y. Koucheryavy, F. Cleary and S. Balasubramaniam, *"Utilizing Neurons for Digital Logic Circuits: A Molecular Communications Analysis,"* in IEEE Transactions on NanoBioscience, vol. 19, no. 2, pp. 224-236, April 2020.

   Summary: For our first journal paper, it was decided to work on a more complex synthetically engineered arrangement of neurons that can form logic gates (Fig. 5.1a). Biocomputing devices can open up possibilities not only for modulation and encoding of information but also for the treatment of neurodegeneration such as epilepsy. Neurons can have their synaptic properties modified in other to evoke logic gating capabilities in a network [14] or take advantage of the influence of non-neuronal cells, e.g. astrocytes, that can be used to help to control synaptic processes [19].
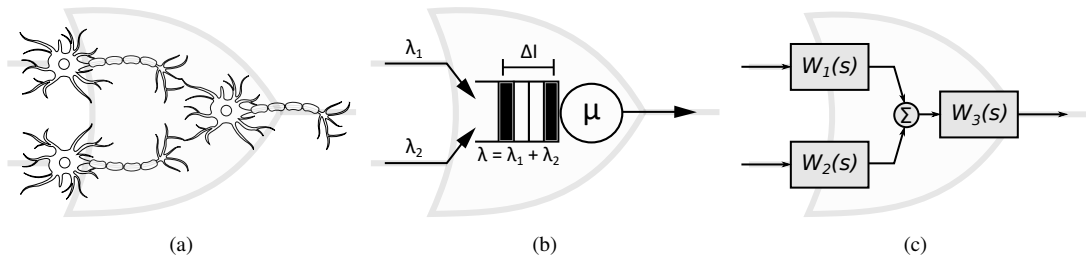
Fig. 5.1 Different models of a biological logic gate; (a) neuronal connection inside gate, (b) queueing-theoretical models for a neuronal logic gate, and (c) transfer-function block equivalent of a neuronal logic gate.

   Contributions: In this paper, we contributed to RQ1 and RQ3, where we proposed a queueing-theoretical model (Fig. 5.1b) for each gate allowing the study of the dynamics of the proposed neuronal logic gates as a single element and, analysing the collective behaviour of the neurons that compose a logic gate. The results suggested higher accuracies when predicting the behaviour of a gate, especially when the mean inter-spike interval (ISI) increased at the input. This sort of prediction could help synthetic

neurobiologists to propose an arrangement capable of smoothing out high-frequency firing caused by neurological disorders such as epilepsy. The results also suggested that the sampling frequency of the spiking train of signals plays a role in the accuracy of the gates and the quality of the proposed model.

2. **FCN** (*Chapter 7*) - G. L. Adonias, H. Siljak, M. T. Barros, N. Marchetti, M. White and S. Balasubramaniam, *"Reconfigurable Filtering of Neuro-Spike Communications using Synthetically Engineered Logic Circuits,"* in Frontiers in Computational Neuroscience, vol. 14, pp. 91-106, October 2020.

Summary: In the second journal publication, systems theory was applied on top of our logic circuits analysis partially contributing to RQ2 and RQ3. In this paper, we proposed computational models of reconfigurable neuronal filters and a transfer function as the basis for the proposed mathematical framework (Fig. 5.1c). The investigation was mainly conducted on the capabilities of a logic circuit to attenuate high-frequency firing of action potentials and how this filtering capability can be controlled through the synaptic properties of the output cell of the whole logic circuit aiming to widen or narrow a specific frequency window. The proposed framework opens new opportunities for the field of *in silico* pharmacology, which is also known as computational therapeutics or computational pharmacology and can be defined as a research field that encompasses the development of techniques for pharmacology hypothesis testing. It uses software to mine and to analyse biological and medical data alongside the generation of *in vitro* data to create and fine-tune a model that could ultimately provide advances in medicine and therapeutics [105].

Contributions: Our results suggested that neuronal logic circuits can work as digital filters that could be fine-tuned after potential deployment inside the human brain through modification of the synaptic weights of its connections. Thus, helping smooth out abnormal frequencies that are mostly evoked by neurological disorders. We

performed analysis on the ratio of frequency response and its analogous metric in decibels, which represents the magnitude (gain) and, showed a clear difference in the levels of attenuation between different neuronal circuits. Also, we proposed a metric of counter-efficiency that suggested specific frequency bands in which different circuit arrangements differed among themselves on their respective optimal performance. This allowed a more scenario-based manipulation of the filter where, for instance, a subject could be awake or asleep. This framework could also provide a platform for the discovery and design of new drugs contributing to the state-of-the-art in synthetic neurobiology and helping to bridge the gap between biophysical models and systems theory engineering.

3. **PHYSBIO** (*Chapter 8*) - G. L. Adonias, H. Siljak, M. T. Barros and S. Balasubramaniam, *"Neuron Signal Propagation Analysis of Cytokine-Storm-induced Demyelination,"* Submitted to Physical Biology Journal, June 2021.

Summary: In the third journal publication, which is currently under review, the structure of the neuron is taken into account. This provides a more in-depth analysis of how external processes and agents can compromise neuronal communications. In this paper, in particular, the effects of a viral infection capable of crossing the blood-brain barrier (BBB) is investigated. Once inside the nervous system, viruses can infect a host cell and replicate themselves triggering an immune response to fight the infection and, as a side effect, damaging healthy tissue.

Contributions: In this work, an end-to-end model that accounts for immune-induced cytokine storms and the demyelination induced by their inflammatory effects is proposed. As discussed in Section 3.2, demyelination affects the propagation and conduction of action potential through the axonal pathway. Therefore, this work also proposed a linear model of demyelination inspired by control systems theory that predicts the signal effects on action potentials that are expected from a demyelinated axon. The

model also maps components regarding spike width, peak potential and delay for spike initiation.

4. **TNSRE** (*Chapter 9*) - G. L. Adonias, C. Duffy, M. T. Barros, C. McCoy and S. Balasubramaniam, *"Analysis of LPC-induced Demyelination on Neural Molecular Communications,"* Submitted to IEEE Transactions on Neural Systems and Rehabilitation Engineering, August 2021.

Summary: Our fourth and last journal submission, currently under review, also focuses on the structure of the neuron and it shows, allied with wet-lab experiments, how fast toxic substances such as lysolecithin induce demyelination and, it provides an insight into the remyelination process which can not bring the myelin sheath back to its original proportion.

Contributions: Using a myelination index calculated with microscopic images of brain slices, this work proposes a model for demyelination under three different scenarios: neuronal compartments (single neuron), bipartite synapse and neuronal network. Therefore, giving us the possibility of predicting the spiking rate of neurons under demyelination or remyelination processes.

5. **NANOCOM** (*Chapter 10*) - G. L. Adonias, M. T. Barros, L. Doyle, and S. Balasubramaniam, *"Utilising EEG Signals for Modulating Neural Molecular Communications,"* in Proceedings of the 5th ACM International Conference on Nanoscale Computing and Communication 2018 (ACM NanoCom '18), Reykjavik, Iceland, Sep. 2018.

Summary: An important feature of neuronal networks is the ability to modulate sensory, motor and cognitive information [29, 106]. Therefore, the modulation of artificial information was the first application addressed in the first conference publication (NANOCOM). This publication proposed a system that can predict the activity of a network of neurons [107] and send information that defines the probability of

vacant periods that implanted nano-devices can use to stimulate neurons, e.g. light stimulation [53, 55, 56, 70], aiming to minimise interference with the natural signalling (see Fig. 5.2). This work helped to understand the possibility of potential disruption caused by a synthetically engineered component, such as a neuronal logic gate.
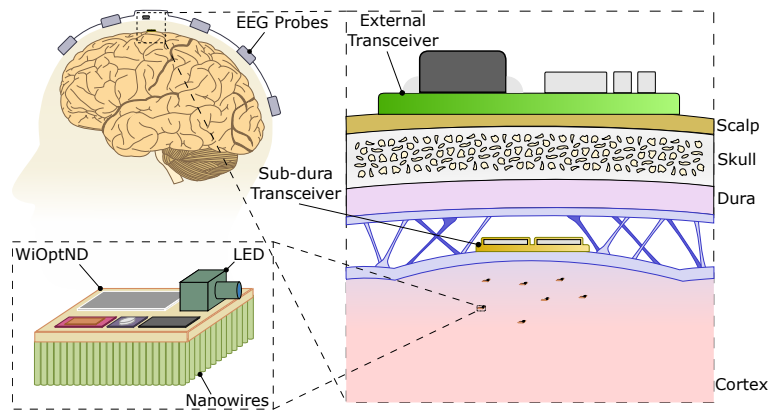
Fig. 5.2 Architecture of a EEG-WiOptND-powered system for the insertion of artificial data into the brain [108].

It was considered that the neurons fire spikes at a rate following a *Poisson* process and they had different spike firing probabilities providing a highly stochastic communication channel. A neuronal network with different types of neurons is simulated with a stimulation point for each cell to represent their spontaneous firing and a few points for artificial stimulation that was chosen based on the neuron's connection probability and topology of the network inferred from the raster plot in [107].

Contributions: A numerical analysis was performed on the data collected from the simulations to show how the capacity and the information rate of the channel would behave with the increase in artificial bits transmitted. The results suggest that we can achieve higher capacity with a lower range of transmitted bits, while the information rate oscillates at high values of the mid-range quantity of transmitted bits. This publication partially addresses RQ1 showing that a synthetically engineered light-sensible neuron can be controllable over specific periods for the dispatch of artificial

information through the cortex and, possibly, for the replacement of malfunctioning neurons.

6. **MOLCOM** (*Chapter 11*) - G. L. Adonias, A. Yastrebova, M. T. Barros, S. Balasubramaniam, and Y. Koucheryavy, *"A Logic Gate Model based on Neuronal Molecular Communication Engineering,"* in Proceedings of the 4th Workshop on Molecular Communications, Linz, Austria, Apr. 2019.

Summary: Lastly, in our second conference publication (MOLCOM), we partially investigated RQ1 and RQ3 by engineering the synapses in a three-neuron arrangement where two neurons act as inputs and one as the output of the gate. From this computational model, we were able to expand the analysis into a more information-theoretical approach which resulted in our first journal publication (TNB).

Contributions: We proposed eight different arrangements with diverse types of neurons in which five of the configurations worked as OR gates and the other three as AND gates. We also identified that not only their connections but the types of neurons played a role in the gating performance of the computing function.

PUBLICATION 1: UTILIZING NEURONS FOR DIGITAL LOGIC CIRCUITS: A MOLECULAR COMMUNICATION ANALYSIS

Utilizing Neurons for Digital Logic Circuits: A Molecular Communications Analysis

Geofly L. Adonias, Anastasia Yastrebova, Michael Taynnan Barros, Yevgeni Koucheryavy *Senior Member, IEEE*, Frances Cleary, and Sasitharan Balasubramaniam, *Senior Member, IEEE*

Abstract—With the advancement of synthetic biology, several new tools have been conceptualized over the years as alternative treatments for current medical procedures. As part of this work, we investigate how synthetically engineered neurons can operate as digital logic gates that can be used towards bio-computing inside the brain and its impact on epileptic seizure-like behaviour. We quantify the accuracy of logic gates under high firing rates amid a network of neurons and by how much it can smooth out uncontrolled neuronal firings. To test the efficacy of our method, simulations composed of computational models of neurons connected in a structure that represents a logic gate are performed. Our simulations demonstrate the accuracy of performing the correct logic operation, and how specific properties such as the firing rate can play an important role in the accuracy. As part of the analysis, the mean squared error is used to quantify the quality of our proposed model and predict the accurate operation of a gate based on different sampling frequencies. As an application, the logic gates were used to smooth out epileptic seizure-like activity in a biological neuronal network, where the results demonstrated the effectiveness of reducing its mean firing rate. Our proposed system has the potential to be used in future approaches to treating neurological conditions in the brain.

Index Terms—Logic gates, synthetic biology, nano communications, nanonetworks, Boolean algebra.

I. INTRODUCTION

It has been over a decade since *Molecular Communications* (MC) was introduced as a new communication paradigm aiming to conceptualize and build communication systems inspired by natural biological processes [1]–[4]. One of those MC systems is known as *neuro-spike communication* [5], where information is transferred between two neurons through an electro-chemical process which triggers an electrical impulse called *action potentials*. We are interested in the interchangeable action potentials information that comprises of

Fig. 1. Neuronal logic gate inside a cortical column.

periods with high membrane polarization, i.e. spikes, which is more suitable to analyse neural activity in population settings. This information can not only be encoded using any of the already proposed encoding techniques [6], [7], but also be modulated [8]–[10] mimicking a traditional communication system, and potentially presenting itself as a tool for cognitive enhancement and treatment of neurodegenerative diseases [11], [12].

In the 1940s, McCulloch and Pitts envisioned that the brain would be composed of units with logic gating capabilities [13]. During that time, the interest in their work in neuroscience was poor simply because neuronal cells are much more dynamic than simple digital logic gates, and there were no tools available to control such biological activity. However, since published, their seminal work contributed to advancements in artificial neural network and machine learning theories [14]. Recently, the interest in creating biological logic gates for the brain is picking up due to the emergence of cellular reprogramming towards augmenting their functioning through synthetic biology [15]. The vision of creating logic operating engineered systems to interact between natural cells and engineered cells (i.e. bio-nano machines) has the potential to create better alternatives for the treatment of diseases at the cellular level by allowing the control of their dynamics [16].

The idea of using cells in the brain as computing agents has been recently progressed by many works. One example is the work of Vogels and Abbott [17], where they investigated the signal propagation in networks of integrate-and-fire

43

models of neurons and found that by either strengthening or weakening specific synapses, different types of logic gates may arise within the network. Goldental et al. [14], used neurons function and communication dynamics to propose dynamic logic gates that work based on their historical activities, interconnection profiles, as well as the frequency of stimulation at the input terminals. Song *et al* [18] took a different approach, where they proposed that the interaction of astrocytes in a tripartite synapse may be able to control the logic gate performance of neurons. Although they are also working with non-neuronal cells, the neurons used are all of the same morphological and electrical types. Even with this tremendous effort, these works don't explore the full impact of logic gate plurality inside a type-rich biological neuronal network (Fig. 1). Further investigation of novel logic gate constructions are needed towards more computing reliability within the chaotic activity within these networks.

Synthetic Biology has achieved success in modifying or inheriting new functions in biological cellular systems and communications [19], [20]. For the past few years, we have seen quite a lot of progress in the manipulation and engineering of the behaviour of mammalian cells [21]. This paved the way for more sophisticated approaches with regards to neuronal and non-neuronal cells (e.g. astrocytes) that can be synthetically engineered to enable control of their dynamic behaviour and functionality, aiming at the correction of abnormalities at a cellular level. With the advance of synthetic biology and nano-scale networks [22], many components ranging from logic gates [14], [17], [23], [24] to integrated circuits such as oscillators [25] have also emerged. To date, there has not been a direct application of synthetic biological-based logic gates for neurological diseases.

In light of numerous applications that can have an impact on biological systems [26], researchers have been investigating computational modelling of neurodegenerative diseases such as Alzheimer's disease (AD) [27], Parkinson's disease (PD) [28] and Epilepsy [29]. Neurodegenerative diseases can be seen as a progressive loss of specific neuronal populations that could lead to death or a disabled life. The modelling of those degeneration processes may help substantially improve our understanding which in turn has the potential to speed up the research of new therapeutic solutions. This work is inspired by the medical challenges in Epilepsy, to deliver a new system that uses synthetic biology and molecular communications. The treatment of Epileptic seizures is truly challenging, where drugs are not effective or have horrendous side effects [30]. At the same time, deep-brain stimulation techniques are not patient-friendly and Epilepsy correcting surgery has tremendously negative effects on the lifestyle of patients [31].

Information processing in the brain involves the propagation of action potentials through countless numbers of specific neuronal networks. This enables the brain to process various types of information that can range from controlling the functions of organs within an organism to coding and storing long-term memory, as examples. The synchronous uncontrolled firing of spikes in large regions of the brain that can occur spontaneously can be related to neurological diseases, and one example is epilepsy [32]. Based on this, spiking firing filtering techniques based on synthetic logic gates using, such as, digital logic gates that can improve the control of neuron activity to normal levels. This novel system can play an important role in smoothing out uncontrolled neuronal firing and consequently reducing the effects of seizures. The practical positioning of those gates also poses an issue on the feasibility of this solution. A suitable way of achieving this efficient insertion and positioning would be by using gene therapy techniques that may be invasive [33] or noninvasive [34] with the dispatch of the synthetic circuits through the bloodstream. To the best of our knowledge, there is no work in the literature on neuronal logic gates that are applicable as potential treatments for neurological disorders.

In this paper, we present a novel theoretical system that couples neuronal logic gates in a biological network of neurons. We investigate the effects of filtering high-frequency multi-unit firing caused by Epileptic seizures by randomly distributed logic gates within a validated computational framework. Unlike the aforementioned works, this paper does not perform any fine-tuning in the network, where the gates are built with three models of neurons with different morpho-electrical characteristics between each other. In our study, the type-rich neuron environment is taken into consideration for improved integration with the existing functioning network. To help quantify the ability of processing spiking information, we developed a queueing theory model that analyses the mean squared error (MSE) as a function of the inter-spike interval (ISI) at different sampling frequencies. Our work is built on top of our previous efforts [23] which only analyzed the performance of the gates as isolated units for three different inter-spike intervals (ISI) using a constant stimulus. The main contributions of this paper are as follows:

- **Neuronal logic gates are built, controlled and simulated within large neuronal networks using computational models of neurons** [35]. We use three models of neuron cells to create a single synthetic logic gate capable of performing logic operations at a cellular level. Two of them act as inputs so the output cell can receive stimuli from natural synaptic connections avoiding bias towards the intensity of any external stimulation.
- **Analysis of performance for the gates simulated in isolation and inside a network of neurons.** We analyze the dynamic behaviour of neuronal communications that could affect the operation of the gate and consequently the network, quantified in terms of accuracy. It is expected that this analysis gives an insight into how parameters of the synaptic connection and morpho-electrical characteristics of the cell, as well as the firing rate, would affect how accurately the gates process the inputs.
- **Proposal of a queuing model for the input and gating of action potentials as units of information.** The advantage of a queueing-theoretical model is that complex neuronal networks can be studied as a single element representing the collective behaviour of those cells. The model is capable of predicting the accuracy of the synthetic gates, and this is validated using mean

squared error (MSE) as a function of the inter-spike interval (ISI) at different sampling frequencies.

- **We quantify the impact of randomly placed logic gates in smoothing seizure-like activity.** Based on the presented model of seizure-like activity, we manipulate the neuronal ionic concentration of K and Na to regulate the spiking rate when the disease is triggered. We couple this model with our computational framework and evaluate the decrease in mean spiking rate when neuronal logic gates are placed inside the biological neuron network.

The remainder of this paper is organized as follows, in Section II an overview of neuronal properties and how they communicate with each other is provided. The construction of neuronal logic gates, their diverse types and the queue-theoretical analysis are discussed in Section III. Section IV, presents a mathematical framework of the role played by ionic dynamics on seizure-like events is presented. Section V contains all details regarding the simulation, network connectivity and its parameters, and the results from those simulations are presented and discussed in Section VI. Finally, in Section VII the conclusions for this work are presented.

II. NEURON COMMUNICATION BACKGROUND

Neuronal network communications allow the propagation of spikes through a population of neurons transferring information inside the brain. Bio-computing approaches based on the communication of neurons will rely on this propagation behaviour and its relation to the neuron properties as well as the characterization of neuronal communications. Therefore, before presenting the model of logic gates using neurons (Section III), the morpho-electrical characteristics, the columnar and laminar organization properties of neurons as well as the compartmentalized Hodgkin-Huxley model for neuronal communications will be introduced.

A. Neuron Properties

Neuronal cells can be classified in terms of their morphology, electrophysiology, projections, position in the brain and the proteins and genes they express. The models of neurons used in this work, collected from [35], are classified only based on their morphological and electrical properties (morpho-electrical characteristics) as well as which cortical layer they are from (columnar and laminar organization). The classification method used in this work is detailed below.

1) Morpho-electrical Characteristics: Well-established features in the soma of the cell and its dendritic and axonal arbours are sufficient for the classification of different morphological cells. In terms of size, cortical neurons can be categorized as small neurons $(8 - 16\,\mu m)$ along with neurons from the hippocampus, olfactory bulb and dorsal horn. Axonal features play a major role in distinguishing inhibitory types while excitatory types can be better identified by their dendritic features [35].

Different morphological types (m-types) of cells can have diverse firing patterns. These patterns are generated in response to the injection of step currents in cortical neurons. From the 11 different electrical types (e-types) identified by
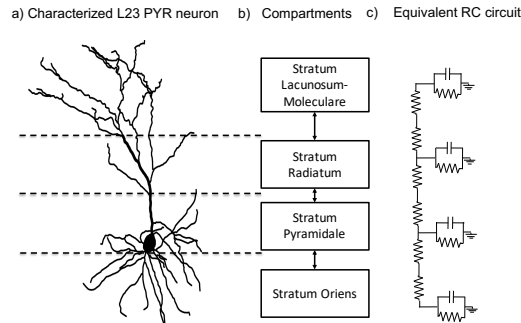
Fig. 2. Cell comparmentalization; a) A morphological structure of a layer 2/3 pyramidal neuron, b) Compartment model of a Layer 2 pyramidal neuron including 4 compartments: stratum oriens, stratum pyramidale, stratum radiatum and stratum lacunosum-moleculare, c) The equivalent RC circuit module.

Markram et al [35], all m-types used in this work are burst Non-accommodating (bNAC) e-types.

2) Columnar and Laminar Organization of the Cortex: The cerebral cortex is composed of neurons arranged into six horizontally and dispersed layers. These layers have different characteristics such as thickness, size, cell type and cell density showing a "laminar" organization and subdividing the cortex into disparate regions and areas. These layers are known as (1) Molecular layer, (2) External granular layer, (3) Pyramidal layer, (4) Inner granular layer, (5) Ganglionic layer and (6) Multiform layer.

Despite the horizontal layering, cortical regions display vertical connections that are of prime importance and take two forms: mini-columns (also called, micro-columns) with approximately $30 - 50\,\mu m$ in diameter and when activated by peripheral stimuli, it generates the macro-columns, with a diameter of approximately $0.4 - 0.5$ mm [36].

B. Neuronal Communications

1) Neuron-to-neuron Communication: Communication between neurons is performed through electrochemical synapses. Action potentials travel down the axon of the pre-synaptic cell and by the time it reaches the axon terminal, it stimulates the release of synaptic vesicles inside the synaptic cleft. These vesicles contain neurotransmitters that bind to neuro-receptors in the dendrites of the postsynaptic cell, on the other end of the synaptic cleft, either depolarizing the membrane. The depolarization starts in a potential state of approximately -65 mV and moves up to the point it reaches a threshold which is high enough to trigger the initiation of an action potential (excitatory) or polarizing the membrane even more, which in turn blocks the postsynaptic cell of firing any spikes (inhibitory) [23], [37]. In larger networks, the balance between inhibitory and excitatory connections helps in encoding information through the neuronal network [38].

After the membrane potential reaches its maximum peak of depolarization, it starts to repolarize itself towards its resting potential right after a spike is fired. The potential gets

hyperpolarized for a very short period which is known as *refractoriness* and can be subdivided into *absolute* and *relative*. During the absolute refractory period (ARP), the cell is unable to fire again regardless of how strong the stimuli are and it takes about $1-2$ ms followed by the relative refractory period (RRP) during which a cell can fire again if the applied stimulus is stronger than it was when applied at its resting state [37].

To model such a complex system, we present a simplification of the model that is used in the NEURON simulator [39] based on the compartmentalized Hodgkin-Huxley model which is one of the most biologically plausible models for computational neuroscience [40]. We adopt the same approach as the Hodgkin-Huxley due to its mathematical tractability. In this model, the cell is broken down into J equal length parts, and the spike propagation is modelled in one compartment travelling to all others (Fig. 2).

We can describe a single compartment model with the following proposed by Pospischil *et al* [41]

$$C_m \frac{\mathrm{d}V}{\mathrm{d}t} = -g_{leak}(V - E_{leak}) - I_{Na} - I_K - I_M - I_T - I_L, \quad (1)$$

where V is the membrane potential, C_m is the specific capacitance of the membrane, g_{leak} is the resting (leak) membrane conductance, E_{leak} is its reversal potential. I_{Na} and I_K are the sodium and potassium currents responsible for action potentials respectively, I_M is a slow voltage-dependent potassium current responsible for spike frequency adaptation, I_L is a high-threshold calcium current and I_T is a low-threshold calcium current. These voltage-dependent currents are variants of the same generic equation which is described as

$$I_x = g_x m^M h^H (V - E_x), \quad (2)$$

where the current I_x is expressed as the product of the synaptic conductance, g_x, activation (m) and inactivation (h) variables, respectively, and the difference between membrane potential V and the reversal potential E_x. Some ionic gates, such as Potassium, do not have inactivation variables so its activation is represented by the variable n, and described as follows

$$I_x = g_x n^N (V - E_x). \quad (3)$$

The gating of the channel is derived from the following first-order kinetic scheme

$$C \underset{\beta(\mathrm{V})}{\overset{\alpha(\mathrm{V})}{\rightleftharpoons}} O, \quad (4)$$

where O and C are the open and closed states of the gate, and $\alpha(V)$ and $\beta(V)$ are the transfer rates for each respective direction. The variables m, n and h represent the fraction of independent gates in the open state, following the conventional approach introduced by [42] and stated as

$$\frac{\mathrm{d}m}{\mathrm{d}t} = \alpha_m(V)(1 - m) - \beta_m(V)m, \quad (5)$$

$$\frac{\mathrm{d}n}{\mathrm{d}t} = \alpha_n(V)(1 - n) - \beta_n(V)n, \quad (6)$$

$$\frac{\mathrm{d}h}{\mathrm{d}t} = \alpha_h(V)(1 - h) - \beta_h(V)h. \quad (7)$$

To consider conductance-based inputs to the neuron in (1), it is necessary to add the effects from the propagation and reception of neurotransmitters from another neuron in the synaptic cleft. We present a simplified model of the synaptic input from pre-synaptic cells, in which the neurotransmitter-activated ion channels (I_{syn}) is represented as an explicitly time-dependent conductance (g_{syn}), and it is defined as [43]

$$I_{\mathrm{syn}} = g_{\mathrm{syn}} (V - E_{\mathrm{syn}}), \quad (8)$$

where the parameter E_{syn} as well as g_{syn} are used to describe the many different synapses types. E_{syn} may assume different values according to receptor types, the four major transmitters used for communication in the nervous systems are listed in Table I [43], where GABA means *gamma*-Aminobutyric acid with two different classes "A" and "B" and NMDA means N-Methyl-d-aspartic acid.

TABLE I
E_{syn} FOR DIFFERENT RECEPTORS.

Neurotransmitter	Neuroreceptor	E_{syn} (mV)
Glutamate	Non-NMDA	0
Glutamate	NMDA	0
GABA	GABA$_A$	-70
GABA	GABA$_B$	-100

Based on this, g_{syn} can be defined as through a superposition of exponentials

$$g_{\mathrm{syn}} = \sum_f \bar{g}_{\mathrm{syn}} \, \mathrm{e}^{-(t - t^{(f)})/\tau} \, H(t - t^{(f)}), \quad (9)$$

where τ is a time constant, $\bar{g}_{\mathrm{syn}}$ is the peak synaptic conductance, $t^{(f)}$ is the arrival time of a presynaptic action potential and $H(\cdot)$ is the Heaviside step function. The $t^{(f)}$ has a non-null value only when the membrane potential of the presynaptic compartment V_{pre} crosses a threshold th_{pre}, indicating a spike has occurred. This threshold-crossing mechanism for spike propagation is known as *event-based synapse* and it can be defined as

$$t^{(f)} = \begin{cases} t^{(f)}, & \text{if } V_{pre} \geq th_{pre} \\ \emptyset, & \text{otherwise.} \end{cases} \quad (10)$$

This can be thought of for each synaptic event as several neurotransmitters are released and bound to the postsynaptic terminal [44].

Extending from (1) to include a new current term that comprises of the compartments that synapses may occur, we simply added the term (8) on the right-hand side, as follows

$$C_m \frac{\mathrm{d}V}{\mathrm{d}t} = -I_{leak} - I_{Na} - I_{K_d} - I_M - I_T - I_L - I_{\mathrm{syn}}, \quad (11)$$

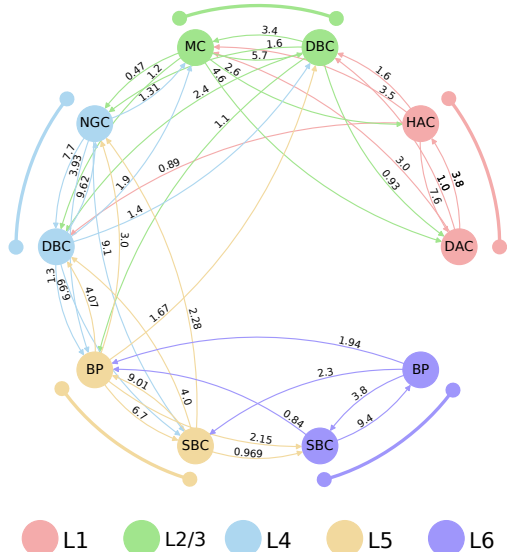where $I_{leak} = g_{leak}(V - E_{leak})$.

Fig. 3. Graphical visualization of network connectivity and each connection probability (in percentage) between pairs of neurons.

In Section II-A, we presented the differences of morpho-electrical characteristics of neurons and their columnar and laminar organization that create a variety of neuronal networks with different types of cells. To incorporate these properties into the model presented in this section we need to use three different approaches. Their morphological properties will dictate the number of compartments of a cell type, which probably indicates that pyramidal, granule and fusiform cells will have different V propagation patterns based on their different number of compartments. For example, in Fig. 2, we divided a layer 2 pyramidal neuron into 4 compartments (*stratum oriens*, *stratum pyramidale*, *stratum radiatum* and *stratum lacunosum-moleculare*). By using the NEURON simulator, we can capture morphological properties with precision through the validated models of Markram et al [35] in which compartments are already provided. In a similar manner, also using the models from [35], it is necessary to change the following parameters in order to shape the electrical characteristics and obtain a type-specific spiking activity, other than the types already available: m, n, h, $\alpha(V)$, $\beta(V)$, g_x, g_{syn}, and initial values of E_{leak} and E_{syn}. Lastly, based on the cell type, we define a network of excitatory neurons that consider the connection probabilities between them as defined in the *Neocortical Microcircuit Collaboration Portal*[1]. We use a simple directed graph to capture this network connectivity pattern, as shown in Fig. 3. Since the model presented in that portal went through a complete validation work, and since we use their models including the constrains of connection probabilities and synaptic weight, our model is in accordance to their computational approach and simulations.

[1] https://bbp.epfl.ch/nmc-portal/welcome

2) Role of the Threshold in Event-based Synapses: As aforementioned in Section II-B1, for a spike to be fired, the membrane potential of the cell compartment to reach a threshold during its depolarization state, the threshold for spike initiation varies with stimuli, cell type and the history of activity of the cell. It is not yet clear what characteristics can cause this variability which may affect the performance of the gate. According to Platkiewicz and Brette [45], even though the concept of spike threshold may be different for *in vivo*, *in vitro* and computational experiments, the threshold in brain cells depends on several parameters such as stimulus, type of cells, synaptic conductances and properties of ionic channels.

For a synapse, with each action potential arrival at the presynaptic terminal at time $t^{(f)}$, a specific number of neurotransmitters may be released into the synaptic cleft and has a probability of binding to the neuroreceptors at the postsynaptic cell. This release process is proportional to the shape and energy of the incoming action potential. An event-based synapse mimics this chemical process and sends an event with a synaptic weight to the postsynaptic cell that may trigger an action potential and consequently propagate information through the network.

To the best of our knowledge, there are no works that utilize realistic models of neurons, and especially the neuron models proposed by Markram *et al* [35], where the gates are constructed from heterogeneous neuronal arrangements and controlled by their respective threshold for event-based synapses.

III. NEURONAL DIGITAL LOGIC GATES AND CIRCUITS

In this section, we describe the construction of neuronal logic gates and how queueing theory can be applied to neuronal circuits to predict and assess how the stimuli in the pre-synaptic terminal are being processed by the post-synaptic cell.

A. Single Logic Gates

Eight neuronal logic gates were built, including five different OR gates and three different AND gates. The truth table for both of these types of gates is depicted in Table II.

TABLE II
TRUTH TABLE FOR BOTH GATE TYPES.

Truth Table			
I_1	I_2	O_{AND}	O_{OR}
0	0	0	0
0	1	0	1
1	0	0	1
1	1	1	1

For an AND gate, both inputs must be non-null to have a non-null output. On the other hand, an OR gate can send out non-null outputs not only when both inputs are active but also when either one of them is active while the other is not. All cell types used to build the gates are listed in Table III [35], [46].

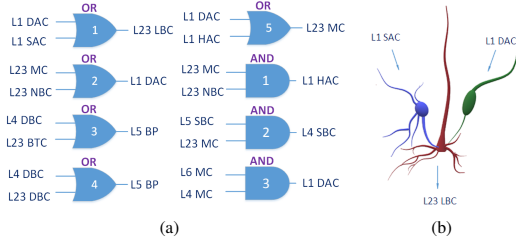| Cell Types		
L1	DAC	Descending Axon Cell
	HAC	Horizontal Axon Cell
	SAC	Small Axon Cell
L2/3	MC	Martinotti Cell
	NBC	Nest Basket Cell
	BTC	Bitufted Cell
	DBC	Double Bouquet Cell
	LBC	Large Basket Cell
L4	DBC	Double Bouquet Cell
	SBC	Small Basket Cell
	MC	Martinotti Cell
L5	BP	Bipolar Cell
	SBC	Small Basket Cell
L6	MC	Martinotti Cell

Fig. 4. Neuronal logic gates; (a) set of neuronal logic gates built using the models of neurons shown in Table III in a traditional representation and (b) potential real connection of neurons as a gate (merely illustrative).

Fig. 5. Basic simulation with inputs $[0,0]$, $[0,1]$, $[1,0]$ and $[1,1]$ for both OR and AND gates with a 10-ms time slot. Inputs 1 and 2 are the first and second rows respectively, the last row is the output.

For each gate, three different types of cells were arranged in a way that two of them should operate as the inputs of the gate and the third one as the output (Fig. 4(b)). The idea is to keep the inner connections of the gate, i.e. the connection between the inputs cells with the output cell, fixed at their default parameters and respective connection probabilities according to the type of cells being connected.

Combinations of cells (as illustrated in Fig. 4(a)) were created largely based on their respective connection probabilities. Since the synaptic weight was kept at a fixed starting value, the higher the probability of two cells establishing a synapse, the higher the influence of the pre-synaptic cell on the post-synaptic cell. In this case, OR gates should have stronger inner connections when compared to AND gates so we can achieve the desired behaviour, as presented in Table II.

In this work, a simple *On-Off Keying (OOK)* modulation is implemented where a spike is considered as a bit '1' and its absence a bit '0' in each time slot (usually 5 ms long) for the inputs into the synthetic gates. The example spikes that propagate along each neuron of a gate is illustrated in Fig. 5. When reproducing a $[1,1]$ input with both L1-HAC and L1-DAC cells (Fig. 5 left side), the spikes should arrive at L23-MC with a minimum amount of time shift between the spikes to avoid misprocessing of the inputs by the output cell.

B. Queuing Theory in Neuronal Circuits

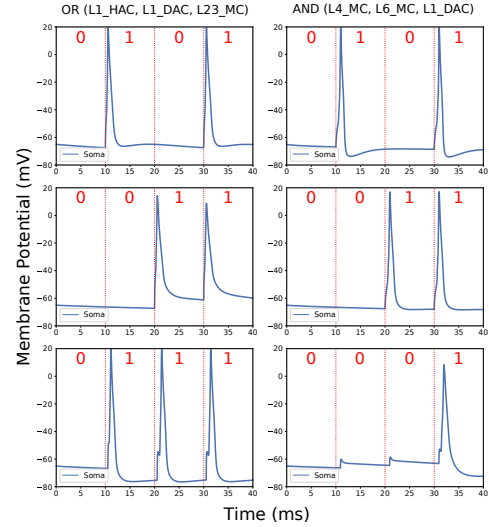Queueing theory is applied in our analysis to evaluate the response time and accuracy of the proposed neuronal logic gates. When looking into the times of arrival of spikes, in other words, considering only the electrical behaviour of an electrochemical synapse, even though there are two inputs, we assume that there is only one queue at the server in which the inputs arrive at a unified rate. At any given moment, only one impulse is carried by the cell and any impulse coming at a rate higher than the service rate may be lost, otherwise, the cell may be able to carry the stimulus and fire again if the input is strong enough to trigger an action potential. The server utilization over a certain period, however, depends on the rate of the impulse arrival to the presynaptic terminal.

1) Queueing Analysis: Consider three neuronal cells arranged as a gate, as illustrated in Fig. 4(b), in which two of them are inputs 1 and 2, respectively, and the third cell is the output. We assume that inputs 1 and 2 have *poissonic* rates of λ_1 and λ_2 spikes per second, respectively, and the output cell "processes" those inputs with a rate of μ spikes per second.

Let's also consider that each input has an individual inter-spike interval, ΔI_1 and ΔI_2, and an inter-neuronal spike interval between both inputs, ΔI_N. It is safe to assume that from the perspective of the output cell, the inputs have a merged rate, λ, defined as [47]

$$\lambda = \lambda_1 + \lambda_2, \qquad (12)$$

which means that there is only one input with rate λ and, analogously, ΔI_N as a unified inter-spike interval. In other words, inputs arrive at time $t^{(f)} + k \cdot \Delta I_N$, as depicted in (10), where k is a zero-indexed order of arrival.

The system now looks like a single-queue and single-server (Fig. 6). However, if $\mu < \lambda$, there will be no waiting time and, any spike that is not processed on a first come first serve basis, will be lost.
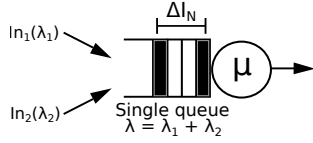
Fig. 6. Illustration of merged rates of pre-synpatic spikes into a single queue to be processed by a single server as described in Section III-B1. ΔI_N may have different values for OR and AND gates.

In the case of an OR gate, the output cell should fire when either of the inputs or even both of them fire, hence

$$\Delta I_{1,2} \geq 2 \cdot \Delta I_N, \tag{13}$$

on the other hand, a cell working as an AND gate should fire only when both inputs fire together. So

$$\Delta I_{1,2} \leq Rp + \Delta I_N. \tag{14}$$

where Rp is the refractory period of the output cell. There are different rules for the value of ΔI_N when either input fires (OR gate) or both inputs fire (both gates), thus

$$\begin{cases} \Delta I_N \geq Rp, & \text{either input fires,} \\ 0 \leq \Delta I_N \leq t_s, & \text{both inputs fire,} \end{cases} \tag{15}$$

where t_s is some threshold in milliseconds allowing the cell to process neighbouring spikes as $[1,1]$ input.

If an input arrives with time $t^{(f)}$ (9), then the probability of another input arriving **before** $t^{(f)} + t_s$ is

$$P(1|[t^{(f)}, t^{(f)} + t_s]) = 1 - e^{-\lambda t_s} \tag{16}$$

where for an AND gate, the smaller the t_s, the better to evoke a spike in the output. In the case of an OR gate, we are also interested in another input arriving **after** $t^{(f)} + t_s$, which will transform into

$$P(1|[t^{(f)}, t^{(f)} + t_s]) = e^{-\lambda t_s} \tag{17}$$

Using both (16) and (17) and by setting a probability threshold for the reconstruction of the queue, it is possible to predict the output of the server with server rate μ which is based on the type of gate and the rate λ and then calculate the accuracy in relation to the expected output in which both inputs are known. This accuracy should be compared to the approach for calculating the difference between the actual output of the gate and the expected output. The model is further validated in Section VI-A, where we employ the Mean Squared Error (MSE) analysis.

IV. IONIC CONCENTRATION DYNAMICS ON SEIZURE-LIKE EVENTS

Modelling of neurodegenerative diseases is a hot topic under the area of computational pathology. Many models have been proposed with great advancements on their validation through wet-lab experiments [48]–[50]. They generally are based on different modelling approaches. However, approximations of their neural activity can be relied on conventional approaches

to not particularly describe the disease but to quantify the impact of it on the general biological system functions [51].

The Hodgkin-Huxley equations, used in our modelling, make the reasonable assumption that intra- and extracellular ion concentrations of sodium and potassium are constant although it is not clear yet how valid this assumption can be for other cases. In mammalian brains, typical ionic currents may have a higher impact on ion concentrations because the neurons are small and the networks are very dense [52]. By looking at their dynamics, one can regulate the spiking rates obtained by the conventional Hodgkin-Huxley model and mimic both the normal and seizure-like neural activity.

Several types of epilepsy have been implicated with deficiencies in extracellular potassium ($[K]_o$) regulation. In order to take into account the effects of ion accumulation and regulation, let's first present the reversal potential E_x (Section II-B, Equations (2) and (3)) in terms of the instantaneous intra- and extracellular ion concentrations

$$E_{Na} = 26.64 \cdot \ln\left(\frac{[Na]_o}{[Na]_i}\right), \tag{18}$$

$$E_K = 26.64 \cdot \ln\left(\frac{[K]_o}{[K]_i}\right). \tag{19}$$

where E_{Na} and E_K are the reversal potential of the Sodium and Potassium channels respectively.

The dynamics of the concentration of extracellular potassium and intracellular sodium ions are given by

$$\tau \frac{d[K]_o}{dt} = \gamma\beta I_K - 2\beta\tilde{I}_{\text{pump}} - \tilde{I}_{\text{glia}} - \tilde{I}_{\text{diff}}, \tag{20}$$

$$\tau \frac{[Na]_i}{dt} = -\gamma I_{Na} - 3\tilde{I}_{\text{pump}}, \tag{21}$$

where the concentrations are in mM, $\tau = 10^3$ balances the time units, $\gamma = 4.45 \times 10^{-2}$ is a factor that converts the membrane currents into mM/s, $\beta = 7$ is the ratio of intracellular to extracellular volume and I_K and I_{Na} refer to the ionic currents first described in Equations 2 and 3. The pump, glia and diffusion molar currents (also measured in mM/s) are given by

$$\tilde{I}_{\text{pump}} = \rho \left(\frac{1}{1 + e^{(8.33 - 0.33[Na]_i)}}\right) \cdot \left(\frac{1}{1 + e^{(5.5 - [K]_o)}}\right), \tag{22}$$

$$\tilde{I}_{\text{glia}} = G \left(1 + e^{(7.2 - 0.4[K]_o)}\right)^{-1}, \tag{23}$$

$$\tilde{I}_{\text{diff}} = \varepsilon([K]_o - k_{\text{bath}}), \tag{24}$$

where the default parameters are set as $\rho = 1.25$ mM/s, $G = 66.666$ mM/s, and $\varepsilon = 1.333$ Hz and $k_{\text{bath}} = 4$ mM represents the potassium concentration in the reservoir. The intracellular potassium ($[K]_i$) and extracellular sodium ($[Na]_o$) concentrations are obtained as

$$[K]_i = 140 \text{ mM} + (18 \text{ mM} - [Na]_i), \tag{25}$$

$$[Na]_o = 144 \text{ mM} - \beta([Na]_i - 18 \text{ mM}), \qquad (26)$$

where it is assumed the total amount of sodium is conserved, sodium is transported across the membrane predominantly through sodium membrane current and there is a relation between the transport of both sodium and potassium [52].

V. SIMULATION MODEL

In this section, the simulation model for a single neuronal logic gate as well as the application case-study scenario for the suppression of epilepsy, are presented.

A. Single Gate

The single neuronal logic gates were simulated in two ways. First, they were individually analyzed and simulated in isolation, where their respective accuracy values were evaluated and those results were fitted to the model described in Section III-B1. In isolated form, their configuration is illustrated in Fig. 4(b).

For all simulations, intrinsic parameters of the cell were kept at their default values (such as the length and diameter of each compartment of the cell), and all other parameters of the simulator required to reproduce the desired behaviour are shown in Table IV, where synaptic weight influences the spiking behaviour of one neuron has on another through either exciting or inhibiting the post-synaptic cell by setting to positive or negative values respectively; the time slot for sampling the spike train is set to 5 ms as a fair amount of time to account for absolute and relative refractory periods [37]; the *noise* object is set to 1 to mimic a *Poisson* firing; *tau* is the decay time constant of the synapse; *threshold* accounts for the detection of a synaptic event as described in Section II-B; *delay* is the time between source crossing *threshold* and delivery event to target; the threshold for spike detection is used to sample the spike trains into bits where any potential higher than 0 mV in a specific time slot is a bit "1". The values of Rp and t_s are only used when simulating the queue model and they are not part of the simulation of the network.

TABLE IV
PARAMETERS FOR SIMULATION.

Simulation Parameters	
Synaptic weight	0.04 μS
Simulation time	1 s
Time slot	5 ms
NetStim.noise	1
ExpSyn.tau	2
NetCon.threshold (AND)	-64 mV
NetCon.threshold (OR)	5 mV
NetCon.delay	0
Threshold (spike detection)	0 mV
Rp	5 ms
t_s	0 ms

1) Accuracy: All gates were tested in terms of accuracy with variations in a few parameters to test their performance. These parameters include their firing rate, λ, and the synaptic threshold, th. As mentioned earlier in Section III-A, we are using an OOK modulation to discretize the spiking activity into binary code. Action potentials can shift and get slightly delayed during propagation, and this is due to axonal characteristics. This emphasizes the importance of having a time slot with a fair length of time so there is a fair distinction between different input combinations. The accuracy will measure how correct the bit train is from the output cell with regards to the ideal output that would be generated by an error-free logic gate. In the simulations, random spike trains following a *Poisson* process were stimulated. *Poisson* process usually provides good approximations of the randomness of spike trains across several trials [53]. For each simulation, since the input is random, the number of spikes fired between both inputs with the same rate is approximately the same.

The accuracy is calculated according to the following equation [54]:

$$A(E[Y]; Y) = \frac{P_{1,1} + P_{0,0}}{P_{1,1} + P_{1,0} + P_{0,1} + P_{0,0}} \qquad (27)$$

where $P_{Y,E[Y]}$ is the probability of Y given $E[Y]$ in which Y is the actual output and $E[Y]$ is the expected one and $Y \& E[Y] \in \{0, 1\}$. $P_{Y,E[Y]}$ can be analogously defined as the conditional probabilities in a binary symmetric channels (BSC). Hence, $P_{0,0} = 1 - P_{1,0}$, and $P_{0,1} = 1 - P_{1,1}$. We can calculate $P_{1,1}$, for example, basically by counting the number of bits there are for each input-output combination, for example, the number of times bit 1 was sent and bit 1 was received ($\#B_{1,1}$) and, also, bit 1 was sent and bit 0 was received ($\#B_{0,1}$), then $P_{1,1} = \#B_{1,1}/(\#B_{1,1} + \#B_{0,1})$.

It is expected that the threshold for a synaptic event will impact the accuracy results. As stated in Section II-B, the threshold of the cell for initiation of an action potential is dynamic and besides the synaptic events arriving at its pre-synaptic terminals, morphological and electrical characteristics of the cell also play a role as well as the rate with which these events arrive. This means that a small change in the way a post-synaptic neuron detects an input triggers changes in other processes that affect the depolarization of its membrane. This can lead to low accuracy results where false positive or false negative results emerge affecting the system reliability.

2) Mean Squared Error (MSE): To validate the model proposed in Section III-B, we estimated how far away from our predictions were from the values of accuracy by using *Mean Squared Error*. MSE is a way to measure the quality of an estimator, and in our case, we want to determine the effectiveness of our model concerning the real accuracy of the gate operation.

Consider that A is the actual accuracy obtained from the real output and that $\overline{A}$ is the predicted accuracy estimated by our model, then the MSE for each point can be calculated as

$$MSE = \frac{1}{a} \sum_{i=1}^{a} (A_i - \overline{A}_i)^2, \qquad (28)$$

where a is the number of accuracy values. The value of a is the bandwidth of the spiking activity or the number of different frequencies with which the simulation is performed.

B. Neuronal Activity Behavior During Epileptic Seizures

Neuronal synchronization is the basis for fundamental brain processes. In neurological diseases, such as epilepsy, neuronal synchronicity, as well as the balance between excitation and inhibition in populations of cortical neurons, can be modified [55], [56].

In this work, a study on brain seizures is conducted by simulating the activity of neurons grouped in a cortical column and by reproducing the stages of spikes before, during, after, and recovery periods of epileptic seizures with a dynamic firing rate. The frequencies for stimulation varies according to results published by Alvarado-Rojas *et al* [55]. In a simulation with time $T = 1000$ ms, the ranges of the firing rate γ (spikes/s) for the various stages of the epileptic seizure in the network are based on the following values

$$\gamma = \begin{cases} 10 - 30, & \text{if } T \leq 300, \\ 10 - 70, & \text{if } 300 < T \leq 650, \\ 70 - 180, & \text{if } 650 < T \leq 750, \\ 0 - 10, & \text{if } T > 750, \end{cases} \quad (29)$$

where the evoked activity of the network also follows a *Poisson* process. This procedure can also be described with the pseudo-code presented in Algorithm 1.

Algorithm 1 Development of Epileptic Seizure Model

1: **Inputs:**
   $\gamma = \{30, 70, 180, 10\}$
   $T = \{0, 300, 650, 750, 1000\}$
2: **Initialize:**
   $\mathcal{C} = \{c_1, ..., c_n\}$
3: **for** $c \in \mathcal{C}$ **do**
4:   **for** $i : 0 \rightarrow \text{length}(\gamma)$ **do**
5:     stimulate c at $(\gamma_i, [T_i, T_{i+1}])$
6:   **end for**
7: **end for**

Neuronal AND logic gates were inserted inside a network with 10 neurons (two neurons per cortical layer) which was built as a simpler model of a cortical micro-column to help evaluate the effects of logic gates inside a neuronal network that simulated different stages of an epileptic seizure. The positioning of the gates between cortical layers is depicted in Fig. 7.

VI. RESULTS AND DISCUSSIONS

In this section, we present a discussion over the results for the logic gate analysis and its epilepsy case study.

A. Logic Gate Performance

For the single gate performance accuracy, we use the configurations that are presented in Fig. 4(a). In the simulations with isolated gates, two different analyses were performed.
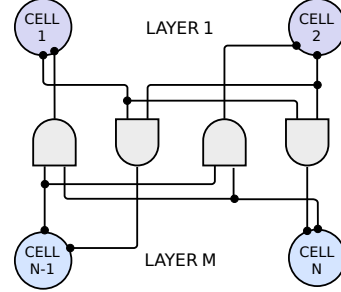

Fig. 7. Schematic of the connection of the neuronal logic gates in between the N cells that forms the network with M layers. In this work $N = 10$ and $M = 5$ where there are N/M cells per layer. The placement of a logic gate in the network require the breakage of the natural connections between the cells.

First, the spiking rate was increased and the accuracy of the gates were computed, and the simulations used the parameters shown in Table IV. In both Figs. 8(a) and 8(b), the accuracy decreases as the firing rate increases, but they are decreasing at different rates due to their different behaviours as shown in Table II and Fig. 5. Even though the different versions of both types of gates have very similar values of accuracy, in Fig. 8(a) all of the AND gates configurations have very similar behaviour, this may be due to the fact that, as depicted in Table II, there is only one way for the gate to fire which decreases the chances of misprocessing the inputs. Meanwhile, since OR gates have more ways of firing an output (Table II), the different arrangements may be affecting the processing of the inputs by the output considering that the gates have a bit less similar performance between each other when compared to the performance of AND gates. Fig. 8(b) shows that OR 2 slightly stands out in performance with better accuracy compared to the other OR gates. To obtain the mean and standard deviation, the simulation ran five times.

Second, two gates were picked out, one of each type (OR2 because it showed a better accuracy in Fig. 8(b) and, AND1 was actually picked at random since all AND gates have a similar performance), and the accuracy was computed based on both the accuracy and the threshold at the presynaptic compartment. In Fig. 9, it is noticeable that the accuracy has a relationship with the threshold, th_{pre} in (10), and spiking rate of the neurons, $\lambda_{1,2}$ in (12). As previously discussed, it is expected that event-based thresholds impact the accuracy results of the logic gates. Since the threshold for initiation of an action potential of biological neurons is dynamic, and not static as some artificial models of neurons, the spiking rate is also considered as dynamic since the synaptic events arriving at a postsynaptic cell, morphological and electrical characteristics of the cell also play a role [45]. Generally speaking, lower spiking rates with higher thresholds negatively affects the accuracy of both types of gates. The results presented are based on the mean from three simulation runs.

The effect of shifting the synchronization of the spikes by up to 4 ms was also analyzed. The results, depicted in Table V, did not show any specific trend when the shift was

TABLE V
ACCURACY MEAN AND STANDARD DEVIATION VALUES FOR DIFFERENT DELAYS BETWEEN INPUTS.

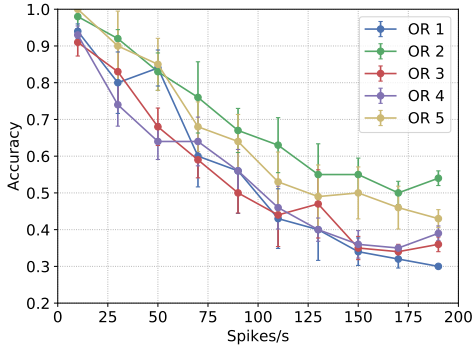|	Effect of Delay on Accuracy							
Types	AND 1	AND 2	AND 3	OR 1	OR 2	OR 3	OR 4	OR 5
Mean	0.9660	0.9530	0.9954	0.7595	0.8595	0.7630	0.7615	0.7720
Std Dev	0.00577	0.00604	0.00603	0.02871	0.02752	0.03059	0.03405	0.03039

(a)

(a)

(b)
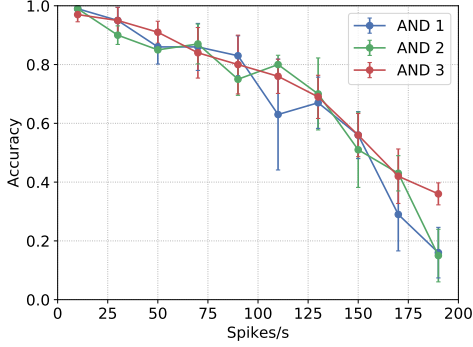
(b)

Fig. 8. Mean and standard deviation of the accuracy for the (a) three AND gates and (b) five OR gates. Five simulations were performed for each rate and the firing of the spikes follows a *Poisson* process.
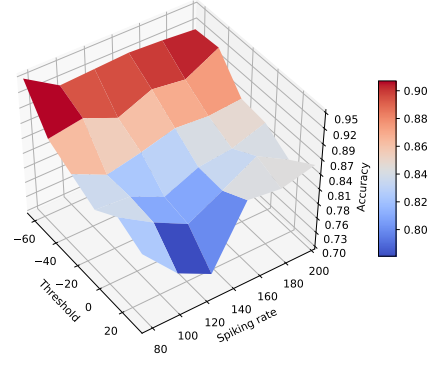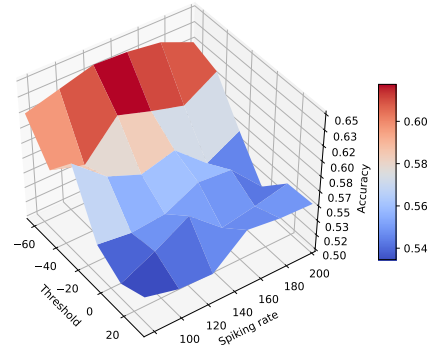
Fig. 9. Spiking rate λ, threshold th and mean accuracy Acc for gates (a) AND1 and (b) OR2.

increased. For the AND gates, the accuracy remained above 95%, which represent a difference of at least 9% concerning OR gates where the highest performance is approximately 86%. The highest standard deviation for an AND gate is still over 50 times smaller than the highest value for an OR gate, as aforementioned, this may be due to their different gating behaviours.

The prediction model was analyzed in relation to ΔI_N and its performance is presented for two gates *AND1* (Fig. 10(a)) and *OR2* (Fig. 10(b)). These accuracy values were calculated with a five-millisecond time slot for the discretization analysis of the output cells. The other performances were omitted to avoid redundancy but MSE values are presented in Fig. 11 for all of the eight built gates. The results presented in Fig. 10

shows that for the AND gates, the model results in slightly higher accuracy compared to the OR gate. This difference between types of gates reveals itself for the other six gates, four of the OR type and two of the AND type.

In Fig. 11, the sampling frequency was changed to evaluate how the shift among bits from both inputs affect the results of our model in comparison with the real firing of the gates.

Figs. 11(a)-11(c) shows the MSE for AND gates with ΔI_N equal to 1, 3, and 5 ms respectively. On the other hand, Figs. 11(d)-11(f) show results for the same analysis but OR gates. In both scenarios, the best MSE was for a time slot with a length of 1 ms, even though an action potential takes a longer period than the firing as well as the duration to pass the absolute refractory period. For all gate models, the MSE
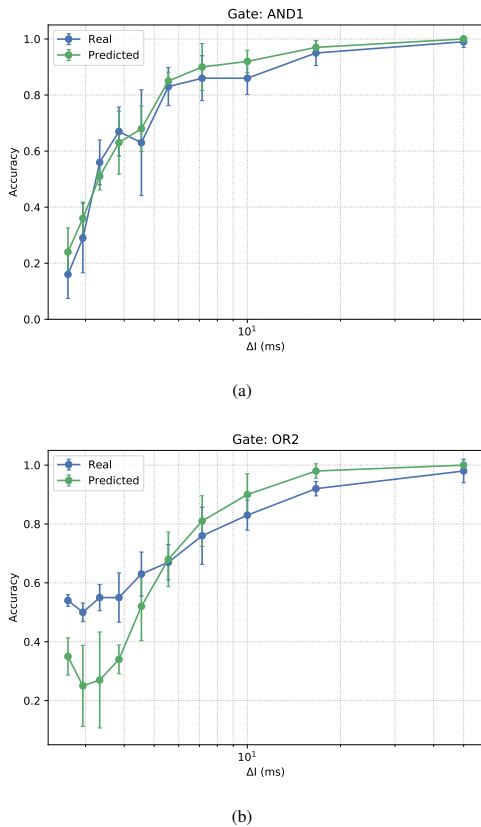
(a)

(b)

Fig. 10. Real and predicted mean and standard deviation of the accuracy for an (a) AND gate type 1 and (b) OR gate type 2 in relation to the ISI. Predicted results obtained from the implementation of the model proposed in Section III-B1.

is quite low showing the robustness of developing gates from the various types of neurons. The changes in the curves can be explained as a result of the influence of different types of gates, the variety of morphological types of cells that compose a gate and to the sampling frequency of spike trains during numerical analysis.

B. Epilepsy Case Study

When simulating a network of cells susceptible to epileptic seizures, the analysis was performed in both cases (with and without logic gates within the network). Only one type of AND gate was used in random positions within the network (as illustrated in Fig. 7) that is composed of L23-MC, L23-NBC and L1-HAC cells. The placement of the AND gates was chosen at random and we start placing the gates inside the network at regions with high connections to other cells.

Fig. 12 shows the effect of increasing or decreasing the intensity of an ionic current while the other is kept constant with their initial value. This specific simulation based on the model presented in Section IV was performed with a

single Hodgkin-Huxley compartment during 400 ms while an external current (10 μA/cm^2) is injected into the compartment in between 100 and 300 ms. The goal of an external stimulus is to evaluate whether there was any spontaneous spike evoked during the simulation. As we can observe, the dynamics between the K and Na influences the spiking rate of the neurons. Based on this, we can replicate the different seizure-like events that are described in Equation (29) with the appropriate ion values.

Figure 13(b) shows how placing a higher number of gates inside the network may help filter out high frequencies of firing by decreasing the average firing rate of the network. This effect is visually shown in Fig. 13(a), where during the seizure, which is possible to generate by manipulating I_K and I_{Na} (Fig. 12), the entire network resulted in lower levels of activity with 16 gates in comparison with the network that did not contain any gates.

VII. CONCLUSION

Even though around 50 million people worldwide suffer from Epilepsy, it is estimated that 10% of the world population will have a seizure during their lifetime without even being an epileptic person. In this paper, the performance of neuronal logic gates was presented as isolated units and their positive effect by smoothing out the high-frequency firing activity of several brain cells that occur during seizures. This approach requires that the cells involved in the gating process should be synthetically engineered and strategically positioned depending on the network connectivity to improve results.

Part of this work included a proposed model based on queue theory concepts that can predict how accurate a specific gating unit can be based on the input and threshold of the output cell. The model showed, in the worst scenario, for OR gates, an MSE of 0.025 while for AND gates this value is of 0.006. The results also show that the sampling frequency of the spike train plays a role in the accuracy of the gates and the quality of the model.

Although this paper only concentrated on the treatment of seizures in the brain, logic gates can also be applied for the encoding of information and have the potential to use synthetic biology to create medical bio nano-machines to improve the quality of life of people with neurodegenerative diseases and enhanced information processing inside the brain.

REFERENCES

[1] T. Nakano, "Molecular communication: A 10 year retrospective," *IEEE Transactions on Molecular, Biological and Multi-Scale Communications*, vol. 3, no. 2, pp. 71–78, June 2017.

[2] I. F. Akyildiz, M. Pierobon, S. Balasubramaniam, and Y. Koucheryavy, "The internet of bio-nano things," *IEEE Communications Magazine*, vol. 53, no. 3, pp. 32–40, 2015.

[3] L. Felicetti, M. Femminella, G. Reali, P. Gresele, M. Malvestiti, and J. N. Daigle, "Modeling CD40-Based Molecular Communications in Blood Vessels," *IEEE Transactions on NanoBioscience*, vol. 13, no. 3, pp. 230–243, Sep. 2014.

[4] L. Felicetti, M. Femminella, G. Reali, and P. Liò, "Applications of molecular communications to medicine: A survey," *Nano Communication Networks*, vol. 7, pp. 27 – 45, 2016.

[5] E. Balevi and O. B. Akan, "A Physical Channel Model for Nanoscale Neuro-Spike Communications," *IEEE Transactions on Communications*, vol. 61, no. 3, pp. 1178–1187, March 2013.

(a) 1 ms.

(b) 3 ms.
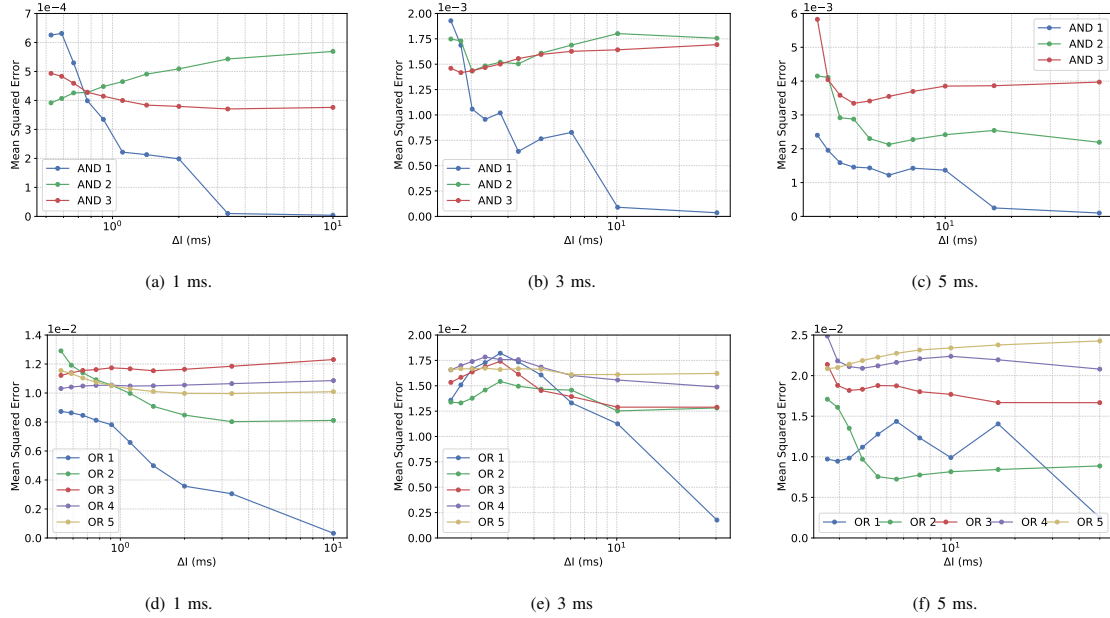
(c) 5 ms.

(d) 1 ms.

(e) 3 ms

(f) 5 ms.

Fig. 11. Mean Squared Error between the predicted accuracy by the model described in Section III-B1 and accuracy calculated with real output. Spike trains were sampled at different time slots. Figures 11(a), 11(b) and 11(c) show the MSE for all AND gates and Figures 11(d), 11(e) and 11(f) show the MSE for all OR gates.
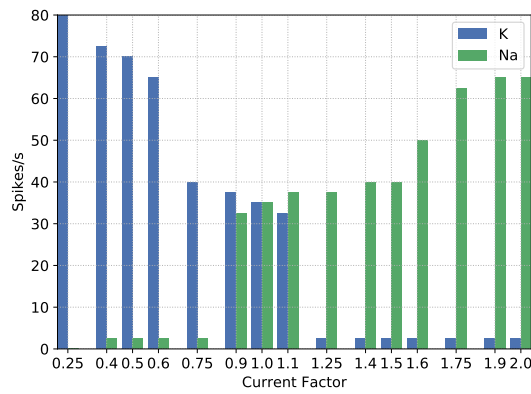

Fig. 12. The effect of multiplying the current factor to the ionic currents. When analyzing I_K, I_{Na} was kept at their default operation, and vice-versa. It is noticeable how the firing rate increases to values within the range presented in Eq. (29) with the increase of the intensity of ionic currents.

[6] S. Thorpe, A. Delorme, and R. V. Rullen, "Spike-based strategies for rapid processing," *Neural Networks*, vol. 14, no. 6, pp. 715 – 725, 2001.

[7] F. Zeldenrust, W. J. Wadman, and B. Englitz, "Neural Coding With Bursts – Current State and Future Perspectives," *Frontiers in Computational Neuroscience*, vol. 12, p. 48, 2018.

[8] G. L. Adonias, M. T. Barros, L. Doyle, and S. Balasubramaniam, "Utilising EEG Signals for Modulating Neural Molecular Communications," in *5th ACM International Conference on Nanoscale Computing and Communication 2018 (ACM NanoCom'18)*, Reykjavik, Iceland, Sep.

2018.

[9] C. P. Billimoria, R. A. DiCaprio, J. T. Birmingham, L. F. Abbott, and E. Marder, "Neuromodulation of spike-timing precision in sensory neurons," *Journal of Neuroscience*, vol. 26, no. 22, pp. 5910–5919, 2006.

[10] G.-S. Yi, J. Wang, X.-L. Wei, K.-M. Tsang, W.-L. Chan, and B. Deng, "Neuronal spike initiation modulated by extracellular electric fields," *PLOS ONE*, vol. 9, no. 5, pp. 1–10, 05 2014.

[11] J. Choe, B. A. Coffman, D. T. Bergstedt, M. D. Ziegler, and M. E. Phillips, "Transcranial Direct Current Stimulation Modulates Neuronal Activity and Learning in Pilot Training," *Frontiers in Human Neuroscience*, vol. 10, p. 34, 2016.

[12] C. Agustín-Pavón and M. Isalan, "Synthetic biology and therapeutic strategies for the degenerating brain," *BioEssays*, vol. 36, no. 10, pp. 979–990, 2014.

[13] W. S. McCulloch and W. Pitts, "A logical calculus of the ideas immanent in nervous activity," *The bulletin of mathematical biophysics*, vol. 5, no. 4, pp. 115–133, Dec 1943.

[14] A. Goldental, S. Guberman, R. Vardi, and I. Kanter, "A computational paradigm for dynamic logic-gates in neuronal activity," *Frontiers in Computational Neuroscience*, vol. 8, p. 52, 2014.

[15] J. Larouche and C. A. Aguilar, "New technologies to enhance in vivo reprogramming for regenerative medicine," *Trends in biotechnology*, 2018.

[16] T. Miyamoto, S. Razavi, R. DeRose, and T. Inoue, "Synthesizing Biomolecule-Based Boolean Logic Gates," *ACS Synthetic Biology*, vol. 2, no. 2, pp. 72–82, 2013, pMID: 23526588.

[17] T. P. Vogels and L. F. Abbott, "Signal propagation and logic gating in networks of integrate-and-fire neurons," *Journal of Neuroscience*, vol. 25, no. 46, pp. 10 786–10 795, 2005.

[18] T. Song, P. Zheng, M. D. Wong, and X. Wang, "Design of logic gates using spiking neural p systems with homogeneous neurons and astrocytes-like control," *Information Sciences*, vol. 372, pp. 380 – 391, 2016.

[19] S. A. Benner and A. M. Sismour, "Synthetic biology," *Nature Reviews Genetics*, vol. 6, no. 7, pp. 533–543, 2005.

[20] M. J. Smanski, H. Zhou, J. Claesen, B. Shen, M. A. Fischbach, and C. A. Voigt, "Synthetic biology to access and expand nature's chemical
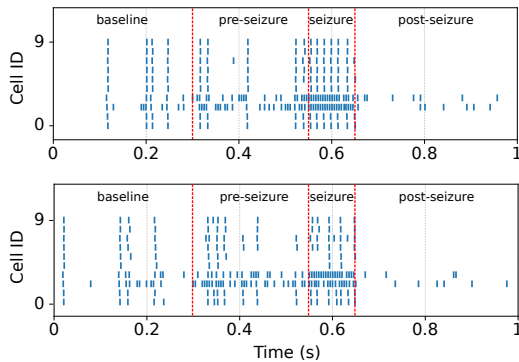
(a) Zero (top) and 16 (bottom) gates in the network.
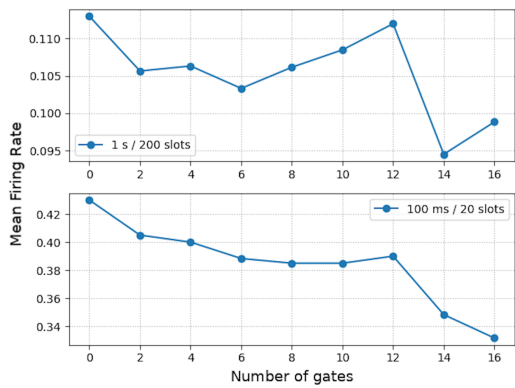
(b) Mean firing rate of the network.

Fig. 13. Simulation of epileptic seizures in a network with 10 neurons (2 neurons per cortical layer), stimulation performed in cells at layer 2/3. (a) Raster plot of the network with no gates inserted and natural connections only (top) as illustrated in Fig. 3; and raster plot of the network with 16 neuronal logic gates (bottom), natural connections are broken where gates are placed as depicted in Fig. 7; (b) Mean firing rate in the network as more and more gates are placed within it; top graph shows the firing rate of the whole network for all stages as shown in Fig. 13(a); bottom graph shows the firing rate for the whole network but only for the seizure stage.

diversity," *Nature Reviews Microbiology*, vol. 14, p. 135, Feb 2016, review Article.

[21] F. Lienert, J. J. Lohmueller, A. Garg, and P. A. Silver, "Synthetic biology in mammalian cells: next generation research tools and therapeutics," *Nature Reviews Molecular Cell Biology*, vol. 15, no. 2, pp. 95–107, 2014.

[22] I. F. Akyildiz, F. Brunetti, and C. Blázquez, "Nanonetworks: A new communication paradigm," *Computer Networks*, vol. 52, no. 12, pp. 2260–2279, 2008.

[23] G. L. Adonias, A. Yastrebova, M. T. Barros, S. Balasubramaniam, and Y. Koucheryavy, "A Logic Gate Model based on Neuronal Molecular Communication Engineering," in *Proceedings of the 4th Workshop on Molecular Communications*, Linz, Austria, Apr. 2019.

[24] J. Hasty, D. McMillen, and J. J. Collins, "Engineered gene circuits," *Nature*, vol. 420, no. 6912, p. 224, 2002.

[25] D. Morse and P. Sassone-Corsi, "Time after time: inputs to and outputs from the mammalian circadian oscillators," *Trends in neurosciences*, vol. 25, no. 12, pp. 632–637, 2002.

[26] R.-S. Wang, A. Saadatpour, and R. Albert, "Boolean modeling in systems biology: an overview of methodology and applications," *Physical Biology*, vol. 9, no. 5, p. 055001, sep 2012.

[27] W. Hao and A. Friedman, "Mathematical model on Alzheimer's disease," *BMC Systems Biology*, vol. 10, no. 1, p. 108, 2016.

[28] S. Bakshi, V. Chelliah, C. Chen, and P. H. van der Graaf, "Mathematical Biology Models of Parkinson's Disease," *CPT: Pharmacometrics & Systems Pharmacology*, vol. 8, no. 2, pp. 77–86, 2019.

[29] F. Fröhlich, M. Bazhenov, V. Iragui-Madoz, and T. J. Sejnowski, "Potassium dynamics in the epileptic cortex: New insights on an old topic," *The Neuroscientist*, vol. 14, no. 5, pp. 422–433, 2008, pMID: 18997121.

[30] A. Morano, L. Iannone, C. Palleria, M. Fanella, A. T. Giallonardo, G. De Sarro, E. Russo, and C. Di Bonaventura, "Pharmacology of new and developing intravenous therapies for the management of seizures and epilepsy," *Expert opinion on pharmacotherapy*, vol. 20, no. 1, pp. 25–39, 2019.

[31] M. C. Li and M. J. Cook, "Deep brain stimulation for drug-resistant epilepsy," *Epilepsia*, vol. 59, no. 2, pp. 273–290, 2018.

[32] V. K. Jirsa, W. C. Stacey, P. P. Quilichini, A. I. Ivanov, and C. Bernard, "On the nature of seizure dynamics," *Brain*, vol. 137, no. 8, pp. 2210–2230, 06 2014.

[33] Y.-C. Chen *et al.*, "A NeuroD1 AAV-Based Gene Therapy for Functional Brain Repair after Ischemic Injury through In Vivo Astrocyte-to-Neuron Conversion," *Molecular Therapy*, 2019.

[34] C.-Y. Lin *et al.*, "Non-invasive, neuron-specific gene therapy by focused ultrasound-induced blood-brain barrier opening in Parkinson's disease mouse model," *Journal of Controlled Release*, vol. 235, pp. 72 – 81, 2016.

[35] H. Markram *et al.*, "Reconstruction and Simulation of Neocortical Microcircuitry," *Cell*, vol. 163, no. 2, pp. 456–492, 2015.

[36] A. Peters, "The morphology of minicolumns," in *The neurochemical basis of autism*. Springer, 2010, pp. 45–68.

[37] A. Mishra and S. K. Majhi, "A comprehensive survey of recent developments in neuronal communication and computational neuroscience," *Journal of Industrial Information Integration*, vol. 13, pp. 40 – 54, 2019.

[38] S. Zhou and Y. Yu, "Synaptic E-I Balance Underlies Efficient Neural Coding," *Frontiers in Neuroscience*, vol. 12, p. 46, 2018.

[39] N. T. Carnevale and M. L. Hines, *The NEURON Book*, 1st ed. New York, NY, USA: Cambridge University Press, 2009.

[40] L. Long and G. Fang, *A Review of Biologically Plausible Neuron Models for Spiking Neural Networks*. America Institute of Aeronautics and Astronautics, 2010.

[41] M. Pospischil, M. Toledo-Rodriguez, C. Monier, Z. Piwkowska, T. Bal, Y. Frégnac, H. Markram, and A. Destexhe, "Minimal hodgkin–huxley type models for different classes of cortical and thalamic neurons," *Biological cybernetics*, vol. 99, no. 4-5, pp. 427–441, 2008.

[42] A. L. Hodgkin and A. F. Huxley, "A quantitative description of membrane current and its application to conduction and excitation in nerve," *The Journal of physiology*, vol. 117, no. 4, pp. 500–544, 1952.

[43] C. Koch, *Biophysics of computation: information processing in single neurons*. Oxford university press, 2004.

[44] I. F. Akyildiz, M. Pierobon, and S. Balasubramaniam, "An Information Theoretic Framework to Analyze Molecular Communication Systems Based on Statistical Mechanics," *Proceedings of the IEEE*, vol. 107, no. 7, pp. 1230–1255, July 2019.

[45] J. Platkiewicz and R. Brette, "A Threshold Equation for Action Potential Initiation," *PLOS Computational Biology*, vol. 6, no. 7, pp. 1–16, 07 2010.

[46] H. Markram, M. Toledo-Rodriguez, Y. Wang, A. Gupta, G. Silberberg, and C. Wu, "Interneurons of the neocortical inhibitory system," *Nature Reviews Neuroscience*, vol. 5, no. 10, pp. 793–807, 2004.

[47] R. Cowan, "The uncontrolled traffic merge," *Journal of Applied Probability*, vol. 16, no. 2, p. 384–392, 1979.

[48] E. Toivari, T. Manninen, A. K. Nahata, T. O. Jalonen, and M.-L. Linne, "Effects of transmitters and amyloid-beta peptide on calcium signals in rat cortical astrocytes: Fura-2am measurements and stochastic model simulations," *PloS one*, vol. 6, no. 3, p. e17914, 2011.

[49] M. T. Barros, W. Silva, and C. D. M. Regis, "The multi-scale impact of the alzheimer's disease on the topology diversity of astrocytes molecular communications nanonetworks," *IEEE Access*, vol. 6, pp. 78 904–78 917, 2018.

[50] D. Reato, M. Cammarota, L. C. Parra, and G. Carmignoto, "Computational model of neuron-astrocyte interactions during focal seizure generation," *Frontiers in computational neuroscience*, vol. 6, p. 81, 2012.

[51] J. C. Wooley, H. S. Lin, N. R. Council *et al.*, "Computational modeling and simulation as enablers for biological discovery," in *Catalyzing inquiry at the interface of computing and biology*. National Academies Press (US), 2005.

[52] E. Barreto and J. R. Cressman, "Ion concentration dynamics as a mechanism for neuronal bursting," *Journal of Biological Physics*, vol. 37, no. 3, pp. 361–373, Jun 2011.

[53] R. E. Kass and V. Ventura, "A Spike-Train Probability Model," *Neural Computation*, vol. 13, no. 8, pp. 1713–1720, 2001.

[54] N. Hanisch and M. Pierobon, "Digital modulation and achievable information rates of thru-body haptic communications," in *Disruptive Technologies in Sensors and Sensor Systems*, vol. 10206. International Society for Optics and Photonics, 2017, p. 1020603.

[55] C. Alvarado-Rojas, K. Lehongre, J. Bagdasaryan, A. Bragin, R. Staba, J. Engel, V. Navarro, and M. LE VAN QUYEN, "Single-unit activities during epileptic discharges in the human hippocampal formation," *Frontiers in Computational Neuroscience*, vol. 7, p. 140, 2013.

[56] J. Du, V. Vegh, and D. C. Reutens, "Small changes in synaptic gain lead to seizure-like activity in neuronal network at criticality," *Scientific Reports*, vol. 9, no. 1, p. 1097, 2019.

Yevgeni Koucheryavy received his Ph.D. degree from Tampere University of Technology in 2004. He is a professor with the Unit of Electrical Engineering, Tampere University. His current research interests include various aspects in heterogeneous wireless communication networks and systems, the Internet of Things and its standardization, and nanocommunications. He is an Associate Technical Editor for the IEEE Communications Magazine and an Editor for the IEEE Communications Surveys and Tutorials.

Geoflly L. Adonias is currently a Ph.D. student at the Telecommunications Software & Systems Group (TSSG), Waterford Institute of Technology (WIT), Ireland, under the Science Foundation Ireland (SFI) CONNECT Project for future networks and communications. He received his B.Eng. in Electrical Engineering from the Federal Institute of Education, Science and Technology of Paraíba (IFPB), Brazil, in 2017. His current research interests include Nano-scale Communications, Digital Signal Processing and Wireless Networks.

Frances Cleary is a Research Division Manager in TSSG-WIT. Her groups research thematic areas of interest include Bio-Nano Communication, Virtual & Augmented Reality and Pervasive sensing, Embedded Systems Communications. Frances has worked in multiple research roles from Project Coordinator, Business Development Manager, Technical lead and now as Research Division Manager. The research Division specifically focuses on the application of ICT technologies across the Healthcare and Transport sectors.

Anastasia Yastrebova has received her B.Sc. in the field of Information Technology and Communication Systems from the Bonch-Bruevich Saint-Petersburg State University of Telecommunications, Russia, in 2017 and M.Sc. (dist.) in Information Technology from Tampere University (former Tampere University of Technology), Finland, in 2019. She is currently Research Scientist at the Technical Research Centre of Finland, VTT Ltd. Her research interests include molecular communications, heterogeneous wireless communication networks, and next-generation communication systems.

Sasitharan Balasubramaniam (Sasi) received his Bachelors of Engineering (Electrical and Electronic) and PhD (Computer Science) degrees from the University of Queensland, Australia, in 1998 and 2005, respectively, and Masters of Engineering Science (Computer and Communication Engineering) degree in 1999 from the Queensland University of Technology, Australia. After completion of his PhD, Sasi joined the Telecommunications Software & Systems Group (TSSG), Waterford Institute of Technology, Ireland where his research focused on bio-inspired communication networks. In 2009, he successfully received the Science Foundation Ireland Starter Investigator Research Grant, which allowed him to create a Bio-Inspired Research Unit. In 2013, Sasi joined the Department of Electronics and Communication Engineering, Tampere University of Technology, Finland, where in 2014 he received the Academy of Finland Research Fellow grant. As of 2019, Sasi is the Director of Research for the TSSG, and is the Principal Investigator for the recently funded Science Foundation Ireland (SFI) VistaMilk research centre, as well as a Funded Investigator for the SFI CONNECT and SFI FutureNeuro research centres. Sasi has published over 100 journal and conference papers, and actively participates in various conference committees. He is currently the Chair of the Steering Committee for ACM NanoCom, a conference which he co-founded. He is currently an editor for the IEEE Letters of the Computer Society, Elsevier Nano Communication Networks, as well as Elsevier Digital Communication Networks journals. He was a past Associate Editor for the IEEE Internet of Things Journal. In 2018, Sasi was also the IEEE Nanotechnology Council Distinguished Lecturer. His current research interests include molecular and nano communications, terahertz communication for 6G, as well as the Internet of Nano Things. Sasi is currently an IEEE Senior Member.

Michael Taynnan Barros is currently the recipient of the Marie Skłodowska-Curie Individual Fellowship (MSCA-IF) at the BioMediTech Institute of the Tampere University, Finland. He received his Ph.D. in Telecommunication Software at the Waterford Institute of Technology, Ireland, in 2016, M.Sc. degree in Computer Science at the Federal University of Campina Grande, Brazil, in 2012 and B.Tech. degree in Telematics at the Federal Institute of Education, Science and Technology of Paraíba, Brazil, in 2011. He has authored or co-authored over 60 research papers in various international flagship journals and conferences in the areas of wireless communications, molecular and nanoscale communications as well as bionanoscience. He is also a reviewer for many journals and participated as technical program committee and reviewer for various international conferences. Research interests include Internet of BioNanoThings, molecular communications, bionanoscience and 6G Communications.

PUBLICATION 2: RECONFIGURABLE FILTERING OF NEURO-SPIKE COMMUNICATIONS USING SYNTHETICALLY ENGINEERED LOGIC CIRCUITS

Reconfigurable Filtering of Neuro-Spike Communications using Synthetically Engineered Logic Circuits

Geoflly L. Adonias [1,*], **Harun Siljak** [2], **Michael Taynnan Barros** [3], **Nicola Marchetti** [2], **Mark White** [4] **and Sasitharan Balasubramaniam** [1]

[1] *Telecommunications Software & Systems Group, Waterford Institute of Technology, Waterford, Ireland*
[2] *CONNECT Centre, Trinity College Dublin, Dublin, Ireland*
[3] *CBIG at Biomeditech, Faculty of Medicine and Health Technology, Tampere University, Tampere, Finland*
[4] *Research, Innovation & Graduate Studies, Waterford Institute of Technology, Waterford, Ireland*

Correspondence*:
Geoflly L. Adonias
gadonias@tssg.org

ABSTRACT

High-frequency firing activity can be induced either naturally in a healthy brain as a result of the processing of sensory stimuli or as an uncontrolled synchronous activity characterizing epileptic seizures. As part of this work, we investigate how logic circuits that are engineered in neurons can be used to design spike filters, attenuating high-frequency activity in a neuronal network that can be used to minimize the effects of neurodegenerative disorders such as epilepsy. We propose a reconfigurable filter design built from small neuronal networks that behave as digital logic circuits. We developed a mathematical framework to obtain a transfer function derived from a linearization process of the Hodgkin-Huxley model. Our results suggest that individual gates working as the output of the logic circuits can be used as a reconfigurable filtering technique. Also, as part of the analysis, the analytical model showed similar levels of attenuation in the frequency domain when compared to computational simulations by fine-tuning the synaptic weight. The proposed approach can potentially lead to precise and tunable treatments for neurological conditions that are inspired by communication theory.

Keywords: neuron, hodgkin-huxley, linear model, transfer function, systems theory, epilepsy, filter.

1 INTRODUCTION

Seizure dynamics with either spontaneous and recurrent profiles can occur even in healthy patients during the processing of sensory stimuli or it could manifest itself as an uncontrolled synchronous neural activity in large areas of the brain (Jirsa et al., 2014). Any disruption to the mechanisms that inhibit action potential initiation or the stimulation of processes that facilitate membrane excitation, can prompt seizures. Tackling this disease efficiently is an existing clinical issue where new approaches are constantly being investigated in order to provide precise and reliable strategies in inhibiting or disrupting seizure-triggering populations

23 of neurons. For example, controlling neuron firing threshold can most likely prevent seizure activity, which
24 can often be achieved at a single neuron level (Scharfman, 2007).

25 The development of techniques for the treatment of this type of neurodegenerative disorder is challenging
26 not only due to the complexity of the brain function and structure but also as a result of the invasiveness and
27 discomfort caused by today's most common neurostimulation or surgery approaches (Rolston et al., 2012).
28 However, due to the lack of success in non-invasive approaches, the immediate future epilepsy treatment
29 will still see invasive methods. This approach must achieve population-level control with state-of-the-art
30 technology in not only neuroengineering but must also integrate other disciplines. Recent advancements in
31 nanotechnology, for instance, have been enabling the development of novel devices at the nano-scale that
32 are capable of improving bio-compatibility. Nanotechnology-based treatment also includes advantages in
33 the treatment precision, patient comfort as well as longer treatment lifetime. However, there still remain
34 numerous challenges in the use of nanotechnology. For example, the passage of chemicals through the
35 blood-brain barrier (BBB) is among the many challenges that disrupt the efficiency of nanoparticles-
36 mediated drug delivery functioning. Challenges still remain as to how nanoparticles that pass through
37 the BBB will diffuse towards specific neural populations. However, if the drug-loaded nanoparticles can
38 be delivered at sufficient concentrations and accurately to a specific location, this can influence neural
39 activities (Bennewitz and Saltzman, 2009; Veletić et al., 2019). As an example, drug delivery targets
40 specific neurodegeneration promoting factors (Feng et al., 2019) by performing a drug-induced control over
41 intracellular, extracellular and synaptic properties that regulate spiking activity (Blier and De Montigny,
42 1987).

43 Previous studies on the firing response of neurons have investigated the filtering capabilities either due to
44 realistic synaptic dynamics (Brunel et al., 2001; Moreno-Bote and Parga, 2004) or by naturally manipulating
45 the resting potential of voltage-dependent active conductances of a neuron enhancing its temporal filtering
46 properties (Fortune and Rose, 1997; Motanis et al., 2018). On the other hand, existing analyses do not
47 account for the many molecular control mechanisms that may influence the synaptic activity, e.g. drug. In
48 the case of seizures, the understanding of the drug-induced firing response may allow further analysis on
49 the impact of high-frequency firing on the neural tissue as well as how to desynchronize or slow it down.
50 Frequency-domain analysis has been performed on top of linear models of the Hodgkin-Huxley (HH)
51 formalism to investigate not only the transmission of information through the use of subthreshold electrical
52 stimulation (Khodaei and Pierobon, 2016) but also the influence of axonal demyelination on the propagation
53 of action potentials (Chaubey and Goodwin, 2016). Although Hodgkin-Huxley is not the only neuron model
54 available in the literature, it is one of the most plausible models for computational neuroscience (Long and
55 Fang, 2010). Other proposed models are, for example, integrate-and-fire, Izhikevich and Fitzhugh-Nagumo
56 models (Mishra and Majhi, 2019).

57 The manipulation of cellular activity, such as neuronal spiking activity, using molecules complexes to
58 mimic logic gates and transistors has also been proposed in the literature. One example is the work of Vogels
59 and Abbott (2005), in which the propagation of neuronal signals in networks of integrate-and-fire models
60 of neurons was investigated and they found that different types of logic gates may arise within the network
61 by either strengthening or weakening specific synapses. Goldental et al. (2014) used identical neurons
62 to propose dynamic logic gates that work based on their historical activities, interconnection profiles, as
63 well as the frequency of stimulation at their input terminals. In our previous works (Adonias et al., 2019;
64 Adonias et al., 2020), we developed several logic gates arranged in groups of three heterogeneous models of
65 neurons, with two working as inputs and one as the output, and performed a queueing-theoretical analysis
66 aiming at the study of such a complex network as a single element behaving as the collective of those

67   cells. Irrespective of the tremendous efforts from the scientific community, these works do not provide a
68   framework of reconfigurable circuits that could pave the way for more sophisticated approaches for neuron
69   control. Further investigation of novel neuronal electronic components constructions is needed to develop
70   bio-compatible and reliable solutions that can address defective neuronal networks. While the scientific
71   community has been witnessing remarkable progress in the manipulation and engineering of the behavior
72   of mammalian cells (Lienert et al., 2014), the existing models do not yield analytical expressions that could
73   be used to model drug-induced filtering capabilities of a neuron and, in particular, incorporating computing
74   paradigms. The main focus of this work is to lay the ground-work of analytical models for digital filters
75   that are designed and engineered into neurons, potentially leading to the development of novel epilepsy
76   treatments.
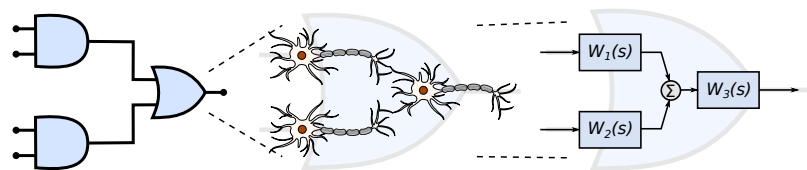
Figure 1. Engineered neuronal digital logic circuit, where each gate is composed of three neurons and each block $W_i(s)$ represents one neuron as a transfer function to enable communication metric analysis .

77   In this work, we propose a mathematical framework aiming at the interpretation of the filtering capabilities
78   in small populations of neurons that are engineered into a logic circuit (Figure 1). The circuit aims to
79   reduce the firing rates from its inputs by performing the binary logic as well as integrating reconfigurability,
80   where the different logic circuit arrangements, as well as logic gate types, can be tuned to change the
81   filtering properties. To achieve that in our mathematical framework, we modify parameters on the logic
82   circuit transfer function, derived from the linear interpretation of the Hodgkin-Huxley neuronal model.
83   These parameters are related to neuronal and synaptic properties of a neuro-spike communication, such
84   as conductances and weight, and can potentially be achieved through the sustained administration of a
85   specific drug. Our mathematical framework is, from an application point-of-view, a design platform for
86   neuroscientists in creating filtering solutions for smoothing out the effects of neurological diseases that
87   require the minimization of firing activity. The framework models the effects of drug-induced molecular
88   changes in models of neurons aiming to control the neuronal activity of a synthetic engineered cell, however,
89   the fabrication and specifications of such a drug are out of the scope of this paper. The contributions of this
90   paper are as follows:

91   • **Neuronal logic circuits are built** using computational models of neurons and this arrangement is
92   expected to be capable of acting as digital filters, converging four inputs into one output with a shift in
93   attenuation driven by modifications to the synaptic weight.

94   • **A mathematical framework is proposed** paving the way for the design of neuronal digital filters to
95   help suppress the destructive effects of neurodegenerative diseases. This framework should enable
96   the relationship between biophysical models and drug design, facilitating scientists control over the
97   behavior of the filters.

98   • **Analysis of the performance of the neuronal filters** in terms of accuracy and of signal power
99   attenuated by the circuit. This analysis gives an insight into how parameters such as weight or
100   frequency at the input would affect the performance of such filters.

The remainder of this paper is as follows, Section 2.1 briefly describes how neurons differ between each other and how they communicate with one another. In Section 2.2, we explain how neurons can function as non-linear electronic circuits based on the seminal work of Hodgkin and Huxley (1952) and we also describe the process of linearization aiming to derive a transfer function of the filter model. The filter design is explained in Section 2.3 which also covers how neurons are represented as compartments and connected to form logic gates and, consequently, to form logic circuits. In Section 3, we present the results that are discussed in Section 4 and, finally, the conclusions are presented in Section 5.

2 MATERIAL AND METHODS

2.1 Neuronal Communication

To be able to synthetically implement complex functions inside the brain, we must control how the neurons exchange information using the propagation of action potentials inside a network of neurons. The number of excitatory and inhibitory connections between neurons determines the spatio-temporal dynamics of the action potentials propagation (Zhou et al., 2018). Efficient coding and modulation of neuronal information have been used to implement bio-computational approaches in our previous work (Adonias et al., 2020). Bio-computing can be created from neuronal networks that are engineered to function as logic circuits through controlling the neuro-spike communication and curbing the signal propagation dynamics between the neurons.

We aim to investigate the neuronal and synaptic properties in constructing logic circuits that perform the filtering of spikes in small populations from the somatosensory cortex. The cortex is responsible for most of the signal processing performed by the brain and comprises a rich variety of morpho-electrical types of neuronal and non-neuronal cells. We will take into account these characteristics in the construction of our mathematical framework that is used to design the circuits.

2.1.1 Properties of a Neuron

Neurons are divided into three main parts: dendrites, soma and axon. Dendrites receive stimuli from other cells and the way these dendritic trees are projected onto neighboring neurons in a network helps to classify neuron morphological types. The axon passes stimuli forward to cells connected down the network through its axon terminals and the soma is the main body of the neuron. Each neuron's response to a stimulus will dictate the electrophysiological neuron type. The soma is where most proteins and genes are produced and where stimuli are generated and fired down the axon.

Besides the way dendrites are projected, the proteins and genes that neurons express and their morphological and electrophysiological characteristics are important for the classification of different types of neurons. One of the most comprehensive works on neuronal modelling, by Markram et al. (2015), classifies the neurons from the rat's somatosensory cortex based on their morpho-electrical properties (morphological and electrical characteristics) as well as the cortical layer they belong (columnar and laminar organization).

2.1.1.1 *Morpho-electrical Characteristics*

Even though all neurons used in this work can assume different morphological structure, it is exactly by analyzing their axonal and dendritic ramification that we can have a good enough categorization of their respective morphological types. Regardless of their types, neurons in the cortical layer are considered of small sizes (8 - $16\,\mu$m). Furthermore, inhibitory neurons can be better identified by their axonal features

4

140 while excitatory neurons can be more easily classified based on their dendritic features (Markram et al.,
141 2015). Each morphological type (m-type) can fire different spiking patterns and this may affect the gating
142 capabilities of neurons due to the fluctuations on precise spike timing. Markram et al. (2015) categorized
143 11 different electrical types (e-types) of neurons, hence, 11 different ways of firing a spike train generated
144 in response to an injected step current.

2.1.1.2   *Cortical Organization*

146 The cerebral cortex comprises six distinguished horizontal layers of neurons, with each layer having
147 particular characteristics such as cell density and type, layer size and thickness. This horizontal
148 configuration is also known as a "laminar" organization, where the layers are identified as (1) Molecular
149 layer, which contains only a few scattered neurons and consists mostly of glial cells and axonal and
150 dendritic connections of neurons from other layers; (2) External granular layer, containing several stellate
151 and small pyramidal neurons; (3) Pyramidal layer, contains non-pyramidal and pyramidal cells of small
152 and medium sizes; (4) Inner granular layer, predominantly populated with stellate and pyramidal cells,
153 this is the target of thalamic inputs; (5) Ganglionic layer, containing large pyramidal cells that establish
154 connections with subcortical structures; and (6) Multiform layer, populated by just a few large pyramidal
155 neurons and a good amount of multiform neurons, which sends information back to the thalamus. All
156 layers may contain inter-neurons bridging two different brain regions.

157 The neurons are not just stacked one on top of another suggesting a horizontal organization, indeed
158 vertical connections are also found in between the neurons from either the same or different layers. This
159 allows another type of classification known as mini-columns (also called, micro-columns) with a diameter
160 of 30 - 50 μm and when activated by peripheral stimuli, they are seen as macro-columns, with a diameter
161 of 0.4 - 0.5 mm (Peters, 2010). This will create network topologies with intrinsic characteristics, e.g.
162 connection probabilities between neurons, that influence the signal propagation to converge into either a
163 specific pattern or flow.

### 2.1.2   Neuron-to-neuron Communication

165 The communication between a pair of neurons is done through the diffusion of neurotransmitters in
166 the synaptic cleft; this process is triggered by an electrical impulse reaching the axon terminals of the
167 transmitting cell characterizing an electrochemical signalling process known as the *synapse*. Action
168 potentials propagate down the axon of the pre-synaptic cell, which is the sender cell, and when reaching
169 the axon terminals also known as pre-synaptic terminals, it triggers the release of vesicles containing
170 neurotransmitters into the synaptic cleft, which is the gap between a pre- and a post-synaptic terminal,
171 as illustrated in Figure 2. Those neurotransmitters will probabilistically bind to neuro-receptors located
172 at the post-synaptic terminals, i.e. dendrites (Balevi and Akan, 2013), triggering the exchange of ions
173 through the membrane that can either excite or inhibit the cell, depending on the type of neurotransmitters
174 that were received. In our work, we focus on the synaptic weight between the pre- and post-synaptic
175 terminals. The synaptic weight is a measure of how much influence the pre-synaptic stimuli have on
176 the post-synaptic cell and it is known to have its value best approximated to the time integral of the
177 synaptic conductance (Gardner, 1989). Furthermore, the value of synaptic conductance in the post-synaptic
178 terminal is driven by the number of neurotransmitters bound to neuroreceptors (Guillamon et al., 2006).
179 We illustrate the synaptic weight, in Figure 2, as red neurotransmitters which should have their release
180 from the pre-synaptic terminals induced by the administration of a specific drug.

181 In an excitatory synapse, the membrane potential of the post-synaptic cell, which rests at approximately
182 -65 mV, will start depolarizing itself until it reaches a threshold, th, for action potential initiation. On the
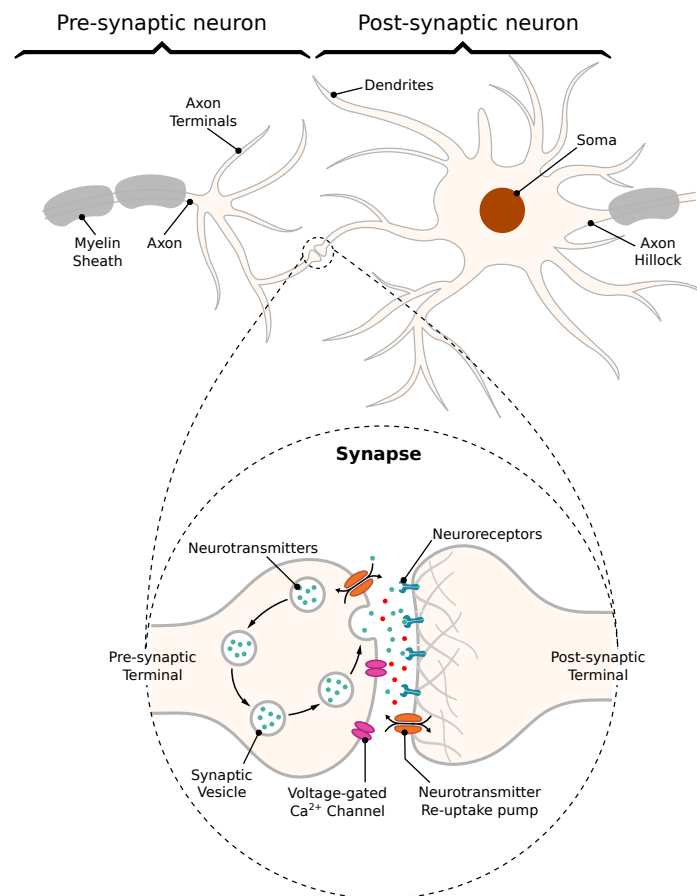
Figure 2. Schematic of a *synapse*; action potentials traveling down the axon trigger the release of neurotransmitters into the cleft between pre- and post-synaptic terminals, traveling towards neuroreceptors on the other end leading to changes on membrane conductance that can either excite or inhibit the post-synaptic neuron.

other hand, if the synapse is inhibitory, the membrane should get even more polarized making it nearly impossible for the cell to fire a spike and not allowing the propagation of any signal down the network from the inhibited cell. After reaching th, the membrane potential should increase towards a maximum peak of depolarization, and then the cell will start the process of repolarization towards its resting potential. For a brief moment, the potential inside the cell will cross the level of potential when at rest making the membrane hyperpolarized, which is a period known as the *refractory period* and it can be further subdivided as *absolute* and *relative*. The absolute refractory period (ARP) lasts around 1 - 2 ms during which the neuron is unable to fire again regardless of the strength of the stimuli; then, it is followed by the relative refractory period (RRP) during which a response in the potential of the cell may be evoked depending on the strength of the stimuli (Mishra and Majhi, 2019).

2.2 Electronic Interpretation of a Neuron Model

194   The main structures of a neuron, previously mentioned in Section 2.1.1, can assume different shapes and
195 spatial structures that play an important role in determining its input and output relationship. By sectioning
196 the neuron into several compartment models, we are able to account for the influence that individual
197 compartments have on the communication process of the neuron. Even though we consider the same
198 value of resting potential for all compartments of the cell, there is some discussion on whether different
199 compartments have different potentials when at rest (Hu and Bean, 2018).

200   We aim to develop a transfer function for the neuron-spike response, or output ($V(s)$), to a particular
201 spike input ($I(s)$). Using a transfer function for each neuron which is represented as a single compartment,
202 we are able to efficiently associate the configuration of the filters with the structure of the neural network as
203 well as the individual characteristics of each neuron. On top of that, we also are able to focus on frequency
204 domain for an effective spike firing filtering. We rely on the electronic interpretation of the Hodgkin-Huxley
205 model of neuron action potentials, which is made based on the neuronal cable theory assumptions on the
206 static ionic channels conductance. In this section, we provide the details of the development of the transfer
207 function, which is built on the linearization process of the Hodgkin-Huxley neuron model.

2.2.1 Hodgkin-Huxley Formalism

209   As aforementioned in Section 1, neurons can perform spike filtering tasks either by manipulating ionic
210 conductances, such as sodium and potassium conductances, from within the cell (Fortune and Rose, 1997)
211 or by working on the extracellular environment where the synapse occurs (Brunel et al., 2001; Moreno-Bote
212 and Parga, 2004). Furthermore, filtering capabilities may vary according to the non-linearities of the
213 neuron's activity and action potential propagation. In order to design an efficient filtering process, we will
214 need to eliminate the non-linearities so we can directly link neurons properties to the filtering behavior
215 and adjust these properties according to a desired filtering performance level. We consider the Hodgkin
216 and Huxley non-linear model (Pospischil et al., 2008) as our basic model since it perfectly describes the
217 influence of ionic conductance and synaptic conductance in the propagation of the action potentials. We
218 assume that parts of the neuron will constitute a compartment, which results in the electric circuit in Fig. 3A
219 when applying the conventional neural cable theory.
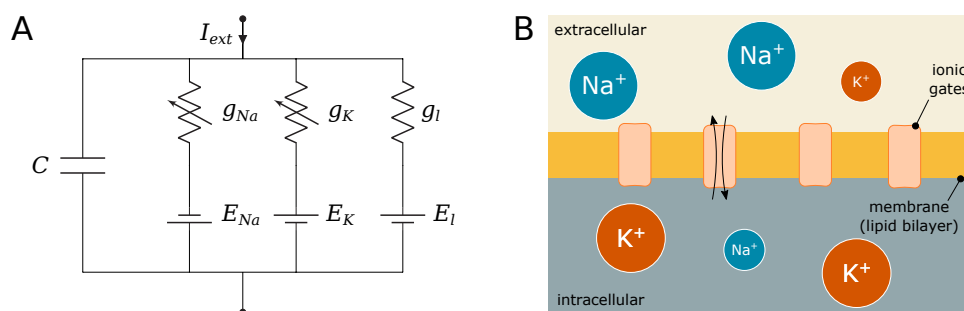
Figure 3. Hodgkin-Huxley (HH) model: **(A)** Electronic circuit representation and **(B)** Equivalent biological HH compartment; the lipid bilayer is modeled as C, the conductances g represent how open or close the ionic gates are and the gradient of ions between the intra- and extra-cellular space define the reversal potentials E.

220   Figure 3 depicts C as the membrane capacitance, each voltage-gated ionic channel represented by its
221   respective conductances g_{Na} and g_K and the leak channel by the linear conductance g_l. The membrane
222   capacitance is proportional to the surface area of the neuron and, along with its resistance, dictates how fast
223   its potential responds to the ionic flow. The ratio between intra- and extra-cellular ions define the reversal
224   potentials $E_{Na, K, l}$ establishing a gradient that will drive the flow of ions (Barreto and Cressman, 2011).

225   When an external stimulus, I_{ext}, is presented, it triggers either the activation or inactivation of the ionic
226   channels that allow the exchange of ions that result in depolarization (or hyperpolarization when inhibitory)
227   of the membrane of the cell. These dynamics are modeled as

$$C\frac{\mathrm{d}V}{\mathrm{d}t} = -I_l - I_{Na} - I_K + I_{ext}, \tag{1}$$

228   where V is the membrane potential and I_x are the ionic currents where x represents either a specific ion
229   (Na, K) or the leak channel (l). Those currents are described as

$$I_l = g_l(V - E_l), \tag{2}$$

$$I_{Na} = g_{Na}m^3h(V - E_{Na}), \tag{3}$$

$$I_K = g_K n^4(V - E_K), \tag{4}$$

230   where m and h are the activation and inactivation variables of the sodium channel, respectively, and n is the
231   activation variable of the potassium channel, following the conventional approach described by Hodgkin
232   and Huxley (1952) and stated as

$$\frac{\mathrm{d}m}{\mathrm{d}t} = \alpha_m(V)(1 - m) - \beta_m(V)m, \tag{5}$$

$$\frac{\mathrm{d}h}{\mathrm{d}t} = \alpha_h(V)(1 - h) - \beta_h(V)h, \tag{6}$$

$$\frac{\mathrm{d}n}{\mathrm{d}t} = \alpha_n(V)(1 - n) - \beta_n(V)n, \tag{7}$$

233   in which the values of the rate constants α_i and β_i for the i-th ionic channel can be defined as

$$\alpha_m = \frac{0.1(V + 40)}{1 + e^{-(V+40)/10}}, \tag{8}$$

$$\beta_m = 4e^{-(V+65)/20}, \tag{9}$$

$$\alpha_h = 0.07e^{-(V+65)/20}, \tag{10}$$

$$\beta_h = \frac{1}{1 + e^{-(V+35)/10}}, \tag{11}$$

$$\alpha_n = \frac{0.01(V + 55)}{1 - e^{-(V+55)/10}}, \tag{12}$$

$$\beta_n = 0.125 e^{-(V+65)/80}. \tag{13}$$

234   The membrane capacitance is proportional to the size of the cell, and on the other hand, the bigger
235 the cell diameter, the lower the spontaneous firing rate (Sengupta et al., 2013). Furthermore, each ionic
236 channel can be studied as containing one or more physical gates which can assume either a permissive or
237 a non-permissive state when controlling the flow of ions. The channel is open when all gates are in the
238 permissive state, and it is closed when all of them are in the non-permissive state (Baxter and Byrne, 2014).

2.2.2 Hodgkin-Huxley Linear Model

240   In order to derive a transfer function for the Hodgkin-Huxley model, we must consider each neuron as
241 a system that is linear and time-invariant (LTI). If the system is non-linear, then a linearization process
242 should be done before any frequency analysis is performed. For a more detailed analysis on the procedures
243 for linearization of the Hodgkin-Huxley model, the reader is referred to (Koch, 2004; Mauro et al., 1970;
244 Sabah and Leibovic, 1969; Chandler et al., 1962).

245   The linearization process requires that we reconsider the electronic components in each neuron
246 compartment to adequately eliminate trivial relationships. Membranes with specific types of voltage-
247 and time-dependent conductances can behave as if they had inductances even though neurobiology
248 does not possess any coil-like elements. This modification will transform the behavior of non-linear
249 components towards linearization, resulting in a proportional relationship between the voltage and current
250 changes (Koch, 2004).

251   Every linearization process is performed for small variations around a fixed point, hereafter denominated
252 by δ, and in the case of the Hodgkin-Huxley model, this fixed point should be the steady-state (resting
253 state) of the system. Because the sodium activation generates a current component that flows in an opposite
254 direction compared to that of a passive current, the branch concerning the sodium activation should
255 have components with negative values while the branches regarding potassium activation and sodium
256 inactivation should have components with positive values (Sabah and Leibovic, 1969). The linear version
257 of the circuit of Figure 3A is illustrated in Figure 4, where C is the membrane capacitance, g_n, g_m and g_h
258 are the conductances of the inductive branches connected in series with their respective inductances L_n,
259 L_m and L_h derived from the linearization process and $G_T = G_L + G_K + G_{Na}$ is the total pure membrane
260 conductance.

261   Let us consider the membrane potential deviation, δV, around some fixed potential. Thus, we can express
262 the response of the circuit to small-signal inputs as

$$C\frac{d\delta V}{dt} = I_{ext} - \delta I_l - \delta I_K - \delta I_{Na}, \tag{14}$$

263 where $\delta I_{l,Na,K}$ are current variations at any given steady-state and can be defined as
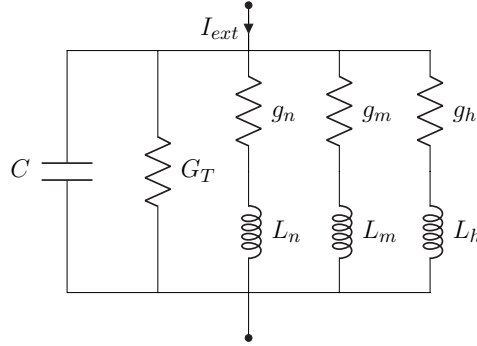
Figure 4. Hodgkin-Huxley linear circuit model representation.

$$\delta I_l = g_l \delta V, \tag{15}$$

$$\delta I_K = G_K \delta V + 4 g_K n_\infty^3 (V - E_K) \delta n, \tag{16}$$

$$\delta I_{Na} = G_{Na} \delta V + 3 g_{Na} m_\infty^2 h_\infty (V - E_{Na}) \delta m + g_{Na} m_\infty^3 (V - E_{Na}) \delta h, \tag{17}$$

264 where $G_{K,Na}$ are pure conductances of potassium and sodium and G_L the pure leak conductance expressed
265 as

$$G_L = \bar{g}_l, \tag{18}$$

$$G_K = \bar{g}_K n_\infty^4, \tag{19}$$

$$G_{Na} = \bar{g}_{Na} m_\infty^3 h_\infty, \tag{20}$$

266 where $\bar{g}_{K,Na}$ are the maximum attainable conductances, and δn, δm and δh are small variations around the
267 steady-state of the activation and inactivation variables n, m and h which are written as

$$\frac{d\delta n}{dt} = \frac{d\alpha_n}{dV} \delta V - (\alpha_n + \beta_n) \delta V - n_\infty \left(\frac{d\alpha_n}{dt} - \frac{d\beta_n}{dt} \right) \delta V, \tag{21}$$

$$\frac{d\delta m}{dt} = \frac{d\alpha_m}{dV} \delta V - (\alpha_m + \beta_m) \delta V - m_\infty \left(\frac{d\alpha_m}{dt} - \frac{d\beta_m}{dt} \right) \delta V, \tag{22}$$

$$\frac{d\delta h}{dt} = \frac{d\alpha_h}{dV} \delta V - (\alpha_h + \beta_h) \delta V - h_\infty \left(\frac{d\alpha_h}{dt} - \frac{d\beta_h}{dt} \right) \delta V, \tag{23}$$

268   as a function of the derivative of the rate constants $\alpha_{n,m,h}$ and $\beta_{n,m,h}$, and n_∞, m_∞ and h_∞ are the
269   steady-state values of m, n and h defined as

$$n_\infty = \frac{\alpha_n}{\alpha_n + \beta_n},\tag{24}$$

$$m_\infty = \frac{\alpha_m}{\alpha_m + \beta_m},\tag{25}$$

$$h_\infty = \frac{\alpha_h}{\alpha_h + \beta_h},\tag{26}$$

270   and the conductances, $g_{n,m,h}$, and inductances, $L_{n,m,h}$, of the inductive branches are defined as

$$g_n = \frac{4\bar{g}_K n_\infty^3 (V - E_K) \left[\left.\frac{d\alpha_n}{dV}\right|_r - n_\infty \left.\frac{d(\alpha_n + \beta_n)}{dV}\right|_r \right]}{\alpha_n + \beta_n},\tag{27}$$

$$L_n = \frac{1}{g_n(\alpha_n + \beta_n)},\tag{28}$$

$$g_m = \frac{3\bar{g}_{Na} m_\infty^2 h_\infty (V - E_{Na}) \left[\left.\frac{d\alpha_m}{dV}\right|_r - m_\infty \left.\frac{d(\alpha_m + \beta_m)}{dV}\right|_r \right]}{\alpha_m + \beta_m},\tag{29}$$

$$L_m = \frac{1}{g_m(\alpha_m + \beta_m)},\tag{30}$$

$$g_h = \frac{\bar{g}_{Na} m_\infty^3 (V - E_{Na}) \left[\left.\frac{d\alpha_h}{dV}\right|_r - h_\infty \left.\frac{d(\alpha_h + \beta_h)}{dV}\right|_r \right]}{\alpha_h + \beta_h},\tag{31}$$

$$L_h = \frac{1}{g_h(\alpha_h + \beta_h)}.\tag{32}$$

271   Each channel has a probability of being open which represents the fraction of gates in that channel that
272   are in the permissive state (Gerstner et al., 2014). The gating variables are described by the coupling of
273   the conductances $g_{n,m,h}$ and their respective inductances $L_{n,m,h}$ which are functions of the rate constants
274   representing the transition from permissive to non-permissive state, $\alpha(V)$, and vice-versa, $\beta(V)$ which
275   should take a short period of time, $\tau = [\alpha(V) + \beta(V)]^{-1}$, to eventually reach a steady-state value, α_∞ and
276   β_∞ (Koslow and Subramaniam, 2005).

277   Borrowing concepts from systems theory such as frequency analysis of LTI systems, as a standard
278   procedure for the analysis of linear differential equations as simpler algebraic expressions, see (Nise, 2015),
279   and the linearization of non-linear systems for the reason previously mentioned at the beginning of this
280   section, we derived a transfer function in the *Laplace* domain for the linear system from Figure 4. The
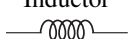
281 relationship between the different elements of the circuit and their respective impedance and admittance
282 values from the *Laplace* transforms are depicted in Table 1.

Table 1. Impedance relationships for capacitors, resistors and inductors.

Component	Impedance	Admittance
Capacitor	$\dfrac{1}{Cs}$	Cs
Resistor	R	$G = \dfrac{1}{R}$
Inductor	Ls	$\dfrac{1}{Ls}$

283 Therefore, the relationship between the output and the input of the system in the frequency domain is
284 expressed as

$$\frac{V(s)}{I(s)} = \frac{s^3 L_n L_m L_h}{\{L_n L_m L_h [s^4 C + s^3 (G_T + g_n + g_m + g_h)] + s^2 (L_m L_h + L_n L_h + L_m L_h)\}} \tag{33}$$

285 where $s = \sigma + j\omega$ is a complex variable; $j = \sqrt{-1}$ and $\omega = 2\pi f$, where f is the frequency in Hertz. Let
286 us rewrite Eq. (33) as

$$W(s) = C^{-1} \frac{s}{s^2 + sC^{-1}(G_T + g_n + g_m + g_h) + C^{-1}(L_m^{-1} + L_n^{-1} + L_h^{-1})}. \tag{34}$$

287 Now, denoting $\gamma = G_T + g_n + g_m + g_h$ and $\lambda^{-1} = L_n^{-1} + L_m^{-1} + L_h^{-1}$ and performing a few algebraic
288 manipulations, we end up with the following transfer function for the filter model

$$W(s) = \gamma^{-1} \frac{C^{-1}\gamma s}{s^2 + C^{-1}\gamma s + \lambda^{-1}C^{-1}}. \tag{35}$$

289 For frequency response analysis, we observe the behaviour of $W(j\omega)$, i.e. substitute $s = j\omega$. For $\omega \to 0$,
290 $W(j\omega)$ behaves like ω; for $\omega \to \infty$ it behaves like $\frac{1}{\omega+1}$, i.e. in both cases it tends to zero, and hence
291 demonstrates the behaviour of a second-order band-pass filter (BPF). It corresponds to the canonical form
292 $\frac{K(\omega_0/Q)s}{s^2+(\omega_0/Q)s+\omega_0^2}$ where $K = \gamma^{-1}$ is the gain, $Q = \gamma^{-1}\sqrt{C\lambda^{-1}}$ is the selectivity and $\omega_0 = \sqrt{\lambda^{-1}C^{-1}}$ is
293 the peak frequency of the filter. This agrees with findings from previous literature on the matter (Plesser
294 and Geisel, 1999) that concluded the periodicity of a stimulus is optimally encoded by a neuron only in a
295 specific spectral window.

2.3 Transfer Function Filter Design

297 Given the transfer function for a neural compartment in the previous section, we now progress towards
298 a transfer function for the spike filter. The filter is comprised of neurons that are particularly chosen to
299 have a network that will behave as a digital gate and a small population that will behave as a circuit that

300 implements the filter. Our aim is to capture the relationship between compartments as well as neuron
301 connections so we can build a transfer function for the filter while considering neuron connection variables
302 (synaptic conductance and synaptic weight) that allow easy reconfiguration of the filtering process. The
303 linearization process combined with the analysis of the neuron communications is the driver of the filtering
304 process, which also allows the derivation of a filter transfer function which is detailed below.

305 2.3.1 Biological Logic Gates and Circuits

306   Synthetic biology is the technology that allows the control of the neurons' internal process in order to
307 construct non-natural activity and functioning of neurons, e.g. logic gates (Larouche and Aguilar, 2018).
308 Synthetic logic operations inspire scientists to address the challenges posed by novel synthetic biomedical
309 systems, such as biocompatibility and long-term use.
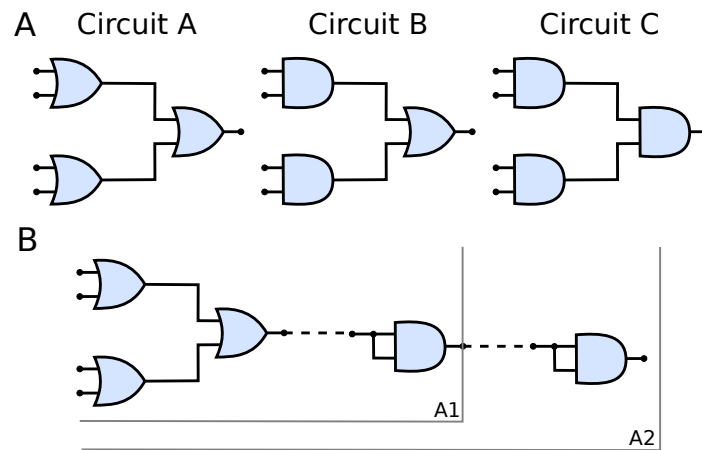
Figure 5. (A) Schematic of circuits A, B and C and (B) The connection of AND gates in cascade to circuit A. $A1$ refers to the arrangement described by a single AND gate connected to the output of the circuit A and $A2$ refers to another AND gate connected to the output of $A1$ arrangement, i.e. two AND gates in cascade with circuit A. Analogous nomenclature is employed for both circuits B, as in B1/B2 and C, as in C1/C2.

310   Figure 5A shows the three types of the circuit we have built and analyzed in this work. From circuits A to
311 C, the number of OR gates is decreased; when compared to AND gates, OR gates are quite permissive. In
312 our previous study

313   Given that several factors such as connection probability, type of cell, and different numbers of
314 compartments (as discussed in Section 2.3.2) among different types of neurons may influence its gating
315 capabilities. This variation on the quantity of compartments could also lead to variations on periods for
316 the action potential to reach the post-synaptic terminals and start the synapse process. Furthermore, cells
317 with bigger sizes of soma may take more time and amount of stimuli to reach threshold for action potential
318 initiation (Sengupta et al., 2013), thus, also affecting the way a neuronal logic gate would work regarding
319 a specific morphological neuronal type. For that reason, it is safe to keep two cells fixed as inputs (as
320 illustrated in Figure 1) and then deploy an arrangement with which its performance has been previously
321 assessed, allowing us to be fairly certain about how the synthetic gate or circuit should behave. Each neuron

322 is represented by a block, $W_i(s)$ for the i-th neuron, and its representation in the frequency domain is
323 proposed in Equation (35) and further detailed in Subsection 2.3.2.

2.3.2 Compartmental Modelling

325   Neurons are very complex structures with numerous ramifications and several factors that contribute
326 to their highly non-linear dynamism. Aiming to make the comprehension of such a complex electrical
327 behavior easier, one employs a widely used technique called "compartmental modelling". Since different
328 neurons have different morphologies, the mechanism of determining the number of compartments will
329 be based on estimating the length of a specific neuronal structure. For instance, a varying length of axon,
330 which will reflect in different quantities of compartment in series, where we will have a fixed size for
331 each segment of the axon representing one compartment. This is a very natural and elegant way to model
332 dynamic systems as multiple interconnected compartments where each compartment is described by its
333 own set of equations, carrying the influence of one compartment to the next reproducing the behavior of
334 the whole neuron.

335   Observing the neuron as a set of compartments described by transfer functions equivalent to that of (35),
336 the neuronal morphology of a pyramidal cell, as illustrated in Figure 6A, (or any cell for that matter) can
337 be modeled as an electrical circuit as shown in the topology of Figure 6B; the dendritic ramifications are
338 modeled as a combination of serial and parallel connections terminanting in the soma which is connected to
339 the axon modeled as a series of compartments; its interpretation in terms of filtering is given in Figure 6C.
340 The effect of a serial connection of two compartments is one of set-intersection when observed in the
341 frequency domain: two bandpass filters in series pass only the frequencies that exist in both of their
342 passbands. On the other hand, a parallel connection has a set-union effect, a parallel connection of filters
343 will pass all the frequencies in both their passbands. As such, a large network (tree) of such compartments
344 with similar bands combined in a cell, and cells combined in a group of cells will exhibit asymptotic
345 bandpass behavior as well.
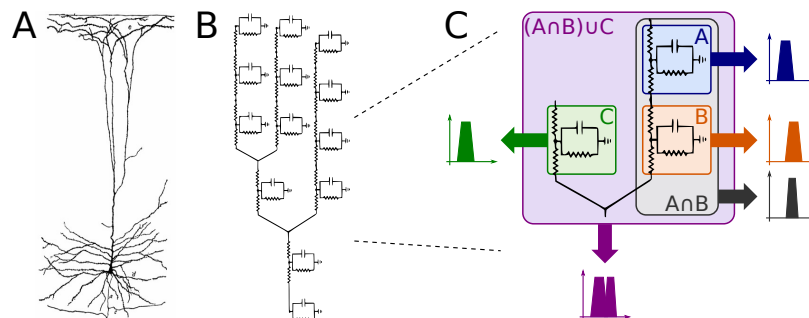
Figure 6. Compartmental neuron representation: **(A)** Natural topology of a pyramidal cell, **(B)** Electronic
circuit compartments and **(C)** Effects of serial and parallel connections between compartments.

346   Every single compartment, each represented by one transfer function, is grouped in trees of three cells
347 (Figure 1) forming a logic gate; the three gates are connected into a tree of their own, as illustrated in
348 Figure 5A, forming a logic circuit. All of the cells are represented with the same form of the transfer
349 function,

14

$$W_i(s) = \zeta_i \gamma_i^{-1} \frac{C_i^{-1}\gamma_i s}{s^2 + C_i^{-1}\gamma_i s + \lambda_i^{-1}C_i^{-1}}, \ i = 1, \ldots, 9 \tag{36}$$

with symbols defined previously, and a new parameter ζ_i describing the synaptic weight for the ith cell; ζ_i acts as a tunable gain for the neurons.

Using the parameters from (Mauro et al., 1970) aiming to keep them within the physically sensible orders of magnitude, we obtain the reference values of $\bar{\gamma} = 0.0024$, $\bar{\lambda} = 119$, $\bar{C} = 1$ and $\bar{\zeta} = 1$, and the values for 9 cells were generated multiplying these reference values by a uniformly distributed random variable in the range $(0, 1)$. This kind of distribution is widely used to describe experiments where an arbitrary result should lie between certain boundaries, and in our case boundaries are defined by reasonable orders of magnitude around values made available by previous studies; keeping exactly the same parameters for all cells in the cascade is not realistic. The total transfer function of this system is

$$W = ((W_1 + W_2)W_3W_7 + (W_4 + W_5)W_6W_8)W_9, \tag{37}$$

and its frequency response (Bode plot) for the relevant range of frequencies in our applications (Wilson et al., 2004) is shown in Figure 7B.
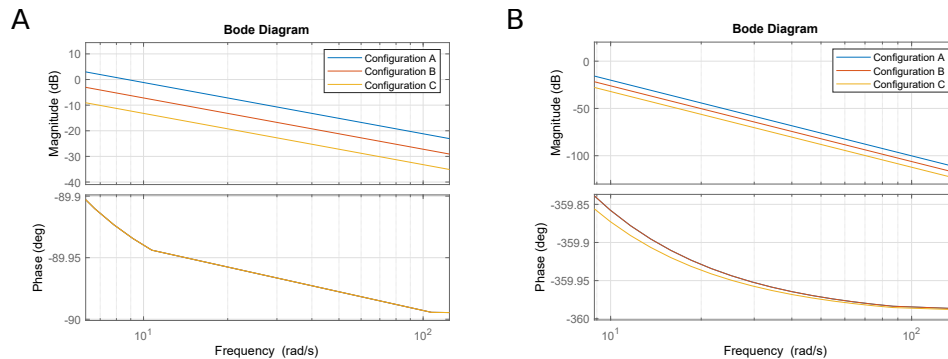
Figure 7. Bode plots: **(A)** Single second-order bandpass filter approximation and **(B)** Filter structure from Eq. (37)

Let us now observe three cases concerning the choice of ζ_i values. In the first case, we keep all of them at unity and consider it our base case for this part of the analysis (and to keep it aligned with the rest of the paper, we call it *Circuit B*). In the second case, we double the values of ζ_3 and ζ_6, which corresponds to the manipulation of the output cell for the two input gates in *Circuit A*. In our linear model, this is equivalent to doubling ζ_9 and leaving everything else intact. Finally, in the third case, we manipulate the output cell of the last gate by halving its synaptic conductance (*Circuit C*). This effectively means that the three cases are $\zeta_{9B} = 1$, $\zeta_{9A} = 2$ and $\zeta_{9C} = 1/2$, respectively. Since the tunable gain ζ_9 of the gate W_9, is the tunable gain of the whole system W according to (37), its change would offset the frequency response along the ordinate axis, i.e. lower gains (lower conductance) would suppress the unwanted frequencies in a better way, while higher gains would do the opposite. This is demonstrated in Figure 7A. The process of

371 the analysis is summarized in Algorithm 1 and a summary with all elements from both the original and
372 linearized versions of the Hodgkin-Huxley as well as the transfer function model is presented in Table 2.

1 **Initialize:**
2 $\Gamma = \{\gamma_1, \ldots, \gamma_9\} \in (0, \bar{\gamma})$
3 $\Lambda = \{\lambda_1, \ldots, \lambda_9\} \in (0, \bar{\lambda})$
4 $\mathcal{C} = \{C_1, \ldots, C_9\} \in (0, \bar{C})$
5 $Z = \{\zeta_1, \ldots, \zeta_9\} \in (0, \bar{\zeta})$
6 **for** $1 \leq i \leq 9$ **do**
7 $W_i \leftarrow \zeta_i \gamma_i^{-1} \frac{C_i^{-1} \gamma_i s}{s^2 + C_i^{-1} \gamma_i s + \lambda_i^{-1} C_i^{-1}}$
8 **end**
9 $W_B \leftarrow ((W_1 + W_2) W_3 W_7 + (W_4 + W_5) W_6 W_8) W_9$
10 $W_A \leftarrow 2 W_B$
11 $W_C \leftarrow 0.5 W_B$
12 Plot frequency response: W_A, W_B, W_C

Algorithm 1: Linear model filter analysis

373 Alternatively, as we suggested earlier, a single transfer function of a compartment serves as an
374 approximation of the entire system due to the effects of repeated bandpass filtering in Figure 6C. In
375 such case, we observe 20 dB/decade slope in the Bode plot shown in Figure 7A (as compared to 80
376 dB/decade slope in Figure 7B) and the same offset of $20 \cdot \log_{10} 2 \approx 6$ dB in case of halving/doubling the
377 synaptic weight. Since the filter is of a band-passing nature, it is only natural that, around the resonant
378 frequency, lower and higher frequency amplitudes should be ideally attenuated towards zero. Thus, it is
379 worth mentioning that in both cases depicted here, the part of the frequency response with the cusp is at
380 very low frequencies, so it is not visible in the relevant part of the spectrum. As such, the filter behaves as a
381 low pass filter for all practical considerations.

3 RESULTS

382 In this section, we discuss the simulation results concerning the reconfigurable logic gates as well as the
383 circuits. For all simulations, intrinsic parameters of the cell were kept at their default values (such as the
384 length and diameter of each of their compartments) meaning that nothing concerning their morphological
385 properties was changed, the spike trains fed to the input of the circuits followed a *Poisson* process and
386 the threshold for spike detection and data analysis was 0 mV where any potential higher than that in a
387 specific time slot would be considered a bit "1", characterizing the use of a simple *On-Off Keying (OOK)*
388 modulation which was implemented where a spike is considered as a bit '1' and its absence a bit '0' in each
389 time slot. The cell models and information on their respective connection probabilities between different
390 pair of neurons were obtained from the work of Markram et al. (2015), and then we used NEURON and
391 Python for simulation and data analysis (Carnevale and Hines, 2009; Hines et al., 2009). The source-code
392 of our simulations is publicly available on a GitHub repository[1].

3.1 Reconfigurable Logic Gates

394 In this work, we call "reconfigurable" logic gates, the gates that work by changing the synaptic weight
395 between the connections of both input cells with the output cell in a neuronal logic gate structure. Aiming

---

[1] https://github.com/gladonias/neuronal-filters

     16

Table 2. Summary of elements described in the proposed model.

Element	Description
C	Membrane capacitance
g_{Na}, g_K, g_l	Sodium, potassium and leak conductances
E_{Na}, E_K, E_l	Sodium, potassium and leak reversal potentials
I_{ext}	External stimulus
I_{Na}, I_K, I_l	Ionic current for the sodium, potassium and leak channels
V	Membrane potential
m, h	Sodium activation and inactivation variables
n	Potassium activation variable
α, β	Rate constants for m, h and n from permissive to non-permissive state and vice-versa
δ	Small variation around the steady-state
G_T	Total pure conductance
G_{Na}, G_K, G_L	Sodium, potassium and leak pure conductances
$\bar{g}_{Na}, \bar{g}_K, \bar{g}_l$	Maximum attainable sodium, potassium and leak conductances
$m_\infty, h_\infty, n_\infty$	Steady-state values of m, h and n
g_m, g_h, g_n	Conductances of the inductive branches
L_m, L_h, L_n	Inductances of the ionic paths
W	Transfer function of the filter
K, Q, ω_0	Gain, selectivity and peak frequency of the filter
ζ	Synaptic weight

396 to measure individual gate accuracy, the spike trains in the inputs were randomly produced but we control
397 their frequency variation, in other words, for each simulation, the frequency at all inputs was the same and
398 any change in the frequency was performed for all inputs of the gates meaning that none of the simulations
399 account for different frequency values between different inputs in a single simulation. The accuracy is
400 a simple but powerful measure for the performance of the gates, with which we intend to analyze the
401 effects of the dynamics of the cell on the output of the circuit when comparing this output with the ideal
402 response of the circuit derived from its truth-table. The accuracy is calculated according to the following
403 equation (Hanisch and Pierobon, 2017):

$$A(E[Y]; Y) = \frac{P_{1,1} + P_{0,0}}{\displaystyle\sum_Y \sum_{E[Y]} P_{Y,E[Y]}}, \tag{38}$$

404 where $P_{Y,E[Y]}$ is the probability of Y given $E[Y]$ in which Y is the actual output and $E[Y]$ is the expected
405 output and $Y \,\&\, E[Y] \in \{0,1\}$. $P_{Y,E[Y]}$ resembles the conditional probabilities in a binary symmetric
406 channel (BSC). Thus, $P_{0,0} = 1 - P_{1,0}$, and $P_{0,1} = 1 - P_{1,1}$. It is possible to calculate $P_{1,1}$, for instance,
407 by counting the number of bits there are for each input-output combination. In other words, considering
408 $\#B_{i,j}$ the number of times a bit i was received when bit j was sent knowing that $i \,\&\, j \in \{0,1\}$, then
409 $P_{1,1} = \#B_{1,1}/(\#B_{1,1} + \#B_{0,1})$.

410   Given the objective of obtaining a behavior similar to an OR gate, the synaptic weight should be set to
411 $0.06\,\mu$S, meaning that the pre-synaptic stimuli will drive a higher influence on the depolarization of the
412 post-synaptic cell. On the other hand, for an AND behavior, the weight is set to $0.03\,\mu$S, which reduces the

413 influence of a single spike and look to a response of the post-synaptic neuron only when two spikes arrive
414 very close to each other in terms of time. This is conducted so we have acceptable levels of accuracy when
415 compared to the expected outputs of the gate.
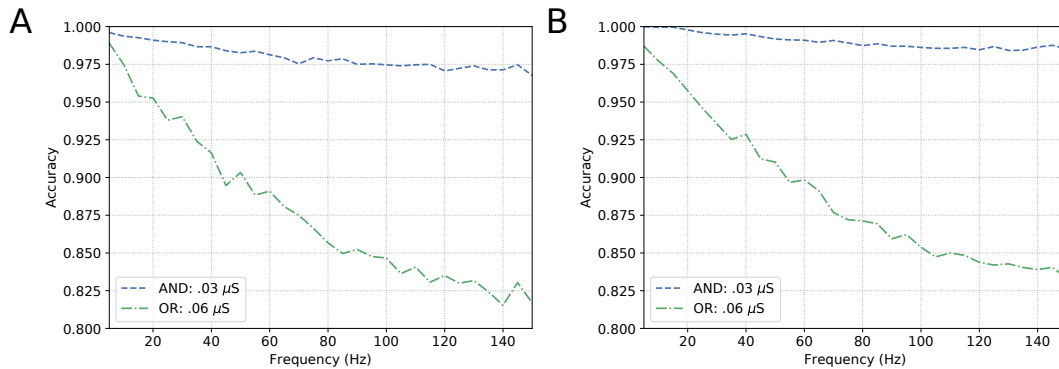
Figure 8. Analysis on reconfigurable logic gates with neurons of types (A) L23-MC, L23-NBC and L1-DAC and (B) L23-MC, L23-NBC and L1-HAC.

416 Figures 8 show similar responses when gates originally built to be of a specific kind. This means either
417 OR or AND gates can change their configurations that drives their gating capabilities by modifying the
418 synaptic weight between the connections of the input cells and the output cell. Although there is quite a
419 visible difference between the performance of AND and OR gates, even at high frequencies (150 Hz), the
420 accuracy of the reconfigurable logic gates remains above 80%.

421 3.2 Neuronal Logic Circuits

422 Once the reconfigurable behavior of the gates is assessed, they are connected to other gates to form a
423 logic circuit. The performance is measured employing a ratio (frequency response), i.e. the number of
424 spikes (bits '1') in the output divided by the nominal input frequency, in Hertz. This ratio is also known as
425 the magnitude, or gain when evaluating the data in decibels. Following the approach for individual gates,
426 the inputs are random and the frequency is increased uniformly. Since the gates showed similar accuracy
427 when increasing the input frequency, we picked the one analyzed in Figure 8A for our circuit analysis with
428 a reconfigurable logic gate, modifying only the output gate's synaptic properties.

429 Figures 9A show the results for the circuits in Figure 5A. As expected, Circuit C has a stronger attenuation
430 of the signals passing through it, and this is mainly due to the fact it is an arrangement with three AND
431 gates and, based on the truth table, an AND gate only responds to stimuli if all its inputs are active at the
432 same time. The magnitude in decibels shown in Figure 9B follow a standard presentation of the response
433 of digital filters.

434 In the non-linear case of the system, the filtering is even better than what the linear model would promise,
435 i.e. the suppression of unwanted frequencies is better due to superexponential decay. Let us compare
436 Figure 7B and Figure 9B. The linear model suggests that a constant difference of 6 dB is to be expected
437 if the synaptic weight of the output cell is halved (or doubled), and a linear, constant amplitude drop. In
438 the nonlinear model, we do observe a 20 dB/decade drop and 6 dB difference at relevant frequencies, but
439 instead of a linear trend, we observe a convex response, which helps in attenuating high frequencies faster

75
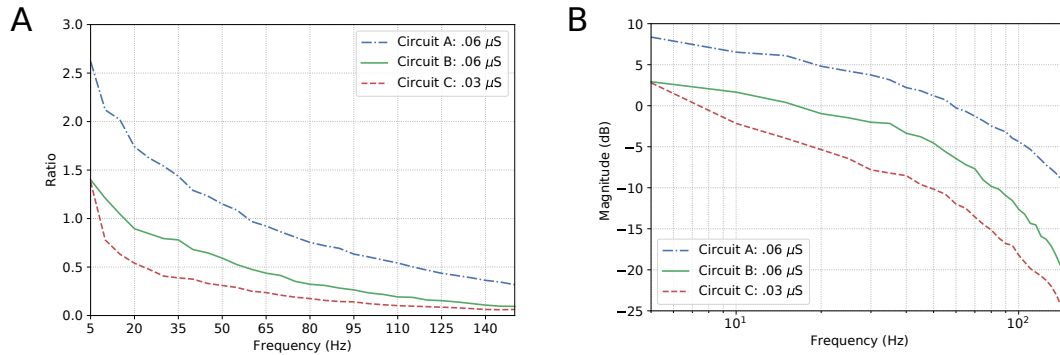
Figure 9. Effects of dynamic changes to the synaptic weight in circuits A, B and C; (A) Frequency response and (B) Magnitude in decibels.

440 than we would expect from the linear model. This is because the linear model is accurate in a neighborhood
441 of the point at which it was linearized.

442   Now, let us consider $H(\nu)$ as the response of an ideal low-pass filter, and $W(\nu)$ the response of the
443 proposed neuronal filter, the counter-efficiency of W given H is calculated as

$$\psi(W|H) = \int_0^{\nu_c} |W(\nu) - H(\nu)| \, d\nu + \int_{\nu_c}^{\nu_f} |W(\nu)| \, d\nu \tag{39}$$

444 where ν_c is the cut-off frequency and ν_f is the last evaluated frequency (in this relationship, the lower the
445 value, the more efficient the filter is). Since, in terms of magnitude, a frequency band when cut by an ideal
446 filter should be attenuated towards negative infinity ($-\infty$), we have to pick a limit for the calculation of the
447 area under the curves. In our case, after a visual inspection, the baseline for calculation chosen was -25
448 dB, because this is the closest integer value to the lowest values of magnitude.
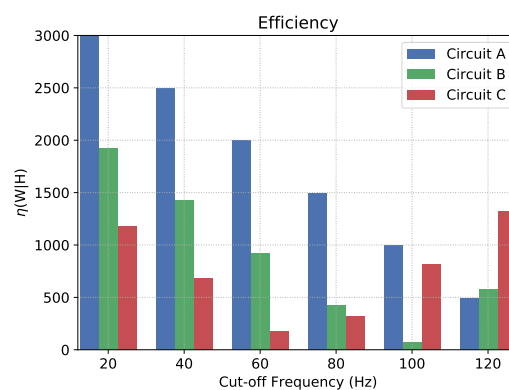
Figure 10. Counter-efficiency of the circuits when compared to ideal filters (the lower the value, the better the filter's performance).

76

449   Figure 10 depicts the counter-efficiency analysis performed for the three circuits. As it is shown, for
450   different frequency bands we have some circuits performing better than others. Also, each circuit has a
451   preferable frequency band for achieving maximum efficiency. For frequencies lower than or equal to 80 Hz,
452   Circuit C seems the most efficient, especially at 60 Hz, while frequencies around 100 Hz show Circuit B as
453   the most efficient which is also the band where it performs the best. Circuit A, on the other hand, has its
454   best performance for 120 Hz, and probably for higher frequencies as well if the trend continues.

455   This shift in performance may allow us to control which type of circuit we want to activate inside the
456   brain depending on which activity the subject is performing at the time, e.g. being awake or being asleep.
457   These changes may be induced by the intake of specific drugs that alter synaptic properties in a neuronal
458   connection.

459   Figure 11 shows a parallel analysis between the magnitude in dB and the accuracy of the filters with
460   AND gates in cascade. Each circuit is identified by a pair of characters, the first is the letter referring to the
461   circuit analyzed, the second is how many AND gates were connected in cascade. For example, $A2$ means
462   Circuit A with two AND gates in cascade, as illustrated in Figure 5B.
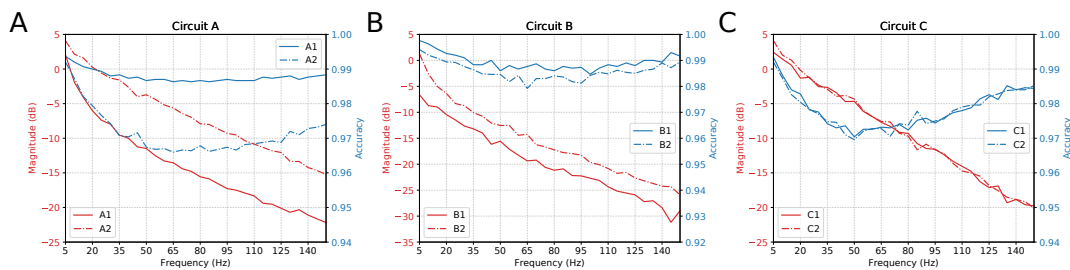
Figure 11. Parallel between Magnitude (dB) and Accuracy of the circuits with AND gates in cascade.

463   The results suggest that, by increasing the number of gates in cascade, we have to deal with attenuation
464   in the network due to propagation caused by specific characteristics of the cell, such as the connection
465   probability; hence, the more gates in cascade the worse the performance of the circuit. Also, even though
466   the ratio keeps going downwards, at some point, the accuracy will start to shoot up. With careful evaluation,
467   the dip in the accuracy along mid-range frequencies is very low in terms of scale, showing a difference of
468   only around 0.03 on the values of accuracy.

4   DISCUSSION

469   Synaptic weight plays a role in the influence of the pre-synaptic stimuli and its impact on the post-synaptic
470   neuron and has a value proportional to the synaptic conductance (Gardner, 1989) which is driven by the
471   amount and type of neurotransmitters that are being bound to the post-synaptic terminals. The higher
472   the connection probability between pairs of neurons, the stronger the influence of a specific synaptic
473   weight. This is due to the proportional relationship that the weight has with each synaptic connection that
474   individually releases a certain amount of neurotransmitters, hence, different neuron types may affect the
475   influence of a fixed value of synaptic weight. This explains how the accuracy values fluctuate between
476   different types of gates and circuits as shown in Fig. 11. Within a larger network spatial dimension, the

477   types of neurons may drive a higher accuracy fluctuation since the network connection exhibits different
478   synaptic weights between each other.

479   With our model, we have mainly investigated the attenuation on the spiking frequency for three different
480   types of circuits in which we decrease the number of OR gates by replacing them with AND gates.
481   We were also able to have the fine-tuning synaptic properties showing a difference of around 5 dB in
482   performance between the curves in Figure 9B. Changes in the synapse are also considered (Vogels and
483   Abbott, 2005), either by strengthening or weakening specific synaptic connections, logic gates were
484   built within a homogeneous network of integrate-and-fire neurons. Moreover, the experiments conducted
485   by (Goldental et al., 2014) followed a procedure that enforced stimulations on neuronal circuits within
486   a network of cortical cells *in-vitro* and they do propose other types of gates such as XOR and NOT.
487   Furthermore, we increased the number of AND gates in a cascade-like manner in order to confirm that
488   the longer the line of cascade gates, the more attenuated the signal should be if none of those elements
489   receives any kind of external stimuli despite the spike coming from the circuit, and this result is depicted
490   in Figure 11. A peak value in the difference of around 8 dB occurs in Circuit A, decreasing to around
491   5 dB in Circuit B and there is a small difference in Circuit C. The transfer function derived from the
492   Hodgkin-Huxley linear model suggests a band-pass behavior of the system (Plesser and Geisel, 1999) for
493   very low frequencies leaving us with a low-pass filter acting on higher frequencies ranging from 5 to 150
494   Hz. Considering the time for a spike to be fired that comprises depolarization, repolarization, and refractory
495   period, higher frequencies will lead to saturation and non-realistic behavior of neuronal firing.

496   Our results, therefore, suggest that neuronal logic circuits can be used to construct also digital filters,
497   filtering abnormal high-frequency activity which can have many sources including neurodegenerative
498   diseases. A metric of counter-efficiency was also proposed, which should show how far apart the real results
499   are from the ideal cases. We found that frequency bands were found to be of optimal value for different
500   types of circuits such as 60 Hz for circuit C, 100 Hz for circuit B, and 120 Hz for circuit A, as shown
501   in Figure 10. Based on the presented results, we demonstrate that by reconfiguring the gates inside the
502   digital filters we can shift the intensity with how we attenuate the spiking frequency allowing an on-the-fly
503   adaptation of the filtering tasks depending on the activity that is being performed by the subject where, for
504   instance, circuit C should outperform both A and B for frequencies lower than or equal to 80 Hz.

505   The envisioned application of the proposed mathematical framework is for in-silico pharmacology and
506   how it can be used to provide advanced prediction supporting computational strategies to test drugs. Since
507   drug design and discovery in neuroscience are very challenging, especially due to the complexity of
508   the brain and the significant impediment of the blood-brain barrier (BBB) imposes on the delivery of
509   therapeutic agents to the brain. The success rate for approval by competent authorities of such drugs is less
510   than 10%. Such a low rate is attributed not only to factors related to the disease itself, such as complexity,
511   slow development, and gradual onset but also, to the limited availability of animal models with good
512   predictive validity and the limited understanding of the biological side of the brain (Geerts et al., 2020).
513   The system model derived from a set of coupled neuron compartments can help push forward the design of
514   these neuronal filters and provide a platform for *in silico* drug-induced treatments on top of engineered
515   biological models of neurons. A platform that could lead to cost-effective drug development and analysis of
516   potential bio-computational units capable of enhancing signal processing in the brain, as well as predicting
517   long-term effects of using a specific drug are potential uses of the proposed mathematical framework.

5 CONCLUSION

518 In this work, we proposed a reconfigurable spike filtering design using neuronal networks that behave as a
519 digital logic circuit. This approach requires the cells to be sensitive to modifications through chemicals
520 delivered through several proposed methods available in the literature. From the Hodgkin-Huxley action
521 potential model we developed a mathematical framework to obtain the transfer function of the filter. This
522 required a linearization of the Hodgkin-Huxley model that changes the cable theory simplification for each
523 cell compartment. To evaluate the system, we have used our transfer function as well as the NEURON
524 simulator to show how the frequency of operation, logic circuit configuration as well as logic circuit
525 size can affect the accuracy and efficiency of the signal propagation. We observed that all-ANDs circuit
526 produces more accurate results concerning their truth-table when compared to all-ORs. In addition, the
527 results show that each digital logic circuit is also reconfigurable in terms of cut-off frequency of the filter,
528 by manipulating the types of gates in the last layer of the circuit.

529 We believe the proposed filter design and its mathematical framework will contribute to synthetic biology
530 approaches for neurodegenerative disorders such as epilepsy, by showing how the control of cellular
531 communication inside a small population can affect the propagation of signals. For future work, we plan
532 the use of non-neuronal cells, e.g. astrocytes, for the control of gating operations and the assessment of
533 neuronal filtering capabilities at a network level. Treatment techniques based on this method can be a
534 radical new approach to reaching precision and adaptable outcomes, inspired from electronic engineering
535 as well as communication engineering. Such techniques could tackle at a single-cell level, neurons affected
536 by seizure-induced high-frequency firing or bypass neurons that have been affected by a disease-induced
537 neuronal death and degeneration, thus keeping the neuronal pathway working at a performance as optimal
538 as possible.

CONFLICT OF INTEREST STATEMENT

AUTHOR CONTRIBUTIONS

541 GA performed the simulations and wrote the first draft of the manuscript. HS performed the control-
542 theoretic analysis. GA, HS and MB performed the data analysis. SB, NM, MB and MW led the work
543 development. All authors contributed to manuscript writing and revision. All authors also have read and
544 approved the submitted version.

FUNDING

REFERENCES

548 Adonias, G. L., Yastrebova, A., Barros, M. T., Balasubramaniam, S., and Koucheryavy, Y. (2019). A
549   Logic Gate Model based on Neuronal Molecular Communication Engineering. In *Proceedings of the*
550   *4th Workshop on Molecular Communications* (Linz, Austria), 15–16

Adonias, G. L., Yastrebova, A., Barros, M. T., Koucheryavy, Y., Cleary, F., and Balasubramaniam, S. (2020). Utilizing Neurons for Digital Logic Circuits: A Molecular Communications Analysis. *IEEE Transactions on NanoBioscience* 19, 224 – 236. doi:10.1109/TNB.2020.2975942

Balevi, E. and Akan, O. B. (2013). A Physical Channel Model for Nanoscale Neuro-Spike Communications. *IEEE Transactions on Communications* 61, 1178–1187. doi:10.1109/TCOMM.2012.010213.110093

Barreto, E. and Cressman, J. R. (2011). Ion concentration dynamics as a mechanism for neuronal bursting. *Journal of Biological Physics* 37, 361–373. doi:10.1007/s10867-010-9212-6

Baxter, D. A. and Byrne, J. H. (2014). Dynamical Properties of Excitable Membranes. In *From Molecules to Networks*, eds. J. H. Byrne, R. Heidelberger, and M. N. Waxham (Boston: Academic Press), chap. 14. 3rd edn., 409 – 442. doi:https://doi.org/10.1016/B978-0-12-397179-1.00014-2

Bennewitz, M. F. and Saltzman, W. M. (2009). Nanotechnology for Delivery of Drugs to the Brain for Epilepsy. *Neurotherapeutics* 6, 323 – 336. doi:https://doi.org/10.1016/j.nurt.2009.01.018. Nontraditional Epilepsy Treatment Approaches

Blier, P. and De Montigny, C. (1987). Modification of 5-HT neuron properties by sustained administration of the 5-HT1A agonist gepirone: Electrophysiological studies in the rat brain. *Synapse* 1, 470–480. doi:10.1002/syn.890010511

Brunel, N., Chance, F. S., Fourcaud, N., and Abbott, L. F. (2001). Effects of Synaptic Noise and Filtering on the Frequency Response of Spiking Neurons. *Phys. Rev. Lett.* 86, 2186–2189. doi:10.1103/PhysRevLett. 86.2186

Carnevale, N. T. and Hines, M. L. (2009). *The NEURON Book* (New York, NY, USA: Cambridge University Press), 1st edn.

Chandler, W., Fitzhugh, R., and Cole, K. S. (1962). Theoretical Stability Properties of a Space-Clamped Axon. *Biophysical Journal* 2, 105 – 127. doi:https://doi.org/10.1016/S0006-3495(62)86844-1

Chaubey, S. and Goodwin, S. J. (2016). A Unified Frequency Domain Model to Study the Effect of Demyelination on Axonal Conduction. *Biomedical Engineering and Computational Biology* 7, BECB.S38554. doi:10.4137/BECB.S38554

Feng, T., Huang, X., Ni, R., Suen, W. L. L., and Chau, Y. (2019). Nanoparticles for drug delivery targeting neurodegeneration in brain and eye. In *Nanomaterials for Drug Delivery and Therapy*, ed. A. M. Grumezescu (William Andrew Publishing). 149 – 183. doi:https://doi.org/10.1016/B978-0-12-816505-8. 00006-0

Fortune, E. S. and Rose, G. J. (1997). Passive and Active Membrane Properties Contribute to the Temporal Filtering Properties of Midbrain Neurons In Vivo. *Journal of Neuroscience* 17, 3815–3825. doi:10.1523/JNEUROSCI.17-10-03815.1997

Gardner, D. (1989). Noise modulation of synaptic weights in a biological neural network. *Neural Networks* 2, 69 – 76. doi:https://doi.org/10.1016/0893-6080(89)90016-6

Geerts, H., Wikswo, J., van der Graaf, P. H., Bai, J. P., Gaiteri, C., Bennett, D., et al. (2020). Quantitative Systems Pharmacology for Neuroscience Drug Discovery and Development: Current Status, Opportunities, and Challenges. *CPT: Pharmacometrics & Systems Pharmacology* 9, 5–20. doi:10.1002/psp4.12478

Gerstner, W., Kistler, W. M., Naud, R., and Paninski, L. (2014). *Neuronal dynamics: From single neurons to networks and models of cognition and beyond* (Cambridge, UK: Cambridge University Press)

Goldental, A., Guberman, S., Vardi, R., and Kanter, I. (2014). A computational paradigm for dynamic logic-gates in neuronal activity. *Frontiers in Computational Neuroscience* 8, 52. doi:10.3389/fncom. 2014.00052

595 Guillamon, A., McLaughlin, D. W., and Rinzel, J. (2006). Estimation of synaptic conductances. *Journal of*
596 *Physiology-Paris* 100, 31 – 42. doi:https://doi.org/10.1016/j.jphysparis.2006.09.010. Theoretical and
597 Computational Neuroscience: Understanding Brain Functions

598 Hanisch, N. and Pierobon, M. (2017). Digital modulation and achievable information rates of thru-body
599 haptic communications. In *Disruptive Technologies in Sensors and Sensor Systems* (International Society
600 for Optics and Photonics), vol. 10206, 1020603

601 Hines, M., Davison, A., and Muller, E. (2009). NEURON and Python. *Frontiers in Neuroinformatics* 3, 1.
602 doi:10.3389/neuro.11.001.2009

603 Hodgkin, A. L. and Huxley, A. F. (1952). A quantitative description of membrane current and its application
604 to conduction and excitation in nerve. *The Journal of physiology* 117, 500–544

605 Hu, W. and Bean, B. P. (2018). Differential Control of Axonal and Somatic Resting Potential by Voltage-
606 Dependent Conductances in Cortical Layer 5 Pyramidal Neurons. *Neuron* 97, 1315 – 1326.e3. doi:https:
607 //doi.org/10.1016/j.neuron.2018.02.016

608 Jirsa, V. K., Stacey, W. C., Quilichini, P. P., Ivanov, A. I., and Bernard, C. (2014). On the nature of seizure
609 dynamics. *Brain* 137, 2210–2230. doi:10.1093/brain/awu133

610 Khodaei, A. and Pierobon, M. (2016). An intra-body linear channel model based on neuronal subthreshold
611 stimulation. In *2016 IEEE International Conference on Communications (ICC)*. 1–7. doi:10.1109/ICC.
612 2016.7511483

613 Koch, C. (2004). *Biophysics of Computation: Information Processing in Single Neurons* (New York:
614 Oxford University Press), chap. Linearizing Voltage-Dependent Currents. Computational Neuroscience.
615 232–247

616 Koslow, S. and Subramaniam, S. (2005). *Databasing the Brain: From Data to Knowledge*
617 *(Neuroinformatics)* (Wiley)

618 Larouche, J. and Aguilar, C. A. (2018). New technologies to enhance in vivo reprogramming for
619 regenerative medicine. *Trends in biotechnology*

620 Lienert, F., Lohmueller, J. J., Garg, A., and Silver, P. A. (2014). Synthetic biology in mammalian cells:
621 next generation research tools and therapeutics. *Nature Reviews Molecular Cell Biology* 15, 95–107.
622 doi:10.1038/nrm3738

623 Long, L. and Fang, G. (2010). A Review of Biologically Plausible Neuron Models for Spiking Neural
624 Networks. In *AIAA Infotech@Aerospace 2010* (America Institute of Aeronautics and Astronautics),
625 1–14. doi:10.2514/6.2010-3540

626 Markram, H. et al. (2015). Reconstruction and Simulation of Neocortical Microcircuitry. *Cell* 163,
627 456–492. doi:10.1016/j.cell.2015.09.029

628 Mauro, A., Conti, F., Dodge, F., and Schor, R. (1970). Subthreshold Behavior and Phenomenological
629 Impedance of the Squid Giant Axon. *The Journal of General Physiology* 55, 497–523. doi:10.1085/jgp.
630 55.4.497

631 Mishra, A. and Majhi, S. K. (2019). A comprehensive survey of recent developments in neuronal
632 communication and computational neuroscience. *Journal of Industrial Information Integration* 13, 40 –
633 54. doi:10.1016/j.jii.2018.11.005

634 Moreno-Bote, R. and Parga, N. (2004). Role of synaptic filtering on the firing response of simple model
635 neurons. *Phys. Rev. Lett.* 92, 028102. doi:10.1103/PhysRevLett.92.028102

636 Motanis, H., Seay, M. J., and Buonomano, D. V. (2018). Short-Term Synaptic Plasticity as a Mechanism for
637 Sensory Timing. *Trends in Neurosciences* 41, 701 – 711. doi:https://doi.org/10.1016/j.tins.2018.08.001.
638 Special Issue: Time in the Brain

639   Nise, N. S. (2015). *Control Systems Engineering* (California State Politechnic University, Pomona: Wiley),
640   7 edn.

641   Peters, A. (2010).   *The Morphology of Minicolumns* (Boston, MA: Springer US), chap. 4.   45–68.
642   doi:10.1007/978-1-4419-1272-5_4

643   Plesser, H. E. and Geisel, T. (1999). Bandpass properties of integrate-fire neurons. *Neurocomputing* 26-27,
644   229 – 235. doi:https://doi.org/10.1016/S0925-2312(99)00076-4

645   Pospischil, M., Toledo-Rodriguez, M., Monier, C., Piwkowska, Z., Bal, T., Frégnac, Y., et al. (2008).
646   Minimal Hodgkin–Huxley type models for different classes of cortical and thalamic neurons. *Biological
647   Cybernetics* 99, 427–441. doi:10.1007/s00422-008-0263-8

648   Rolston, J. D., Englot, D. J., Wang, D. D., Shih, T., and Chang, E. F. (2012). Comparison of seizure control
649   outcomes and the safety of vagus nerve, thalamic deep brain, and responsive neurostimulation: evidence
650   from randomized controlled trials. *Neurosurgical Focus FOC* 32, E14

651   Sabah, N. and Leibovic, K. (1969). Subthreshold Oscillatory Responses of the Hodgkin-Huxley Cable
652   Model for the Squid Giant Axon. *Biophysical Journal* 9, 1206 – 1222. doi:https://doi.org/10.1016/
653   S0006-3495(69)86446-5

654   Scharfman, H. E. (2007). The Neurobiology of Epilepsy. *Current Neurology and Neuroscience Reports* 7,
655   348–354. doi:10.1007/s11910-007-0053-z

656   Sengupta, B., Faisal, A. A., Laughlin, S. B., and Niven, J. E. (2013). The Effect of Cell Size and Channel
657   Density on Neuronal Information Encoding and Energy Efficiency. *Journal of Cerebral Blood Flow &
658   Metabolism* 33, 1465–1473. doi:10.1038/jcbfm.2013.103. PMID: 23778164

659   Veletić, M., Barros, M. T., Balasingham, I., and Balasubramaniam, S. (2019). A Molecular Communication
660   Model of Exosome-Mediated Brain Drug Delivery.   In *Proceedings of the Sixth Annual ACM
661   International Conference on Nanoscale Computing and Communication* (New York, NY, USA:
662   Association for Computing Machinery), NANOCOM '19, 1–7. doi:10.1145/3345312.3345478

663   Vogels, T. P. and Abbott, L. F. (2005). Signal propagation and logic gating in networks of integrate-and-fire
664   neurons. *Journal of Neuroscience* 25, 10786–10795. doi:10.1523/JNEUROSCI.3508-05.2005

665   Wilson, C. J., Weyrick, A., Terman, D., Hallworth, N. E., and Bevan, M. D. (2004).   A Model of
666   Reverse Spike Frequency Adaptation and Repetitive Firing of Subthalamic Nucleus Neurons. *Journal of
667   Neurophysiology* 91, 1963–1980. doi:10.1152/jn.00924.2003. PMID: 14702332

668   Zhou, Y., Peng, Z., Seven, E. S., and Leblanc, R. M. (2018).   Crossing the blood-brain barrier with
669   nanoparticles. *Journal of Controlled Release* 270, 290 – 303. doi:https://doi.org/10.1016/j.jconrel.2017.
670   12.015

CHAPTER 8

PUBLICATION 3: NEURON SIGNAL PROPAGATION ANALYSIS OF CYTOKINE-STORM-INDUCED DEMYELINATION

Neuron Signal Propagation Analysis of Cytokine-Storm-induced Demyelination

Geoflly L. Adonias, Harun Siljak, Michael Taynnan Barros, and Sasitharan Balasubramaniam

Abstract—**Throughout history, infectious diseases pandemics have been showing humanity how vulnerable we are and, also, how they can induce a mindset shift concerning social and economic aspects. While numerous yet unknown factors are being investigated in terms of the distributed damage that a viral infection can do to the human body, recent studies have also shown that the infection can lead to lifelong sequelae that could affect other parts of the body, and one example is the brain. As part of this work, we investigate how viral infection can affect the brain by modelling and simulating a neuron's behaviour under demyelination that is affected by the cytokine storm. We quantify the effects of cytokine-induced demyelination with an end-to-end phenomenological model on the propagation of action potential signals within a neuron. We used information and communication theory analysis on the signal propagated through the axonal pathway under different intensity levels of demyelination to analyse these effects. Our simulations demonstrate that virus-induced degeneration can play a role in the signal power and spiking rate which compromise the propagation and processing of information between neurons. We also propose a transfer function that models these attenuating effects that degenerate the action potential and has the potential to be used as a framework for the analysis of virus-induced neurodegeneration and pave the way to an improved understanding of virus-induced demyelination.**

Index Terms—**Neuron, Action Potential, Demyelination, Molecular Communications, Cytokine Storm, Hodgkin-Huxley.**

I. INTRODUCTION

The recent outbreak of the **coronavirus disease 2019** (COVID-19) pandemic caused by the **severe acute respiratory syndrome coronavirus 2** (SARS-CoV-2) has shaken society as a whole, leaving a long-lasting impact on people's health. As a result, scientists from multidisciplinary fields

have been joining efforts and resources towards the study of not only the epidemiologic characteristics and transmission dynamics of the virus, but also of the physiological damage to the human body as the infection is prolonged. SARS-CoV-2 is well known for affecting primarily the respiratory system and can potentially leave lifelong sequelae in tissues and organs. Furthermore, there has been an increase in works that suggest SARS-CoV-2 may be able to invade the nervous system [1]–[4] and elicit neurodegeneration [5], [6] where sequelae may have other detrimental effects on patients' lives post-infection.

Viruses that present the ability to infect nerve cells are known to exhibit *neurotropic* properties and can also be called *neuroinvasive*. By infecting cells in the nervous system and replicating themselves within it, these viruses can negatively impact neurological functions and even cause severe nerve damage by triggering a pro-inflammatory immune response [6]. Unfortunately, SARS-CoV-2 is not the only virus that exhibits this kind of behaviour, for example, it has been shown that the Zika virus (ZKV) [7] can infect the peripheral nervous system (PNS) and, sometimes, spread to the central nervous system (CNS). Furthermore, viruses such as the human immunodeficiency virus (HIV) [8], can infect the CNS and cause **neuroinflammation** which induced by an immune response of the body and, consequently, lead to neurodegeneration [9]. A growing amount of data from the past few years support the hypothesis that chronic damage caused by different infectious agents can lead to neurodegeneration [10], as early experimental models of virus-induced demyelination have indicated [11].

Viruses are known for causing dramatic structural and biochemical changes to the host cell, by hijacking and exhausting its machinery for replication until, eventually, the cell is killed. This viral manipulation of a host cell provokes neuroinflammatory defence mechanisms that can be characterised by numerous toxic-metabolic derangements, such as cytokine storms (Fig. 1(a)). Such inflammation could potentially lead to several types of neurodegeneration, including **demyelination**. As cytokines are released to fight the infection, healthy tissues could be affected as a "collateral damage" of the fight against infectious agents [12]. Other types of coronavirus have been known to cause demyelination, such as the murine coronavirus (M-CoV), which has been identified to cause demyelinating disease and, even after the virus is cleared from the CNS, the demyelination can continue for a few months [12]. This behaviour also matches findings on SARS-CoV-1, which reports a decrease in viral titers as clinical disease worsens [13]. M-CoV is a type of coronavirus of the same genus (*betacoronavirus*) as SARS-CoV-2, and it is believed to be 43.8%-48%
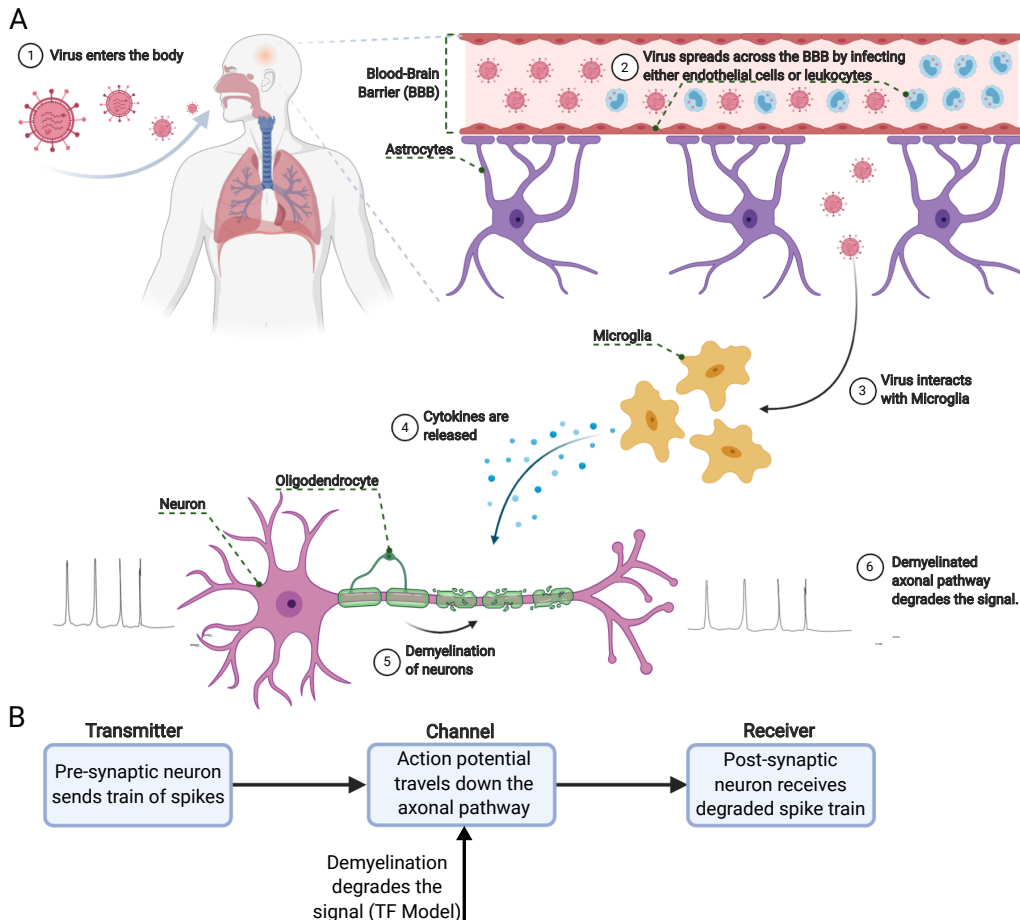
Fig. 1. Pathogenesis of a virus-induced demyelination.

similar to this novel coronavirus [14]. SARS-CoV-2, when compared to SARS-CoV-1, triggers lower levels of interferons and pro-inflammatory cytokines and chemokines. However, it is capable of infecting and replicating a significantly higher amount of viruses in human tissues [15].

This paper presents a systems-theory-based analysis of the demyelination that is, either directly or indirectly, caused by viral infections from the perspective of MC, more specifically, a neuro-spike MC. The goals of this paper are (1) to propose a model extension coupled with computational analysis on the Hodgkin-Huxley formalism to account for the effects of cytokine storms indirectly caused by viral infections; (2) to provide insights on how the demyelination will affect the neuronal information along the axonal pathway; and (3) to provide a transfer function (TF) model that describes the effects of the membrane action potential caused by the degeneration of the myelin sheath. This TF can be considered fundamentally as a model of the demyelination process itself. It is intrinsically tied with the behaviour of equivalent resistance-capacitance (RC) circuits, but at the same time, has a reduced complexity

as it opts for exponential asymptotics. Given that complex cascades of equivalent simple blocks (in our scenario, myelin sheaths) are traditionally well-approximated by first-order transfer functions with time delay and the underlying physical rationale, our model joins the family of established, applicable biophysical transfer function models. We expect that these analyses not only could pave the way for more in-depth studies that can support *in vitro* and *in vivo* experimental works on the neurological effects induced by neurotropic viral infections, but also serve as a prediction tool that can help to guide future experimental works. It may even be necessary that, as the demyelinating scenarios get more and more biologically plausible, future works may have to fine-tune some of the parameters, e.g. regarding the type of cell or the intensity of cytokine-storm-induced demyelination, of the proposed model in order to have an analysis as accurate as possible.

The contributions of this work are as follows:

- *A mathematical model that serves as a building block for a transfer function of the signal propagation:* We present a model inspired by the well-documented fact that viral

Publication 3: Neuron Signal Propagation Analysis of Cytokine-Storm-induced Demyelination

infections trigger cytokine storms and lead us towards a general transfer function that accounts for the propagation of the signal. The cytokine storms are countermeasures of the immune system against the infection. We investigate the signal power, the signal attenuation and magnitude-squared coherence (MSC) analysis of the axonal pathway as a communication channel.

- *An analysis of the effects of demyelination on the neuronal action potential propagation:* We conduct a variety of analyses, such as latency, attenuation and spiking rate, on the spike trains that pass through a demyelinated pathway. Furthermore, we also analyse how the intensity of cytokines storms correlates with the amount of attenuation present in the signal at the output of the neuron.

- *A transfer function model that accounts for the effects of the demyelination-induced attenuation:* We propose a transfer function that describes the transition of a healthy to an unhealthy neuron. The model accounts for sheath-by-sheath demyelination which affects membrane potential, peak times and spike width. This should lead to more in-depth analysis and open a new view on demyelination modelling, especially those triggered by a neurotropic viral infection and how it affects the transmembrane molecular exchange (i.e. exchange of ions and release of neurotransmitters) of the neurons.

II. Background and Literature Review

The virus replication process exhausts host cells leading to the activation of the immune system, which calls for the work of macrophages. Those are types of cells of the immune system, and their resident in the brain is the microglia [1], [4]. Macrophages secret pro-inflammatory cytokines such as interleukin-1 (IL-1), interleukin-6 (IL-6) and tumor necrosis factor *alpha* (TNF-α) aiming to fight the infection. These cytokines exert cytotoxic effects on neurons and glial cells, e.g. oligodendrocytes, damaging the myelin sheaths which are responsible for providing support and insulation to axons [16]. The dynamics of cytokine storms and their efficiency in fighting infections without further cellular damage become of increased attention to measure the neuroinflammatory effects of COVID-19. Ludwig et al. [17] found out that as the neuropathy is more severe, the higher the serum concentration of TNF-α and IL-6. This matches more recent results found by Chen et al. [18] and Song et al. [19], cytokine levels concerning the severity of COVID-19 cases. They identified a positive correlation between the levels of cytokines and the severity of the COVID-19 cases, meaning that the more severe the COVID-19 cases were, the higher were the levels of cytokines, which can lead to demyelinating lesions [5], [20].

On the other hand, the dynamics of a cytokine storm can be similar for different inflammatory scenarios, yielding the need for a more general approach that evaluates cytokine dynamics. An example is the work of Waito et al. [21] in which they match recordings of 13 different cytokines with a model of non-linear ordinary differential equations. Likewise, Yiu et al. [22] analysed the dynamics of cytokine storms and provided evidence for how cytokines induce or inhibit other cytokines. Additionally, some pieces of literature report the effects of cytokine storms on specific neuronal and non-neuronal structures. For instance, the work of Bitsch et al. [23] shows a negatively correlated relationship between the amount of microglia-produced TNF-α and the concentration of myelin oligodendrocyte glycoprotein (MOG). It shows that the more TNF-α there is, the less MOG oligodendrocytes will produce, compromising the myelin sheath structure. On the other hand, Redford et al. [24] showed how the number of axons found in sciatic nerves is affected. They found that the more the concentration of TNF-α is increased, the more axons are found to be damaged. However, the complete biophysical models of these various effects to neurons caused by infection, particularly infections from COVID-19, require urgent attention since correct treatment procedures for acute infection damage can benefit from mathematical modelling.

In the past decade, Molecular Communications (MC) has been improving biological models by accounting for the communication of cells using their signalling mechanisms as information carriers [25]. MC is a new field that is looking to characterise and engineer biological cells using concepts from communication engineering and networking [26]–[28], it bridges electrical and communications engineering, molecular biology and biomedical engineering and provides complete end-end models of biophysical transmission of molecules, their propagation, and their reception [29]–[32]. A recent survey [33] reports numerous works concerning the use of MC for the analysis and modelling of infectious diseases. However, accounts for the effects of infections are still missing from a biophysical approach even within MC models, as the COVID-19 effects are many, and the molecular interactions with the body can be used to predict the behaviour of a population of cells, even tissues and organs. The emergence of novel MC models for biophysical processes, such as the demyelination induced by COVID-19, delivers an in-depth analysis of tissue behaviour that is needed for treatments based on synthetic biology. Even further targeted drug delivery technology can alleviate the cytokine storms effects on neurons and provoke the restoration of the myelin sheath [34].

III. End-to-end Computational Model for a Cytokine-storm-induced Demyelination

Models that describe the dynamics and evolution of cytokine concentrations, without regard to the cells that secrete or are affected by them, have been proposed by Yiu et al. [22]. This model was extended by coupling together with a neuronal model that implements the behaviour of a myelinated axon [35]. By extending these models, we performed simulations with the default parameters of the cell (such as the length and diameter of each of their compartments) based on the original model. Therefore, the myelin sheath properties concerning their morphological characteristics were not modified or changed. We studied and quantified the propagation of action potentials on a Layer 5 (L5) pyramidal neuron mimicking damage to its myelin sheath. All simulations were performed with extensions to the NEURON Simulator [36].
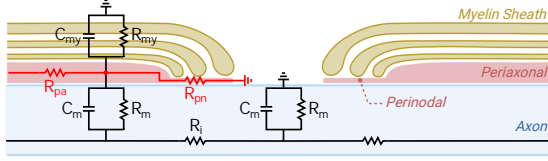
Fig. 2. Schematic of the equivalent myelinated axon circuit, with added periaxonal (P_a) and paranodal (P_n) axial resistances [35].

A. Cytokine Signalling in Microglia

The growth and decay of an individual cytokine's response to its given initial state are first represented by a second-order, linear, time-invariant ordinary differential equation. Denoting the serum concentration, $\rho(t)$ in pg/mL, and its rate of change, $\Delta_\rho(t)$, it can be represented in a vector-matrix form as follows

$$\begin{bmatrix} \dot{\rho}(t) \\ \dot{\Delta}_\rho(t) \end{bmatrix} = \begin{bmatrix} 0 & 1 \\ -a & -b \end{bmatrix} \begin{bmatrix} \rho(t) \\ \Delta_\rho(t) \end{bmatrix}, \begin{bmatrix} \rho(0) \\ \Delta_\rho(0) \end{bmatrix} \text{given,} \quad (1)$$

where the initial concentration, $\rho(0) = 0$, is referenced to the cytokine's basal level, and the initial rate of change, $\Delta_\rho(0)$, is stimulated by the TGN1412 infusion (see [22] for further details). Also, a and b are positive constants that express the sensitivity of the cytokine's acceleration to concentration and rate of change.

The cytokine's response modes are characterised by the eigenvalues, λ_1 and λ_2 (rad/day), of the stability matrix of the system, and this is as follows

$$\begin{bmatrix} \dot{\rho}(t) \\ \dot{\Delta}_\rho(t) \end{bmatrix} = \begin{bmatrix} 0 & 1 \\ -\lambda_1\lambda_2 & (\lambda_1 + \lambda_2) \end{bmatrix} \begin{bmatrix} \rho(t) \\ \Delta_\rho(t) \end{bmatrix}, \begin{bmatrix} \rho(0) \\ \Delta_\rho(0) \end{bmatrix} \text{given.} \quad (2)$$

The parameters are chosen to minimize the error between the cytokine concentration and the clinical trial measurements performed in [22]. For TNF-α, $\lambda_1 = \lambda_2 = -2.63$ and $\Delta_\rho(0) = 32821$. In this work, we will be investigating the inflammatory effects of TNF-α, as this cytokine is well-known for its pro-inflammatory properties.

B. Conduction Through a Myelinated Axon

It is well known that some neurons contain a myelin sheath wrapped around sections of their axons. Myelin sheath helps propagate electrical impulses, known as action potentials (AP) or spikes, and avoid significant attenuation due to parallel synaptic processes. According to Cohen et al. [35], the myelin sheath dynamics can be described using circuit theory (Fig. 2). This circuit is then coupled with the Hodgkin-Huxley (HH) circuit model [37], which describes the membrane potential dynamics in neurons.

Axial resistance, R_i ($\Omega \cdot \text{cm}^{-1}$), of the axon core, can be defined as the ratio between axial resistivity, r_i ($\Omega \cdot \text{cm}$), and the cross-sectional area of the axon core, and this is described as

$$R_i = \frac{4r_i}{\pi d^2}, \quad (3)$$

where d (nm) is the axon core diameter. Let δ_{pa} (nm) be the radius of the periaxonal space, then

$$\delta_{pa} = \frac{1}{2}\left[-d + \sqrt{d^2 + \left(\frac{4r_{pa}}{\pi R_{pa}} \right)} \right], \quad (4)$$

where the axial resistance in the periaxonal space, R_{pa} ($\text{G}\Omega \cdot \text{cm}^{-1}$), is calculated as the ratio between periaxonal resistivity, r_{pa} ($\Omega \cdot \text{cm}$), and periaxonal cross-sectional area. In this case, the axon core cylinder is surrounded by both the periaxonal and perinodal spaces forming a "larger" axon cylinder of diameter $d + 2\delta_{pa}$, thus

$$R_{pa} = \frac{r_{pa}}{\pi \delta_{pa}(d + \delta_{pa})}, \quad (5)$$

and, an analogous calculation can be performed for δ_{pn} (nm), r_{pn} ($\Omega \cdot \text{cm}$) and R_{pn} ($\text{T}\Omega \cdot \text{cm}^{-1}$).

Recognising that a myelin sheath is an in-series compaction of n layers, the radial resistance of the sheath, R_{my} ($\text{k}\Omega \cdot \text{cm}^2$), is the sum of the resistance of each myelin membrane, R_{mm} ($\text{k}\Omega \cdot \text{cm}^2$), formulated as

$$R_{my} = \sum_{i=1}^{n} R_{mm_i}, \quad (6)$$

and, the radial capacitance of the myelin sheath, C_{my} ($\mu\text{F} \cdot \text{cm}^{-2}$), may vary inversely to the sum of the capacitances of each of its composing membranes, C_{mm} ($\mu\text{F} \cdot \text{cm}^{-2}$), thus

$$\frac{1}{C_{my}} = \sum_{i=1}^{n} \frac{1}{C_{mm_i}}, \quad (7)$$

where the resistance and capacitance of a single myelin membrane are R_{mm} and C_{mm}, respectively. Based on this, equations (6) and (7) can be represented in terms of the number of myelin lamellae, n_{my}, as follows

$$n_{my} = \frac{R_{my}}{2R_{mm}} = \frac{C_{mm}}{2C_{my}}. \quad (8)$$

For a more detailed analysis of the myelin sheath's modelling, the reader is referred to the work of Cohen et al. [35]. Each of the of the lamellae that composes the whole myelin sheath is modelled with the same set of parameters. This is basically an assumption that each myelin lamellae is identical to the other and that the degeneration caused by the demyelination affects the myelin sheath proportionally.

C. Cytokine-induced Demyelination

As previously discussed in Section I, the literature indicates that, as microglias release pro- and anti-inflammatory to fight the infection, demyelination may also occur as a side effect and, consequently, compromise the neuronal signal propagation. There are numerous pieces of evidence linking cytokine storms to neurodegeneration [17], [21]–[23], however to the best of our knowledge, none of them goes as far as linking the storm's intensity to an approximate number of myelin lamellae, n_{my}. A linear regression ($R = 0.508$, $p = 0.001$) applied by Ludwig et al. [17] to their own data reveals a proportional relationship between the severity of

the neuropathy, ζ, (in our scenario, the neuropathy is the demyelination) and the serum concentration of TNF-α, $\rho(t)$, as

$$\zeta(t) = 20.727 - 0.9228 \cdot \rho(t). \tag{9}$$

Even though the cytokine dynamics in [22] are triggered by a specific antibody, the proportionality presented in Equation 9 is also suggested by the works of Hartung [38] and Empl et al. [39]. In this relationship, the stronger the cytokine storm is, the more severe the degeneration of the myelin sheaths. Furthermore, in this work, we are using data from [35] as a reference to indicate healthy myelin with 13 lamellae. In [17], the severity of the neuropathy was defined by scoring four nerve functions as '0' for typical values of the nerve, '1' for affected nerves (either decreased amplitude and/or decreased nerve conduction velocity) and '2' for no stimulation possible. As we are looking at it from the perspective of n_{my}, we had to re-scale these scores by applying linear interpolation to indicate approximately how many sheaths are being degraded. Therefore, building on top of their findings we hypothesise that the worst-case scenario would have a score of 8 (four nerve functions multiplied by two – no stimulation possible) which indicates $n_{my} = 0$ and the best-case scenario would have a score of 0 indicating $n_{my} = 13$. Similar experiments conducted by the scientific community potentially on top of this work can re-scale $\zeta(t)$ depending on their reference of normal myelination as the number of myelin sheaths may vary among different types of neurons from different parts of either the CNS or the PNS.

The model proposed by [17] addresses neuropathies in the PNS in which peripheral neurons are myelinated by Schwann cells. On the other hand, this work examines neuropathies in the CNS where myelination is mainly controlled by oligodendrocytes. Even though oligodendrocytes and Schwann cells can express different types of myelin proteins, a major difference would be that oligodendrocytes can myelinate several axons at the same time while Schwann cells can wrap around only a single axon at a time [40], [41]. In terms of myelination processes, both types of cells are quite similar and the model itself already leaves room for improvement as the parameters may be finely tuned as soon as new evidence is presented in the literature.

D. A Linear Model of Demyelination

The linearisation process aims to find a linear approximation of a nonlinear system, i.e. the Hodgkin-Huxley model, at an equilibrium point. This means that for small variations around said point, the linear system should behave similarly to the nonlinear system [42]. The linear model is the result of the process of linearisation applied to the conventional (nonlinear) Hodgkin-Huxley model. In this process, the dynamics of the ionic channels are "lost", the components that represent each channel (e.g. variable conductance and a voltage source) are "reduced" to a static conductance and an inductance. As the demyelination only affects the RC circuits coupled to the internodal compartments, the electronic elements for the axon should remain in their default parameters and the myelin
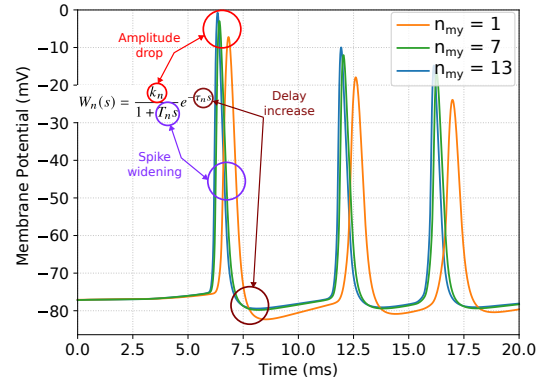
Fig. 3. Mapping of the model components and the effects on the propagated signal, and illustration of signal behaviour as it transitions from healthy to unhealthy state.

sheath RC circuits be affected by the inflammatory effects of a cytokine storm. Based on a given healthy neuron, we want to predict the signal effects on spike trains that are expected from a demyelinated neuron. Let n, the number of the myelin sheaths, be a tunable parameter of the model (in this section, we refer to n_{my} as n for clarity of index notation). This mechanism is depicted in the block diagram in Fig. 1(b).

In telecommunication systems, the study of damage and degradation often asks for a model of damage effects which could explain how healthy (i.e., signals characteristic to the system without damage) transition into faulty signals (i.e., signals characteristic to the damaged system). Observing faulty signals resulting from the propagation of standard signals through a transfer function superimposed on the original system is a well-established concept; examples of its application include modelling of cables [43]. It makes intuitive sense to observe such a transfer function as taking the healthy system's output and delivering the faulty, unhealthy signal as the faulty output, which results in signal degradation for a worsening channel it traverses. In our case, this means that we will construct a transfer function which, for an input that represents a healthy neuronal signal, delivers an output equivalent to that of a demyelinated neuron. The opposite process, in which an "adaptor" transfer function would convert a signal from a deteriorated neuron into one of a healthy neuron, is anti-causal as it would have to introduce negative time delays in the signal.

In this regard, when we speak of our *model*, we have the transfer function in mind. Our model's *input* is the series of spikes produced by a healthy pre-synaptic neuron and the model's *output* is the series of spikes a demyelinated neuron would fire, as illustrated in Fig. 1(b). The model *parameters* are factors in the transfer function; their value depends on the number of myelin sheaths we desire the demyelinated neuron to have. Hence, the number of myelin sheaths is a tunable scalar value characterising the model. Now that we have established the processing chain, the choice for the

transfer function is made by observing the general trends in the output signals for various values of n. Namely, as seen in Fig. 3, the transfer function emulating the effect of myelin deficiency needs to allow for the attenuation of the signal, widening of the spikes, and overall propagation delay. An obvious candidate is the traditional First Order Plus Time Delay (FOPTD) function [44], given by

$$W_n(s) = \frac{k_n}{1 + T_n s} e^{-\tau_n s},\tag{10}$$

where we assume that the parameters k_n, T_n and τ_n have different values for different values of n. While those values could be tabulated and looked up for specific values of n, we set a more ambitious goal of determining the laws according to which they change. Here we make a hypothesis that they follow exponential law (namely, $\log k_n = a_0 \cdot a_r^n$, $T_n = T_o \cdot T_r^n$ and $\tau_n = \tau_0 \cdot \tau_r^n$), based on the following reasoning.

Turning a healthy signal into a deteriorated one in our model is a process of cancelling the effect of passing through some of the sheaths. For example, if the healthy baseline signal is achieved with $n = 13$, emulation of $n = 10$ can be interpreted as undoing the effect of $\Delta n = 3$ sheaths, i.e. the effect of a cascade of three blocks representing a "sheath undo function". This approximation is good for larger Δn, as it allows for the approximations like $(1 + T\bar{s})^{\Delta n} \approx 1 + T^{\Delta n}s$, i.e. giving rise to a $T_n \sim e^n$ law. In Section IV, we revisit this hypothesis, both in terms of the exponential law's existence and in terms of the domain of accuracy. Introducing exponential laws for the coefficients in this transfer function gives us the final form of our transfer function, which is represented as

$$W_n(s) = \frac{e^{a_0 \cdot a_r^n}}{1 + T_0 \cdot T_r^n s} e^{-\tau_0 \cdot \tau_r^n s} = \frac{e^{a_0 \cdot a_r^n - \tau_0 \cdot \tau_r^n s}}{1 + T_0 \cdot T_r^n s}.\tag{11}$$

The final form of equation 11 suggests the rationale behind suggesting exponential behaviour of $a = \log k$ instead of k itself: in the s-domain, we obtain a function of the form $\frac{e^{(\alpha + \beta s)}}{\gamma + \delta s}$, which in turn in the Fourier domain corresponds to $\frac{e^{(\alpha + j\beta\omega)}}{\gamma + j\delta\omega}$. Knowing that the behaviour of the myelin circuit originates from connections of R (purely passive, real impedance) and C (purely active, imaginary impedance), it is expected to observe this symmetric real-imaginary coupling of terms.

The knowledge about the equivalent model of the myelin circuit, a ladder of resistors and capacitors supports the choice of FOPTD, and this is known as a convenient model for large RC circuits [45]. Namely, the circuit consists of linear components and as such can be represented by a linear model. Furthermore, with the increasing order of such a linear model, there is a necessity to replace it with a simpler first-order model such as FOPTD as it grows and will keep the complexity of the model low while retaining accuracy.

FOPTD is not an uncommon choice in biophysics, where it has been used to model glucose control [46], because they are simple for identification [44] and for quick and accurate tuning of the controllers that can regulate their behaviour [47].

Nonetheless, our model may help in designing chemical control loops for myelin reinforcement in a similar manner.

To verify the quality of the model, we introduce a metric based on root mean square error (RMSE):

$$M_n = 20 \log_{10}\left(\frac{RMSE_{N,n}}{RMSE_{W,n}}\right).\tag{12}$$

Here, $RMSE_{W,n}$ stands for the RMSE of the output of our transfer function W_n compared to the actual output signal for n sheaths, i.e. if the m is the number of samples, which is represented as

$$RMSE_{W,n} = \sqrt{\frac{1}{m}\sum_{i \geqslant 1}(x_{n,i} - x_{W,i})^2}.\tag{13}$$

Analogously, we can find the value for $RMSE_{N,n}$ which corresponds to the RMSE of the output signal produced by another model N compared to the nth actual output signal. The quantity M_n is positive where our model W_n is more accurate (has lower RMSE) than the model N we are comparing to it.

Certainly, the parameters might eventually change, however, qualitatively speaking, changes in axon structure from different neurons should exhibit similar behaviour to each other. For example, some delay on signal propagation may be introduced due to different axonal lengths [48] but, it should not affect the shape of the action potentials as it is the case with axons that have been demyelinated. Further more, the transfer function works on sub-threshold neuronal signalling and this stimulation technique usually does not lead to the firing of action potentials even though it can still fire depending on the intensity of the stimuli. Our aim is to apply a similar approach to Khodaei and Pierobon [49] to study the impact on the signalling caused by the demyelination that may have been indirectly caused a viral infection.

E. Signal Analysis

Visually, we first noticed subtle shifts in amplitude (peak potential reached by the membrane) and in time (spikes were taking longer to reach their peak values). We then decided to quantify these shifts, both in amplitude and in time, on average, by proposing a metric that we called **relative mean shift**. For the analysis on time shift, we consider the points in time where each spike peaked at the input as T_{in}^k, where $k = \{1, 2, 3, ..., K\}$ identifies the order of each spike and, T_{out}^k as the peak times at the output. Thus, we define the relative mean time shift, $\overline{\delta_t}$ (ms), as

$$\overline{\delta_t} = \frac{1}{K}\sum_{k=1}^{K}(T_{out}^k - T_{in}^k),\tag{14}$$

analogously, we can define the relative mean amplitude shift, $\overline{\delta_v}$ (mV), with V_{in}^k and V_{out}^k as the peak amplitudes of spike k at the input (spike peak observed in the soma) and output (spike peak observed in the axon), respectively.

As there is an average shift in time inside the channel itself due to demyelination, we also expect an increase in **latency** as we decrease n_{my}. In order words, latency is the time interval between the input and the output, and it often occurs due
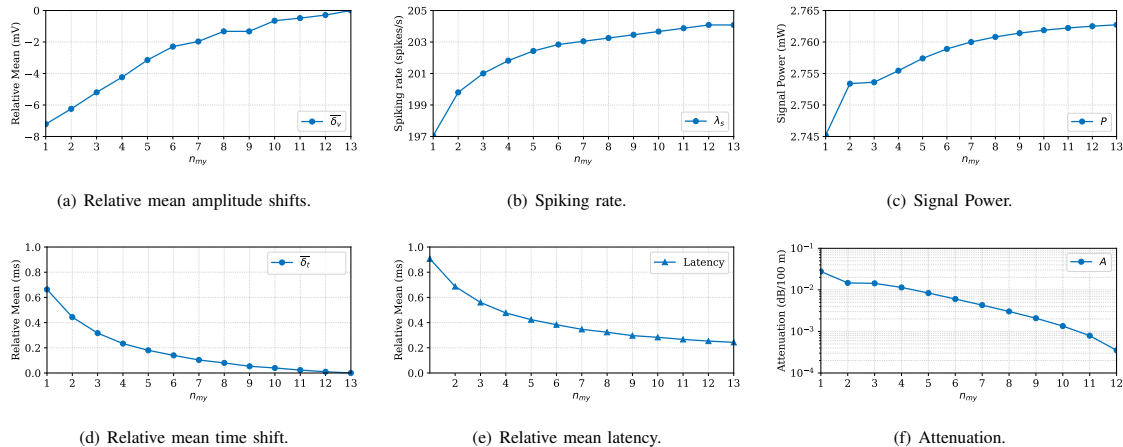
(a) Relative mean amplitude shifts.

(b) Spiking rate.

(c) Signal Power.

(d) Relative mean time shift.

(e) Relative mean latency.

(f) Attenuation.

Fig. 4. Measurements of attenuation and delay. All results except for Fig. 4(e), use the signal $n_{my} = 13$ as their input and $1 \leqslant n_{my} \leqslant 12$ as the output. Fig. 4(e) uses the recordings from the soma of the neuron and is compared with $1 \leqslant n_{my} \leqslant 13$.

to the channel or network's intrinsic characteristics. In our scenario, we are looking for the time the first spike peaked at the output, concerning the point when this same spike peaked at the soma of the neuron. Later, analogous to the relationship between $\overline{\delta_t}$ and the latency, we decided to look into a potential attenuation on the power of the signal, P (mW), as we have already discussed a relatively heavy mean attenuation in the membrane potential, $\overline{\delta_v}$. Let us define P as

$$P = \lim_{J \to \infty} \left(\frac{1}{2J+1} \sum_{j=-J}^{J} |x[j]|^2 \right), \tag{15}$$

where in a set of J samples, $x[j]$ corresponds to the potential of the membrane at the j-th sample.

We also quantified the attenuation of the signal, A in dB/100 m, which is the gradual loss of power of a signal over its propagation through the channel. Depending on the attenuation coefficient, one can calculate more accurately the attenuation in a specific material. For our analysis, we used the generic form of attenuation for RF cables. This decision is based on the fact that the axonal pathway is modelled using cable theory as a leaky cable. Thus,

$$A = 10 \cdot \log_{10} \left(\frac{P_i}{P_o} \right), \tag{16}$$

where P_i and P_o, in W, are the input and output power of the signal. In this analysis, the input is the spike train through a healthy neuron and the output would be the spike train through a demyelinated one.

Lastly, we also analysed the relation between the reference spike train ($n_{my} = 13$) and all other demyelinating scenarios ($1 \leqslant n_{my} \leqslant 12$). The intention is to understand how much power is being transferred between each pair of signals. With that in mind, we applied a coherence (C_{xy}) metric, which is described as

$$C_{xy}(\omega) = \frac{S_{xy}(\omega)^2}{S_{xx}(\omega) S_{yy}(\omega)}, \tag{17}$$

where $S_{xy}(\omega)$ is the cross-spectral density between the two signals and, $S_{xx}(\omega)$ and $S_{yy}(\omega)$ are the power spectrum densities of input and output, respectively.

IV. COMPUTATIONAL RESULTS AND DISCUSSION

Let us consider the proportionality between the severity of the neuropathy, $\zeta(t)$, and the number of myelin lamellae, n_{my}, as described in Section III-C. Our analysis consisted of an evaluation of the neuronal behaviour and spike propagation under normal circumstances ($n_{my} = 13$), followed by an analysis on the demyelination by decreasing n_{my}. The objective is to understand what happens to the neuronal information when travelling through a demyelinated axonal pathway. In other words, we are looking at the signalling within a single neuron that has been impacted by the demyelination on its own, rather than signals that have changed from pre-synaptic neurons that may be affected by cytokine storms. The neuron receives an external current of 3 nA for 15 ms starting at time $t = 2.5$ ms in a 20-ms simulation. The spikes evoked under normal circumstances are considered our input of the channel, and the spikes at the far end of the axon are the output. The axon itself is our communication channel, while the demyelination is acting as an attenuator for the channel, as illustrated in Fig. 1.

A. Analysis of a Demyelination-induced Channel Attenuation

The results for $\overline{\delta_v}$ and $\overline{\delta_t}$ from Equation (14) are shown in Figs. 4(a) and 4(d), respectively. The former shows that membrane potential is on average affected by an eight-fold decrease. This matches fundamental computational neuroscience theory on neuronal modelling which states that a neuron

(a) Signal coherence with $n_{my} = 1$.

(b) Signal coherence with $n_{my} = 12$.

(c) Mean and standard deviation of the signal coherence for all n_{my}.
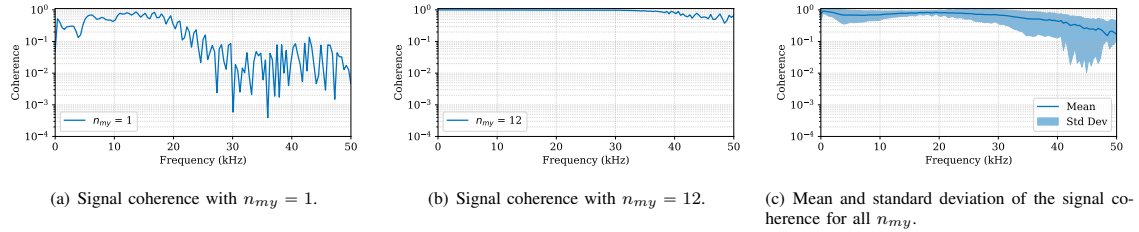
Fig. 5.   Signal coherence between $n_{my} = 13$ and (a) $n_{my} = 1$; (b) $n_{my} = 12$; and, (c) mean and standard deviation of the signal coherence with $1 \leqslant n_{my} \leqslant 12$.

(a) Time offset of spike peaks

(a) Ratio of spike amplitudes

(b) Time offset of spike onsets

(b) Ratio of pulse widths
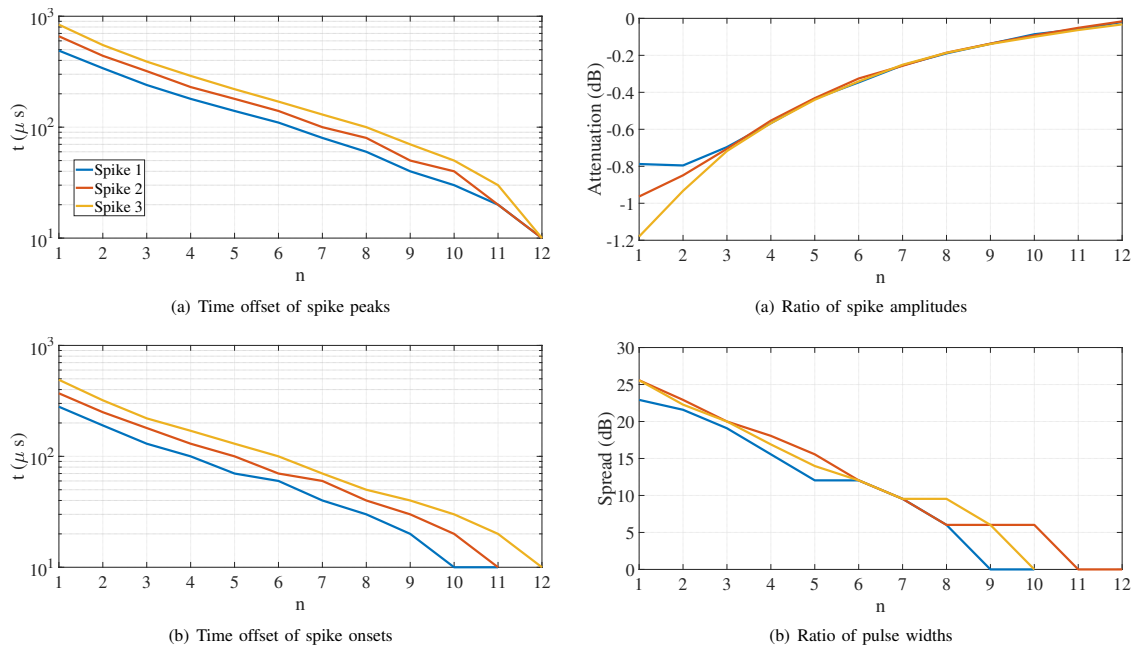
Fig. 6.   Exponential relationships between signals from different demyelinated neurons compared to the healthy $n = 13$ case.

Fig. 7.   Exponential relationships between signals from different demyelinated neurons compared to the healthy $n = 13$ case.

gradually leaks a small amount of the input signal as it travels through it, and this "leak" worsens on unmyelinated cables [50], [51]. On the other hand, from the latency data (Fig. 4(e)), we notice that there is a subtle "lag" for the signal to travel across the axon even under normal circumstances matching findings in the literature [52] for models of CNS demyelination. This is most likely due to a maximum conduction speed inherent in the axonal membrane itself. As we go from our worst scenario towards a regular healthy myelin sheath, there is a massive decrease of about 73% in the latency.

Fig. 4(b) depicts how the spiking rate is affected by the demyelination. As we expected, as the spikes start to get wider and far from each other, the spiking rate gets lower. This corroborates findings on demyelination-induced effects on spiking rate [53]. The rate at which a neuron fires action potentials is significant for modulating and encoding neuronal

information in cognitive, sensory and motor functions.

Fig. 4(c) shows that the decrease in signal power is quite subtle, and from the worst-case scenario to the best, there is a difference of less than $20\,\mu\mathrm{W}$. This indicates how demyelination affects the energy consumption per unit time used to propagate the axon's action potentials. As the signal starts to get degraded, it is less and less likely a spike would be evoked at the post-synaptic neurons connected to a demyelinated cell [51]. Demyelination does not affect only the post-synaptic neuron by reducing the chances of evoking post-synaptic potential, but it can compromise the spiking rate of the demyelinated neuron itself. Furthermore, we decided to investigate the attenuation caused by the demyelination from a more generic communication systems point of view as expressed in Equation 16. The results presented in Fig. 4(f) show how the signal is more attenuated as we remove each

myelin sheath. It not only shows consistency between our results and validates our hypothesis but also supports findings on failing pre-synaptic AP due to demyelinating diseases [51]. We decided to sweep through the entire range of the number of myelin sheaths instead of emphasising the cytokine storm time-dependency because it made more sense as we wanted to identify every potential demyelination effect to the axonal pathway.

Lastly, Fig. 5 shows the results for the signal coherence. In Fig. 5(a), we show the coherence with regards to our worst scenario, $n_{my} = 1$, in which there clearly are more oscillations in lower frequency bands when compared to Fig. 5(b). Fig. 5(b) shows the coherence for a light demyelination, $n_{my} = 12$, where only 1 sheath has been removed with regards to a healthy scenario, $n_{my} = 13$. Fig. 5(c), describes the mean and standard deviation of how the coherence values ($1 \leqslant n_{my} \leqslant 12$) fluctuate in the $0 - 50$kHz spectrum. Neuronal coherence has been known to serve neuronal communication as an indicator of the efficiency of the exchange of information [54]. In this work, it is noticeable how coherence measurements show higher instability for severely demyelinated neurons in comparison with light demyelination for low- and mid-frequency ranges. As demyelination worsens, so does the reliability of the information going down the axonal channel. All coherence plots showed some fluctuations for the higher end of the frequency range. We believe the fluctuations in the coherence plots is a finite window effect. In other words, the Fast Fourier Transform (FFT) implicitly filters the data with a rectangular time-domain filter, which is a sinc-shaped filter in the frequency domain. For this reason, we are bound to get those lobes.

B. The Linear Model Identification and Verification

Let us observe the changes that the output of a neuron goes through when n varies, and understand these dynamics as depicted in Fig. 3. Reduction in the number of myelin sheaths (n, $1 \leqslant n \leqslant 13$) causes an increasing delay in the signal, i.e., spikes start later in neurons with less myelin, and they take longer to reach the peak value (in this section, we also refer to n_{my} as n for improved consistency with Section III-D). On the other hand, in terms of the shape of the spikes, we observe the effect on the spike height and the spike width (full width at half maximum, FWHM) also in Fig. 3. This solution was adopted by identifying a suitable transfer function.

In Figs. 6(a) and 6(b) we verify that time intervals represented here correspond to $\Delta t = t_n - t_{13}$ for $1 \leqslant n \leqslant 12$, i.e., they are the "lag" observed between 13-sheath neuron, which will be the input to our model and other analysed scenarios that the model needs to approximate well, given the value of $n < 13$.

At this point, we can say that (1) for $1 \leqslant n \leqslant 10$, we see an exponential decay in the "lag" as n grows; (2) spike onsets reach the values observed in $n = 13$ one by one (1st spike for $n = 10$, 2nd for $n = 11$, 3rd for $n = 12$) while all the peaks reach the $n = 13$ time values in the same case of $n = 12$. The first conclusion suggests that we will have a transport delay term $e^{-\tau_n s}$ in the transfer function, in which the delay τ_n

will be an exponential function of n. The second conclusion suggests that this term cannot explain all of the dynamics: some of the lag is contributed by a real pole $-1/T_n$, i.e. a term $(1 + T_n s)^{-1}$ in the transfer function. Furthermore, after $n = 10$, the delay term vanishes and the only effect seen is the one of the pole (we will ignore this effect, as our approximation focus will be for the interval up to $n = 10$). Again, given the linearity of the log plot, i.e. exponential nature of the curve, it is expected that T_n is an exponential function of n.

In Figs. 7(a) and 7(b) we observe the behaviour of logarithms of spike amplitudes and pulse widths in the region of interest, which suggests (1) time-invariance of the system, as all three pulses collapse in the same amplitude curve, and (2) that the change in the pulse width requires the real pole $-1/T_n$. This reasoning, graphically presented in Fig. 3, confirms our hypothesis about the applicability of the FOPTD transfer function (10) and its exponential coefficients from Equation (11).

The identified parameters of the model 11 are $a_0 = 0.35$, $a_r = 0.7$, $\tau_0 = 54.42$, $\tau_r = 0.66$, $T_0 = 20.27$ and $T_r = 0.8$. Those values were found with the Levenberg-Marquardt [55] numerical optimisation. The iterative procedure was conducted by determining the values of k_n, τ_n, T_n for $n = 6$, then using those values as initial guesses for $n = 5$ and $n = 7$, and subsequent values. The relationship between exponential approximation, or linearisation in the *log*-domain, and the best choice of coefficients without exponential law assumption is shown in Fig. 8(a).

It is expected that this would be a good approximation for the observed signals in the "exponential domain", $1 \leqslant n \leqslant 10$. While the approximation can be accurate outside of this domain as well, we focus on applicability within the range, and we verified it using the RMSE metric introduced earlier in Equation (12). For larger values of n, our numerical estimation found τ to be zero, hence it could not be shown in a *log* plot.

Fig. 8(b), representing M_n for $1 \leqslant n \leqslant 12$, gives the answer to the following question: if one ignores the variability in n and replaces every output signal (x_n) with (a) one of a completely deteriorated neuron $N = 1$, (b) averagely damaged neuron $N = 6$, or (c) a healthy neuron $N = 13$, how high is the amplitude of error, compared to that of our model. As expected, for $n = N$ this ratio goes down to $-\infty$ dB as the approximation with exact signals is perfect. However, for any other value, even $N \pm 1$, our approximation is superior (i.e., above 0 dB). It is important to emphasise that, as observed in Figs. 4- 8, this demyelinating behaviour can be caused by other sources of degeneration. However, there are no claims those results are caused **only** by virus infections, rather we can say that it is clear from the literature that there is a specific demyelination caused by viruses and, we proposed a phenomenological model that takes into account the potential effects indirectly caused by a viral infection into the nervous system.

V. CONCLUSION

In this work, we proposed an end-to-end model that takes advantage of the fact that viruses can invade the nervous system and affect the brain. This model expresses the dynamics

(a) Parameter estimation for the transfer function.

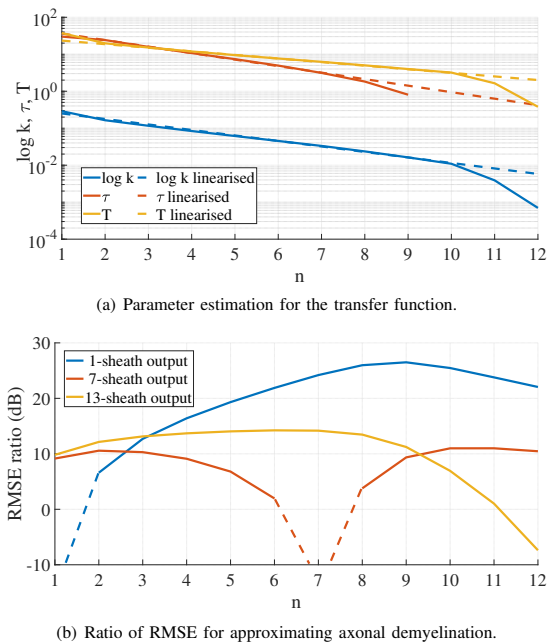(b) Ratio of RMSE for approximating axonal demyelination.

Fig. 8. Estimation and performance for a linear model of demyelination; (a) Estimated parameters of the transfer function, and their exponential approximation and, (b) Ratio of the RMSE for approximating a demyelinated with the single sheath case, average demyelinated neuron, or a healthy neuron and RMSE for approximating the demyelinated neurons with our transfer function.

of a cytokine storm and its relation to the amount of demyelination that may subject to a neuron. From evidence found in the literature, we developed a phenomenological model capable of mimicking cytokine-storm-induced demyelination's degenerative effects. We also proposed a transfer function aiming towards a linear model of the demyelination. Using traditional control and systems theory, we propose a FOPTD function that could help the design of chemical control loops for the reinforcement of myelin. It is important to emphasise that, even though we believe the linear approach described in this work can be a stepping stone for more complex systems, the whole system itself is highly non-linear. Thus, this should be taken into account as it can affect the accuracy of future synthetically engineered therapeutics.

Although the discovery and design of new drugs is a timely effort that require multidisciplinary teams working together, it is important to not only understand what computational tools can offer to improve the accuracy of proposed approaches but also to reproduce cells and molecules interactions as an area of computed-aided drug development. We believe that this model can help bio-technologists as well as pharmacologists to design drugs that will be able to minimise and, hopefully, neutralise the impact of cytokine storms on myelin sheaths. This could be achieved by adding new modules to the model to facilitate the remyelination of axons and, even though the process of remyelination rarely regenerates the myelin sheaths back to their original state [56], this approach could be used

to determine the treatment strategy required to remyelinate the neuron towards a state as close as possible to a healthy fully myelinated neuron.

The results show that the demyelination induced by the cytokine storm not only degrades the signal but also compromises the signal propagation inside the axon. The signal is attenuated and shifted in time and influences the release of excitatory neurotransmitters into the synaptic cleft. This whole analysis led to the development of a transfer function that fundamentally represents the process of demyelination itself. It not only decreases the level of complexity of the system linking itself with the behaviour of an RC circuit but also underlies the physical rationale of the system by applying biophysically plausible transfer function models. We believe that the proposed models will contribute to bioengineering approaches for neurodegeneration, especially demyelinating disease.

For future work, we plan to couple our computational modelling with wet-lab experiments to assess and improve our model's accuracy. There are many other interesting experiments to be done on top of the current work, one example would be whether cytokines diffusion would behave differently in distinct parts of the brain as they also may present different diffusion coefficients that need to be further investigated. Also, different viral infections can trigger cytokine storms with different concentration levels and many of those levels may be similar to one another depending on whether there are any similarities between the viruses under analysis. We expect that our proposed technique could pave the way for more sophisticated and precise approaches for the treatment of neurodegeneration.

REFERENCES

[1] A. S. Zubair, L. S. McAlpine, T. Gardin, S. Farhadian, D. E. Kuruvilla, and S. Spudich, "Neuropathogenesis and Neurologic Manifestations of the Coronaviruses in the Age of Coronavirus Disease 2019: A Review," *JAMA Neurology*, 05 2020. [Online]. Available: https://doi.org/10.1001/jamaneurol.2020.2065

[2] I. Sanclemente-Alaman *et al.*, "Experimental Models for the Study of Central Nervous System Infection by SARS-CoV-2," *Frontiers in Immunology*, vol. 11, p. 2163, 2020. [Online]. Available: https://doi.org/10.3389/fimmu.2020.02163

[3] V. Montalvan, J. Lee, T. Bueso, J. De Toledo, and K. Rivas, "Neurological manifestations of COVID-19 and other coronavirus infections: A systematic review," *Clinical Neurology and Neurosurgery*, vol. 194, p. 105921, 2020. [Online]. Available: https://doi.org/10.1016/j.clineuro.2020.105921

[4] E. Song *et al.*, "Neuroinvasion of SARS-CoV-2 in human and mouse brain," *Journal of Experimental Medicine*, vol. 218, no. 3, Jan 2021, e20202135. [Online]. Available: https://doi.org/10.1084/jem.20202135

[5] L. Zanin *et al.*, "SARS-CoV-2 can induce brain and spine demyelinating lesions," *Acta Neurochirurgica*, vol. 162, no. 7, pp. 1491–1494, Jul 2020. [Online]. Available: https://doi.org/10.1007/s00701-020-04374-x

[6] Y. Wu, X. Xu, Z. Chen, J. Duan, K. Hashimoto, L. Yang, C. Liu, and C. Yang, "Nervous system involvement after infection with COVID-19 and other coronaviruses," *Brain, Behavior, and Immunity*, vol. 87, pp. 18 – 22, 2020. [Online]. Available: https://doi.org/10.1016/j.bbi.2020.03.031

[7] Y. Oh *et al.*, "Zika virus directly infects peripheral neurons and induces cell death," *Nature Neuroscience*, vol. 20, no. 9, pp. 1209–1212, Sep 2017. [Online]. Available: https://doi.org/10.1038/nn.4612

[8] V. Valcour *et al.*, "Central Nervous System Viral Invasion and Inflammation During Acute HIV Infection," *The Journal of Infectious Diseases*, vol. 206, no. 2, pp. 275–282, 05 2012, on behalf of the RV254/SEARCH 010 Study Group. [Online]. Available: https://doi.org/10.1093/infdis/jis326

[9] Y. Cheng, D. Skinner, and T. Lane, "Innate Immune Responses and Viral-Induced Neurologic Disease," *Journal of Clinical Medicine*, vol. 8, no. 1, p. 3, Dec 2018. [Online]. Available: http://doi.org/10.3390/jcm8010003

[10] G. De Chiara, M. E. Marcocci, R. Sgarbanti, L. Civitelli, C. Ripoli, R. Piacentini, E. Garaci, C. Grassi, and A. T. Palamara, "Infectious Agents and Neurodegeneration," *Molecular Neurobiology*, vol. 46, no. 3, pp. 614–638, Dec 2012. [Online]. Available: https://doi.org/10.1007/s12035-012-8320-7

[11] M. C. Dal Canto and S. G. Rabinowitz, "Experimental models of virus-induced demyelination of the central nervous system," *Annals of Neurology*, vol. 11, no. 2, pp. 109–127, 1982. [Online]. Available: https://onlinelibrary.wiley.com/doi/abs/10.1002/ana.410110202

[12] S. A. Stohlman and D. R. Hinton, "Viral Induced Demyelination," *Brain Pathology*, vol. 11, no. 1, pp. 92–106, 2001. [Online]. Available: https://doi.org/10.1111/j.1750-3639.2001.tb00384.x

[13] A. A. Dandekar and S. Perlman, "Immunopathogenesis of coronavirus infections: implications for SARS," *Nature Reviews Immunology*, vol. 5, no. 12, pp. 917–927, Dec 2005. [Online]. Available: https://doi.org/10.1038/nri1732

[14] M. Geldenhuys *et al.*, "A metagenomic viral discovery approach identifies potential zoonotic and novel mammalian viruses in Neoromicia bats within South Africa," *PLOS ONE*, vol. 13, no. 3, pp. 1–27, 03 2018. [Online]. Available: https://doi.org/10.1371/journal.pone.0194527

[15] H. Chu *et al.*, "Comparative replication and immune activation profiles of SARS-CoV-2 and SARS-CoV in human lungs: an ex vivo study with implications for the pathogenesis of COVID-19," *Clinical Infectious Diseases*, 04 2020. [Online]. Available: https://doi.org/10.1093/cid/ciaa410

[16] T. D. Merson, M. D. Binder, and T. J. Kilpatrick, "Role of Cytokines as Mediators and Regulators of Microglial Activity in Inflammatory Demyelination of the CNS," *NeuroMolecular Medicine*, vol. 12, no. 2, pp. 99–132, Jun 2010. [Online]. Available: https://doi.org/10.1007/s12017-010-8112-z

[17] J. Ludwig *et al.*, "Cytokine expression in serum and cerebrospinal fluid in non-inflammatory polyneuropathies," *Journal of Neurology, Neurosurgery & Psychiatry*, vol. 79, no. 11, pp. 1268–1274, 2008. [Online]. Available: https://doi.org/10.1136/jnnp.2007.134528

[18] G. Chen *et al.*, "Clinical and immunological features of severe and moderate coronavirus disease 2019," *The Journal of Clinical Investigation*, vol. 130, no. 5, pp. 2620–2629, 5 2020. [Online]. Available: https://doi.org/10.1172/JCI137244

[19] P. Song, W. Li, J. Xie, Y. Hou, and C. You, "Cytokine storm induced by SARS-CoV-2," *Clinica Chimica Acta*, vol. 509, pp. 280–287, 2020. [Online]. Available: https://www.sciencedirect.com/science/article/pii/S0009898120302813

[20] A. Zoghi, M. Ramezani, M. Roozbeh, I. A. Darazam, and M. A. Sahraian, "A case of possible atypical demyelinating event of the central nervous system following COVID-19," *Multiple Sclerosis and Related Disorders*, vol. 44, p. 102324, 2020. [Online]. Available: https://doi.org/10.1016/j.msard.2020.102324

[21] M. Waito *et al.*, "A Mathematical Model of Cytokine Dynamics During a Cytokine Storm," in *Mathematical and Computational Approaches in Advancing Modern Science and Engineering*, J. Bélair *et al.*, Eds. Cham: Springer International Publishing, 2016, pp. 331–339. [Online]. Available: http://doi.org/10.1007%2F978-3-319-30379-6_31

[22] H. H. Yiu, A. L. Graham, and R. F. Stengel, "Dynamics of a Cytokine Storm," *PLOS ONE*, vol. 7, no. 10, pp. 1–15, 10 2012. [Online]. Available: https://doi.org/10.1371/journal.pone.0045027

[23] A. Bitsch, T. Kuhlmann, C. Da Costa, S. Bunkowski, T. Polak, and W. Brück, "Tumour necrosis factor alpha mRNA expression in early multiple sclerosis lesions: Correlation with demyelinating activity and oligodendrocyte pathology," *Glia*, vol. 29, no. 4, pp. 366–375, 2000. [Online]. Available: https://doi.org/10.1002/(SICI)1098-1136(20000215)29:4⟨366::AID-GLIA7⟩3.0.CO;2-Y

[24] E. J. Redford, S. Hall, and K. J. Smith, "Vascular changes and demyelination induced by the intraneural injection of tumour necrosis factor," *Brain*, vol. 118, no. 4, pp. 869–878, 08 1995. [Online]. Available: https://doi.org/10.1093/brain/118.4.869

[25] T. Nakano, M. J. Moore, F. Wei, A. V. Vasilakos, and J. Shuai, "Molecular Communication and Networking: Opportunities and Challenges," *IEEE Transactions on NanoBioscience*, vol. 11, no. 2, pp. 135–148, 2012.

[26] B. D. Unluturk, S. Balasubramaniam, and I. F. Akyildiz, "The Impact of Social Behavior on the Attenuation and Delay of Bacterial Nanonetworks," *IEEE Transactions on NanoBioscience*, vol. 15, no. 8, pp. 959–969, 2016.

[27] I. F. Akyildiz, M. Pierobon, and S. Balasubramaniam, "An Information Theoretic Framework to Analyze Molecular Communication Systems Based on Statistical Mechanics," *Proceedings of the IEEE*, vol. 107, no. 7, pp. 1230–1255, 2019.

[28] G. L. Adonias, C. Duffy, M. T. Barros, C. E. McCoy, and S. Balasubramaniam, "Analysis of the Information Capacity of Neuronal Molecular Communications under Demyelination and Remyelination," *IEEE Transactions on Neural Systems and Rehabilitation Engineering*, pp. 1–1, 2021.

[29] G. D. Ntouni, A. E. Paschos, V. M. Kapinas, G. K. Karagiannidis, and L. J. Hadjileontiadis, "Optimal detector design for molecular communication systems using an improved swarm intelligence algorithm," *Micro & Nano Letters*, vol. 13, no. 3, pp. 383–388, Mar. 2018. [Online]. Available: https://doi.org/10.1049/mnl.2017.0489

[30] M. Kuscu, E. Dinc, B. A. Bilgin, H. Ramezani, and O. B. Akan, "Transmitter and Receiver Architectures for Molecular Communications: A Survey on Physical Design With Modulation, Coding, and Detection Techniques," *Proceedings of the IEEE*, vol. 107, no. 7, pp. 1302–1341, 2019. [Online]. Available: https://doi.org/10.1109/JPROC.2019.2916081

[31] P. Hou, A. W. Eckford, and L. Zhao, "Analysis and Design of Two-Hop Diffusion-Based Molecular Communication With Ligand Receptors," *IEEE Access*, vol. 8, pp. 189 458–189 470, 2020. [Online]. Available: https://doi.org/10.1109/ACCESS.2020.3032009

[32] C. A. Söldner, E. Socher, V. Jamali, W. Wicke, A. Ahmadzadeh, H. G. Breitinger, A. Burkovski, K. Castiglione, R. Schober, and H. Sticht, "A Survey of Biological Building Blocks for Synthetic Molecular Communication Systems," *IEEE Communications Surveys Tutorials*, vol. 22, no. 4, pp. 2765–2800, 2020. [Online]. Available: https://doi.org/10.1109/COMST.2020.3008819

[33] M. T. Barros, M. Veletić, M. Kanada, M. Pierobon, S. Vainio, I. Balasingham, and S. Balasubramaniam, "Molecular Communications in Viral Infections Research: Modelling, Experimental Data and Future Directions," *Accepted in IEEE Transactions on Molecular, Biological and Multi-Scale Communications.*, 2021. [Online]. Available: https://doi.org/10.1109/TMBMC.2021.3071780

[34] Y. Chahibi, "Molecular communication for drug delivery systems: A survey," *Nano Communication Networks*, vol. 11, pp. 90–102, 2017. [Online]. Available: https://doi.org/10.1016/j.nancom.2017.01.003

[35] C. C. H. Cohen *et al.*, "Saltatory Conduction along Myelinated Axons Involves a Periaxonal Nanocircuit," *Cell*, vol. 180, no. 2, pp. 311–322.e15, Jan 2020. [Online]. Available: https://doi.org/10.1016/j.cell.2019.11.039

[36] N. T. Carnevale and M. L. Hines, *The NEURON Book*, 1st ed. New York, NY, USA: Cambridge University Press, 2009.

[37] A. L. Hodgkin and A. F. Huxley, "A quantitative description of membrane current and its application to conduction and excitation in nerve," *The Journal of physiology*, vol. 117, no. 4, pp. 500–544, 1952.

[38] H.-P. Hartung, "Immune-mediated demyelination," *Annals of Neurology*, vol. 33, no. 6, pp. 563–567, 1993. [Online]. Available: https://doi.org/10.1002/ana.410330602

[39] M. Empl, S. Renaud, B. Erne, P. Fuhr, A. Straube, N. Schaeren–Wiemers, and A. Steck, "TNF-alpha expression in painful and nonpainful neuropathies," *Neurology*, vol. 56, no. 10, pp. 1371–1377, 2001. [Online]. Available: https://doi.org/10.1212/WNL.56.10.1371

[40] K. Bhatheja and J. Field, "Schwann cells: Origins and role in axonal maintenance and regeneration," *The International Journal of Biochemistry & Cell Biology*, vol. 38, no. 12, pp. 1995–1999, 2006. [Online]. Available: https://www.sciencedirect.com/science/article/pii/S1357272506001634

[41] N. Baumann and D. Pham-Dinh, "Biology of Oligodendrocyte and Myelin in the Mammalian Central Nervous System," *Physiological Reviews*, vol. 81, no. 2, pp. 871–927, 2001, pMID: 11274346. [Online]. Available: https://doi.org/10.1152/physrev.2001.81.2.871

[42] G. L. Adonias, H. Siljak, M. T. Barros, N. Marchetti, M. White, and S. Balasubramaniam, "Reconfigurable Filtering of Neuro-Spike Communications Using Synthetically Engineered Logic Circuits," *Frontiers in Computational Neuroscience*, vol. 14, p. 91, 2020. [Online]. Available: https://www.frontiersin.org/article/10.3389/fncom.2020.556628

[43] R. Pintelon and L. Van Biesen, "Identification of transfer functions with time delay and its application to cable fault location," *IEEE Transactions on Instrumentation and Measurement*, vol. 39, no. 3, pp. 479–484, 1990. [Online]. Available: https://doi.org/10.1109/19.106276

[44] K. R. Sundaresan and P. R. Krishnaswamy, "Estimation of time delay time constant parameters in time, frequency, and laplace domains," *The Canadian Journal of Chemical Engineering*, vol. 56, no. 2, pp. 257–262, 1978. [Online]. Available: https://doi.org/10.1002/cjce.5450560215

[45] J. Juchem, K. Dekemele, A. Chevalier, M. Loccufier, and C.-M. Ionescu, "First order plus frequency dependent delay modeling: New perspective or mathematical curiosity?" in *2019 IEEE International Conference on Systems, Man and Cybernetics (SMC)*. IEEE, 2019, pp. 2025–2030.

[46] T. G. Farmer, T. F. Edgar, and N. A. Peppas, "Effectiveness of Intravenous Infusion Algorithms for Glucose Control in Diabetic Patients Using Different Simulation Models," *Industrial & Engineering Chemistry Research*, vol. 48, no. 9, pp. 4402–4414, May 2009. [Online]. Available: https://doi.org/10.1021/ie800871t

[47] R. Padma Sree, M. Srinivas, and M. Chidambaram, "A simple method of tuning PID controllers for stable and unstable FOPTD systems," *Computers & Chemical Engineering*, vol. 28, no. 11, pp. 2201–2218, 2004. [Online]. Available: https://doi.org/10.1016/j.compchemeng.2004.04.004

[48] D. Debanne, E. Campanac, A. Bialowas, E. Carlier, and G. Alcaraz, "Axon Physiology," *Physiological Reviews*, vol. 91, no. 2, pp. 555–602, 2011, pMID: 21527732. [Online]. Available: https://doi.org/10.1152/physrev.00048.2009

[49] A. Khodaei and M. Pierobon, "An intra-body linear channel model based on neuronal subthreshold stimulation," in *2016 IEEE International Conference on Communications (ICC)*, May 2016, pp. 1–7.

[50] C. Eliasmith and C. Anderson, *Neural Engineering: Computation, Representation, and Dynamics in Neurobiological Systems*, ser. A Bradford book. MIT Press, 2003.

[51] M. S. Hamada *et al.*, "Loss of Saltation and Presynaptic Action Potential Failure in Demyelinated Axons," *Frontiers in Cellular Neuroscience*, vol. 11, p. 45, 2017. [Online]. Available: https://doi.org/10.3389/fncel.2017.00045

[52] Y. Bando *et al.*, "Differential changes in axonal conduction following CNS demyelination in two mouse models," *European Journal of Neuroscience*, vol. 28, no. 9, pp. 1731–1742, 2008. [Online]. Available: https://doi.org/10.1111/j.1460-9568.2008.06474.x

[53] J. S. Coggan *et al.*, "Imbalance of ionic conductances contributes to diverse symptoms of demyelination," *Proceedings of the National Academy of Sciences*, vol. 107, no. 48, pp. 20602–20609, 2010. [Online]. Available: https://doi.org/10.1073/pnas.1013798107

[54] J.-M. Schoffelen, R. Oostenveld, and P. Fries, "Neuronal Coherence as a Mechanism of Effective Corticospinal Interaction," *Science*, vol. 308, no. 5718, pp. 111–113, 2005. [Online]. Available: https://doi.org/10.1126/science.1107027

[55] J. J. Moré, "The levenberg-marquardt algorithm: implementation and theory," in *Numerical analysis*. Springer, 1978, pp. 105–116. [Online]. Available: https://doi.org/10.1007/BFb0067700

[56] R. J. M. Franklin and C. ffrench Constant, "Remyelination in the CNS: from biology to therapy," *Nature Reviews Neuroscience*, vol. 9, no. 11, pp. 839–855, Nov 2008. [Online]. Available: https://doi.org/10.1038/nrn2480

Harun Siljak received his bachelor and master degrees in Automatic Control and Electronics from the University of Sarajevo in 2010 and 2012, respectively and his PhD degree in Electrical and Electronics Engineering from the International Burch University, Sarajevo, in 2015. He is an assistant professor at the School of Engineering, Trinity College Dublin. During his earlier Marie Curie fellowship at TCD, he merged complex systems science and reversible computation in a new toolbox for wireless communications, mainly for control and optimisation of large antenna arrays. The tools developed during the project found their application in quantum computation and communications, as well as molecular and neuronal communications. He serves as an associate editor for the EURASIP Journal on Wireless Communications and Networking, and science communication officer for the Western Balkans Chapter of Marie Curie Alumni Association and MAT-DYN-NET COST Action.

Michael Taynnan Barros is an Assistant Professor (Lecturer) since June 2020 in the School of Computer Science and Electronic Engineering at the University of Essex, UK. He is also a MSCA-IF Research Fellow (part-time) at the Tampere University, Finland. He received the PhD in Computer Science at the Waterford Institute of Technology in 2016. He has over 70 research peer-reviewed scientific publications in top journals and conferences such as Nature Scientific Reports, IEEE Transactions on Communications, IEEE Transactions on Vehicular Technology, in the areas of molecular and unconventional communications, biomedical engineering, bionano science and Beyond 5G. Since 2020, he is a review editor for the Frontiers in Communications and Networks journal in the area of unconventional communications. He also served as guest editor for the IEEE Transactions on Molecular, Biological and Multi-Scale Communications and Digital Communications Networks journals. He received the CONNECT Prof. Tom Brazil Excellence in Research Award in 2020. Dr Barros current research interests include molecular communications, Biocomputing, Internet of Bio-NanoThings and 6G.

Sasitharan Balasubramaniam (Sasi) received his Bachelors of Engineering (Electrical and Electronic) and PhD (Computer Science) degrees from the University of Queensland, Australia, in 1998 and 2005, respectively, and Masters of Engineering Science (Computer and Communication Engineering) degree in 1999 from the Queensland University of Technology, Australia. He is currently an Associate Professor with the Department of Computer Science & Engineering, University of Nebraska-Lincoln, USA. He was previously a recipient of the Science Foundation Ireland Starter Investigator Research Grant and the Academy of Finland Research Fellow grant. Sasi has published over 100 journal and conference papers, and actively participates in various conference committees. He is currently the Chair of the Steering Committee for ACM NanoCom, a conference which he co-founded. He is currently an Associate Editor for IEEE Transactions on Mobile Computing and IEEE Transactions on Molecular, Biological, and Multi-scale Communications. He was a past Associate Editor for the IEEE Internet of Things Journal. In 2018, Sasi was also the IEEE Nanotechnology Council Distinguished Lecturer. His current research interests include molecular and nano communications, terahertz communication for 6G, as well as the Internet of Nano Things.

Geoflly L. Adonias is currently a Ph.D. candidate at the Walton Institute for Information and Communication Systems Science (formerly TSSG), Waterford Institute of Technology (WIT), Ireland, under the Science Foundation Ireland (SFI) CONNECT Project for future networks and communications. He received his B.Eng. in Electrical Engineering from the Federal Institute of Education, Science and Technology of Paraíba (IFPB), Brazil, in 2017. His current research interests include Nano-scale Communications, Digital Signal Processing and Wireless Networks.

CHAPTER 9

PUBLICATION 4: ANALYSIS OF LPC-INDUCED DEMYELINATION ON NEURONAL MOLECULAR COMMUNICATIONS

Analysis of the Information Capacity of Neuronal Molecular Communications under Demyelination and Remyelination

Geoflly L. Adonias, Conor Duffy, Michael Taynnan Barros,
Claire E. McCoy, and Sasitharan Balasubramaniam

Abstract—Demyelination of neurons can compromise the communication performance between the cells as the absence of myelin attenuates the action potential propagated through the axonal pathway. In this work, we propose a hybrid experimental and simulation model for analyzing the demyelination effects on neuron communication. The experiment involves locally induced demyelination using *Lysolecithin* and from this, a myelination index is empirically estimated from analysis of cell images. This index is then coupled with a modified Hodgkin-Huxley computational model to simulate the resulting impact that the de/myelination processes has on the signal propagation along the axon. The effects of signal degradation and transfer of neuronal information are simulated and quantified at multiple levels, and this includes (1) compartment per compartment of a single neuron, (2) bipartite synapse and the effects on the excitatory post-synaptic potential, and (3) a small network of neurons to understand how the impact of de/myelination has on the whole network. By using the myelination index in the simulation model, we can determine the level of attenuation of the action potential concerning the myelin quantity, as well as the analysis of internal signalling functions of the neurons and their impact on the overall spike firing rate. We believe that this hybrid experimental and *in silico* simulation model can result in a new analysis tool that can predict the gravity of the degeneration through the estimation of the spiking activity and vice-versa, which can minimize the need for specialised laboratory equipment needed for single-cell communication analysis.

Index Terms—Re/Demyelination, Lysolecithin (LPC), Hodgkin-Huxley model, Myelination Index, Molecular Communications.

I. INTRODUCTION

With the ever-growing knowledge of the biological processes involved in the regeneration of nerve tissues, a better understanding of these events is crucial for the creation of more robust models that could accelerate the development of targeted therapeutics against neurodegeneration [1]. For example, multiple sclerosis (MS) is an autoimmune demyelinating disease (DD), characterised by localised destruction of protective myelin sheaths around axons and subsequent impairment of neuronal function and action potential (AP) propagation, leading to the formation of sclerotic plaques across the central nervous system (CNS). In relapse-remitting MS (RRMS), demyelination is caused by abnormal peripheral immune invasion of the CNS and inflammatory attack against the myelin sheath, most notably from activated T-cells [2]. This form of the disease is characterised by "attacks" (relapse), followed by periods of recovery (remitting), where innate repair mechanisms of the CNS restore damaged myelin in a process known as **remyelination**. However, MS can also manifest in the form of primary progressive MS (PPMS), where demyelination is continuous and remyelination mechanisms appear to be dysfunctional [3]. It is, therefore, of considerable interest to develop therapies that can promote or restore remyelination, with current research approaches including stem cell therapeutics, biomaterial construct implants and nanoparticle or extracellular vesicle treatment formulations, among others [4]–[7].

The drug *Lysolecithin* (LPC) has been widely used for years to experimentally induce demyelination in neurons from both the central and peripheral nervous systems (PNS). Many studies have taken advantage of LPC to help characterise experimental models in terms of its morphology by light and electron microscopy, electrophysiology and biochemistry. The various uses and validity of organotypic cerebellar slice cultures in studying demyelinating disease have been thoroughly reviewed by Doussau and colleagues [9], identifying the culture system as the easiest way to replicate the various stages of myelination, demyelination and remyelination that are of interest outside of *in vivo* models. These cultures faithfully retain the cytoarchitecture and neuronal networks of the cerebellar cortex *in vitro* for weeks to months, allowing for long-term investigations of novel therapeutics and sufficient recovery time following a demyelinating insult to observe remyelination. Furthermore, the neurons in these slice cultures retain electrophysiological characteristics, such as Purkinje cells forming new synapses with targets upon stimulation [10]. Crucially to study remyelination, cells at all stages of the oligodendroglia lineage are retained in the organotypic cerebellar slice culture [11].

Turning to LPC specifically, this was first demonstrated to induce demyelination in organotypic cerebellar slice cultures by Birgbauer and colleagues in 2004, as observed by immunostaining for myelin basic protein (MBP), myelin oligodendrocyte glycoprotein (MOG), and 2', 3'-cyclic nucleotide 3'-phosphodiesterase (CNPase), followed by recovery and subsequent remyelination [12]. This approach to inducing demyelination has been used in several studies to date, including a demonstration that the MS therapy fingolimod can promote remyelination [13], validation of an immune-mediated technique for inducing demyelination [14] and characterization of the critical pro-remyelination properties of microglia [8], [15]. Furthermore, focal injections of LPC to the spinal cord (Fig. 1) are a frequently-used *in vivo* model of demyelination [16], thus using an LPC-based *in vitro* model is attractive to screen potential treatments before commencing *in vivo* studies.

The findings on the demyelination and remyelination processes observed with the help of the wet-lab experiments will allow the construction of a more refined and accurate computational simulation model and, possibly, shine light on the way neurons encode information. In the last few years, there has been an increasing number

PUBLICATION 4: ANALYSIS OF LPC-INDUCED DEMYELINATION ON NEURONAL MOLECULAR COMMUNICATIONS
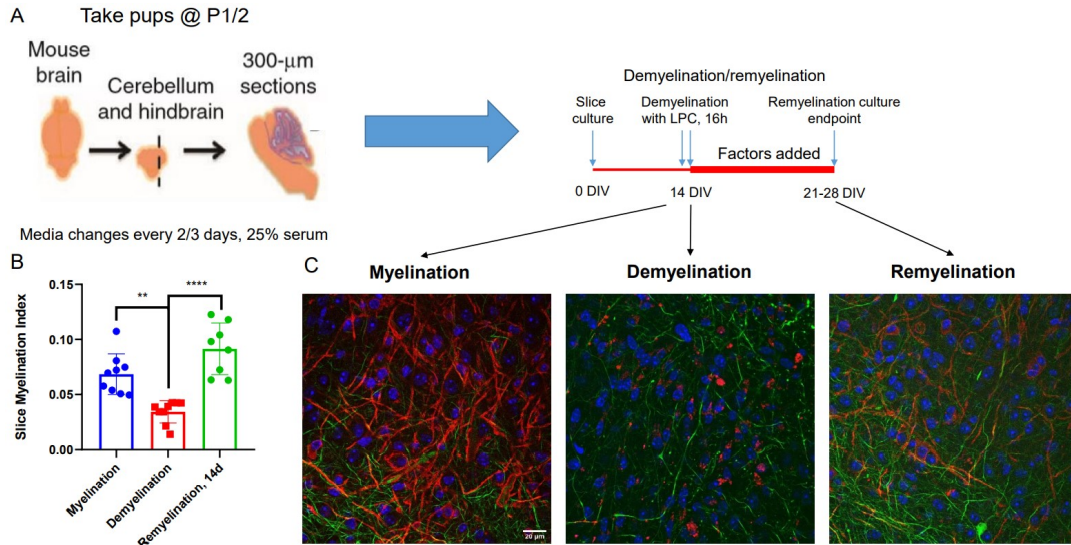
Fig. 1. (A) Schematic of organotypic brainstem and cerebellum slice culture model set-up. Drawings of mouse brains borrowed from Miron et al [8]. (B) Average myelination indices of slices in myelination, demyelination and remyelination conditions. Each datapoint represents the index of a single slice. ** $= p < 0.01$, **** $= p < 0.0001$, one-way ANOVA with post-hoc Sidak's multiple comparisons test. Graph generated in GraphPad Prism. (C) Representative images of myelination, demyelination and remyelination staining under confocal microscopy, composite images. Blue = DAPI, Green = NFH, Red = MBP.

of scientists that started to look at alternative coding techniques, some of them imposing profound implications on the field of neural computation [17]. **Firing rate coding** [17], [18] is a technique where the rate with which spikes are being fired is proportional to the strength of the stimuli. Several other coding techniques have also been proposed as alternatives such as rank order coding or sparse coding, where these techniques take into account that real neurons use spikes that are followed by refractory periods which should play a role in information encoding. One of the simplest techniques proposed is to just count the number of action potentials fired during a particular period, and this is referred to as **count coding** [17]. With this coding technique, the maximum amount of information transmitted by N neurons is $\log_2(N+1)$ bits. Another alternative method is to check for the presence of an action potential in a specific time window. In this technique, the presence of a firing will be considered a bit "1" and its absence a bit "0", and this is referred to as **binary coding** [17], [19]. For a binary code, the maximum amount of information transmitted by N neurons is equal to $\log_2(2^N)$ bits. More complex encoding techniques have also been proposed. Such approaches use the precise time of each spike on each input to increase the maximum amount of information transmitted by a group of neurons. In this case, the maximum amount of information transmitted by N neurons in a time window of t ms, where the spikes can be timed with a precision of 1 ms, is $N \cdot \log_2(t)$ bits. Thus, this encoding technique is known as **temporal coding** or **timing coding** [17], [20].

This model should be able to play a significant role in the analysis of the impact that demyelination and remyelination will have on the neuronal signalling communication process and should also be used to add a new analysis tool for wet-lab experimentalists without the need for specialised equipment. This hybrid computational simulation and experimental model has the potential to improve both sides of the study and bring together scientists and researchers from different disciplines by unifying their findings and validating their data for a more reliable analysis of the demyelination and remyelination processes on the

molecular aspect of neuronal communications.

The objective of this paper is to computationally validate the data collected from wet-lab experiments on LPC-induced demyelination and to analyse its impact on the communication once the demyelinated neuron is partially remyelinated. The contributions of this paper are:

- **A novel hybrid wet-lab-computational model:** We describe the construction of a wet-lab dataset of myelination under conditions of LPC-induced demyelination and subsequent remyelination, alongside undisturbed myelination controls, suitable for input to a computational model. By utilising a method of analysis from neuronal molecular communications, we use this hybrid model to understand the signal propagation behaviour as they propagate through the axonal pathway.

- **Modelling of the spiking rate for myelin-deficient neurons:** As proposed in the literature, spike firing usually follows a *Poisson* process [21], [22]. The rate and pattern of firing can defer between different demyelination intensities leading to the modelling of their respective behaviour into known distributions.

- **Multi-perspective theoretical analysis of LPC-induced demyelination:** Communication metrics (e.g., channel capacity, attenuation and time delay) analysis are presented and discussed on the effects of demyelination from three different perspectives, (1) single neuron and the signal propagation through axonal compartments, (2) bipartite synapse and the effects on the excitatory post-synaptic potential and, (3) small neuronal network of 27 cells is analysed to determine the network communication when a neuron starts to demyelinate.

The remainder of this paper is as follows in Section II we present the methodologies applied for both the wet-lab experiments and the computational simulations for analysis and validation of data from LPC-induced demyelination. In Section III, we present and discuss our results from (1) single neuron, (2) bipartite synapse and (3) small neuronal network perspectives and, finally, in Section IV, we conclude

this analysis and discuss potential future works.

II. MATERIALS AND METHODS

A. LPC-induced Demyelination

1) Animals and Tissue Preparation: All experiments were conducted in accordance with EU and Health Products Regulatory Authority guidelines. A breeding colony of wild-type C57BL/6J mice was maintained in the Biomedical Research Facility in the Royal College of Surgeons in Ireland using mice obtained from The Jackson Laboratory. Organotypic brain slice cultures of the brainstem and cerebellum were established to examine demyelination and remyelination *ex vivo*, based on the protocol described by Doussau and colleagues [9]. Briefly, the cerebellum and brainstem were cut into slices 300 μm thick along the sagittal axis using a McIlwain Tissue Chopper. Slices were separated in slice culture media (46.55% Minimum Essential Medium (MEM), 25% heat-inactivated horse serum, 25% Earl's balanced salt solution, 1% glutamine, 1% 100 U/mL P/S, 1.45% glucose 45, final concentration 6.5 mg/mL) and transferred onto 0.4 μm Millipore mesh membrane inserts inside 6-well plates containing 1 mL of slice culture media. Typically 6-7 slices were obtained per brain, and the slices from each brain were distributed across separate wells, with 6 slices per culture well. Slices were then cultured at 37 °C, 5% oxygen, with fresh slice culture media, exchanged every 2-3 days, for a total of 14 days *in vitro* (d.i.v.).

2) Demyelination and Remyelination: To induce demyelination, the drug lysolecithin (LPC) was applied to 14 d.i.v. cultures at a concentration of 0.5 mg/mL for 16 hours. LPC was then withdrawn, the cultures were washed once in slice culture media before being transferred and maintained in fresh media for a 24-hour recovery period. Slices were then allowed to remyelinate for a further 14 days *in vitro*, with media changes every 2-3 days as before.

3) Immunofluorescence and Fluorescent Microscopy: Immunofluorescent staining and fluorescent microscopy were used to evaluate the extent of myelination in organotypic brain slice cultures. Cultures were washed once in PBS before fixation with 4% paraformaldehyde solution (PFA) for 45 minutes, at which point PFA was withdrawn and cultures ready for staining. Cultures were first blocked for 3 hours using a 2% horse serum, 10% goat serum, 1% BSA, 0.25% Triton-X-100, 1 mM HEPES solution in PBS at room temperature. The mesh insert membranes were then cut and slices transferred to 24-well plates for staining. Primary antibodies for anti-NFH (1:2000) and anti-MBP (1:600) were then applied in the block solution, 400 μL/well for 2 days at 4 °C. Slices were then washed with shaking three times at room temperature in PBS-0.01% Triton-X-100, 1 hour per wash, before applying AlexaFluor secondary antibodies - 1:500 anti-chicken AlexaFluor 488, 1:500 anti-rat AlexaFluor 568, in block solution, 400 μL/well overnight at 4°C. Slices were then counterstained with DAPI –1:30,000 of stock in PBS, 500 μL per well – for ten minutes before washing three times in PBS-0.01% Triton-X-100 as before. Slices were mounted with ProLong Gold and were labelled with randomly generated 6-digit numbers corresponding to treatment or control conditions, to introduce blinding during image acquisition.

Slices were imaged using a Zeiss 710 confocal microscope at 40x magnification. Three representative image stacks were acquired per slice, using Z-stack imaging at 0.5 μm intervals across 10 μm. Images were then analysed in ImageJ for co-localisation of MBP to NFH (neurofilament protein H) to assess the extent of myelination in each slice. A myelination index (ι_{my}), ranging from 0 to 1, was calculated for each z-stack by dividing the amount of co-localisation by the total amount of NFH, and averages for each slice calculated by pooling

Slice 16 of 21 in stack (top)   Slice 5 of 21 in stack (bottom)
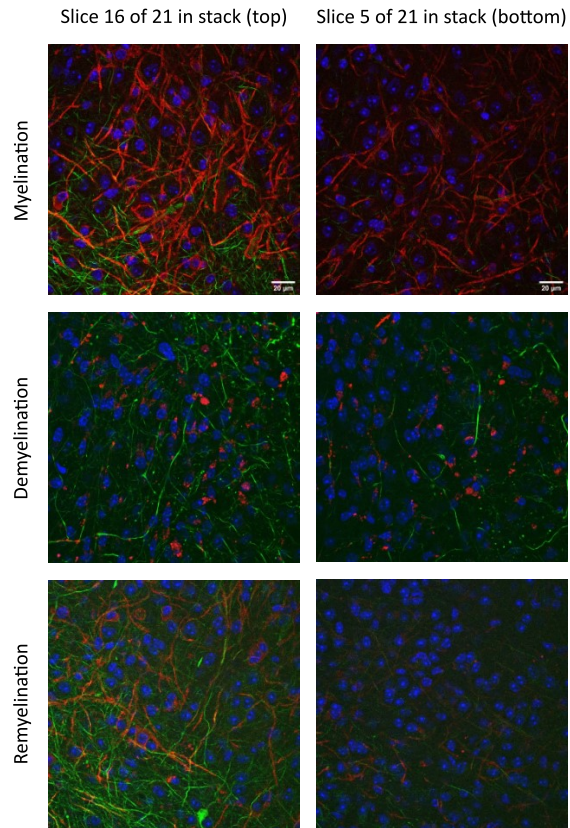
Fig. 2. Comparison of staining quality at the top (slice 16 of 21, **2.5** μm below surface) and bottom (slice 5 of 21, **8** μm below surface) of image stacks under confocal microscopy. Composite images, Blue = DAPI, Green = NFH, Red = MBP.

myelination indices from representative images together. The indices obtained are, therefore, a measure of myelin sheaths overlaid on axon fibres, relative to total axon density. A graphical illustration of tissue analysis and slice culture model set-up are shown in Fig. 1, with a description of the culture set-up, the timeline for introducing LPC for demyelination at day 14, and the stop point for remyelination in Fig. 1(a). Taking the average myelination index for each slice we confirm that introduction of LPC for 16h produced a significant decrease in myelination, allowing a 14-day recovery period following LPC withdrawal, we observed a significant restoration of myelin sheaths in the remyelination conditions as measured by the myelination index relative to demyelination slices, Fig. 1(b). Representative images for each condition are also shown for illustrative purposes in Fig. 1(c). As can be seen in the "Myelination" image, prior to application of LPC clear (red) myelin sheaths can be observed overlaid on (green) axons. Following LPC application, substantially less myelin stain can be observed in the "Demyelination" image, and what myelin is present does not form clear sheath structures, most likely debris. In the "remyelination" image, taken 14 days following LPC withdrawal, myelin in sheath structures can be observed again laid over axons, though perhaps less pronounced or thinner than the myelination condition. This is an expected characteristic of repaired myelin sheaths. It is therefore clear that the myelination index measurement is reflective

PUBLICATION 4: ANALYSIS OF LPC-INDUCED DEMYELINATION ON NEURONAL MOLECULAR COMMUNICATIONS

A

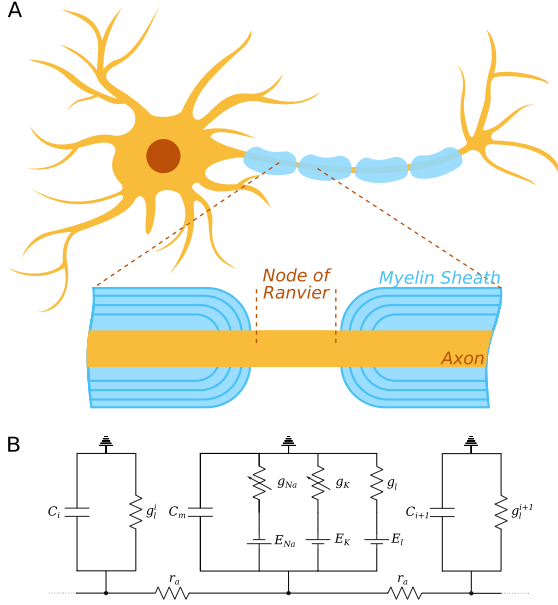

B

Fig. 3. Illustration of an axonal pathway with a (A) detail of a *Node of Ranvier* and two internodes, respectively, (B) Hodgkin-Huxley circuit model with parameter detailed description provided in Section II-B; the parameters C_i and g_l^i and their subsequent myelinated compartments are described by equations (14) and (15), respectively.

of clear differences in myelination of axons. For that reason, for computational analysis, indices were restricted to the top $3.5\,\mu m$ of each $10\,\mu m$ stack captured across slices and conditions which, visually, it is clear that NFH staining was of superior quality in the regions of the slice closer to the surface, as seen in Fig. 2.

B. Computational Model for Axonal Demyelination

The axon under analysis in this work is modelled according to the Hodgkin-Huxley formalism [23] with modifications proposed by Quandt and Davis [24], as depicted in Fig. 3, where the parameters are described in Table I.

When an external stimulus, I_{ext}, is applied, it triggers either the activation or inactivation of the ionic channels that allow the exchange of ions that result in depolarisation (or hyperpolarize when it is inhibited) of the membrane of the cell. These dynamic changes in the voltage and current of each ion diffusion through the membrane are modelled as

$$C\frac{\mathrm{d}V}{\mathrm{d}t} = -I_l - I_{Na} - I_K - I_{syn} + I_{ext}, \tag{1}$$

where V is the membrane potential, I_x are the ionic currents, where x represents either a specific ion (Na, K) or the leak channel (l). Those currents are represented as

$$I_l = g_l(V - E_l), \tag{2}$$

$$I_{Na} = g_{Na}m^3h(V - E_{Na}), \tag{3}$$

$$I_K = g_K n^4(V - E_K), \tag{4}$$

Element	Value	Unit
Membrane capacitance (C_m)	1	μF/cm^2
Axon radius (δ_a)	5	μm
Node length (L_n)	4	μm
Internodal distance (d_i)	2	mm
Internal resistance (r_a)	100	$\Omega\cdot$cm
Myelin sheath (w)	200	wraps
Sodium reversal potential (E_{Na})	53	mV
Potassium reversal potential (E_K)	-74	mV
Leak reversal potential (E_l)	-60	mV
Sodium conductance density (G_{Na})	1200	mS/cm^2
Potassium conductance density (G_K)	90	mS/cm^2
Leak conductance density (G_l)	20	mS/cm^2
Internodal membrane conductance (g_i)	0.3	mS/cm^2
Temperature (T)	37	°C
Time step (dt)	0.25	μs
Q_{10}	3.0	-

where m and h are the activation and inactivation variables of the sodium (Na) channel, respectively, and n is the activation variable of the potassium (K) channel. Following the approach proposed by Hodgkin and Huxley [23], those variables are represented below as x and their dynamics are described as

$$\frac{\mathrm{d}x}{\mathrm{d}t} = \alpha_x(V)(1-x) - \beta_x(V)x, \tag{5}$$

in which the values of the rate constants α_i and β_i for the i-th ionic channel can be defined as

$$\alpha_m = \frac{0.1(V+40)}{1+e^{-(V+40)/10}}, \tag{6}$$

$$\beta_m = 4e^{-(V+65)/20}, \tag{7}$$

$$\alpha_h = 0.07e^{-(V+65)/20}, \tag{8}$$

$$\beta_h = \frac{1}{1+e^{-(V+35)/10}}, \tag{9}$$

$$\alpha_n = \frac{0.01(V+55)}{1-e^{-(V+55)/10}}, \tag{10}$$

$$\beta_n = 0.125e^{-(V+65)/80}. \tag{11}$$

We also integrated a process into the model for the synaptic inputs from pre-synaptic cells in which the ionic channels that are activated will release neurotransmitters that are diffused into the synaptic cleft towards neuroreceptors at the post-synaptic cell. This relationship is represented as

$$I_{syn} = g_{syn}(V - E_{syn}), \tag{12}$$

where the synaptic conductance, g_{syn}, and the synaptic reversal potential, E_{syn}, are used to describe many different types of synapses, and the latter may assume different values according to the types of neuroreceptors. The four major transmitters used for communication in the nervous systems are listed in Table II [25], [26].

The g_{syn} can be described as a superposition of exponentials and is represented as

PUBLICATION 4: ANALYSIS OF LPC-INDUCED DEMYELINATION ON NEURONAL MOLECULAR COMMUNICATIONS

Neurotransmitter	Neuroreceptor	E_{syn} (mV)
Glutamate	Non-NMDA	0
Glutamate	NMDA	0
GABA	$GABA_A$	−70
GABA	$GABA_B$	−100
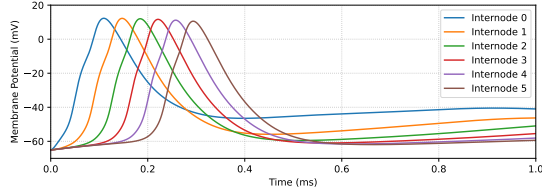
(a) Action potential propagation on an axon fully myelinated.
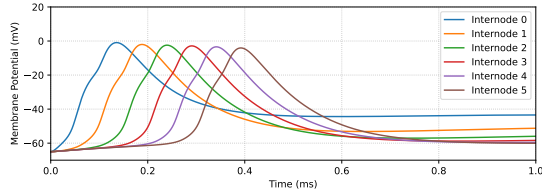
(b) Action potential propagation on an axon with half of its normal myelination levels.

Fig. 4. Parallel for action potential propagations between a fully myelinated and a partially (50%) demyelinated axon.

$$g_{\text{syn}} = \sum_f \bar{g}_{\text{syn}} \, e^{-(t-t^{(f)})/\tau} \, H(t - t^{(f)}), \qquad (13)$$

where τ is a time constant, $\bar{g}_{\text{syn}}$ is the peak synaptic conductance, $t^{(f)}$ is the arrival time of a pre-synaptic action potential and $H(\cdot)$ is the Heaviside step function [25]. As we have investigated in [27], the membrane potential that reaches the pre-synaptic terminals can affect the probability of releasing neurotransmitters. Consequently, anything that would affect this potential could also indirectly lead to changes in the release of neurotransmitters. In other words, it is not only the synaptic current (Equation 12), but also all other ionic currents that can influence the release of neurotransmitters and consequently compromise the integrity of the signal being propagated down the neuronal network.

The modifications, proposed by Quandt and Davis [24], on the original Hodgkin-Huxley model is to incorporate the dynamics of myelination and understand the signal propagation per compartment, by including the capacitance of the internode (C_i), which is represented as

$$C_i = \frac{2\pi\,\delta_a\,d_i\,C_m}{\iota_{my}w + 1}, \qquad (14)$$

and the assumption that the internode have a specific leak conductance (g_l^i), which is represented as

$$g_l^i = \frac{2\pi\,\delta_a\,d_i\,g_i}{\iota_{my}w + 1}, \qquad (15)$$

where ι_{my} is the myelination index described in Section II-A.3. The myelinated compartments (also called internode compartments) are modelled as not having ionic channels. This is mainly because as the

myelin sheath provides insulation, it also blocks the ionic channels in the axonal membrane, not allowing the free movement and exchange of ions between intra- and extra-cellular mediums. Furthermore, both the C_i and g_l^i values are heavily influenced by the number of myelin wraps, w, as shown in equations (14) and (15) and, as w decreases due to demyelination, it negatively impacts the speed and potential responses concerning the propagation of the signal.

An axon with six internodes and seven nodes of *Ranvier* was built as illustrated in Fig. 3. The simulations were conducted using the NEURON simulation environment with Python [28], [29]. Each point of stimulation was set at 200 spikes per second following a *Poisson* process [22] unless otherwise stated. Five simulations were conducted for each value of ι_{my} starting at full myelination (100%) and decreasing at 12.5% intervals until it reaches 12.5%, hereafter considered as full demyelination (see Section II-A). Each spike is represented as a bit '1' and its absence is represented as a bit '0' in a specific time slot. In this work, the time slot for sampling the neuronal binary information is 5 ms. This is short enough to detect less than a single spike and account for its refractory periods. The cells were connected following a standard procedure with the `NetCon` object that defines a synaptic connection. We are not using any morphological-type-related connection probability as the neurons are modelled in a generic structure and behaviour. The network arrangement does not follow any structure in particular, e.g. cortical layers, instead it was arranged in a cubic shape (more details in Section III-D) where there was a single synapse per connection and, a single connection where needed.

III. RESULTS AND DISCUSSION

A. Demyelination and Remyelination of Slice Cultures

Following the 16-hour treatment with 0.5 mg/mL LPC, we observed a significant reduction in the myelination of neurons as determined by the average myelination index of slices relative to untreated controls ($p < 0.01$, one-way ANOVA and Sidak's multiple comparisons posthoc test). LPC-induced demyelination was observed to be of a similar magnitude in our hands as reported by several other groups [13], [14], [30]. Following 14 days of recovery post-LPC-induced demyelination in brain slice media, remyelination was observed that was significantly greater than the demyelination time-point as determined by the myelination index ($p < 0.0001$, one-way ANOVA and Sidak's multiple comparisons posthoc test).

The average myelination index of each slice was used to determine the success and overall extend of LPC-induced demyelination and remyelination; however, individual myelination indices of each captured image were also recorded as part of the analysis process.

B. Compartmental Analysis

To understand the dynamics of action potential propagation in the axonal pathway, our modelling process should account for the effects of myelinated and non-myelinated sections of the axon. For that reason, we are using the multi-compartmental modelling framework [31] to help put together a detailed representation of the axon that would provide us with enough information regarding the electrical behaviour of the neuronal membrane.

In this work, we have modelled the axon with Hodgkin-Huxley compartments for the nodes of *Ranvier* and the myelinated internode compartments. As indicated in Section II-B, even though both use the same framework, the internodes are modelled slightly differently to account for the myelin sheaths. Then, we decided to start our analysis on the neuron itself, in other words, on the behaviour of the membrane per compartment (Fig. 4). The model used follows the description from Section II-B aiming to understand how partially
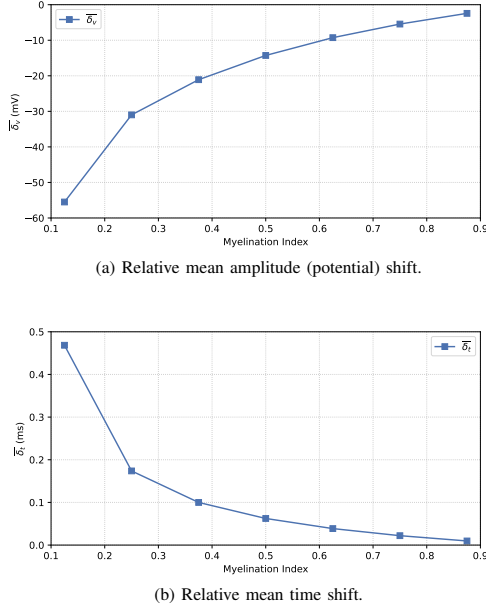
Publication 4: Analysis of LPC-induced Demyelination on Neuronal Molecular Communications

(a) Relative mean amplitude (potential) shift.

(b) Relative mean time shift.

Fig. 5. Relative mean shift in relation to a fully myelinated neuron.

Fig. 6. Bipartite synapse with demyelinated pre-synaptic neuron.

Fig. 7. Capacity, C(X;Y) and mean mutual information, I(X;Y), for peer-to-peer analysis of a pre-synaptic demyelinated neuron.

myelinated neurons, i.e. under either demyelination or remyelination conditions, affects the propagation of action potentials per neuronal compartment. Fig. 4 shows how a neuron with half of its normal myelin, Fig. 4(b), compared to a fully myelinated neuron shown in Fig. 4(a). The results depicts not only a delay for the action potential to reach its peak in all compartments but also shows how damages to the myelin sheath can affect the value of membrane potential reached. For that reason, we decided to numerically evaluate by how much the shift in peak time and amplitude changes as the demyelination worsens and, analogously, the changes due to remyelination processes.

1) Relative Mean Shift: Visually, we first noticed subtle shifts in amplitude (peak potential reached by the membrane) and in time (spikes were taking longer to reach their peak values). We then decided to quantify these shifts, both in amplitude and in time, on average, by proposing a metric that we called **relative mean shift**. For the analysis on time shift, we consider the points in time where each spike peaked at the input as T_{in}^k, where $k = \{1, 2, 3, ..., K\}$ identifies the order of each spike and, T_{out}^k as the peak times at the output. Thus, we define the relative mean time shift, $\overline{\delta_t}$ (ms), as

$$\overline{\delta_t} = \frac{1}{K} \sum_{k=1}^{K} (T_{out}^k - T_{in}^k). \quad (16)$$

Analogously, we can define the relative mean amplitude shift, $\overline{\delta_v}$ (mV), with V_{in}^k and V_{out}^k as the peak amplitudes of spike k at the input and output, respectively.

As illustrated in Fig. 5, the difference in the average membrane potential in relation to a full myelinated neuron is considerably damaging to the signal propagation through the axonal pathway. At 12.5% myelination, the difference is almost 60 mV shown in Fig. 5(a) and this is enough to not even consider the signal travelling down the axon as a spike. The degradation in the membrane potential is not linear, where its logarithmic-shaped curve illustrates a much steeper
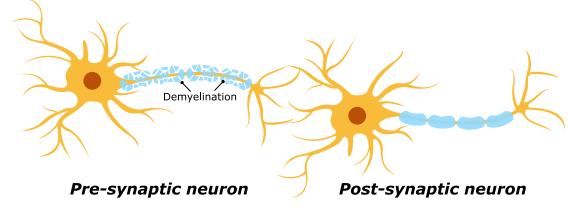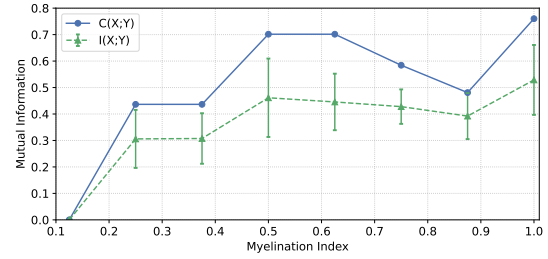
degeneration for the lower half of the indices when compared to the upper half as the mean shift in amplitude starts to plateau as it approaches full myelination. Analogous to the effects on membrane potential, Fig. 5(b) shows how the peak times of the action potentials are delayed as ι_{my} decreases. The negative-exponentially-shaped curve depicts a smoother increase in the mean time shift for higher indices. Both results in Fig. 5 match findings in Cohen et al [32], where they identified longer onset latencies and lower peak amplitudes in the conduction of action potentials along myelinated axons on models of L5 pyramidal cells.

C. Bipartite Synapse Analysis

From the perspective of information and communication theory, the neuron can be seen as peers in the nervous system characterising a peer-to-peer communication system [33]. Even though the bit transmission may be affected by the refractory period of a recently fired action potential, depending on the intensity of the stimuli, new bits may still be transmitted during relative refractory periods. Furthermore, if the post-synaptic neuron does not manage to evoke a subsequent action potential, there will be no waiting queue [26] which characterises the channel as *memoryless*. This means that any spike not propagated, because the post-synaptic neuron is unable to fire at the time the pre-synaptic stimuli arrives, will be lost. A pair of neurons, one acting as the transmitter, known as pre-synaptic neuron and, the other acting as the receiver, called a post-synaptic neuron, form a bipartite synapse as shown in Fig. 6. A synaptic connection between only two neurons is considered a single input single output (SISO) communication channel [22] and can be evaluated as such using well-known metrics from information and communication theory such as capacity [34], [35].

1) Channel Capacity: Shannon's entropy of a discrete random variable x and probability mass function $p(x)$ can be used in biological systems to represent information as bits in several processes and is defined as
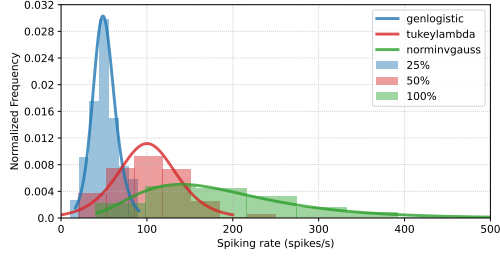
(a) Spiking rate distributions for different ι_{my}.

(b) Interspike intervals (ISI) distributions for different ι_{my}.

Fig. 8. Distributions for spiking rate and interspike intervals revealing a shift in peak and widening of the curve for different myelination indices.

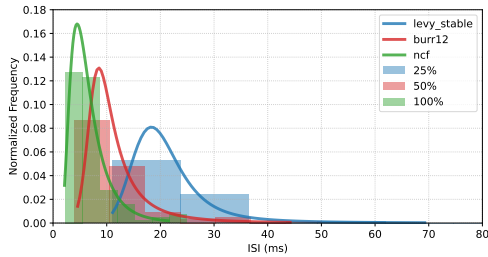(a) Mean and standard deviation for spiking rate on a small neuronal network.

(b) Mean and standard deviation for interspike intervals on a small neuronal network.

Fig. 9. Mean and standard deviation for spiking rate and interspike intervals for the analysis of a network of 27 neurons.

$$H(X) = -\sum_{x \in X}^{P} (x) \log_2 p(x), \tag{17}$$

where $X = \{x_0, x_1\}$.

Additionally, the definition of conditional entropy is based on the conditional and joint distribution of x and y:

$$H(X|Y) = -\sum_{x \in X}\sum_{y \in Y} p(x, y) \log_2 p(x|y), \tag{18}$$

where $Y = \{y_0, y_1\}$.

All the remaining probabilities are defined as follows:
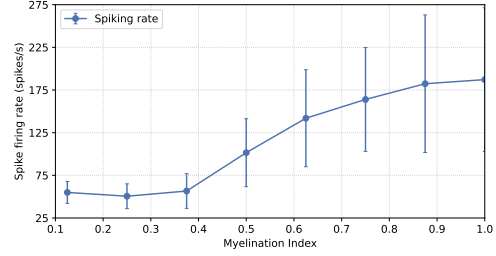
$$p(x) = p(x = x_0) + p(x = x_1), \tag{19}$$

$$p(y) = [p(y = y_0) + p(y = y_1)]\, p(y|x), \tag{20}$$
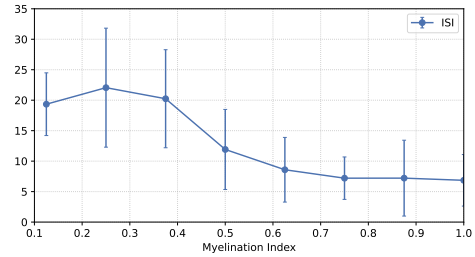
$$p(y = y_0|x = x_0) = 1 - p(y = y_1|x = x_0), \tag{21}$$

$$p(y = y_0|x = x_1) = 1 - p(y = y_1|x = x_1). \tag{22}$$

In other words, we could characterise the destructive effects of demyelination on the propagation of the signal as the probability of receiving a bit '0', i.e. no spike, given that a bit '1' was sent at the input, $p(y = y_0|x = x_1)$ in Eq. (22). Moreover, as the remyelination takes place, there is an increase on the probability of receiving a bit '1', given that a bit '1', i.e. spike, was sent, $p(y = y_1|x = x_1)$ in Eq. (22). This shows how the channel capacity can be affected as the conditional probabilities for receiving a specific bit changes with the degeneration and, eventually the partial regeneration of the myelin sheath.

The mutual information between two variables indicates that the input can be construed as a measure of the "noise" in the channel given the output, and is calculated as

$$\begin{aligned}I(X;Y) &= H(X) - H(X|Y)\\ &= -\sum_{x \in X}\sum_{y \in Y} p(x)p(y|x) \log_2 \frac{p(y|x)}{p(y)},\end{aligned} \tag{23}$$

and the maximum average mutual information in any single use of the channel, known as capacity, which is represented as

$$C(X;Y) = max_{p(x)}I(X;Y). \tag{24}$$

From our simulations, both the capacity and mean mutual information are shown in Fig. 7.

As shown in Fig. 7, there are a few fluctuations which we believe to be due to the randomness of the spikes at the input of a myelinated axon. The mutual information increases in a way that resembles a logarithmic curve, similar to the mean shift in amplitude from Fig. 5(a) and corroborates findings from Veletić et al [33], [36]. The authors showed a similar growth of channel capacity (bits), and information rate (bits per second) which is proportional to capacity values for bipartite synaptic connections.

D. Network Analysis

When part of a larger network, neurons can receive stimuli from several other neurons and pass this information down to many other neurons as well characterising a multiple-input and multiple-output (MIMO) communication channel [37]. For our network analysis, we arranged 27 neurons in a $3 \times 3 \times 3$ cubic structure, with vertical and horizontal connections, but not diagonals; this was a design choice to avoid too much noise at higher spike firing frequencies and still takes advantage of a good connectivity scheme. As with any stochastic system, it is not ideal to force a system's behaviour into a deterministic model, where we need to account for inherent randomness. In this
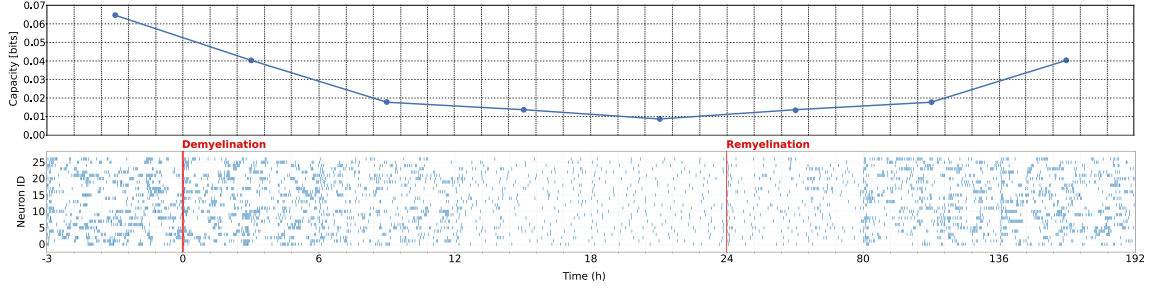
Fig. 10.   Raster plots for different myelination indices showing how capacity is degrated and then regenerated as demyelination and remyelination take place over time.

scenario, the system is our network and as the demyelination gets worse, the spike-firing pattern and rate is negatively compromised. In this scenario, all 27 neurons are demyelinated at the same time and the same proportion, to mimic the process of demyelination for the calculation of ι_{my}, where all neurons in the field of view are demyelinated together.

1) Distribution Fitting: Several works in the literature have hypothesised that neurons follow a *Poisson* process when firing individually, but this may not be the case depending on the connectivity, stimulus and neuronal structure [38]. To assess these conditions, we turn to distribution fitting to help us understand how those differences affect the network as a whole and to reproduce its behaviour. This modelling technique is most commonly done by applying the Kolmogorov–Smirnov (KS) test for goodness of fit [39]. Once the best fit is found for the data, both the histogram of the real data and the probability distribution function, f_x, of the best-fitted distribution are plotted together as shown in Fig 8.

Full myelination in Fig. 8(a) shows similarities to the findings by Platkiewicz and Brette [40] on the threshold for spike initiation which suggests that our results for different levels of demyelination can be a good representation for the validity of *in vivo* and *in vitro* experiments. Furthermore, we have also found strong similarity between our results in Fig. 8(b) and the results presented by Levine and Shefner [41]. Visually, the highly skewed distribution of their data resembles our findings for a *Noncentral F distribution* (n.c.f.) at full myelination. As for the spiking rate, these results suggest our models offer good approximations to provide complementary analysis tool of understanding internal signal propagation properties of the neurons under de/remyelination.

2) Spiking Rate and Interspike Intervals (ISI): One of the first things to indicate changes have happened in the neuronal communication channel is the spiking rate and the ISI. The spiking rate changes with the intensity of the stimulus as a way of encoding and modulating the stimulus with different firing frequencies. However, as neurons inside a network start to attenuate the signal or not pass it along altogether, it affects the rate with which the information is transferred within the network.

To understand what happens to the overall spiking rate inside a network, we decided to calculate its mean and standard deviation as the myelination index changed. As aforementioned in Section II, the myelination index was calculated for several neurons within the field of view for each cortical slice. For that reason, we chose to vary the index and see its effect on the entire network as depicted in Fig. 9.

As expected, Fig. 9(a) shows an increase in the spike firing rate as the myelination index increases. From myelination index of 0.375 onwards it is clear how it increases as a logarithmic-shaped curve, similar to the relative mean amplitude shift, $\bar{\delta}_v$, from Fig. 5(a).

However, there is barely any difference for the three lowest index points. This is an interesting finding from the point of view of communication performance, where myelination index ι_{my} lower than 40% results in information that may be degraded to their worst levels and this change does not differ all the way to the level of 15%. In Fig. 10, it is possible to follow the visual decrease in spiking activity as demyelination progresses up to a point when the remyelination takes over and the restoration of several axonal pathways returns to propagate the action potentials. As the spiking rate is visually affected, so is the channel capacity which follows a similar behaviour as the one depicted in Section III-C, Fig. 7.

Researchers have already shown that action potentials are broadened and the conduction velocity supported by the saltatory nature of the conduction of neuronal potential is prone to failure as the myelin sheath gets more and more damaged [27], [32], [42]. All of the results available in the literature help support our claim that the frequency-dependent spiking activity is highly correlated to the level of demyelination which eventually plateau in both ends, as shown in Fig. 9, where values of ι_{my} less than 0.4 (lower index band) and greater than 0.7 (upper index band) show very subtle variations in comparison to values between 0.4 and 0.7 (middle index band).

IV. CONCLUSION

In this work, we have proposed a new hybrid computational simulation and experimental model to analyze signal propagation along neurons as they undergo demyelination and remyelination. We have analysed the effects of demyelination for three different levels and this includes (1) a single compartment within an axon, (2) bipartite synapse to understand how signal propagation changes as they propagate to the post-synaptic neuron and, (3) the impact of de/remyelination on a neuronal network. Our computational simulations were based on data from wet-lab experiments that used LPC to induce demyelination in slices of the cortical regions of the brain. The results from our computational simulations validated other findings from the literature that suggested the neuronal communication is indeed affected by demyelination. This analysis is based on developing a computational simulation model proposed by Hodgkin-Huxley and integrating it with signalling behaviour that is affected by the changes in the myelin sheaths. Our correlated analysis to the results from literature includes the changes in the amplitude and mean-shift, as well as capacity of information bits propagated between neurons, and the firing spike rate within a network of neurons as they undergo demyelination and remyelination. These approaches could pave the way for novel analytical techniques of neurons that are affected by diseases and their impact on their communication behaviour, by linking the results from wet-lab experiments that can feed into computational simulation models. This in turn can minimize the need for specialized

PUBLICATION 4: ANALYSIS OF LPC-INDUCED DEMYELINATION ON NEURONAL MOLECULAR COMMUNICATIONS

experimental equipment that is needed to investigate changes in the communication behaviour, where the simulation model can provide very fine-grain signalling properties down to the compartment level, as well as between neurons, all the way up to the scale of the network.

ACKNOWLEDGMENT

REFERENCES

[1] W. Huang, W. Chen, and X. Zhang, "Multiple sclerosis: Pathology, diagnosis and treatments (Review)," *Exp Ther Med*, vol. 13, no. 6, pp. 3163–3166, Jun 2017.

[2] C. S. Constantinescu and B. Gran, "The essential role of t cells in multiple sclerosis: A reappraisal," *Biomedical Journal*, vol. 37, no. 2, pp. 34–40, Mar-Apr 2014.

[3] S. Faissner, J. R. Plemel, R. Gold, and V. W. Yong, "Progressive multiple sclerosis: from pathophysiology to therapeutic strategies," *Nature Reviews Drug Discovery*, vol. 18, no. 12, pp. 905–922, Dec 2019.

[4] H.-B. Fan, L.-X. Chen, X.-B. Qu, C.-L. Ren, X.-X. Wu, F.-X. Dong, B.-L. Zhang, D.-S. Gao, and R.-Q. Yao, "Transplanted miR-219-overexpressing oligodendrocyte precursor cells promoted remyelination and improved functional recovery in a chronic demyelinated model," *Scientific Reports*, vol. 7, no. 1, p. 41407, Feb 2017.

[5] C. P. Duffy and C. E. McCoy, "The Role of MicroRNAs in Repair Processes in Multiple Sclerosis," *Cells*, vol. 9, no. 7, 2020.

[6] U. Milbreta, J. Lin, C. Pinese, W. Ong, J. S. Chin, H. Shirahama, R. Mi, A. Williams, M. E. Bechler, J. Wang, C. ffrench Constant, A. Hoke, and S. Y. Chew, "Scaffold-Mediated Sustained, Non-viral Delivery of miR-219/miR-338 Promotes CNS Remyelination," *Molecular Therapy*, vol. 27, no. 2, pp. 411–423, Feb 2019.

[7] A. P. Robinson, J. Z. Zhang, H. E. Titus, M. Karl, M. Merzliakov, A. R. Dorfman, S. Karlik, M. G. Stewart, R. K. Watt, B. D. Facer, J. D. Facer, N. D. Christian, K. S. Ho, M. T. Hotchkin, M. G. Mortenson, R. H. Miller, and S. D. Miller, "Nanocatalytic activity of clean-surfaced, faceted nanocrystalline gold enhances remyelination in animal models of multiple sclerosis," *Scientific Reports*, vol. 10, no. 1, p. 1936, Feb 2020.

[8] V. E. Miron, A. Boyd, J.-W. Zhao, T. J. Yuen, J. M. Ruckh, J. L. Shadrach, P. van Wijngaarden, A. J. Wagers, A. Williams, R. J. M. Franklin, and C. ffrench Constant, "M2 microglia and macrophages drive oligodendrocyte differentiation during cns remyelination," *Nature Neuroscience*, vol. 16, no. 9, pp. 1211–1218, Sep 2013.

[9] F. Doussau, J.-L. Dupont, D. Neel, A. Schneider, B. Poulain, and J. L. Bossu, "Organotypic cultures of cerebellar slices as a model to investigate demyelinating disorders," *Expert Opinion on Drug Discovery*, vol. 12, no. 10, pp. 1011–1022, 2017.

[10] T. Miki, H. Hirai, and T. Takahashi, "Activity-Dependent Neurotrophin Signaling Underlies Developmental Switch of Ca2+ Channel Subtypes Mediating Neurotransmitter Release," vol. 33, no. 48, pp. 18 755–18 763, 2013.

[11] A. Ghoumari, E. Baulieu, and M. Schumacher, "Progesterone increases oligodendroglial cell proliferation in rat cerebellar slice cultures," *Neuroscience*, vol. 135, no. 1, pp. 47–58, 2005.

[12] E. Birgbauer, T. S. Rao, and M. Webb, "Lysolecithin induces demyelination in vitro in a cerebellar slice culture system," *Journal of Neuroscience Research*, vol. 78, no. 2, pp. 157–166.

[13] V. E. Miron, S. K. Ludwin, P. J. Darlington, A. A. Jarjour, B. Soliven, T. E. Kennedy, and J. P. Antel, "Fingolimod (FTY720) Enhances Remyelination Following Demyelination of Organotypic Cerebellar Slices," *The American Journal of Pathology*, vol. 176, no. 6, pp. 2682–2694, Jun 2010.

[14] A. J. Pritchard, A. K. Mir, and K. K. Dev, "Fingolimod Attenuates Splenocyte-Induced Demyelination in Cerebellar Slice Cultures," *PLOS ONE*, vol. 9, 06 2014.

[15] A. F. Lloyd, C. L. Davies, R. K. Holloway, Y. Labrak, G. Ireland, D. Carradori, A. Dillenburg, E. Borger, D. Soong, J. C. Richardson, T. Kuhlmann, A. Williams, J. W. Pollard, A. des Rieux, J. Priller, and V. E. Miron, "Central nervous system regeneration is driven by microglia necroptosis and repopulation," *Nature Neuroscience*, vol. 22, no. 7, pp. 1046–1052, Jul 2019.

[16] N. D. Jeffery and W. F. Blakemore, "Remyelination of mouse spinal cord axons demyelinated by local injection of lysolecithin," *Journal of Neurocytology*, vol. 24, no. 10, pp. 775–781, Oct 1995.

[17] S. Thorpe, A. Delorme, and R. V. Rullen, "Spike-based strategies for rapid processing," *Neural Networks*, vol. 14, no. 6, pp. 715 – 725, 2001.

[18] J. Gautrais and S. Thorpe, "Rate coding versus temporal order coding: a theoretical approach," *Biosystems*, vol. 48, no. 1, pp. 57 – 65, 1998.

[19] M. R. DeWeese and A. M. Zador, "Binary Coding in Auditory Cortex," in *17th Conference on Neural Information Processing Systems*, 2003, pp. 117–124.

[20] K. Aghababaiyan, V. Shah-Mansouri, and B. Maham, "Capacity and Error Probability Analysis of Neuro-Spike Communication Exploiting Temporal Modulation," *IEEE Transactions on Communications*, vol. 68, no. 4, pp. 2078–2089, 2020.

[21] ——, "Axonal Channel Capacity in Neuro-Spike Communication," *IEEE Transactions on NanoBioscience*, vol. 17, no. 1, pp. 78–87, 2018.

[22] E. Balevi and O. B. Akan, "A Physical Channel Model for Nanoscale Neuro-Spike Communications," *IEEE Transactions on Communications*, vol. 61, no. 3, pp. 1178–1187, 2013.

[23] A. L. Hodgkin and A. F. Huxley, "A quantitative description of membrane current and its application to conduction and excitation in nerve," *The Journal of physiology*, vol. 117, no. 4, pp. 500–544, 1952.

[24] F. N. Quandt and F. A. Davis, "Action potential refractory period in axonal demyelination: a computer simulation," *Biological Cybernetics*, vol. 67, no. 6, pp. 545–552, Oct 1992.

[25] C. Koch, *Biophysics of computation: information processing in single neurons*. Oxford university press, 2004.

[26] G. L. Adonias, A. Yastrebova, M. T. Barros, Y. Koucheryavy, F. Cleary, and S. Balasubramaniam, "Utilizing Neurons for Digital Logic Circuits: A Molecular Communications Analysis," *IEEE Transactions on NanoBioscience*, vol. 19, no. 2, pp. 224–236, 2020.

[27] G. L. Adonias, H. Siljak, M. T. Barros, and S. Balasubramaniam, "Neuron Signal Propagation Analysis of Cytokine-Storm induced Demyelination," 2021, submitted for publication in March 2021.

[28] N. T. Carnevale and M. L. Hines, *The NEURON Book*, 1st ed. New York, NY, USA: Cambridge University Press, 2009.

[29] M. Hines, A. Davison, and E. Muller, "NEURON and Python," *Frontiers in Neuroinformatics*, vol. 3, p. 1, 2009.

[30] Y. Dombrowski *et al.*, "Regulatory T cells promote myelin regeneration in the central nervous system," *Nature Neuroscience*, vol. 20, no. 5, pp. 674–680, May 2017.

[31] U. S. Bhalla, *Multi-compartmental Models of Neurons*. Dordrecht: Springer Netherlands, 2012, pp. 193–225.

[32] C. C. H. Cohen *et al.*, "Saltatory Conduction along Myelinated Axons Involves a Periaxonal Nanocircuit," *Cell*, vol. 180, no. 2, pp. 311–322.e15, Jan 2020.

[33] M. Veletić, P. A. Floor, Z. Babić, and I. Balasingham, "Peer-to-Peer Communication in Neuronal Nano-Network," *IEEE Transactions on Communications*, vol. 64, no. 3, pp. 1153–1166, 2016.

[34] C. E. Shannon, "A mathematical theory of communication," *The Bell System Technical Journal*, vol. 27, no. 3, pp. 379–423, 1948.

[35] I. F. Akyildiz and J. M. Jornet, "The internet of nano-things," *IEEE Wireless Communications*, vol. 17, no. 6, pp. 58–63, 2010.

[36] M. Veletić, P. A. Floor, Y. Chahibi, and I. Balasingham, "On the Upper Bound of the Information Capacity in Neuronal Synapses," *IEEE Transactions on Communications*, vol. 64, no. 12, pp. 5025–5036, 2016.

[37] D. Malak, M. Kocaoglu, and O. B. Akan, "Communication theoretic analysis of the synaptic channel for cortical neurons," *Nano Communication Networks*, vol. 4, no. 3, pp. 131–141, 2013.

[38] B. B. Averbeck, "Poisson or Not Poisson: Differences in Spike Train Statistics between Parietal Cortical Areas," *Neuron*, vol. 62, no. 3, pp. 310–311, 2009.

[39] I. Chakravarti, R. Laha, and J. Roy, *Handbook of Methods of Applied Statistics: Techniques of Computation, Descriptive Methods, and Statistical Inference*, ser. Wiley Series in Probability and Mathematical Statistics. Wiley, 1967, vol. 1, pp. 392–394.

[40] J. Platkiewicz and R. Brette, "A threshold equation for action potential initiation," *PLOS Computational Biology*, vol. 6, 07 2010.

[41] M. Levine and J. Shefner, "A model for the variability of interspike intervals during sustained firing of a retinal neuron," *Biophysical Journal*, vol. 19, no. 3, pp. 241–252, 1977.

[42] M. S. Hamada *et al.*, "Loss of Saltation and Presynaptic Action Potential Failure in Demyelinated Axons," *Frontiers in Cellular Neuroscience*, vol. 11, p. 45, 2017.

Geoflly L. Adonias is currently a Ph.D. candidate at the Walton Institute for Information and Communication Systems Science (formerly TSSG), Waterford Institute of Technology (WIT), Ireland, under the Science Foundation Ireland (SFI) CONNECT Project for future networks and communications. He received his B.Eng. in Electrical Engineering from the Federal Institute of Education, Science and Technology of Paraíba (IFPB), Brazil, in 2017. His current research interests include Nano-scale Communications, Digital Signal Processing and Wireless Networks.

Conor Duffy is a PhD candidate in the School of Pharmacy and Biomolecular Sciences at the Royal College of Surgeons in Ireland, under the Irish Research Council Government of Ireland Postgraduate Scholarship Programme. He received his B.Sc in neuroscience from University College Dublin, Ireland in 2017. His current research interests are neuroinflammation and myelin repair, particularly the role of microRNAs in mediating these processes.

Michael Taynnan Barros is currently the recipient of the Marie Skłodowska-Curie Individual Fellowship (MSCA-IF) at the BioMediTech Institute of the Tampere University, Finland. He received his Ph.D. in Telecommunication Software at the Waterford Institute of Technology, Ireland, in 2016, M.Sc. degree in Computer Science at the Federal University of Campina Grande, Brazil, in 2012 and B.Tech. degree in Telematics at the Federal Institute of Education, Science and Technology of Paraíba, Brazil, in 2011. He has authored or co-authored over 60 research papers in various international flagship journals and conferences in the areas of wireless communications, molecular and nanoscale communications as well as bionanoscience. He is also a reviewer for many journals and participated as technical program committee and reviewer for various international conferences. Research interests include Internet of BioNanoThings, molecular communications, bionanoscience and 6G Communications.

Dr Claire E. McCoy is a research scientist and senior lecturer in immunology at the Royal College of Surgeons in Ireland. She leads a research team investigating the impact of the immune system in Multiple Sclerosis, with the aim to understand how manipulation of the immune system may be therapeutically harnessed for the treatment of MS. Claire has published 26 manuscripts in high impact journals and is the recipient of multiple national and international research awards, most notably; the President of Ireland Future Research Leader Award from Science Foundation Ireland. She is co-founder of the All-Ireland MS Research Network and is a funded investigator with FutureNeuro.

Sasitharan Balasubramaniam (Sasi) received his Bachelors of Engineering (Electrical and Electronic) and PhD (Computer Science) degrees from the University of Queensland, Australia, in 1998 and 2005, respectively, and Masters of Engineering Science (Computer and Communication Engineering) degree in 1999 from the Queensland University of Technology, Australia. He is currently an Associate Professor with the Department of Computer Science & Engineering, University of Nebraska-Lincoln, USA. He was previously a recipient of the Science Foundation Ireland Starter Investigator Research Grant and the Academy of Finland Research Fellow grant. Sasi has published over 100 journal and conference papers, and actively participates in various conference committees. He is currently the Chair of the Steering Committee for ACM NanoCom, a conference which he co-founded. He is currently an Associate Editor for IEEE Transactions on Mobile Computing and IEEE Transactions on Molecular, Biological, and Multi-scale Communications. He was a past Associate Editor for the IEEE Internet of Things Journal. In 2018, Sasi was also the IEEE Nanotechnology Council Distinguished Lecturer. His current research interests include molecular and nano communications, terahertz communication for 6G, as well as the Internet of Nano Things.

CHAPTER **10**

PUBLICATION 5: UTILISING EEG SIGNALS FOR MODULATING NEURAL MOLECULAR COMMUNICATIONS

Utilising EEG Signals for Modulating Neural Molecular Communications

Geoflly L. Adonias,
Michael Taynnan Barros
Telecommunications Software and
Systems Group,
Waterford Institute of Technology
Waterford, Ireland
gadonias,mbarros@tssg.org

Linda Doyle
Trinity College Dublin
Dublin, Ireland
linda.doyle@tcd.ie

Sasitharan Balasubramaniam
Dept. of Electronic and
Communication Engineering,
Tampere University of Technology
Telecommunications Software and
Systems Group,
Waterford Institute of Technology
Tampere, Finland, Waterford, Ireland
sasib@tssg.org

ABSTRACT

A major challenge in neuronal molecular communications lies in modulating signals through the neuronal network of the cortex that will minimize interference with the natural signalling. In this paper, we propose the use of Electroencephalogram (EEG) signals as a sensing mechanism to determine spiking interval gaps that can be used to stimulate artificial data transfer in the cortical micro-column.

CCS CONCEPTS

• **Applied computing** → **Life and medical sciences**; *Telecommunications*; *Computational biology*; *Systems biology*;

KEYWORDS

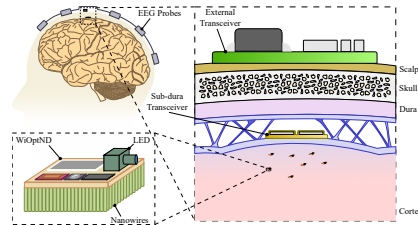Nanonetworks, Molecular Communication, Information Theory, EEG, Optogenetics

1 INTRODUCTION

Recent studies in molecular communication have investigated the maximum capacity of sending information through neurons. A question remains as to how stimulation of neurons to transmit information can be achieved while minimizing interference with natural signalling process. In particular when miniature nanoscale implantables such *Wireless Optogenetics Nanonetworks* (*WiOptND*) are used to stimulate the neurons. One possible approach is to

Figure 1: System Architecture.

integrate a sensing system within the cortex that will sense the neural activities, however, this leads to increased complexity.

The objective of this paper is to present a new form of Brain-Computer Interface (BCI), where the EEG measurements are used to determine the activity of the cortex, which in turn can provide new forms of neuronal molecular communication modulation. The overall proposed system is illustrated in Figure 1. There is a relationship that exists between the neuron firing patterns and the EEG signalling, as shown in Figure 2. A neuron can slow down or speed up its firing rate depending on tasks being performed by the subject. Therefore, based on this, our aim is to transmit information through the low spiking patterns of the neurons, and in particular during the gaps.

2 CORTICAL COLUMN ARTIFICIAL DATA TRANSFER

The Micro-column activity (MCA) depends on parameters regarding its structure such as number, type and configuration of the cells and topology of the column. The EEG signal is measured passed through a band-pass filter for both the *delta* and *gamma* frequency bands with which the power of the *gamma* signal and the phase of the *delta* signal are determined. The multi-unit activity is then predicted by the model proposed by [4] and represented as $S = W_\gamma \omega_\gamma + \Theta_\Delta \omega_\Delta + \varepsilon$, where $\omega_{\gamma,\Delta}$ are the weights of power and phase, W_γ and Θ_Δ are oscillatory power and phase and ε is a constant error term. Further details regarding the statistical estimation of the weights and the use of only *gamma* and *delta* signals can be found in [4].

The probability that k spikes are fired during a giving time interval in which S spikes are expected, is given by $P(k \in S) = S^k e^{-S}/k!$. Therefore, the probability of communication gap, P_{gap}, would be

(a) Evoked EEG.

(b) Spike activity.
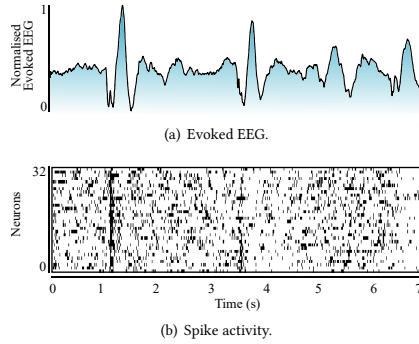
Figure 2: Relationship between the (a) normalised evoked EEG and the (b) spike raster plot data from visual stimuli.

equal to the probability of $k = 0$ spikes. Thus, $P_{gap} = p(x = 0) = e^{-S}$. Time intervals, with duration τ, are discrete time slots in which a single bit is transmitted, and is defined as $\tau = T/N_b$, where T is the total time of observation and N_b is the total number of bits. The information rate, R, which is used to analyse the ability of a sender to communicate multiple bits of information to a receiver, is the maximum average amount of information transferred per unit time and is given as $R = C(X;Y)/\tau$, where $C(X;Y)$ is the maximum average mutual information.

3 RESULTS AND DISCUSSION

In this section, the results obtained from simulations performed using NEURON and Python are presented [1]. The cells models are arranged according to their respective layers and connection probabilities based in [2]. Each column is arranged with one cell per layer and a fractional noise parameter is set to zero so it would be possible to evaluate the interference caused by the free spreading of spikes fired in both single- and multi-unit arrangements. The EEG readings of neuronal activity are based on recordings from a 10-20 electrode system [3]. The data is analysed through a signal processing algorithm to detect gaps that can be used to modulate signals. Based on this, we stimulate the neurons to transmit artificial data within these gaps.

Figure 3(a) depicts how a larger number of transmitted bits along with a lower P_{gap} implies more interference across the column, considering bit sequences randomly generated in relation to P_{gap}, which represents a decrease in the channel capacity between T_x (L23) and R_x (L6). This decay follows the shape of an exponential function getting very close to zero when it approaches 100 transmitted bits.

Figure 3(b), on the left side, shows that neighbouring columns, simulated for 50 transmitted bits and a $P_{gap} = 0.5$, resulting in more interference in the channel which leads to a decrease, by a factor of approximately 2, in the capacity and information rate. The right side illustrates a input probability collected from real EEG readings.

The columnar arrangements were kept the same for all simulations, but any change in their position, connection probability or

(a)

(b)
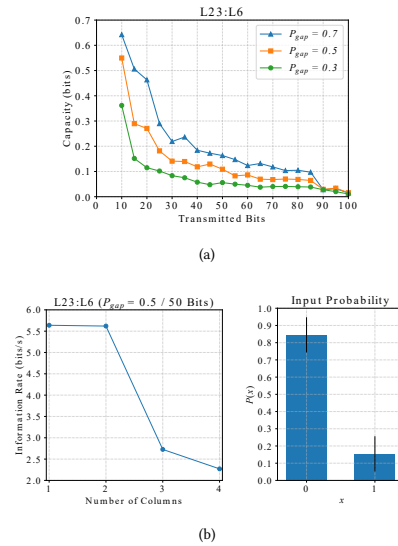
Figure 3: Analysis of the channel regarding the relationship between the (a) capacity and the number of transmitted bits in a 1000 ms simulation and the (b) influence of the number of cortical columns in the information rate (left) and the input probability of the system (right).

the number of dendrites, represents a cascade of events that would lead to performance changes.

4 CONCLUSIONS

Our proposed artificial data transfer system results demonstrates how neighbouring cells represent a significant level of interference even if only one cell is firing spikes. At the same time, the correlation between the EEG signals and spiking activity may vary across situations requiring a careful approach for interpreting the signals. The proposed work can lead to a new form of BCI for neural communication systems and pave the way towards new applications and a more reliable process to enhance the capabilities of the brain by inserting artificial data without interfering with the natural flow of neuronal information.

ACKNOWLEDGMENTS

REFERENCES

[1] Nicholas T. Carnevale and Michael L. Hines. 2009. *The NEURON Book* (1st ed.). Cambridge University Press, New York, NY, USA.
[2] Henry Markram et al. 2015. Reconstruction and Simulation of Neocortical Microcircuitry. *Cell* 163, 2 (2015), 456–492. https://doi.org/10.1016/j.cell.2015.09.029
[3] Michal Teplan. 2002. Fundamentals of EEG measurement. *Measurement science review* 2, 2 (2002), 1–11.
[4] Kevin Whittingstall and Nikos K. Logothetis. 2009. Frequency-Band Coupling in Surface EEG Reflects Spiking Activity in Monkey Visual Cortex. *Neuron* 64, 2 (2009), 281–289. https://doi.org/10.1016/j.neuron.2009.08.016

CHAPTER 11

PUBLICATION 6: A LOGIC GATE MODEL BASED ON NEURONAL MOLECULAR COMMUNICATION ENGINEERING

A Logic Gate Model based on Neuronal Molecular Communication Engineering

Geofly L. Adonias,
Michael Taynnan Barros,
Sasitharan Balasubramaniam
Telecommunications Software & Systems Group
Waterford Institute of Technology
Waterford, Ireland
{gadonias, mbarros, sasib}@tssg.org

Anastasia Yastrebova,
Yevgeni Koucheryavy
Dept. of Electronic and Communication Engineering
Tampere University of Technology
Tampere, Finland
anast.yastrebova@gmail.com
yk@cs.tut.fi

Abstract—The field of Neuroengineering aims to investigate ways to proposed synthetic and controllable Boolean computing inside the brain using neuronal cells based on the existing neuronal computation abilities of the Brain. In this work, we propose the design of AND and OR logic gates using a multicellular Boolean logic operation by engineering the molecular communications of neurons and we evaluate their performance when passing data along as isolated units. The results show higher accuracy values of gate operation for mid-level inter-spike intervals when stimulated with spike trains revealing the role of the frequency of firing and how this impacts on neuronal logic gating.

Index Terms—molecular communication, neuronal network, logic gates, Boolean algebra

I. INTRODUCTION

Recent studies have investigated the computation abilities of the brain following findings that its internal structure might be composed of reliable Boolean building blocks similar to the ones found at the core of today's transistors [1]. A question remains as to how synthetic and controllable engineering of neuronal logic gates can impact on future precision medicine technologies for neurodegenerative diseases.

Neuronal cells send and receive information through the firing of action potentials (AP), i.e. spikes, and depending on the task that is being performed by the brain, a neuron can speed up or slow down its firing rate. This exchange of information through electrochemical signalling between neurons is known as neuro-spike communication and is one of the models of molecular communication proposed in the literature [2]. In this work, we propose the design of logic gates using a multicellular Boolean logic operation by engineering the molecular communications of neurons, based on the neuro-spike signal propagation.

Our objective is to present an analysis from the perspective of molecular communications on the logical Boolean operations of neuronal cells by controlling information processing at a tissue level, for potential reconfiguration of neural circuits or the development of non-surgical neural interfaces, in relation
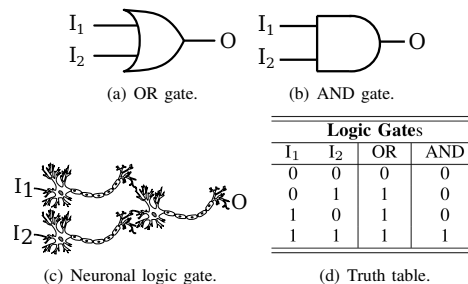
Fig. 1. Logic gates and their truth tables.

	Logic Gates		
I_1	I_2	OR	AND
0	0	0	0
0	1	1	0
1	0	1	0
1	1	1	1

to stimulation frequencies of the input neurons, as illustrated in Fig. 1. The variations in the frequency of stimulation may represent interference in the neuro-spike propagation that could cause loss of information. The performance of the gates is measured in terms of accuracy between the expected output, given with known inputs, and the actual output.

II. NEURONAL DIGITAL LOGIC GATES

The neuron spiking threshold value not only controls the firing rate of a neuron but also plays a role in how it processes information. A neuron follows the *all-or-none* principle to fire a spike. Stereotypically, an AP is initiated only when the membrane potential, $V(\cdot)$, in the cell reaches a certain level, i.e. threshold, th. According to Platkiewicz and Brette [3], the threshold in brain cells depends on several parameters such as stimulus (x), type of cells (α), synaptic conductances ($gSyn$) and properties of ionic channels (E). We use this phenomenon of the neurons to design logic gates and it is defined as

$$AP = \begin{cases} 1, & \text{if } V(x, \alpha, gSyn, E) > th \quad (1) \\ 0, & \text{otherwise} \quad\quad\quad\quad\quad (2) \end{cases}$$

In order to build a single logic gate, three neurons are used, two of them operating as the inputs and the other one as the output, and the synaptic connections between them are made with regards to their respective connection

probabilities. The stimulation may be due to spikes from other neighbouring neurons or can be artificially stimulated using miniature implantables *Wireless Optogenetics Nanonetwork Devices (WiOptND)* [4].

In this work, we use a simple OOK modulation, where a spike is considered as a bit "1" and its absence as a bit "0" in a time slot with τ ms. Both inputs, I_1 and I_2, are stimulated with spike trains with different inter-spike intervals (ISI). The models of neurons were kept in their default configuration except for the threshold for spike initiation that was set to a very low value of -60 mV for both gate types.

For this paper, we present the design of two logic gate types, an OR and an AND gate. Five OR and three AND gates were built for this study with different types of cells but all of them follow the structure/connection depicted in Fig. 1(c) and their behaviour is described by their respective truth tables as shown in Fig. 1(d).

By knowing the type of the gate and the two input spike trains, it is possible to obtain the expected output, $E[Y]$, and then calculate the accuracy of the gate by comparing $E[Y]$ with the actual output, Y. The accuracy, $A(E[Y]; Y)$, is then defined as the ratio of correct classifications to the total number of samples classified, thus

$$A(E[Y]; Y) = \frac{P_{1,1} + P_{0,0}}{P_{0,0} + P_{0,1} + P_{1,0} + P_{1,1}}, \qquad (3)$$

where $P_{Y,E[Y]}$ is the probability of Y given $E[Y]$, where $Y \& E[Y] \in \{0, 1\}$.

III. RESULTS AND DISCUSSION

In this section, the simulations performed with the models of neurons downloaded from the *Digital Reconstruction of Neocortical Microcircuitry* [5] using the *NEURON Simulator* [6] are presented. The models are arranged as isolated cells connected to each other as shown in Fig. 1(c) and do not represent activities as part of a larger network. The type of cells include *Descending Axon (DAC)*, *Horizontal Axon (HAC)*, *Small Axon (SAC)*, *Martinotti (MC)*, *Bitufted (BTC)*, *Double Bouquet (DBC)*, *Bipolar (BP)*, *Large Basket (LBC)*, *Nest Basket (NBC)* and *Small Basket (SBC)*.

In Fig. 2(a), it is possible to verify that different ISI's do not represent drastic changes in the accuracy of the AND gate, where the average accuracy is around 0.353. On the other hand for the gate OR (Fig. 2(b)), we observe an increase of the accuracy with the ISI between $5 - 11$ ms from 0.232 to 1.

In general, Fig. 2 shows that for all gates, an ISI of 8 ms returns the highest values of accuracy and that the higher the frequency of firing, the worse the performance of the gates will be. At the same time, higher ISI's can decrease the accuracy considering that to evoke a spike in the output, the potential summation should increase towards the threshold in a faster pace than the rate with which the cell goes back to its resting potential. We highlight this importance to consider that changes in the parameters of the models may lead to a change of the gate's accuracy.
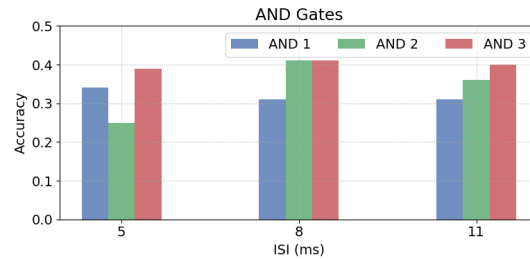
(a) Accuracy for AND gates.
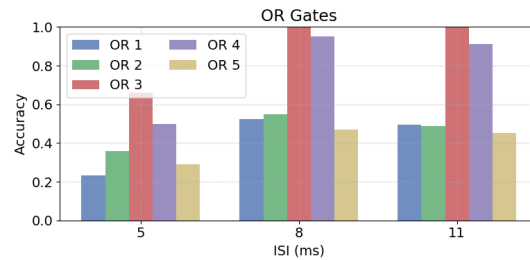
(b) Accuracy for OR gates.

Fig. 2. Accuracy for the AND and OR gates with different ISI's. AND gates: (1) MC, NBC and HAC, (2) SBC, MC and SBC, (3) MC, MC and DAC. OR gates: (1) DAC, SAC and LBC, (2) DBC, BTC and BP, (3) DAC, HAC and MC, (4) MC, NBC and DAC, (5) DBC, DBC and BP.

IV. CONCLUSIONS

In this paper, we designed OR and AND logic gates using the engineering of neuronal molecular communication systems. Our results show how the frequency of firing affects the accuracy of the neuronal digital logic gates, where a mid-level ISI demonstrates to be the most appropriate for high accuracy. For future work, we intend to conduct analysis on logic circuits composed by several gates with a generalised approach to fine-tune the system constructed within a cellular tissue .

REFERENCES

[1] A. Goldental, S. Guberman, R. Vardi, and I. Kanter, "A computational paradigm for dynamic logic-gates in neuronal activity," *Frontiers in Computational Neuroscience*, vol. 8, p. 52, 2014.

[2] N. Farsad, H. B. Yilmaz, A. Eckford, C. B. Chae, and W. Guo, "A Comprehensive Survey of Recent Advancements in Molecular Communication," *IEEE Communications Surveys Tutorials*, vol. 18, no. 3, pp. 1887–1919, thirdquarter 2016.

[3] J. Platkiewicz and R. Brette, "A Threshold Equation for Action Potential Initiation," *PLOS Computational Biology*, vol. 6, no. 7, pp. 1–16, 07 2010. [Online]. Available: https://doi.org/10.1371/journal.pcbi.1000850

[4] S. A. Wirdatmadja *et al.*, "Wireless Optogenetic Nanonetworks for Brain Stimulation: Device Model and Charging Protocols," *IEEE Transactions on NanoBioscience*, vol. PP, no. 99, pp. 1–1, 2017.

[5] H. Markram *et al.*, "Reconstruction and Simulation of Neocortical Microcircuitry," *Cell*, vol. 163, no. 2, pp. 456–492, 2015. [Online]. Available: http://dx.doi.org/10.1016/j.cell.2015.09.029

[6] N. T. Carnevale and M. L. Hines, *The NEURON Book*, 1st ed. New York, NY, USA: Cambridge University Press, 2009.

DISCUSSION

This PhD work has investigated neuron-based molecular communications systems supported by conventional information and communication engineering concepts and metrics, such as attenuation, channel capacity and propagation delay. Because these systems are so unique in approaching the stochasticity of the biological dynamics, there is a chance some challenges that have not even been modelled yet e.g., extremely low propagation speeds and severely susceptible to thermal noise and drifting, are affecting the performance of those communication channels. As scientists validate and propose novel models of these biological processes more efficiently, conventional communication concepts will shift towards a more accurate theory for information and communication systems. This chapter summarises the lessons learnt as well as the contributions from the design and analysis of neuron-based communications systems.
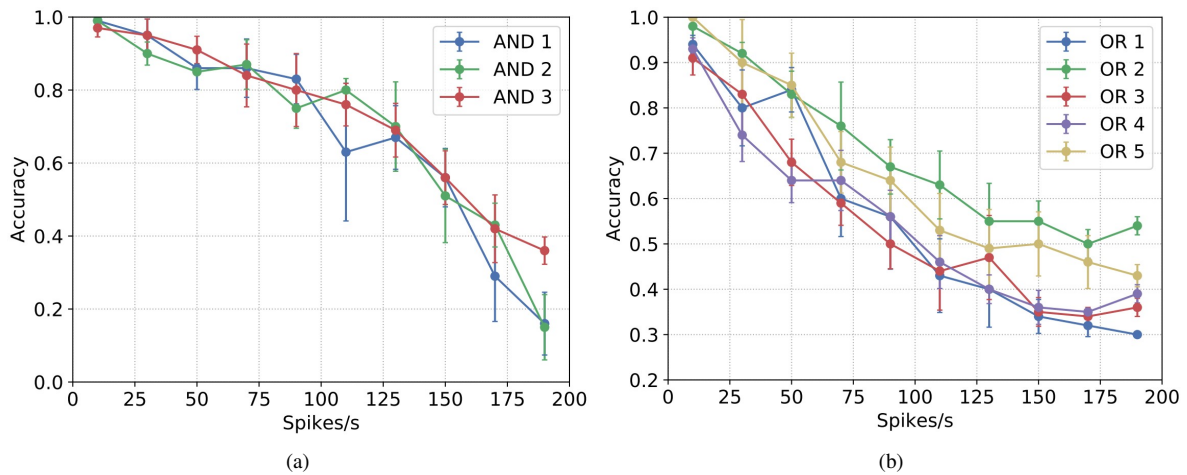
Fig. 12.1 Mean and standard deviation for the (a) three AND gates and (b) five OR gates. Five simulations were performed for each rate and the spiking pattern follows a *Poisson* process.

12.1 DESIGN OF NEURON-BASED MOLECULAR COMMUNI-CATION DEVICES

Several parameters of synaptic communication can be used to influence the weight of a stimulus and the reliability of the propagation of an action potential. One example would be the capability of neurotransmitters to influence synaptic conductance values [109]. The models proposed for the design of logic gates for queue and systems theory analysis of an arrangement of neurons and neuronal logic gates can be mostly fine-tuned for maximum gating performance as suggested by Vogels et al [14] who suggested the weakening or strengthening of synaptic connections lead to a gating behaviour inside a homogeneous network of neurons. Moreover, the experiments conducted by Goldental et al [13] enforced stimulations on neuronal circuits within a network of cortical neurons *in-vitro*. The authors propose different types of gates, such as XOR and NOT. However, they took advantage of the propagation delay to control the output of the neuronal logic gate. Nevertheless, proving biocomputing devices made out of neurons are reaching promising stages of development.

114
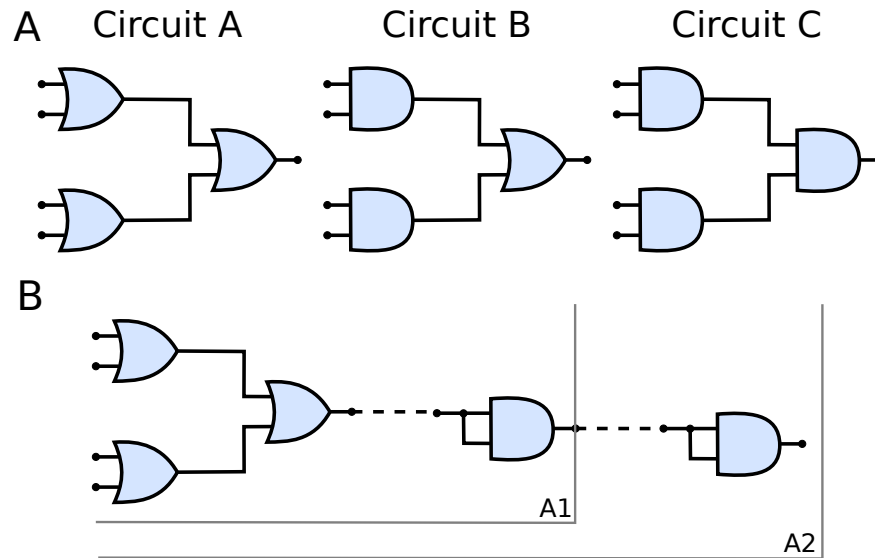
Fig. 12.2 (A) Schematic of circuits A, B and C and (B) The connection of AND gates in cascade to circuit A. *A*1 refers to the arrangement described by a single AND gate connected to the output of the circuit A and *A*2 refers to another AND gate connected to the output of *A*1 arrangement, i.e. two AND gates in cascade with circuit A. Analogous nomenclature is employed for both circuits B, as in B1/B2 and C, as in C1/C2.

Fig. 12.1 shows the performance of the different gate arrangements that were proposed for AND gates (Fig. 12.1a) and OR gates (Fig. 12.1b). As aforementioned above, many of the work published in the literature about neuronal logic gates do not account for missed signals, i.e. spikes that are not passed forward due to effects of the refractory period of a neuron (refer to Section 2.1 for more detailed information on refractory period). As shown in Fig. 12.1b, the three AND gates have quite a similar performance although AND 3 is slightly the best one (refer to Adonias et al. [110] for details on the logic gates). This may be due to the fact there is only a single way for an AND gate to output a signal, meaning that this may play a role in decreasing the chances for the gate to inaccurately process the inputs. On the other hand, OR gates can invoke an output not only when both inputs receive a stimulus but also when either of them is stimulated. The proposed arrangements differ between themselves in terms of accuracy when compared to an ideal OR gate and, it is clear from Fig. 12.1b that OR 2 is the best performing gate.

Not only is the filtering behaviour suggested as a case study but also the idea of analysing the neuronal arrangements as a transfer function derived from the Hodgkin-Huxley linear model corroborates the notion that neurons can help filter out specific frequencies as found in the literature [104]. The transfer function and the queuing theoretical models help researchers approach the challenges of modelling neuron-based communication systems in a relatively simple yet efficient way. The results from this PhD work such as the ones published in Chapter 7, therefore, suggest that neuronal logic circuits can be used to construct more complex "bio-electronic" circuits, such as digital filters, capable of filtering abnormal high-frequency activity which can have many sources including neurodegenerative diseases. The proposed mathematical framework provides a way to understand how arrangements of neurons can act as neuronal digital filters. Furthermore, by providing an insight into how the control of the band-passing frequency could be performed, it is possible that researchers and scientists on precision pharmacology and drug design could take advantage of those findings to develop specific pharmaceuticals able to modify parameters of the neuronal logic gates responsible for its band-passing control. It was demonstrated that by reconfiguring inner parameters of the filters, e.g. gates that make up the filter, it is possible to, by modifying the type of filter (Fig. 12.2), shift the intensity with how specific spike firing frequencies are attenuated on the fly and this adaptation could be tailored to specific tasks performed by the subject.

Fig. 12.2a shows the three types of the circuit that were built and analysed in [111]. From circuits A to C, the number of OR gates is decreased; when compared to AND gates, OR gates are quite permissive as seen in one of our previous studies [110]. Fig. 12.2b shows the connection of up to two AND gates in cascade with the circuits. Each of the circuits was analysed with one and two AND gates in cascade, hence the nomenclature of a letter followed by a number, the letter refers to the type of circuit and the number accounts for how many AND gates are connected in cascade. If using the same type of gates (OR and AND),
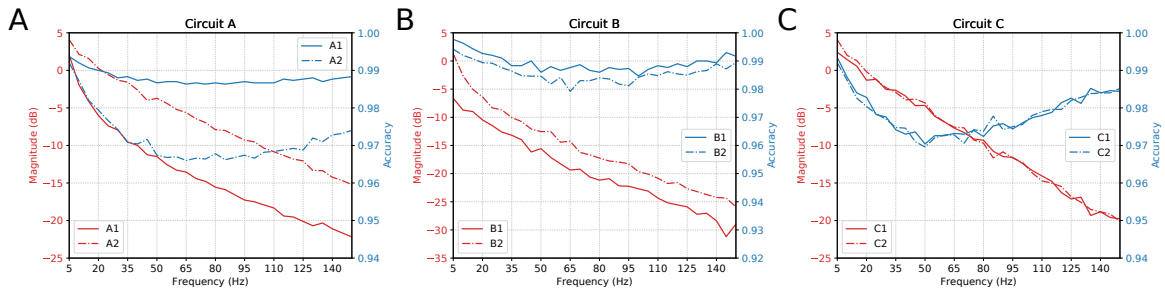
Fig. 12.3 Parallel between Magnitude (dB) and Accuracy of the circuits with AND gates in cascade.

by mixing and matching them into different configurations, we should not expect dramatic changes in the results when compared to the ones presented. However, different types of gates may strongly influence the accuracy and overall performance of the circuit. The results for that analysis in terms of magnitude and accuracy for the circuits are shown in Fig 12.3.

The results shown in Fig 12.3 suggest that an increase in the number of cascading gates will lead to an increase in the attenuation of the signal propagated through the network and this effect is probably specific to some characteristics of the cell, such as the connection probability. Hence, the more gates in the cascade, the worse the performance of the circuit in terms of accuracy. However, when looking from the perspective of filtering high-frequency firing, each of the circuits performs quite well by attenuating the power of higher frequencies for more than -20 dB. Even though the ratio keeps fluctuating, with a careful evaluation, the dip in the accuracy along mid-range frequencies is very subtle in terms of the whole scale, showing a difference of only around 0.03 on the values of accuracy. The possibility of enforcing a drop in higher frequencies can be beneficial for the treatment of certain diseases such as epilepsy which is characterised by high-frequency bursts of spike firing [112]. Although this requires precise characterisation of the neural tissue that would be the "epicentre" of the seizure-like activity, we do not need to know exactly which cell is malfunctioning. In other words, those neuronal circuits can be deployed in a network and, with a sufficient number of

(a)   (b)
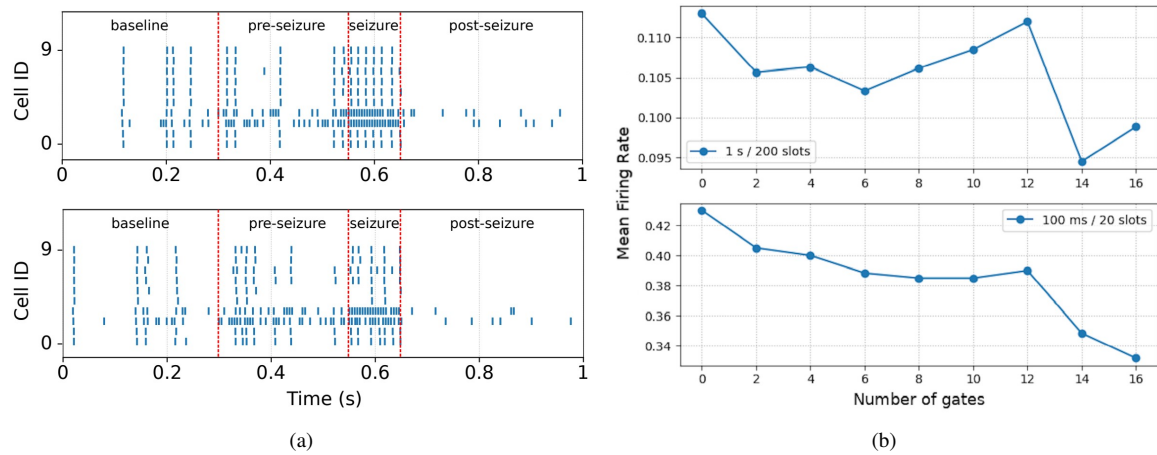
Fig. 12.4 Simulation of epileptic seizures in a network with 10 neurons (2 neurons per cortical layer), stimulation performed in cells at layer 2/3. (a) Raster plot of the network with no gates inserted and natural connections only (top) as illustrated in Fig. 3; and raster plot of the network with 16 neuronal logic gates (bottom), natural connections are broken where gates are placed; (b) Mean firing rate in the network as more and more gates are placed within it; the top graph shows the firing rate of the whole network for all stages as shown in Fig. 13(a); the bottom graph shows the firing rate for the whole network but only for the seizure stage.

them, it is possible to curb the epileptic activity. This shows the relevance of the research described in this PhD work.

The previously mentioned attenuating effects can be seen in Fig. 12.4. A small network, was built for the investigation presented in [110], it contains 10 neurons and the number of AND gates increases from none to 16 inside the network. The AND gates are suggested as a potential solution to smooth out high-frequency spike firing. Fig. 12.4a, show how a stimulation done only in the cells of layer 2/3 behaves as it propagates through other cells in the same network and the difference is visually clear on the frequency of spike firing between a network with no gates (top) and a network with 16 gates (bottom). On the other hand, the mean firing rate (Fig. 12.4b) was also calculated as a function of the number of gates inside the network. As expected mean firing rate of the network decreases as the number of AND gates inside the network increases. This corroborates our hypothesis that neuronal logic gates and, consequently logic circuits, will help to fine-tune the system, providing ways to improve the performance of the disease therapy using biocomputing approaches. The lessons

learnt from those analyses reveal a tendency for AND gates to maintain a better accuracy with the increase of the input frequency compared to OR gates in a relatively large neuronal logic circuit. Moreover, a queuing-theoretical analysis showed remarkable accuracy when predicting the output of the gates under different input frequencies. It was also learnt that our study has demonstrated the fact that each circuit has a preferable frequency band for maximum efficiency when filtering high-frequency spike firing.

12.2 Demyelination Effects on a Neuronal Communication Channel

Myelin sheath is an integral part of some neurons as it provides insulation to the axon and reduces attenuation on the propagation of action potentials through the axonal pathway. The demyelinating disease is a strong factor that leads to other types of neurodegeneration such as multiple sclerosis. One of the causes of demyelinating disease occurs indirectly and it needs other processes, such as immune system responses, to kick-start it. This is the case of viral infections, some viruses can cross the blood-brain barrier and infect the nervous system leading to an immune response that triggers the release of cytokine storm to fight the infection but it can damage healthy tissues, such as the myelin sheath, in the process [81]. The literature has been hinting at this hypothesis, but more in-depth studies are needed because viruses are usually studied from the perspective of their main symptoms. Demyelination can also be induced by known chemicals, this is a process widely used by wet-lab experimentalists and aims at facilitating the analysis of the effects of demyelination and remyelination.

This thesis investigated new computational simulation models to understand how cytokine storms can affect and destroy myelin sheaths and how this affects the communication as well as the effects of chemicals such as lysolecithin. The work described in this thesis does

(a) Action potential propagation on an axon fully myelinated.

(b) Action potential propagation on an axon with half of its normal myelination levels.
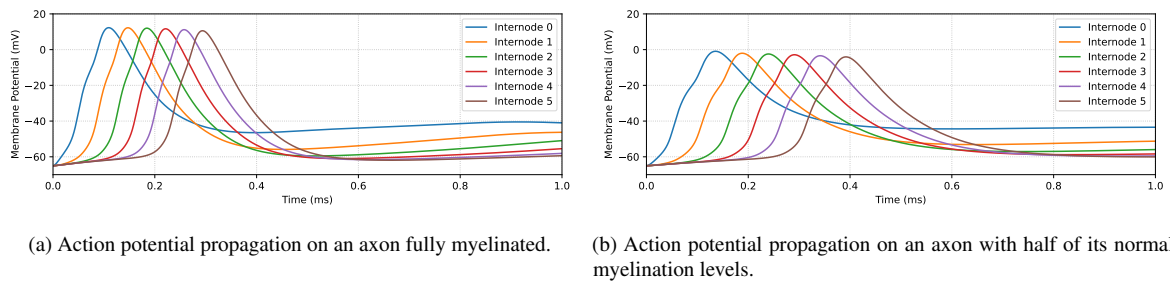
Fig. 12.5 Parallel for action potential propagations between a fully myelinated and a partially (50%) demyelinated axon.

not focus on variations of the input process. The objective of the analysis is, basically, to understand the effects of demyelination on axonal signal propagation and consequences to the communication in a bipartite synapse and relatively larger networks of neurons. The main difference between both causes of demyelination would be the time they take to reach full demyelination. From a cytokine storm perspective, even after the viral infection is cleared from the nervous system, it may take about a few weeks for the demyelination to settle [81]. On the other hand, the use of chemicals such as lysolecithin (LPC) [113] can offer a more timely controlled way of evaluating the demyelinating process, in other words, LPC can fully demyelinate a slice culture in about 24 hours and then the remyelination process should naturally take a couple of weeks. However, it never comes back to its original state (full myelination). The results presented in this thesis have shed light on the relevance of modelling external agents such as cytokine storms and chemicals for a more detailed and accurate analysis of neuron-based molecular communication systems. Along with wet-lab data provided by collaborators, it was possible to understand the dynamics of the demyelination on the propagation of action potentials on neuronal compartments (Fig. 12.5), its influence on the synaptic connection and the effects on a larger neuronal network. This collaboration was very fruitful as it helped make sense of the computational results presented in the paper, it provided background information on the speed with which the demyelination and remyelination occur.

Furthermore, the empirical calculation of the myelination index shed light on a more accurate fine-tuning of the Hodgkin-Huxley model. This collaboration was crucial for preliminary validation of the results and, consequently, a better understanding of wet-lab procedures for the collection of data. The results match other studies that show that action potentials are broadened and the conduction velocity supported by the saltatory nature of the conduction of neuronal potential is prone to failure as the myelin sheath gets damaged [114–116]. This phenomenon can be observed as half of the myelination (Fig. 12.5b), which already present quite a distinct visual attenuation on the potential and on the peak time when compared to a healthy fully-myelinated neuron (Fig. 12.5a). This is an interesting finding for the field of molecular communications as neurotransmitters are released also as a function of the action potentials [117] and with attenuation and delay caused by demyelination, the information that is being transferred can be compromised. For example, the intersymbol interference can be minimised with proper modulation of molecules such as neurotransmitters [118]. In other words, by modulating the quantity of molecules diffused in the medium, we are applying a similar approach to pulse-width modulation, thus, leading to a lower intersymbol interference. The lessons learnt reveal that our analysis corroborates findings from literature that indicates the neuronal communication may be affected by pro-inflammatory immune response inside the brain. Also, the proposed model for demyelination and remyelination show a satisfactory level of effectiveness when combining wet lab and digital simulation platforms that can be used to help design drugs for re-myelination and its relation to axonal signal propagation and subsequent neuronal communication.

CHAPTER 13

CONCLUSION

Several molecular communication systems have been studied in the past few years, e.g. neuro-spike communication, and even though only a small number of those studies focused on the conceptualisation and design of synthetically engineered devices, it is expected that much of this knowledge will soon reach development stages fueled by interdisciplinary advances in nanotechnology, biomedical engineering and synthetic biology. These systems can be presented as a biocompatible interface for a more reliable biological communication system. They would also have the ability to influence the communication at the nanoscale where natural cells interact with bio-nanomachines either reacting to the environment (e.g. cytokines released to fight infections) or for cooperation aiming towards better efficiency. This PhD thesis followed the premise that the union of molecular communications and synthetic biology will allow the communication between neurons (natural and artificial) by manipulating their electrochemical signalling. Neuronal signalling is a short-range communication process between neurons and, sometimes involves non-neuronal cells, e.g. glial cells. Therefore, this theses provided a framework that could lead further study and development of synthetically engineered systems capable of interfacing with natural and other artificial brain cells. This approach could help pave the way for more robust and biologically compatible treatments against neurodegeneration with an increased efficiency.

Neuronal logic gates have been proposed in the literature as one of the building blocks of more complex neuronal circuits. Although we explored three-neuron arrangements for the construction of neuronal logic gates of types AND and OR, it could be the case that a higher number of neurons will be necessary for other types of logic gates. Also, depending on which parameter is under analysis, even AND and OR gates may demand an arrangement with more than three neurons. A framework based on queueing-theoretical concepts has taken into account the time of propagation and arrival of the action potential at the presynaptic terminals of the "output" neuron aiming to predict the neuronal gate performance once it is positioned inside a neuronal network. Thus, this queueing-theoretical analysis could eventually allow experimentalists to understand the impacts of a synthetically engineered neuronal gate even before deployment *in vivo*. A similar approach was applied for the work on filtering high-frequency spike firing, where logic gates constructed from neurons were put together to build a more complex circuit capable of filtering specific frequency bands based on re-arranging logic gates. In this case, our neuronal filter is submitted to traditional circuit modelling as a linear system and each neuronal compartment model described its properties such as ionic channels and synaptic weight. These properties are crucial for the evaluation of how accurately a neuronal logic gate can output an action potential based on its inputs. The proposed gates showed different levels of accuracy which were influenced by not only the neuronal properties but also the spiking rate at the input and, potentially, any "noise" coming from other synaptic processes. The study also observed the ability of AND gates to help smooth out high frequency firing at its inputs which can imply novel treatment of epilepsy. This is because an AND gate only sends an output if there are simultaneous stimuli at its inputs. This way, even if the neurons at the input are under seizure, only an unlikely syncing would "minimise" the filtering efficiency of the gate.

As non-neuronal cells also impact the communication and propagation of neuronal information, so do non-neuronal processes of the body such as immune response to infections

123

caused by external agents. In this thesis, the effects of viral infections have been investigated and among many of the neurodegenerations, it may directly or indirectly cause. Demyelination of neurons is one example. This is because, to fight the infection, cytokine storms that are pro- and anti-inflammatory should be released. For that reason, it has been found that pro-inflammatory cytokines can damage healthy tissue and compromise neuronal communication as myelin sheaths get damaged in the process. Our proposed model of this phenomenon built on top of the current knowledge for known coronaviruses and extended the analysis to the novel coronavirus (SARS-CoV-2) which also indicated the potential of the virus to cause even further damage to the nervous system. Further progressing with studies on demyelination, this thesis also discusses some modelling of LPC-induced demyelination that built on top of wet-lab experimental data. A myelination index metric was coupled to the well known Hodgkin-Huxley model and the analysis showed consistency with the literature. The model also provided an opportunity for experimentalists to speed up their results using a wet-lab-validated model that can easily be fine-tuned for specific analysis. The results showed a heavy influence on the propagation and potential of the signal travelling down a partially myelinated axon although the relationship is not entirely linear. The lower band of the indices presented subtle changes up to the point it increased more linearly in the middle band and it started to plateau again on the upper band of the myelination indices. These results provided an interesting behaviour in how demyelination and remyelination affect neuronal communication as it is not necessary to reach the lowest index point to have a heavy attenuation on the signal and, analogously, it is not necessary to reach the highest index point to have a satisfactory conduction behaviour.

13.1 FUTURE WORKS

There is a long way before we see the everyday use of synthetically designed molecular communication systems for biomedical applications, but the contributions of this thesis is a

stepping stone towards that vision. In the following, future works based on the presented work are shown.

13.1.1 IMPACTS OF NON-NEURONAL CELLS IN THE COMMUNICATION BASED ON ACTION POTENTIAL AND SYNAPSES

It is well known that non-neuronal cells, such as astrocytes, can influence the communication between neurons. Moreover, the use of other cells in the nervous system can help identify points for improvement in the models as more details are being inserted in the model to account for a rich cellular environment. For example, a tripartite synapse can offer an alternative way of controlling the release and diffusion of neurotransmitters that can impact the propagation of action potential over the network. Non-neuronal cells also include the performance of synthetically engineered neurons, especially in terms of biocompatibility and energy efficiency when interfacing with natural neurons.

13.1.2 VALIDATION OF COMPUTATIONAL MODELS WITH WET-LAB EXPERIMENTS

It is only natural for a specific theoretical approach to plateau in terms of how it evolves into more robust models. For that reason, wet-lab experimentalists must find their way to validate the models. The validation may require some fine-tuning or, least likely, drastic changes to the proposed model. This will surely require collaboration between biologists working in the field of neuroscience, synthetic neurobiologists that can program neurons into a computing element, as well as researchers from embedded nanotechnology that could proceed with the implementation of a cell into a chip and then conduct tests that will help validate the model.

13.1.3 REAL IMPLEMENTATION OF NEURON-BASED MOLECULAR COM-MUNICATIONS

The numerical and computational simulation analysis performed in this thesis was put together and adapted from other works in the field with different goals compared to the investigation conducted in this thesis. So, the next step has the potential to be the design and development of proof-of-concept systems capable of validating, even if partially, the theoretical models which could most likely lead to prototypes for future novel devices.

Collaborations with other professionals from different fields will most likely be required for the successful implementation of real neuron-based devices. As molecular communications is a highly interdisciplinary field, the process from research to safe use and deployment may benefit from, for example, biologists, engineers, chemists molecular microbiologists, pharmacists and physicians.

13.1.4 APPLICATION OF NOVEL DISEASE TREATMENT METHODS USING NEURONAL LOGIC CIRCUITS

Even with the current advancements of medicine and biomedical engineering, many of the tools used for the treatment of disease in hard-to-reach places inside the body still poses numerous challenges for the patient, such as bulky equipment, reduced biocompatibility and relatively high maintenance that compromise the patient's lifestyle. For that reason, scientists and researchers have been working on tackling those challenges to develop novel approaches to neurodegeneration based on the concept of neuronal logic gates and circuits.

These circuits should have improved compatibility with the biological medium and demand much less outside maintenance as it could be tailored to a specific activity performed by the patient, such as being asleep or awake, with the use of precise drug delivery or artificial stimulation for example via ultrasound or light stimuli. These novel methods should

account for long-term treatments against neurodegeneration and, probably pave the way for techniques able to enhance the performance of cognitive abilities.

REFERENCES

[1] F. López-Muñoz, J. Boya, and C. Alamo, "Neuron theory, the cornerstone of neuroscience, on the centenary of the Nobel Prize award to Santiago Ramón y Cajal," *Brain Research Bulletin*, vol. 70, no. 4, pp. 391–405, 2006, ISSN: 0361-9230. DOI: https://doi.org/10.1016/j.brainresbull.2006.07.010. [Online]. Available: https://www.sciencedirect.com/science/article/pii/S0361923006002334.

[2] R. Lentini, N. Y. Martín, M. Forlin, L. Belmonte, J. Fontana, M. Cornella, L. Martini, S. Tamburini, W. E. Bentley, O. Jousson, and S. S. Mansy, "Two-Way Chemical Communication between Artificial and Natural Cells," *ACS Central Science*, vol. 3, no. 2, pp. 117–123, Feb. 2017, ISSN: 2374-7943. DOI: 10.1021/acscentsci.6b00330. [Online]. Available: https://doi.org/10.1021/acscentsci.6b00330.

[3] G. Rampioni, F. D'Angelo, M. Messina, A. Zennaro, Y. Kuruma, D. Tofani, L. Leoni, and P. Stano, "Synthetic cells produce a quorum sensing chemical signal perceived by Pseudomonas aeruginosa," *Chem. Commun.*, vol. 54, pp. 2090–2093, 17 2018. DOI: 10.1039/C7CC09678J. [Online]. Available: http://dx.doi.org/10.1039/C7CC09678J.

[4] A. P. Alivisatos, M. Chun, G. M. Church, R. J. Greenspan, M. L. Roukes, and R. Yuste, "The Brain Activity Map Project and the Challenge of Functional Connectomics," *Neuron*, vol. 74, no. 6, pp. 970–974, 2012, ISSN: 0896-6273. DOI: https://doi.org/10.1016/j.neuron.2012.06.006. [Online]. Available: https://www.sciencedirect.com/science/article/pii/S0896627312005181.

[5] F. Lienert, J. J. Lohmueller, A. Garg, and P. A. Silver, "Synthetic biology in mammalian cells: next generation research tools and therapeutics," *Nature Reviews Molecular Cell Biology*, vol. 15, no. 2, pp. 95–107, 2014, ISSN: 1471-0080. DOI: 10.1038/nrm3738.

[6] J. Larouche and C. A. Aguilar, "New technologies to enhance in vivo reprogramming for regenerative medicine," *Trends in biotechnology*, 2018.

[7] Y. Higashikuni, W. C. Chen, and T. K. Lu, "Advancing therapeutic applications of synthetic gene circuits," *Current Opinion in Biotechnology*, vol. 47, pp. 133–141, 2017, Tissue, cell and pathway engineering, ISSN: 0958-1669. DOI: https://doi.org/10.1016/j.copbio.2017.06.011. [Online]. Available: https://www.sciencedirect.com/science/article/pii/S0958166917301106.

[8] L. You, R. S. Cox, R. Weiss, and F. H. Arnold, "Programmed population control by cell–cell communication and regulated killing," *Nature*, vol. 428, no. 6985, pp. 868–871, Apr. 2004, ISSN: 1476-4687. DOI: 10.1038/nature02491. [Online]. Available: https://doi.org/10.1038/nature02491.

[9] A. Tamsir, J. J. Tabor, and C. A. Voigt, "Robust multicellular computing using genetically encoded nor gates and chemical 'wires'," *Nature*, vol. 469, no. 7329, pp. 212–215, Jan. 2011, ISSN: 1476-4687. DOI: 10.1038/nature09565. [Online]. Available: https://doi.org/10.1038/nature09565.

[10] I. F. Akyildiz, F. Brunetti, and C. Blázquez, "Nanonetworks: A new communication paradigm," *Computer Networks*, vol. 52, no. 12, pp. 2260–2279, 2008.

[11] G. Rampioni, L. Leoni, and P. Stano, "Molecular Communications in the Context of "Synthetic Cells" Research," *IEEE Transactions on NanoBioscience*, vol. 18, no. 1, pp. 43–50, 2019. DOI: 10.1109/TNB.2018.2882543.

[12] J. Hasty, D. McMillen, and J. J. Collins, "Engineered gene circuits," *Nature*, vol. 420, no. 6912, p. 224, 2002.

[13] A. Goldental, S. Guberman, R. Vardi, and I. Kanter, "A computational paradigm for dynamic logic-gates in neuronal activity," *Frontiers in Computational Neuroscience*, vol. 8, p. 52, 2014, ISSN: 1662-5188. DOI: 10.3389/fncom.2014.00052.

[14] T. P. Vogels and L. F. Abbott, "Signal propagation and logic gating in networks of integrate-and-fire neurons," *Journal of Neuroscience*, vol. 25, no. 46, pp. 10786–10795, 2005, ISSN: 0270-6474. DOI: 10.1523/JNEUROSCI.3508-05.2005.

[15] D. Morse and P. Sassone-Corsi, "Time after time: Inputs to and outputs from the mammalian circadian oscillators," *Trends in neurosciences*, vol. 25, no. 12, pp. 632–637, 2002.

[16] D. G. Gibson, J. I. Glass, C. Lartigue, V. N. Noskov, R.-Y. Chuang, M. A. Algire, G. A. Benders, M. G. Montague, L. Ma, M. M. Moodie, C. Merryman, S. Vashee, R. Krishnakumar, N. Assad-Garcia, C. Andrews-Pfannkoch, E. A. Denisova, L. Young, Z.-Q. Qi, T. H. Segall-Shapiro, C. H. Calvey, P. P. Parmar, C. A. Hutchison, H. O. Smith, and J. C. Venter, "Creation of a Bacterial Cell Controlled by a Chemically Synthesized Genome," *Science*, vol. 329, no. 5987, pp. 52–56, 2010, ISSN: 0036-8075. DOI: 10.1126/science.1190719. eprint: https://science.sciencemag.org/content/329/5987/52.full.pdf. [Online]. Available: https://science.sciencemag.org/content/329/5987/52.

[17] W. S. McCulloch and W. Pitts, "A logical calculus of the ideas immanent in nervous activity," *The bulletin of mathematical biophysics*, vol. 5, no. 4, pp. 115–133, Dec. 1943, ISSN: 1522-9602. DOI: 10.1007/BF02478259.

[18] M. T. Barros, P. Doan, M. Kandhavelu, B. Jennings, and S. Balasubramaniam, "Engineering calcium signaling of astrocytes for neural–molecular computing logic gates," *Scientific Reports*, vol. 11, no. 1, p. 595, Jan. 2021, ISSN: 2045-2322. DOI: 10.1038/s41598-020-79891-x. [Online]. Available: https://doi.org/10.1038/s41598-020-79891-x.

[19] T. Song, P. Zheng, M. D. Wong, and X. Wang, "Design of logic gates using spiking neural p systems with homogeneous neurons and astrocytes-like control," *Information Sciences*, vol. 372, pp. 380–391, 2016, ISSN: 0020-0255. DOI: 10.1016/j.ins.2016.08.055.

[20] N. Farsad, H. B. Yilmaz, A. Eckford, C. B. Chae, and W. Guo, "A Comprehensive Survey of Recent Advancements in Molecular Communication," *IEEE Communications Surveys Tutorials*, vol. 18, no. 3, pp. 1887–1919, thirdquarter 2016, ISSN: 1553-877X. DOI: 10.1109/COMST.2016.2527741.

[21] M. Pierobon and I. F. Akyildiz, "A physical end-to-end model for molecular communication in nanonetworks," *IEEE Journal on Selected Areas in Communications*, vol. 28, no. 4, pp. 602–611, May 2010, ISSN: 0733-8716. DOI: 10.1109/JSAC.2010. 100509.

[22] M. Moore, A. Enomoto, T. Suda, T. Nakano, and Y. Okaie, "Molecular communication: New paradigm for communication among nanoscale biological machines," *Handbook of Computer Networks: Distributed Networks, Network Planning, Control, Management, and New Trends and Applications*, vol. 3, pp. 1034–1054, 2007.

[23] T. Nakano, "Molecular communication: A 10 year retrospective," *IEEE Transactions on Molecular, Biological and Multi-Scale Communications*, vol. 3, no. 2, pp. 71–78, Jun. 2017, ISSN: 2372-2061. DOI: 10.1109/TMBMC.2017.2750148.

[24] D. P. Martins, M. T. Barros, and S. Balasubramaniam, "Quality and Capacity Analysis of Molecular Communications in Bacterial Synthetic Logic Circuits," *IEEE Transactions on NanoBioscience*, vol. 18, no. 4, pp. 628–639, Oct. 2019, ISSN: 1558-2639. DOI: 10.1109/TNB.2019.2930960.

[25] M. T. Barros, "Ca2+-signaling-based molecular communication systems: Design and future research directions," *Nano Communication Networks*, vol. 11, pp. 103–113, 2017.

[26] L. P. Giné and I. F. Akyildiz, "Molecular communication options for long range nanonetworks," *Computer Networks*, vol. 53, no. 16, pp. 2753–2766, 2009, ISSN: 1389-1286.

[27] G. H. Koenderink, Z. Dogic, F. Nakamura, P. M. Bendix, F. C. MacKintosh, J. H. Hartwig, T. P. Stossel, and D. A. Weitz, "An active biopolymer network controlled by molecular motors," *Proceedings of the National Academy of Sciences*, vol. 106, no. 36, pp. 15 192–15 197, 2009. DOI: 10.1073/pnas.0903974106.

[28] E. Balevi and O. B. Akan, "A Physical Channel Model for Nanoscale Neuro-Spike Communications," *IEEE Transactions on Communications*, vol. 61, no. 3, pp. 1178–1187, Mar. 2013, ISSN: 0090-6778. DOI: 10.1109/TCOMM.2012.010213.110093.

[29] J. Choe, B. A. Coffman, D. T. Bergstedt, M. D. Ziegler, and M. E. Phillips, "Transcranial Direct Current Stimulation Modulates Neuronal Activity and Learning in Pilot Training," *Frontiers in Human Neuroscience*, vol. 10, p. 34, 2016, ISSN: 1662-5161. DOI: 10.3389/fnhum.2016.00034. [Online]. Available: https://www.frontiersin.org/article/10.3389/fnhum.2016.00034.

[30] M. A. Lebedev and M. A. L. Nicolelis, "Brain-machine interfaces: From basic science to neuroprostheses and neurorehabilitation," *Physiological Reviews*, vol. 97, no. 2, pp. 767–837, 2017, PMID: 28275048. DOI: 10.1152/physrev.00027.2016.

[31] F. Zeldenrust, W. J. Wadman, and B. Englitz, "Neural Coding With Bursts – Current State and Future Perspectives," *Frontiers in Computational Neuroscience*, vol. 12, p. 48, 2018, ISSN: 1662-5188. DOI: 10.3389/fncom.2018.00048.

[32] Y. Huang and R. P. N. Rao, "Predictive coding," *Wiley Interdisciplinary Reviews: Cognitive Science*, vol. 2, no. 5, pp. 580–593, 2011, ISSN: 1939-5086. DOI: 10.1002/wcs.142.

[33] R. P. N. Rao and D. H. Ballard, "Predictive coding in the visual cortex: a functional interpretation of some extra-classical receptive-field effects," *Nature Neuroscience*, vol. 2, pp. 79–87, Jan. 1999.

[34] B. A. Olshausen and D. J. Field, "Sparse coding of sensory inputs," *Current Opinion in Neurobiology*, vol. 14, no. 4, pp. 481–487, 2004, ISSN: 0959-4388. DOI: 10.1016/j.conb.2004.07.007.

[35] G. Rinkus, "A cortical sparse distributed coding model linking mini- and macrocolumn-scale functionality," *Frontiers in Neuroanatomy*, vol. 4, p. 17, 2010, ISSN: 1662-5129.

[36] E. T. Rolls and A. Treves, "The neuronal encoding of information in the brain," *Progress in Neurobiology*, vol. 95, no. 3, pp. 448–490, 2011, ISSN: 0301-0082. DOI: 10.1016/j.pneurobio.2011.08.002.

[37] S. Thorpe, A. Delorme, and R. V. Rullen, "Spike-based strategies for rapid processing," *Neural Networks*, vol. 14, no. 6, pp. 715–725, 2001, ISSN: 0893-6080. DOI: 10.1016/S0893-6080(01)00083-1.

[38] A. Luczak, B. L. McNaughton, and K. D. Harris, "Packet-based communication in the cortex," *Nature Reviews Neuroscience – Perspectives*, vol. 16, pp. 1–11, Oct. 2015.

[39] I. F. Akyildiz, M. Pierobon, S. Balasubramaniam, and Y. Koucheryavy, "The internet of bio-nano things," *IEEE Communications Magazine*, vol. 53, no. 3, pp. 32–40, 2015.

[40] M. Kuscu, E. Dinc, B. A. Bilgin, H. Ramezani, and O. B. Akan, "Transmitter and Receiver Architectures for Molecular Communications: A Survey on Physical Design With Modulation, Coding, and Detection Techniques," *Proceedings of the IEEE*, vol. 107, no. 7, pp. 1302–1341, 2019. DOI: 10.1109/JPROC.2019.2916081.

[41] Q. Tang, N. Tummala, S. Gupta, and L. Schwiebert, "Communication scheduling to minimize thermal effects of implanted biosensor networks in homogeneous tissue," *IEEE Transactions on Biomedical Engineering*, vol. 52, no. 7, pp. 1285–1294, 2005. DOI: 10.1109/TBME.2005.847527.

[42] I. F. Akyildiz, F. Fekri, R. Sivakumar, C. R. Forest, and B. K. Hammer, "MoNaCo: Fundamentals of Molecular Nano-Communication Networks," *IEEE Wireless Communications*, vol. 19, no. 5, pp. 12–18, 2012. DOI: 10.1109/MWC.2012.6339467.

[43] U. A. K. Chude-Okonkwo, R. Malekian, B. T. Maharaj, and A. V. Vasilakos, "Molecular Communication and Nanonetwork for Targeted Drug Delivery: A Survey," *IEEE Communications Surveys Tutorials*, vol. 19, no. 4, pp. 3046–3096, 2017. DOI: 10.1109/COMST.2017.2705740.

[44] O. B. Akan, H. Ramezani, T. Khan, N. A. Abbasi, and M. Kuscu, "Fundamentals of Molecular Information and Communication Science," *Proceedings of the IEEE*, vol. 105, no. 2, pp. 306–318, Feb. 2017, ISSN: 0018-9219. DOI: 10.1109/JPROC.2016.2537306.

[45] H. Ramezani and O. B. Akan, "A Communication Theoretical Modeling of Axonal Propagation in Hippocampal Pyramidal Neurons," *IEEE Transactions on NanoBioscience*, vol. 16, no. 4, pp. 248–256, Jun. 2017, ISSN: 1536-1241. DOI: 10.1109/TNB.2017.2688341.

[46] V. K. Jirsa, W. C. Stacey, P. P. Quilichini, A. I. Ivanov, and C. Bernard, "On the nature of seizure dynamics," *Brain*, vol. 137, no. 8, pp. 2210–2230, Jun. 2014, ISSN: 0006-8950. DOI: 10.1093/brain/awu133.

[47] C. Kerr, S. Van Albada, S. Neymotin, G. Chadderdon, P. Robinson, and W. Lytton, "Cortical information flow in parkinson's disease: A composite network/field model," *Frontiers in Computational Neuroscience*, vol. 7, p. 39, 2013, ISSN: 1662-5188. DOI: 10.3389/fncom.2013.00039. [Online]. Available: https://www.frontiersin.org/article/10.3389/fncom.2013.00039.

[48] M. Barros and S. Dey, "Feed-forward and feedback control in astrocytes for ca2+-based molecular communications nanonetworks," *IEEE/ACM Transactions on Computational Biology and Bioinformatics*, pp. 1–1, 2018.

[49] M. U. Ahmed, M. Hanif, M. J. Ali, M. A. Haider, D. Kherani, G. M. Memon, A. H. Karim, and A. Sattar, "Neurological Manifestations of COVID-19 (SARS-CoV-2): A Review," *Frontiers in Neurology*, vol. 11, p. 518, 2020, ISSN: 1664-2295. DOI: 10.3389/fneur.2020.00518. [Online]. Available: https://www.frontiersin.org/article/10.3389/fneur.2020.00518.

[50] A. Orsini, M. Corsi, A. Santangelo, A. Riva, D. Peroni, T. Foiadelli, S. Savasta, and P. Striano, "Challenges and management of neurological and psychiatric manifestations in SARS-CoV-2 (COVID-19) patients," *Neurological Sciences*, vol. 41, no. 9, pp. 2353–2366, Sep. 2020, ISSN: 1590-3478. DOI: 10.1007/s10072-020-04544-w. [Online]. Available: https://doi.org/10.1007/s10072-020-04544-w.

[51] V. Borutaite, A. M. Tolkovsky, M. Fricker, G. C. Brown, and M. Coleman, "Neuronal Cell Death," *Physiological reviews*, 2018.

[52] G.-M. Hariz and K. Hamberg, "Perceptions of Living With a Device-Based Treatment: An Account of Patients Treated With Deep Brain Stimulation for Parkinson's Disease," *Neuromodulation: Technology at the Neural Interface*, vol. 17, no. 3, pp. 272–278, 2014. DOI: https://doi.org/10.1111/ner.12073. eprint: https://onlinelibrary.wiley.com/doi/pdf/10.1111/ner.12073. [Online]. Available: https://onlinelibrary.wiley.com/doi/abs/10.1111/ner.12073.

[53] S. A. Wirdatmadja, M. T. Barros, Y. Koucheryavy, J. M. Jornet, and S. Balasubramaniam, "Wireless Optogenetic Nanonetworks for Brain Stimulation: Device Model and Charging Protocols," *IEEE Transactions on NanoBioscience*, vol. PP, no. 99, pp. 1–1, 2017, ISSN: 1536-1241. DOI: 10.1109/TNB.2017.2781150.

[54] I.-W. Chen, E. Papagiakoumou, and V. Emiliani, "Towards circuit optogenetics," *Current Opinion in Neurobiology*, vol. 50, pp. 179–189, 2018, Neurotechnologies, ISSN: 0959-4388. DOI: https://doi.org/10.1016/j.conb.2018.03.008. [Online]. Available: https://www.sciencedirect.com/science/article/pii/S0959438817302477.

[55] S. Wirdatmadja, P. Johari, A. Desai, Y. Bae, E. K. Stachowiak, M. K. Stachowiak, J. M. Jornet, and S. Balasubramaniam, "Analysis of Light Propagation on Physiological Properties of Neurons for Nanoscale Optogenetics," *IEEE Transactions on Neural Systems and Rehabilitation Engineering*, vol. 27, no. 2, pp. 108–117, 2019. DOI: 10.1109/TNSRE.2019.2891271.

[56] S. Wirdatmadja, J. M. Jornet, Y. Koucheryavy, and S. Balasubramaniam, "Channel Impulse Analysis of Light Propagation for Point-to-Point Nano Communications Through Cortical Neurons," *IEEE Transactions on Communications*, vol. 68, no. 11, pp. 7111–7122, 2020. DOI: 10.1109/TCOMM.2020.3012477.

[57] R. A. Shewcraft, H. L. Dean, M. M. Fabiszak, M. A. Hagan, Y. T. Wong, and B. Pesaran, "Excitatory/Inhibitory Responses Shape Coherent Neuronal Dynamics Driven by Optogenetic Stimulation in the Primate Brain," *Journal of Neuroscience*, vol. 40, no. 10, pp. 2056–2068, 2020, ISSN: 0270-6474. DOI: 10.1523/JNEUROSCI. 1949-19.2020. eprint: https://www.jneurosci.org/content/40/10/2056.full.pdf. [Online]. Available: https://www.jneurosci.org/content/40/10/2056.

[58] A. Caruso, J. Vollmer, M. Machacek, and E. Kortvely, "Modeling the activation of the alternative complement pathway and its effects on hemolysis in health and disease," *PLOS Computational Biology*, vol. 16, no. 10, pp. 1–23, Oct. 2020. DOI: 10.1371/journal.pcbi.1008139. [Online]. Available: https://doi.org/10.1371/journal. pcbi.1008139.

[59] H. Markram *et al.*, "Reconstruction and Simulation of Neocortical Microcircuitry," *Cell*, vol. 163, no. 2, pp. 456–492, 2015, ISSN: 0092-8674. DOI: 10.1016/j.cell.2015. 09.029.

[60] A. Mishra and S. K. Majhi, "A comprehensive survey of recent developments in neuronal communication and computational neuroscience," *Journal of Industrial Information Integration*, vol. 13, pp. 40–54, 2019, ISSN: 2452-414X. DOI: 10.1016/j. jii.2018.11.005.

[61] M. Pospischil, M. Toledo-Rodriguez, C. Monier, Z. Piwkowska, T. Bal, Y. Frégnac, H. Markram, and A. Destexhe, "Minimal Hodgkin–Huxley type models for different classes of cortical and thalamic neurons," *Biological Cybernetics*, vol. 99, no. 4, pp. 427–441, Nov. 2008, ISSN: 1432-0770. DOI: 10.1007/s00422-008-0263-8.

[62] A. L. Hodgkin and A. F. Huxley, "A quantitative description of membrane current and its application to conduction and excitation in nerve," *The Journal of physiology*, vol. 117, no. 4, pp. 500–544, 1952.

[63] L. Long and G. Fang, "A Review of Biologically Plausible Neuron Models for Spiking Neural Networks," in *AIAA Infotech@Aerospace 2010*. America Institute of Aeronautics and Astronautics, 2010. DOI: 10.2514/6.2010-3540.

[64] E. Barreto and J. R. Cressman, "Ion concentration dynamics as a mechanism for neuronal bursting," *Journal of Biological Physics*, vol. 37, no. 3, pp. 361–373, Jun. 2011, ISSN: 1573-0689. DOI: 10.1007/s10867-010-9212-6.

[65] C. Koch, *Biophysics of computation: information processing in single neurons*. Oxford university press, 2004.

[66] B. Sengupta, A. A. Faisal, S. B. Laughlin, and J. E. Niven, "The Effect of Cell Size and Channel Density on Neuronal Information Encoding and Energy Efficiency," *Journal of Cerebral Blood Flow & Metabolism*, vol. 33, no. 9, pp. 1465–1473, 2013, PMID: 23778164. DOI: 10.1038/jcbfm.2013.103. eprint: https://doi.org/10.1038/ jcbfm.2013.103. [Online]. Available: https://doi.org/10.1038/jcbfm.2013.103.

[67] D. A. Baxter and J. H. Byrne, "Dynamical Properties of Excitable Membranes," in *From Molecules to Networks*, J. H. Byrne, R. Heidelberger, and M. N. Waxham, Eds., 3rd, Boston: Academic Press, 2014, ch. 14, pp. 409–442, ISBN: 978-0-12-397179-1. DOI: https://doi.org/10.1016/B978-0-12-397179-1.00014-2. [Online]. Available: http://www.sciencedirect.com/science/article/pii/B9780123971791000142.

[68] J. Gautrais and S. Thorpe, "Rate coding versus temporal order coding: a theoretical approach," *Biosystems*, vol. 48, no. 1, pp. 57–65, 1998, ISSN: 0303-2647. DOI: 10.1016/S0303-2647(98)00050-1.

[69] N. A. Lesica and G. B. Stanley, "Encoding of Natural Scene Movies by Tonic and Burst Spikes in the Lateral Geniculate Nucleus," *Journal of Neuroscience*, vol. 24, no. 47, pp. 10731–10740, 2004, ISSN: 0270-6474. DOI: 10.1523/JNEUROSCI.3059-04.2004.

[70] S. A. Wirdatmadja, S. Balasubramaniam, Y. Koucheryavy, and J. M. Jornet, "Wireless optogenetic neural dust for deep brain stimulation," in *2016 IEEE 18th International Conference on e-Health Networking, Applications and Services (Healthcom)*, Sep. 2016, pp. 1–6. DOI: 10.1109/HealthCom.2016.7749532.

[71] H. Ramezani, T. Khan, and O. B. Akan, "Information Theoretical Analysis of Synaptic Communication for Nanonetworks," in *IEEE INFOCOM 2018 - IEEE Conference on Computer Communications*, 2018, pp. 2330–2338.

[72] M. Veletić, P. A. Floor, Z. Babić, and I. Balasingham, "Peer-to-Peer Communication in Neuronal Nano-Network," *IEEE Transactions on Communications*, vol. 64, no. 3, pp. 1153–1166, 2016.

[73] M. Veletić and I. Balasingham, "An information theory of neuro-transmission in multiple-access synaptic channels," *IEEE Transactions on Communications*, vol. 68, no. 2, pp. 841–853, 2020.

[74] M. T. Barros, "Capacity of the Hierarchical Multi-Layered Cortical Microcircuit Communication Channel," in *Proceedings of the 5th ACM International Conference on Nanoscale Computing and Communication*, ser. NANOCOM '18, Reykjavik, Iceland: Association for Computing Machinery, 2018, ISBN: 9781450357111. DOI: 10.1145/3233188.3233208. [Online]. Available: https://doi.org/10.1145/3233188.3233208.

[75] A. S. Cacciapuoti, M. Caleffi, and A. Piras, "Neuronal Communication: Presynaptic Terminals as Transmitter Array," in *Proceedings of the Second Annual International Conference on Nanoscale Computing and Communication*, ser. NANOCOM' 15, Boston, MA, USA: Association for Computing Machinery, 2015, ISBN: 9781450336741. DOI: 10.1145/2800795.2800800. [Online]. Available: https://doi.org/10.1145/2800795.2800800.

[76] T. Khan, B. A. Bilgin, and O. B. Akan, "Diffusion-Based Model for Synaptic Molecular Communication Channel," *IEEE Transactions on NanoBioscience*, vol. 16, no. 4, pp. 299–308, 2017.

[77] T. Khan and O. B. Akan, "Sum rate analysis of multiple-access neuro-spike communication channel with dynamic spiking threshold," *Nano Communication Networks*, vol. 19, pp. 110–118, 2019, ISSN: 1878-7789. DOI: https://doi.org/10.1016/j.nancom.2019.01.002. [Online]. Available: http://www.sciencedirect.com/science/article/pii/S1878778918301169.

[78] S. Lotter, A. Ahmadzadeh, and R. Schober, *Channel modeling for synaptic molecular communication with re-uptake and reversible receptor binding*, 2019. arXiv: 1912.04025 [q-bio.SC].

[79] R. Miller, "Theory of the normal waking EEG: From single neurones to waveforms in the alpha, beta and gamma frequency ranges," *International Journal of Psychophysiology*, vol. 64, no. 1, pp. 18–23, 2007, Brain Oscillations:Cutting Edges, ISSN: 0167-8760. DOI: 10.1016/j.ijpsycho.2006.07.009.

[80] M. L. Cuzner and W. T. Norton, "Biochemistry of Demyelination," *Brain Pathology*, vol. 6, no. 3, pp. 231–242, 1996. DOI: https://doi.org/10.1111/j.1750-3639.1996.tb00852.x. eprint: https://onlinelibrary.wiley.com/doi/pdf/10.1111/j.1750-3639.1996.tb00852.x. [Online]. Available: https://onlinelibrary.wiley.com/doi/abs/10.1111/j.1750-3639.1996.tb00852.x.

[81] S. A. Stohlman and D. R. Hinton, "Viral Induced Demyelination," *Brain Pathology*, vol. 11, no. 1, pp. 92–106, 2001. DOI: 10.1111/j.1750-3639.2001.tb00384.x. [Online]. Available: https://doi.org/10.1111/j.1750-3639.2001.tb00384.x.

[82] A. Miller, M. Korem, R. Almog, and Y. Galboiz, "Vitamin B12, demyelination, remyelination and repair in multiple sclerosis," *Journal of the Neurological Sciences*, vol. 233, no. 1, pp. 93–97, 2005, Preserve the Neuron., ISSN: 0022-510X. DOI: https://doi.org/10.1016/j.jns.2005.03.009. [Online]. Available: https://www.sciencedirect.com/science/article/pii/S0022510X05000870.

[83] J. R. Plemel, N. J. Michaels, N. Weishaupt, A. V. Caprariello, M. B. Keough, J. A. Rogers, A. Yukseloglu, J. Lim, V. V. Patel, K. S. Rawji, S. K. Jensen, W. Teo, B. Heyne, S. N. Whitehead, P. K. Stys, and V. W. Yong, "Mechanisms of lysophosphatidylcholine-induced demyelination: A primary lipid disrupting myelinopathy," *Glia*, vol. 66, no. 2, pp. 327–347, 2018. DOI: https://doi.org/10.1002/glia.23245. eprint: https://onlinelibrary.wiley.com/doi/pdf/10.1002/glia.23245. [Online]. Available: https://onlinelibrary.wiley.com/doi/abs/10.1002/glia.23245.

[84] O. Fernández, V. Fernández, and M. Guerrero, "Enfermedades desmielinizantes del sistema nervioso central," *Medicine - Programa de Formación Médica Continuada Acreditado*, vol. 11, no. 77, pp. 4601–4609, 2015, ISSN: 0304-5412. DOI: https://doi.org/10.1016/j.med.2015.04.001. [Online]. Available: https://www.sciencedirect.com/science/article/pii/S0304541215000797.

[85] E. M. Rhea and W. A. Banks, "Role of the Blood-Brain Barrier in Central Nervous System Insulin Resistance," *Frontiers in Neuroscience*, vol. 13, 2019, ISSN: 1662-453X. DOI: 10.3389/fnins.2019.00521. [Online]. Available: https://www.frontiersin.org/article/10.3389/fnins.2019.00521.

[86] G. Kreutzberg, "Microglia, the first line of defence in brain pathologies," *Arzneimittel-Forschung*, vol. 45, no. 3A, pp. 357–360, Mar. 1995, ISSN: 0004-4172. [Online]. Available: http://europepmc.org/abstract/MED/7763326.

[87] M. Desforges, A. Le Coupanec, É. Brison, M. Meessen-Pinard, and P. J. Talbot, "Neuroinvasive and Neurotropic Human Respiratory Coronaviruses: Potential Neurovirulent Agents in Humans," in *Infectious Diseases and Nanomedicine I*, R. Adhikari and S. Thapa, Eds., New Delhi: Springer India, 2014, pp. 75–96, ISBN: 978-81-322-1777-0.

[88] Y. Wu, X. Xu, Z. Chen, J. Duan, K. Hashimoto, L. Yang, C. Liu, and C. Yang, "Nervous system involvement after infection with COVID-19 and other coronaviruses," *Brain, Behavior, and Immunity*, vol. 87, pp. 18–22, 2020, ISSN: 0889-1591. DOI: https://doi.org/10.1016/j.bbi.2020.03.031. [Online]. Available: https://doi.org/10.1016/j.bbi.2020.03.031.

[89] Y. Oh *et al.*, "Zika virus directly infects peripheral neurons and induces cell death," *Nature Neuroscience*, vol. 20, no. 9, pp. 1209–1212, Sep. 2017, ISSN: 1546-1726. DOI: 10.1038/nn.4612. [Online]. Available: https://doi.org/10.1038/nn.4612.

[90] V. Valcour *et al.*, "Central Nervous System Viral Invasion and Inflammation During Acute HIV Infection," *The Journal of Infectious Diseases*, vol. 206, no. 2, pp. 275–282, May 2012, on behalf of the RV254/SEARCH 010 Study Group, ISSN: 0022-1899. DOI: 10.1093/infdis/jis326. [Online]. Available: https://doi.org/10.1093/infdis/jis326.

[91] Y. Cheng, D. Skinner, and T. Lane, "Innate Immune Responses and Viral-Induced Neurologic Disease," *Journal of Clinical Medicine*, vol. 8, no. 1, p. 3, Dec. 2018, ISSN: 2077-0383. DOI: 10.3390/jcm8010003. [Online]. Available: http://doi.org/10.3390/jcm8010003.

[92] A. S. Zubair, L. S. McAlpine, T. Gardin, S. Farhadian, D. E. Kuruvilla, and S. Spudich, "Neuropathogenesis and Neurologic Manifestations of the Coronaviruses in the Age of Coronavirus Disease 2019: A Review," *JAMA Neurology*, May 2020, ISSN: 2168-6149. DOI: 10.1001/jamaneurol.2020.2065. [Online]. Available: https://doi.org/10.1001/jamaneurol.2020.2065.

[93] I. Sanclemente-Alaman *et al.*, "Experimental Models for the Study of Central Nervous System Infection by SARS-CoV-2," *Frontiers in Immunology*, vol. 11, p. 2163, 2020, ISSN: 1664-3224. DOI: 10.3389/fimmu.2020.02163. [Online]. Available: https://doi.org/10.3389/fimmu.2020.02163.

[94] V. Montalvan, J. Lee, T. Bueso, J. De Toledo, and K. Rivas, "Neurological manifestations of COVID-19 and other coronavirus infections: A systematic review," *Clinical Neurology and Neurosurgery*, vol. 194, p. 105 921, 2020, ISSN: 0303-8467. DOI: https://doi.org/10.1016/j.clineuro.2020.105921. [Online]. Available: https://doi.org/10.1016/j.clineuro.2020.105921.

[95] E. Song *et al.*, "Neuroinvasion of SARS-CoV-2 in human and mouse brain," *Journal of Experimental Medicine*, vol. 218, no. 3, Jan. 2021, e20202135, ISSN: 0022-1007. DOI: 10.1084/jem.20202135. [Online]. Available: https://doi.org/10.1084/jem.20202135.

[96] M. T. Barros, M. Veletić, M. Kanada, M. Pierobon, S. Vainio, I. Balasingham, and S. Balasubramaniam, "Molecular Communications in Viral Infections Research: Modelling, Experimental Data and Future Directions," *Accepted in IEEE Transactions on Molecular, Biological and Multi-Scale Communications.*, 2021. DOI: 10.1109/TMBMC.2021.3071780. [Online]. Available: https://doi.org/10.1109/TMBMC.2021.3071780.

[97] Y. Chahibi, "Molecular communication for drug delivery systems: A survey," *Nano Communication Networks*, vol. 11, pp. 90–102, 2017, ISSN: 1878-7789. DOI: https://doi.org/10.1016/j.nancom.2017.01.003. [Online]. Available: https://doi.org/10.1016/j.nancom.2017.01.003.

[98] H. K. Charlton Hume, J. Vidigal, M. J. T. Carrondo, A. P. J. Middelberg, A. Roldão, and L. H. L. Lua, "Synthetic biology for bioengineering virus-like particle vaccines," *Biotechnology and Bioengineering*, vol. 116, no. 4, pp. 919–935, 2019. DOI: https: //doi.org/10.1002/bit.26890. eprint: https://onlinelibrary.wiley.com/doi/pdf/10.1002/ bit.26890. [Online]. Available: https://onlinelibrary.wiley.com/doi/abs/10.1002/bit. 26890.

[99] I. F. Akyildiz, M. Pierobon, S. Balasubramaniam, and Y. Koucheryavy, "The internet of Bio-Nano things," *IEEE Communications Magazine*, vol. 53, no. 3, pp. 32–40, Mar. 2015, ISSN: 0163-6804. DOI: 10.1109/MCOM.2015.7060516.

[100] T. Miyamoto, S. Razavi, R. DeRose, and T. Inoue, "Synthesizing Biomolecule-Based Boolean Logic Gates," *ACS Synthetic Biology*, vol. 2, no. 2, pp. 72–82, 2013, PMID: 23526588. DOI: 10.1021/sb3001112.

[101] H. Geerts, J. Wikswo, P. H. van der Graaf, J. P. Bai, C. Gaiteri, D. Bennett, S. E. Swalley, E. Schuck, R. Kaddurah-Daouk, K. Tsaioun, and M. Pelleymounter, "Quantitative Systems Pharmacology for Neuroscience Drug Discovery and Development: Current Status, Opportunities, and Challenges," *CPT: Pharmacometrics & Systems Pharmacology*, vol. 9, no. 1, pp. 5–20, 2020. DOI: 10.1002/psp4.12478. eprint: https://ascpt.onlinelibrary.wiley.com/doi/pdf/10.1002/psp4.12478. [Online]. Available: https://ascpt.onlinelibrary.wiley.com/doi/abs/10.1002/psp4.12478.

[102] O. Feinerman, A. Rotem, and E. Moses, "Reliable neuronal logic devices from patterned hippocampal cultures," *Nature Physics*, vol. 4, no. 12, pp. 967–973, Dec. 2008, ISSN: 1745-2481. DOI: 10.1038/nphys1099. [Online]. Available: https://doi. org/10.1038/nphys1099.

[103] E. S. Fortune and G. J. Rose, "Passive and Active Membrane Properties Contribute to the Temporal Filtering Properties of Midbrain Neurons In Vivo," *Journal of Neuroscience*, vol. 17, no. 10, pp. 3815–3825, 1997, ISSN: 0270-6474. DOI: 10.1523/ JNEUROSCI.17-10-03815.1997. eprint: https://www.jneurosci.org/content/17/10/ 3815.full.pdf. [Online]. Available: https://www.jneurosci.org/content/17/10/3815.

[104] H. E. Plesser and T. Geisel, "Bandpass properties of integrate-fire neurons," *Neurocomputing*, vol. 26-27, pp. 229–235, 1999, ISSN: 0925-2312. DOI: https://doi.org/10. 1016/S0925-2312(99)00076-4. [Online]. Available: http://www.sciencedirect.com/ science/article/pii/S0925231299000764.

[105] S. Ekins, J. Mestres, and B. Testa, "In silico pharmacology for drug discovery: methods for virtual ligand screening and profiling," *British Journal of Pharmacology*, vol. 152, no. 1, pp. 9–20, 2007. DOI: https://doi.org/10.1038/sj.bjp.0707305. eprint: https://bpspubs.onlinelibrary.wiley.com/doi/pdf/10.1038/sj.bjp.0707305. [Online]. Available: https://bpspubs.onlinelibrary.wiley.com/doi/abs/10.1038/sj.bjp.0707305.

[106] C. P. Billimoria, R. A. DiCaprio, J. T. Birmingham, L. F. Abbott, and E. Marder, "Neuromodulation of spike-timing precision in sensory neurons," *Journal of Neuroscience*, vol. 26, no. 22, pp. 5910–5919, 2006, ISSN: 0270-6474. DOI: 10.1523/ JNEUROSCI.4659-05.2006.

[107] K. Whittingstall and N. K. Logothetis, "Frequency-Band Coupling in Surface EEG Reflects Spiking Activity in Monkey Visual Cortex," *Neuron*, vol. 64, no. 2, pp. 281–289, 2009, ISSN: 0896-6273. DOI: 10.1016/j.neuron.2009.08.016. [Online]. Available: http://dx.doi.org/10.1016/j.neuron.2009.08.016.

[108] G. L. Adonias, M. T. Barros, L. Doyle, and S. Balasubramaniam, "Utilising EEG Signals for Modulating Neural Molecular Communications," in *5th ACM International Conference on Nanoscale Computing and Communication 2018 (ACM NanoCom'18)*, Reykjavik, Iceland, Sep. 2018, ISBN: 978-1-4503-5711-1/18/09. DOI: 10.1145/3233188.3236333.

[109] D. Gardner, "Noise modulation of synaptic weights in a biological neural network," *Neural Networks*, vol. 2, no. 1, pp. 69–76, 1989, ISSN: 0893-6080. DOI: https://doi.org/10.1016/0893-6080(89)90016-6. [Online]. Available: http://www.sciencedirect.com/science/article/pii/0893608089900166.

[110] G. L. Adonias, A. Yastrebova, M. T. Barros, Y. Koucheryavy, F. Cleary, and S. Balasubramaniam, "Utilizing Neurons for Digital Logic Circuits: A Molecular Communications Analysis," *IEEE Transactions on NanoBioscience*, vol. 19, no. 2, pp. 224–236, 2020, ISSN: 1558-2639. DOI: 10.1109/TNB.2020.2975942.

[111] G. L. Adonias, H. Siljak, M. T. Barros, N. Marchetti, M. White, and S. Balasubramaniam, "Reconfigurable Filtering of Neuro-Spike Communications Using Synthetically Engineered Logic Circuits," *Frontiers in Computational Neuroscience*, vol. 14, p. 91, 2020, ISSN: 1662-5188. DOI: 10.3389/fncom.2020.556628. [Online]. Available: https://www.frontiersin.org/article/10.3389/fncom.2020.556628.

[112] E. R. G. Sanabria, H. Su, and Y. Yaari, "Initiation of network bursts by Ca2+-dependent intrinsic bursting in the rat pilocarpine model of temporal lobe epilepsy," *The Journal of Physiology*, vol. 532, no. 1, pp. 205–216, 2001. DOI: https://doi.org/10.1111/j.1469-7793.2001.0205g.x. eprint: https://physoc.onlinelibrary.wiley.com/doi/pdf/10.1111/j.1469-7793.2001.0205g.x. [Online]. Available: https://physoc.onlinelibrary.wiley.com/doi/abs/10.1111/j.1469-7793.2001.0205g.x.

[113] F. Doussau, J.-L. Dupont, D. Neel, A. Schneider, B. Poulain, and J. L. Bossu, "Organotypic cultures of cerebellar slices as a model to investigate demyelinating disorders," *Expert Opinion on Drug Discovery*, vol. 12, no. 10, pp. 1011–1022, 2017, PMID: 28712329. DOI: 10.1080/17460441.2017.1356285. eprint: https://doi.org/10.1080/17460441.2017.1356285. [Online]. Available: https://doi.org/10.1080/17460441.2017.1356285.

[114] C. C. H. Cohen *et al.*, "Saltatory Conduction along Myelinated Axons Involves a Periaxonal Nanocircuit," *Cell*, vol. 180, no. 2, 311–322.e15, Jan. 2020, ISSN: 0092-8674. DOI: 10.1016/j.cell.2019.11.039. [Online]. Available: https://doi.org/10.1016/j.cell.2019.11.039.

[115] M. S. Hamada *et al.*, "Loss of Saltation and Presynaptic Action Potential Failure in Demyelinated Axons," *Frontiers in Cellular Neuroscience*, vol. 11, p. 45, 2017, ISSN: 1662-5102. DOI: 10.3389/fncel.2017.00045. [Online]. Available: https://doi.org/10.3389/fncel.2017.00045.

[116] G. L. Adonias, H. Siljak, M. T. Barros, and S. Balasubramaniam, *Neuron Signal Propagation Analysis of Cytokine-Storm induced Demyelination*, Submitted for publication in March 2021., 2021. arXiv: 2103.03790 [q-bio.NC].

[117] J. Yu, H. Qian, and J.-H. Wang, "Upregulation of transmitter release probability improves a conversion of synaptic analogue signals into neuronal digital spikes," *Molecular Brain*, vol. 5, no. 1, p. 26, Aug. 2012, ISSN: 1756-6606. DOI: 10.1186/1756-6606-5-26. [Online]. Available: https://doi.org/10.1186/1756-6606-5-26.

[118] H. Arjmandi, M. Movahednasab, A. Gohari, M. Mirmohseni, M. Nasiri-Kenari, and F. Fekri, "Isi-avoiding modulation for diffusion-based molecular communication," *IEEE Transactions on Molecular, Biological and Multi-Scale Communications*, vol. 3, no. 1, pp. 48–59, 2017. DOI: 10.1109/TMBMC.2016.2640311.